

ADVANCED TOPICS IN SCIENCE AND TECHNOLOGY IN CHINA

Kai Li

Electromagnetic Fields in Stratified Media



ZHEJIANG UNIVERSITY PRESS

浙江大学出版社



Springer

ADVANCED TOPICS IN SCIENCE AND TECHNOLOGY IN CHINA

ADVANCED TOPICS IN SCIENCE AND TECHNOLOGY IN CHINA

Zhejiang University is one of the leading universities in China. In Advanced Topics in Science and Technology in China, Zhejiang University Press and Springer jointly publish monographs by Chinese scholars and professors, as well as invited authors and editors from abroad who are outstanding experts and scholars in their fields. This series will be of interest to researchers, lecturers, and graduate students alike.

Advanced Topics in Science and Technology in China aims to present the latest and most cutting-edge theories, techniques, and methodologies in various research areas in China. It covers all disciplines in the fields of natural science and technology, including but not limited to, computer science, materials science, life sciences, engineering, environmental sciences, mathematics, and physics.

Kai Li

Electromagnetic Fields in Stratified Media

With 100 figures

 ZHEJIANG UNIVERSITY PRESS
浙江大学出版社

 Springer

AUTHOR:

Prof. Kai Li,
The Electromagnetics Academy
Zhejiang University
Yuquan Campus, Hangzhou
310027, China
E-mail: kaili@zju.edu.cn

ISBN 978-7-308-06401-9 **Zhejiang University Press, Hangzhou**
ISBN 978-3-540-95963-2 **Springer Berlin Heidelberg New York**
e-ISBN 978-3-540-95964-9 **Springer Berlin Heidelberg New York**

Series ISSN 1995-6819 Advanced topics in science and technology in China
Series e-ISSN 1995-6827 Advanced topics in science and technology in China

Library of Congress Control Number: 2009920460

This work is subject to copyright. All rights are reserved, whether the whole or part of the material is concerned, specifically the rights of translation, reprinting, reuse of illustrations, recitation, broadcasting, reproduction on microfilm or in any other way, and storage in data banks. Duplication of this publication or parts thereof is permitted only under the provisions of the German Copyright Law of September 9, 1965, in its current version, and permission for use must always be obtained from Springer-Verlag. Violations are liable to prosecution under the German Copyright Law.

© 2009 Zhejiang University Press, Hangzhou and Springer-Verlag GmbH Berlin Heidelberg

Co-published by Zhejiang University Press, Hangzhou and Springer-Verlag GmbH Berlin Heidelberg

Springer is a part of Springer Science+Business Media
springer.com

The use of general descriptive names, registered names, trademarks, etc. in this publication does not imply, even in the absence of a specific statement, that such names are exempt from the relevant protective laws and regulations and therefore free for general use.

Cover design: Frido Steinen-Broo, EStudio Calamar, Spain
Printed on acid-free paper

Preface

The properties of the electromagnetic field over the boundary between two different media like earth and air are much more complicated when the source is on or near the boundary than when it is far away and the incident waves are plane waves. This subject has been intensively investigated for over a century. In the pioneering works of Zenneck and Sommerfeld, analytical solutions are carried out based on a flat-Earth model. With myriad practical applications in subsurface and close-to-the-surface communications, radar, and geophysical prospecting and diagnostics, the subject has been investigated widely and the findings have been summarized in the classic book *Dipole radiation in the presence of a conducting half-space* by Baños (Pergamon Press, Oxford, 1966). Lately, investigations are conducted to extend the two-layered case to three-layered and multi-layered cases, with a long series of papers published. The details of the research findings are well summarized in the book *Electromagnetic waves in stratified media* by Wait (Pergamon Press, New York, 1970) and the book *Lateral Electromagnetic Waves* by King, Owens, and Wu (Springer-Verlag, 1992).

In the past decade, the existence or nonexistence of trapped-surface-wave terms in the solution for a dipole radiating over a dielectric-coated lossy underling medium continued to be a controversial subject. Many investigators have revisited the old problem and some new progress has been made. In this book it is investigated with an emphasis placed on the solution for a dipole radiating over the planar or spherical boundary of a stratified medium. It is concerned with an approximate or rigorous analytical solution of the electromagnetic field radiated by a vertical or horizontal dipole. Usually, a simplified or idealized physical model is founded for a practical problem. Subject to the boundary conditions, the formulas of the electromagnetic field are always represented in the exact form of general integrals. These integrals are then evaluated by using mathematical techniques. The corresponding numerical results are carried out, and the conclusions are drawn.

Chapter 1 presents the historical and technical overview of the electromagnetic fields in stratified media in the past century. In Chapters 2-5, it

is concerned with the approximate solutions for electromagnetic fields radiated by vertical and horizontal electric dipoles in the presence of three- and four-layered regions. Both the trapped surface wave and the lateral wave are addressed specifically. Chapters 6 and 7 deal with the propagation of the electromagnetic waves generated by a dipole on or near the spherical surface of a layered Earth while the transient field excited by delta function and Gaussian currents in a horizontal electric dipole on the boundary between two different media is dealt with in Chapters 8 and 9. In the entire book an $e^{-i\omega t}$ time dependence is assumed and suppressed.

The author would like to express his gratitude to his advisor, Professor Wei-Yan Pan of the China Research Institute of Radiowave Propagation, who introduced him to the fascinating world of electromagnetics. Special thanks are owed to Professor Hong-Qi Zhang of the China Research Institute of Radio Propagation. The author also wishes to thank Professor Seong-Ook Park of the Information and Communications University, Korea and Professor Yi-Long Lu of the Nanyang Technological University, Singapore for their insight suggestions and comments. The author is also grateful to his graduate students at Zhejiang University, especially to Yin-Lin Wang and Yi-Hui Xu. Many thanks are also owed to Professor Kang-Sheng Chen, Professor Xian-Min Zhang, Professor Sai-Ling He, Professor Dong-Xiao Yang, Professor Xi-Dong Wu, and Professor Wen-Yan Yin of Zhejiang University for their helpful support and encouragement. Finally, the author would like to acknowledge the support and guidance of the editorial staff of Zhejiang University Press and Springer.

The author sincerely appreciates the financial support in part of the National Science Foundation of China under Grant 60831002 of Shanghai Jiao Tong University.

The author hopes that the book would help stimulate new ideas and innovative approaches to electromagnetic fields and waves in stratified media in the years to come.

Kai Li
Zhejiang University
August 2008

Contents

1	Historical and Technical Overview of Electromagnetic Fields in Stratified Media	1
1.1	Electromagnetic Wave Along Air-Earth Boundary	1
1.2	Surface Waves Along Surfaces of Stratified Media	3
1.3	Lateral Waves Along the Air-Earth Boundary	6
1.4	Trapped Surface Wave in the Presence of Three-Layered Region	6
1.5	Electromagnetic Field Radiated by a Dipole over Spherical Earth	8
	References	9
2	Electromagnetic Field of a Vertical Electric Dipole in the Presence of a Three-Layered Region	15
2.1	Introduction	15
2.2	The Integrated Formulas for Electromagnetic Field in Air	16
2.3	Field of Vertical Dipole over Dielectric-Coated Perfect Conductor	20
2.3.1	Integrated Formulas of the Electromagnetic Field in Air	20
2.3.2	Evaluations of Trapped Surface Wave and Lateral Wave	21
2.3.3	Final Formulas for the Electromagnetic Field Components	27
2.3.4	Computations and Discussions	28
2.4	Field of Vertical Dipole over Dielectric-Coated Imperfect Conductor	32
2.4.1	Statements of the Problem	32
2.4.2	The Trapped Surface Wave	33
2.4.3	Lateral Wave	35
2.4.4	Final Formulas for the Electromagnetic Field Components	37
2.4.5	Computations and Discussions	38
2.5	Radiation from Vertical Dipole in Three-Layered Region	42
2.5.1	Field of Vertical Dipole in Three-Layered Region	42

2.5.2	Graphical Representations of the Far Field	46
References	53
3	Electromagnetic Field of a Horizontal Electric Dipole in the Presence of a Three-Layered Region	55
3.1	Introduction	55
3.2	Electromagnetic Field of Horizontal Electric Dipole	56
3.2.1	Integrated Formulas for Electromagnetic Field in Air ..	56
3.2.2	Evaluation for the Electric-Type Field	59
3.2.3	Evaluation for the Magnetic-Type Field	62
3.2.4	New Techniques for Determining the Poles λ_E and λ_B ..	65
3.2.5	Final Formulas for Six Field Components.....	68
3.2.6	Computations and Conclusions.....	69
3.3	Radiation of Horizontal Electric Dipole and Microstrip Antenna	73
3.3.1	Radiation of a Horizontal Electric Dipole	73
3.3.2	Microstrip Antenna.....	77
3.3.3	Computations and Discussions	79
3.4	Summary.....	84
References	84
4	Electromagnetic Field of a Vertical Electric Dipole in the Presence of a Four-Layered Region	87
4.1	Introduction	87
4.2	Formulation of Problem	88
4.3	Evaluations of the Trapped Surface Wave and Lateral Wave ..	90
4.4	Computations and Conclusions.....	96
References	99
5	Electromagnetic Field of a Horizontal Electric Dipole in the Presence of a Four-Layered Region	103
5.1	Integrated Formulas for the Electromagnetic Field	103
5.2	Evaluation for the Electric-Type Field	108
5.3	Evaluation for the Magnetic-Type Field	113
5.4	Final Formulas for the Six-Field Components	117
5.5	Computations and Conclusions	118
References	121
6	Electromagnetic Field Radiated by a Dipole Source over a Dielectric-Coated Spherical Earth	123
6.1	Introduction	123
6.2	Electromagnetic Field due to Vertical Electric Dipole	124
6.2.1	Formulations of the Problem.....	124
6.2.2	Determination of the Coefficient A_s	128
6.2.3	Final Formulas of the Electromagnetic Field	131
6.2.4	Computations for Parameters t_s	131

6.2.5	Analysis and Computations	136
6.3	Electromagnetic Field due to Vertical Magnetic Dipole	137
6.4	Electromagnetic Field due to Horizontal Electric Dipole	140
6.5	Summary	144
	References	144
7	Electromagnetic Field of a Dipole Source over the Spherical Surface of Multi-Layered Earth	147
7.1	Introduction	147
7.2	Electromagnetic Field due to Vertical Electric Dipole	149
7.3	Electromagnetic Field due to Vertical Magnetic Dipole	153
7.4	Electromagnetic Field due to Horizontal Electric Dipole	155
7.5	Computations and Conclusions	157
	References	162
8	Exact Transient Field of a Horizontal Electric Dipole on the Boundary Between Two Dielectrics	165
8.1	Introduction	165
8.2	Exact Transient Field with Delta Function Excitation	166
8.2.1	Formal Representations of Time-independent Field due to Horizontal Electric Dipole	166
8.2.2	Time-Dependent Component $E_{2\rho}$	169
8.2.3	Time-Dependent Component $E_{2\phi}$	185
8.2.4	Time-Dependent Component B_{2z}	190
8.2.5	Discussions and Conclusions	193
8.3	Exact Transient Field with Gaussian Excitation	193
8.3.1	Exact Formulas for the Transient Field of Horizontal Dipole Excited by a Gaussian Pulse on the Boundary Between Two Dielectrics	193
8.3.2	Computations and Conclusions	197
	References	199
9	Approximate Transient Field of Horizontal Electric Dipole on the Boundary Between a Homogeneous Isotropic Medium and One-Dimensionally Anisotropic Medium	203
9.1	Statements of Problem	203
9.2	The Approximate Transient Field with Delta Function Excitation	204
9.3	Approximate Formulas for the Transient Field with Gaussian Excitation	212
	References	219
	Index	221

Historical and Technical Overview of Electromagnetic Fields in Stratified Media

The electromagnetic field in stratified media has been intensively investigated for over a century. In this chapter, we conduct a formal review on the electromagnetic field in stratified media. Attention should be paid to early analytical contributions on the electromagnetic field in two half-spaces by Zenneck and Sommerfeld. The subsequent contributions by other pioneers, such as Van der Pol, Baños, Fock, Wait, and King, are outlined. From the new developments on the electromagnetic field of a dipole in the presence of a three-layered region, it is seen that a trapped surface wave can be excited efficiently when both the dipole and the observation point are on or close to the boundary.

1.1 Electromagnetic Wave Along Air-Earth Boundary

The first analytical solution for the propagation of electromagnetic waves along the planar boundary between the air and the Earth was carried out by Zenneck (1907). With the existence and significance of the ionosphere still unknown, a possible explanation was offered that a surface wave could propagate over great distance with low attenuation. The properties of the Zenneck surface wave, a radial cylindrical surface wave, are well described by Barlow and Cullen (1953). The model considered is a conducting or dielectric half-space, for $z \geq 0$, with the conductivity σ_1 and permittivity ε_1 . The air, for $z \leq 0$, has a uniform permittivity ε_0 . It is assumed that both Region 1 and Region 2 are nonmagnetic so that $\mu_1 = \mu_2 = \mu_0$. Thus, the wave numbers of the two regions are

$$k_1 = \beta_1 + i\alpha_1 = \omega \left[\mu_0 \left(\varepsilon_1 + \frac{i\sigma_1}{\omega} \right) \right]^{1/2}, \quad (1.1)$$

$$k_2 = k_0 = \omega \sqrt{\mu_0 \varepsilon_0}. \quad (1.2)$$

When the conditions

$$|k_1|^2 \gg k_2^2 \quad \text{or} \quad |k_1|^2 \geq 9|k_2|^2 \quad (1.3)$$

are satisfied, the simplified formulas are obtained in cylindrical coordinates ρ, ϕ, z readily.

For $z \geq 0$, the field components are expressed by

$$B_{1\phi} = \mu_0 A e^{ik_1 z} H_1^{(1)}(k_2 \rho), \quad (1.4)$$

$$E_{1\rho} = -\frac{\omega}{k_1} B_{1\phi}, \quad (1.5)$$

$$E_{1z} = i \frac{\omega \mu_0 k_2}{k_1^2} A e^{ik_1 z} H_0^{(1)}(k_2 \rho), \quad (1.6)$$

and the corresponding forms, for $z \leq 0$, by

$$B_{2\phi} = \mu_0 A e^{-i(k_2^2/k_1)z} H_1^{(1)}(k_2 \rho), \quad (1.7)$$

$$E_{2\rho} = -\frac{\omega}{k_1} B_{2\phi}, \quad (1.8)$$

$$E_{2z} = i \frac{\omega \mu_0}{k_2} A e^{-i(k_2^2/k_1)z} H_0^{(1)}(k_2 \rho). \quad (1.9)$$

Here H_0 and H_1 are Hankel functions and A is an amplitude that depends on the nature of the unspecified source at the origin. For $k_2 \rho \geq 10$, the Hankel functions can be approximated by

$$H_0^{(1)}(k_2 \rho) \sim \sqrt{\frac{2}{\pi k_2 \rho}} e^{i(k_2 \rho - \pi/4)}, \quad (1.10)$$

$$H_1^{(1)}(k_2 \rho) \sim \sqrt{\frac{2}{\pi k_2 \rho}} e^{i(k_2 \rho - 3\pi/4)}. \quad (1.11)$$

Evidently, it is seen that the far field decreases as $\rho^{-1/2}$ with radial distance ρ and decreases exponentially in a vertical direction. This is the essential characteristic of the Zenneck surface wave.

In pioneering works by Sommerfeld, detailed analysis was carried out on the electromagnetic field radiated by an infinitesimal vertical Hertzian dipole on the surface of the Earth, a lossy homogeneous isotropic half-space (Sommerfeld, 1909). In his classic solution, a radial Zenneck surface wave was contained. This seemed to explain the guiding-wave mechanism for the long-distance transmission of radio signals along the air-earth boundary. In 1919, Weyl published a paper on the same subject and obtained a solution similar to that found by Sommerfeld, but without the term of the Zenneck surface wave (Weyl, 1919). In 1926, Sommerfeld returned to the same problem by using a different approach, and concluded that the term of the Zenneck surface wave was not included in the complete solution for the electromagnetic field (Sommerfeld, 1926). This work confirmed the correctness of Weyl's solution.

Nevertheless, the controversies concerning the existence or nonexistence of the Zenneck surface wave continued for a long time and rekindled many investigators to revisit the subject (Van der Pol, 1930; 1935; Sommerfeld, 1935; North, 1937; Wait, 1953; 1961; 1962; Hill and Wait, 1978; Wait and Hill, 1979). The details are well summarized by Baños (1966), and they are not repeated here. Useful discussions are carried out by Wait (1998a), and Collin (2004b).

1.2 Surface Waves Along Surfaces of Stratified Media

The mechanisms of the propagation of electromagnetic waves over the surfaces of stratified media are depended on the nature of the boundary and the properties of the media. The typical surface waveguides that allow the surface waves to be guided along the boundary surfaces include dielectric-coated plane and cylinder as shown in Fig. 1.1, corrugated metal plane and cylinder in Fig. 1.2, and dielectric rod or optical fiber and dielectric image line in Fig. 1.3.

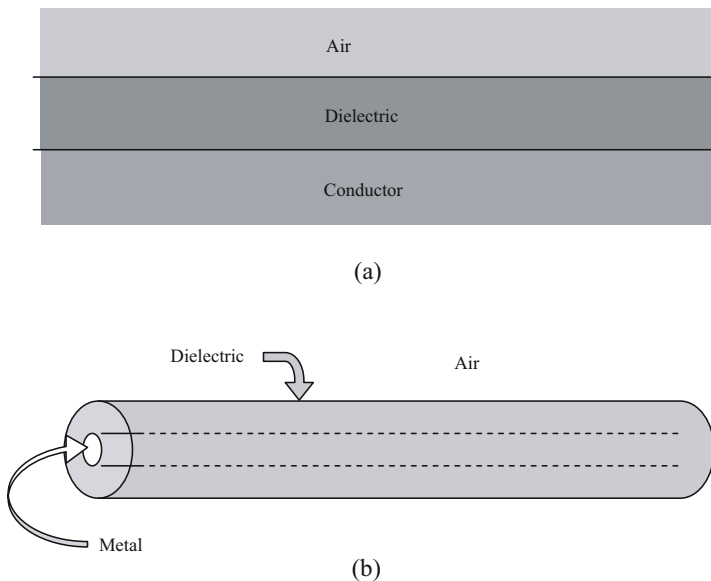


Fig. 1.1. Dielectric-coated metal plane and cylinder

Next, we attempt to describe the properties of the surface waves of the electromagnetic field in the presence of a three-layered region, which are addressed in the dissertation of Zhang (2001). The region of interest consists of the air (Region 0, $z > a$) over a dielectric layer (Region 1, $0 < z < a$) that coats a perfect conductor (Region 2, $z < 0$), as illustrated in Fig. 1.4. The simplified formulas for the electromagnetic field are obtained readily.

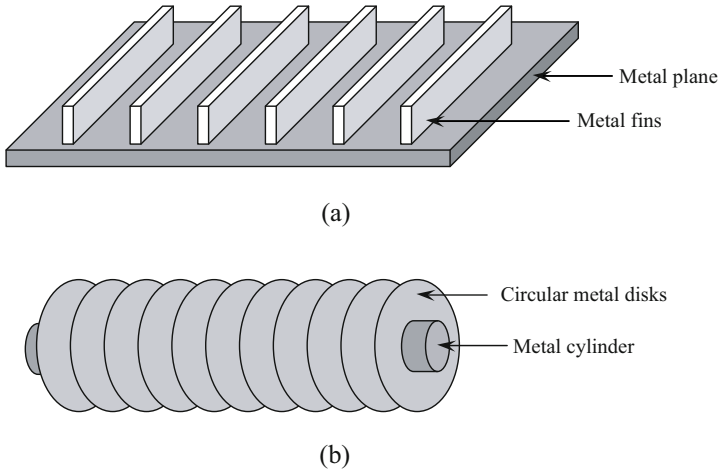


Fig. 1.2. Corrugated metal plane and cylinder

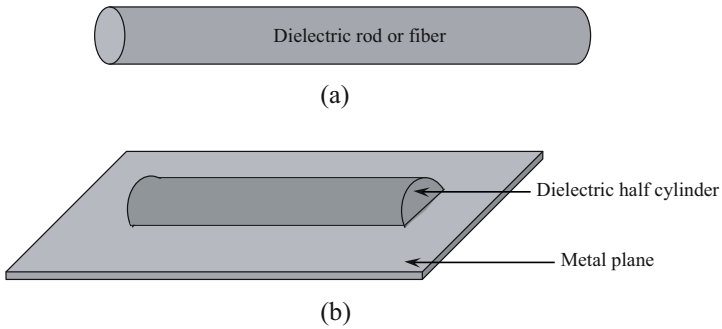


Fig. 1.3. Dielectric rod or fiber and dielectric image line

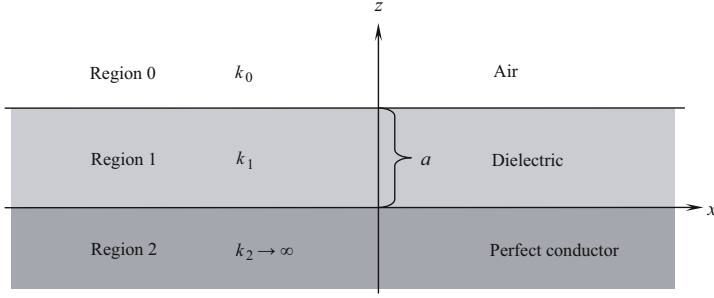
For transverse magnetic (TM) wave, in Region 0,

$$E_x = -Ae^{-K_1 z} e^{i\gamma x}, \quad (1.12)$$

$$E_z = \frac{i\gamma}{K_1} Ae^{-K_1 z} e^{i\gamma x}, \quad (1.13)$$

$$H_y = \frac{i\omega\epsilon_0}{K_1} Ae^{-K_1 z} e^{i\gamma x}. \quad (1.14)$$

In Region 1,

**Fig. 1.4.** Geometry of three-layered region

$$E_x = -B \sin(K_2 z) e^{i\gamma x}, \quad (1.15)$$

$$E_z = -\frac{i\gamma}{K_2} B \cos(K_2 z) e^{i\gamma x}, \quad (1.16)$$

$$H_y = -\frac{i\omega\epsilon_0}{K_2} B \cos(K_2 z) e^{i\gamma x}, \quad (1.17)$$

where γ , K_1 , and K_2 should be satisfied by the following characteristic equations:

$$K_2 \tan(K_2 a) = (\epsilon_1 / \epsilon_0) K_1, \quad (1.18)$$

$$K_2^2 + \gamma^2 = k_0^2, \quad (1.19)$$

$$\gamma^2 - K_1^2 = k_1^2. \quad (1.20)$$

For transverse electric (TE) wave, in Region 0,

$$H_x = A e^{-K_1 z} e^{i\gamma x}, \quad (1.21)$$

$$H_z = \frac{i\gamma}{K_1} A e^{-K_1 z} e^{i\gamma x}, \quad (1.22)$$

$$E_y = -\frac{i\omega\mu_0}{K_1} A e^{-K_1 z} e^{i\gamma x}. \quad (1.23)$$

In Region 1,

$$H_x = B \sin(K_2 z) e^{i\gamma x}, \quad (1.24)$$

$$H_z = \frac{i\gamma}{K_2} B \cos(K_2 z) e^{i\gamma x}, \quad (1.25)$$

$$E_y = -\frac{i\omega\mu_0}{K_2} B \cos(K_2 z) e^{i\gamma x}, \quad (1.26)$$

where

$$K_2 a \tan(K_2 a) = K_1 a, \quad (1.27)$$

$$K_2^2 + \gamma^2 = k_0^2, \quad (1.28)$$

$$\gamma^2 - K_1^2 = k_1^2. \quad (1.29)$$

It follows that the surface wave in the air decreases exponentially in the \hat{z} direction and travels along the \hat{x} direction. It is noted that the wave number in the \hat{x} direction, which is between k_0 and k_1 , is determined by the thickness and nature of the dielectric layer.

1.3 Lateral Waves Along the Air-Earth Boundary

The properties of a lateral electromagnetic wave radiated by vertical and horizontal dipoles on the planar boundary between two different media have been investigated extensively. The details are addressed in an excellent summary by King, Owens and Wu (1992).

The region considered consists of the Earth (Region 1) and the air (Region 2), and both the horizontal dipole and the observation point are located on the boundary in Region 1. The analytical formulas were obtained for the electromagnetic field generated by a horizontal electric dipole in the two different media by King and Wu (1983). It is seen that the far field includes direct wave, ideal reflected wave or ideal image wave, and lateral wave.

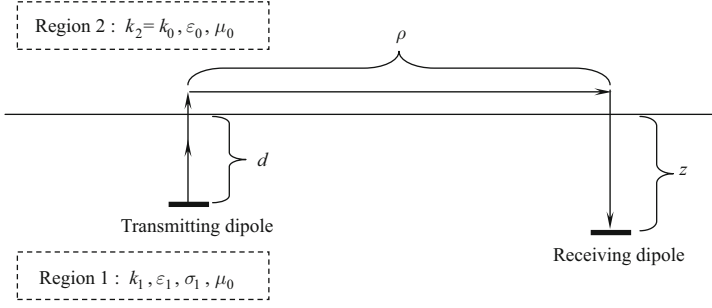
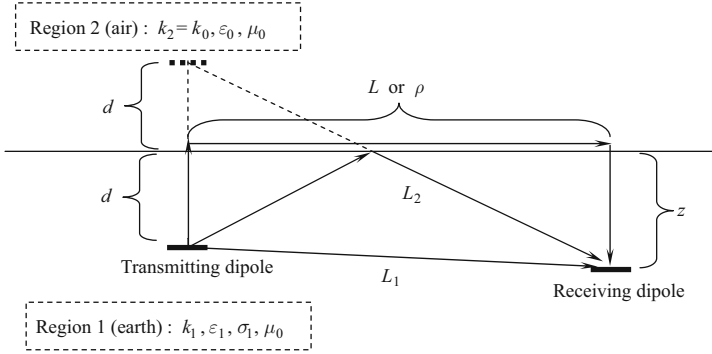
$$E_1(\rho, z) = E_1^{inc}(\rho, z) + E_1^{ref}(\rho, z) + E_1^L(\rho, z), \quad (1.30)$$

where the three terms $E_1^{inc}(\rho, z)$, $E_1^{ref}(\rho, z)$, and $E_1^L(\rho, z)$ stand for the direct wave, the ideal reflected wave, and the lateral wave, respectively.

As illustrated in Fig. 1.5, it is seen that the lateral wave travels from the transmitting dipole a distance d in Region 1 (Earth) to the boundary, then radially along the boundary in Region 2 (Air) a distance ρ , and finally vertically a distance z in Region 1 to the receiving dipole. The paths of the direct wave, the ideal reflected wave, and the lateral wave are shown in Fig. 1.6. The lateral-wave characteristics are well known and addressed specifically in the book by King, Owens, and Wu (1992).

1.4 Trapped Surface Wave in the Presence of Three-Layered Region

The electromagnetic fields of vertical and horizontal electric dipoles on or near the boundary between two different media have been well known in terms of closed-form expressions for many years. When the boundary includes a layer of third material with intermediate properties, the properties of the electromagnetic field radiated by a dipole are in general much more complicated.

**Fig. 1.5.** Apparent path of lateral wave**Fig. 1.6.** Apparent paths of directed wave, image reflected wave, and lateral wave

In early 1990's, the simply analytical formulas were derived for the electromagnetic fields generated by horizontal and vertical electric dipoles in the presence of a three-layered region (King, 1991; 1992; 1993; King and Sandler, 1994b). It was demonstrated that the total field on or near the air-dielectric boundary is determined primarily by lateral wave, where the amplitude of the field along the boundary is $1/\rho^2$.

In the late 1990's, Wait (1998) and Mahmoud (1999) wrote comments on the work by King and Sandler (1994a, 1994b) and considered that the trapped surface wave, varying as $\rho^{-1/2}$ in the far-field region, should not be overlooked in the three-layered case. In the two papers by Collin (2004a; 2004b), the analysis supports the conclusions reached by Wait and Mahmoud. To clarify the controversies concerning the trapped surface wave, the old problem was revisited again by several investigators in the past several years (Zhang and Pan, 2002; Zhang, Li, and Pan, 2003; Zhang et al., 2001, 2005; Li and Lu, 2005b; Liu and Li, 2007).

From the works by Zhang and Pan (2002), it is concluded that the trapped-surface-wave terms, where the amplitude decreases as $\rho^{-1/2}$ along the air-dielectric boundary in the far-field region, can be excited efficiently by a vertical electric dipole in the presence of a three-layered region. The wave

numbers of the trapped surface wave are between the wave number k_0 in the air and the wave number k_1 in the dielectric. It is found that the far field includes the direct wave, ideal reflected wave, lateral wave, and trapped surface wave.

$$E(\rho, z) = E^{inc}(\rho, z) + E^{ref}(\rho, z) + E^L(\rho, z) + E^S(\rho, z), \quad (1.31)$$

where the four terms $E^{inc}(\rho, z)$, $E^{ref}(\rho, z)$, $E^L(\rho, z)$, and $E^S(\rho, z)$ stand for the direct wave, the ideal reflected wave, the lateral wave, and the trapped surface wave, respectively.

1.5 Electromagnetic Field Radiated by a Dipole over Spherical Earth

In practical situations such as dipole radiation over the Earth or sea, when large distances are involved, a spherical model needs to be adopted. An early analytical solution was carried out by Watson (1918), in the case of the earth being a perfect conducting sphere. In his solution, by using a complex plane technique, the original harmonic series is transformed into a series of residues. Lately, based on Watson's theory, this problem was visited by many investigators. Remarkable progress had been made by several pioneers such as Van der Pol (1938), Bremmer (1949; 1954; 1958), Wait (1956b; 1956c; 1962), and Fock (1965). In what follows, we will attempt to describe the works by Fock (1965).

The geometry of interest consists of the spherical Earth (Region 1, $r < a$) and the air (region 0, $r > a$). It is noted that important parameters include the radius a of the Earth and the wave numbers k_1 in the Earth and $k_2 = k_0$ in the air. Let us suppose that a vertical electric dipole is represented by the current density $\hat{z}Idl\delta(x)\delta(y)\delta(z-b)$, where $b = a + z_s$, and $z_s > 0$ denotes the height of the dipole above the surface of the Earth. The approximate formula for the vertical electric field E_r is written in the following form:

$$E_r = E_0 V(x, y_1, y_2, q), \quad (1.32)$$

where

$$E_0 = -\frac{iIdl\eta}{\lambda a} \frac{e^{ik_0 a \theta}}{\sqrt{\theta \sin \theta}}, \quad (1.33)$$

$$V(x, y_1, y_2, q) = e^{i\frac{\pi}{4}} \sqrt{\pi x} \sum_s \frac{W_2(t_s - y_1)}{W_2(t_s)} \frac{W_2(t_s - y_2)}{W_2(t_s)} \frac{e^{it_s x}}{t_s - q^2}, \quad (1.34)$$

where

$$x = \left(\frac{k_0 a}{2} \right)^{1/3} \theta, \quad (1.35)$$

$$y_1 = \left(\frac{2}{k_0 a} \right)^{1/3} k_0 z_s, \quad (1.36)$$

$$y_2 = \left(\frac{2}{k_0 a} \right)^{1/3} k_0 z_r. \quad (1.37)$$

Here η and z_r denote the wave impedance of free space and the height of the observation point, respectively. θ is the angular degree between the dipole and the observation point. It is noted that the parameters t_s ($s = 1, 2, \dots$) are the roots of the following Stokes equation:

$$W_2'(t) - qW_2(t) = 0, \quad (1.38)$$

where

$$q = i \left(\frac{k_0 a}{2} \right)^{1/3} \Delta_g, \quad (1.39)$$

where Δ_g is the normalized surface impedance of the Earth. Eq. (1.32) is the formula for diffraction of ground waves, which is employed in engineering. The function $V(x, y_1, y_2, q)$ indicates the ground-wave attenuation factor, which is determined by the operating frequency, the angular distance between the dipole and the observation point, the conductivity of the Earth, the height of the dipole and that of the observation point, and the radius of the Earth.

If the spherical-Earth surface is coated with layered dielectric, the properties of the electromagnetic field radiated by a dipole are much more complicated. In recent works, the properties were carried out analytically (Pan and Zhang, 2003; Li and Park, 2003; Li, Park, and Zhang, 2004a; 2004b; Li and Lu, 2005a).

References

- Attwood SS (1951) Surface wave propagation over a coated plane conductor, *Journal of Applied Physics*, 22: 504–509.
- Bannister PR and Dube RL (1978) Simple expressions for horizontal electric dipole quasi-static range subsurface-to-subsurface and subsurface-to-air propagation. *Radio Science*, 13: 501–507.
- Baños A Jr (1966) *Dipole Radiation in the Presence of a Conducting Half-Space*. Oxford, UK: Pergamon Press.
- Barlow HM and Cullen AL (1953) Surface wave. *Proceedings of the IEE*, 100: 329–341
- Bremmer H (1949) *Terrestrial Radio Waves*. New York, NY, USA: Elsevier.
- Bremmer H (1954) The extension of Sommerfeld's formula for the propagation of radio waves over a flat earth to different conductivities of the soil. *Physica*, 20: 441–460.

- Bremmer H (1958) Applications of operational calculus to groundwave propagation, particularly for long waves. *IRE Transactions on Antennas and Propagation*, AP-6: 267–274.
- Brown MF, King RWP, and Wu TT (1984) Experiments on the reflection of lateral electromagnetic waves. *Journal of Applied Physics*, 55: 3927–3933.
- Chew WC (1990) *Waves and Fields in Inhomogeneous Media*. New York, NY, USA: Van Nostrand Reinhold.
- Collin RE (2004a) Some observations about the near zone electric field of a hertzian dipole above a lossy earth. *IEEE Transactions on Antennas and Propagation*, 52(11): 3133–3137.
- Collin RE (2004b) Hertzian dipole radiation over a lossy earth or sea: Some early and late 20th century controversies. *IEEE Antennas and Propagation Magazine*, 46(2): 64–79.
- Dunn JM (1984) *Electromagnetic Lateral Waves in Layered Media*. Phd Thesis, Cambridge, MA, USA: Harvard University.
- Dunn JM (1986) Lateral wave propagation in a three-layered medium. *Radio Science*, 21(5): 787–796.
- Fei T, Li LW, Yeo TS, Wang HL, and Wu Q (2007) A comparative study of radio wave propagation over the earth due to a vertical electric dipole. *IEEE Transactions on Antennas and Propagation*, 55(10): 2723–2732.
- Felsen LB and Maruvitz N (1973) *Radiation and scattering of waves*. Englewood Cliffs, USA: Prentice Hall.
- Fock VA (1965) *Electromagnetic Diffraction and Propagation Problems*. Oxford, UK: Pergamon Press.
- Hill DA and Wait JR (1978) Excitation of Zenneck surface wave by a vertical aperture. *Radio Science*, 13(6): 969–977.
- Hill DA and Wait JR (1980) Ground wave attenuation function for a spherical earth with arbitrary surface impedance. *Radio Science*, 15(3): 637–643.
- Houdzoumis VA (1999) Vertical electric dipole radiation over a sphere: character of the waves that propagate through the sphere. *Journal of Applied Physics*, 86: 3939–3942.
- Houdzoumis VA (2000) Two modes of wave propagation manifested in vertical electric dipole radiation over a sphere. *Radio Science*, 35(1): 19–29.
- Ishimaru A (1991) *Electromagnetic Wave Propagation, Radiation and Scattering*. Englewood Cliffs, USA: Prentice Hall.
- King RJ (1969) EM wave propagation over a constant impedance plane. *Radio Science*, 4: 225–268.
- King RWP, Wu TT, and Shen LC (1974) The horizontal wire antenna over a conducting or dielectric half-space: Current and admittance. *Radio Science*, 9: 701–709.
- King RWP, Shen LC, and Wu TT (1975) The dipole antenna with dielectric coating in a relatively medium. *IEEE Transactions on Antennas and Propagation*, AP-23: 57–62.
- King RWP and Sandler BH (1977) Subsurface communication between dipoles in general media. *IEEE Transactions on Antennas and Propagation*, AP-25: 770–775.
- King RWP, deBettencourt JT, and Sandler BH (1979) Lateral-wave propagation of electromagnetic waves in the lithosphere. *IEEE Transactions on Geosciences and Electronics*, GE-17: 86–92.

- King RWP, Sandler BH, and Shen LC (1980) A comprehensive study of subsurface propagation from horizontal electric dipoles. *IEEE Transactions on Geoscience and Remote Sensing*, GE-18: 225–233.
- King RWP (1982) New formulas for the electromagnetic field of a vertical electric dipole in a dielectric or conducting half-space near its horizontal interface. *Journal of Applied Physics*, 53: 8476–8482; (1984) Erratum, 56: 3366.
- King RWP and Wu TT (1983) Lateral waves: Formulas for the magnetic field. *Journal of Applied Physics*, 54: 507–514; (1984) Erratum, 56: 3365.
- King RWP (1984) On the reflection of lateral electromagnetic waves from perpendicular boundaries. *Journal of Applied Physics*, 55: 3916–3926.
- King RWP and Brown MF (1984) Lateral electromagnetic waves along plane boundaries: A summarizing approach. *Proceedings of the IEEE*, 72: 595–611.
- King RWP (1985) Electromagnetic surface waves: New formulas and applications. *IEEE Transactions on Antennas and Propagation*, AP-33: 1204–1212.
- King RWP, Owens M, and Wu TT (1986) Properties of lateral electromagnetic fields and their application. *Radio Science*, 21: 12–23.
- King RWP (1986) Properties of the lateral electromagnetic field of a vertical dipole and their application. *IEEE Transactions on Geoscience and Remote Sensing*, GE-24: 813–825.
- King RWP and Prasad S (1986) *Fundamental Electromagnetic Theory and Application*. Englewood Cliffs, USA: Prentice-Hall.
- King RWP (1988a) Lateral electromagnetic pulses generated by a vertical electric dipole on a plane boundary between dielectrics. *Journal of Electromagnetic Waves and Applications*, 2: 225–243.
- King RWP (1988b) The Propagation of signals along a three-layered region: Microstrip. *IEEE Transactions on Microwave Theory and Techniques*, 36: 1080–1086.
- King RWP (1989a). Lateral electromagnetic waves from a horizontal antenna for remote sensing in the ocean. *IEEE Transactions on Antennas and Propagation*, 37: 1250–1255.
- King RWP (1989b) Lateral electromagnetic pulses generated on a plane boundary between dielectrics by vertical and horizontal dipole source with Gaussian pulse excitation. *Journal of Electromagnetic Waves and Applications*, 2: 589–597.
- King RWP (1990a) Electromagnetic field of a vertical dipole over a imperfect conducting half-space. *Radio Science*, 25: 149–160.
- King RWP (1990b) Lateral electromagnetic waves and pulses on open microstrip. *IEEE Transactions on Microwave Theory and Techniques*, 38: 38–47.
- King RWP (1991) The electromagnetic field of a horizontal electric dipole in the presence of a three-layered region. *Journal of Applied Physics*, 69(12): 7987–7995.
- King RWP (1992) Electromagnetic field of dipoles and patch antennas on microstrip. *Radio Science*, 27: 71–78.
- King RWP, Owens M, and Wu TT (1992) *Lateral Electromagnetic Waves: Theory and Applications to Communications, Geophysical Exploration, and Remote Sensing*. New York, NY, USA: Springer-Verlag.
- King RWP (1993) The electromagnetic field of a horizontal electric dipole in the presence of a three-layered region: supplement. *Journal of Applied Physics*, 74(8): 4845–4548.

- King RWP and Sandler SS (1994a) The electromagnetic field of a vertical electric dipole in the presence of a three-layered region. *Radio Science*, 29(1): 97–113.
- King RWP and Sandler SS (1994b) The electromagnetic field of a vertical electric dipole over the earth or Sea. *IEEE Transactions on Antennas and Propagation*, 42(3): 382–389.
- King RWP and Sandler SS (1998) Reply. *Radio Science*, 33(2): 255–256.
- King RWP, Fikioris GJ, and Mack RB (2002) *Cylindrical Antennas and Array*. Cambridge, UK: Cambridge University Press.
- Kong JA (2005) *Electromagnetic Wave Theory*. Cambridge, MA, USA: EMW Publishing.
- Li K and Park SO (2003) Electromagnetic field in the air generated by a horizontal electric dipole located in the spherical electrically earth coated with a dielectric layer. *Journal of Electromagnetic Waves and Applications*, 17(10): 1399–1417.
- Li K, Park SO, and Zhang HQ (2004a) Electromagnetic field in the presence of a three-layered spherical region. *Progress In Electromagnetics Research*, PIER 45: 103–121. Cambridge, MA, USA: EMW Publishing.
- Li K, Park SO, and Zhang HQ (2004b) Electromagnetic field over the spherical earth coated with N-layered dielectric. *Radio Science*, 39, RS2008, doi:10.1029/2002RS002771.
- Li K and Lu Y (2005a). Electromagnetic Field from a Horizontal Electric Dipole in the spherical electrically earth Coated with N-layered dielectrics. *Progress In Electromagnetics Research*, PIER 54: 221–244. Cambridge, MA, USA: EMW Publishing.
- Li K and Lu Y (2005b) Electromagnetic field generated by a horizontal electric dipole near the surface of a planar perfect conductor coated with a uniaxial layer. *IEEE Transactions on Antennas and Propagation*, 53(10): 3191–3200.
- Liu L and Li K (2007) Radiation from a vertical electric dipole in the presence of a three-layered region. *IEEE Transactions on Antennas and Propagation*, 55(12): 3469–3475.
- Lytle RJ, Miller EK, and Lager DL (1976) A physical explanation of electromagnetic surface wave formulas. *Radio Science*, 11: 235–243.
- Mahmoud SF (1999) Remarks on “The electromagnetic field of a vertical electric dipole over the earth or sea”. *IEEE Transactions on Antennas and Propagation*, 46(12): 1745–1946.
- Margetis D (2001) Exactly calculable field components of electric dipoles in planar boundary. *Journal of Mathematical Physics*, 42: 713–745.
- Margetis D (2002) Radiation of horizontal electric dipole on large dielectric sphere. *Journal of Mathematical Physics*, 43: 3162–3201.
- Mei JP and Li K (2007) Electromagnetic field from a horizontal electric dipole on the surface of a high lossy medium coated with a uniaxial layer. *Progress In Electromagnetics Research*, PIER 73: 71–91. Cambridge, MA, USA: EMW Publishing.
- Norton KA (1936) The propagation of radio waves over the surface of the earth and in the upper atmosphere. *Proceeding of the IRE*, 24: 1367–138.
- Norton KA (1937) The propagation of radio waves over the surface of the earth and in the upper atmosphere. *Proceeding of the IRE* 25: 1203–1236.
- North KA (1941) The calculations of ground-wave field intensity over a finitely conducting spherical earth. *Proceedings of the IRE*, 29: 623–639.

- Pan WY (1985) Surface wave propagation along the boundary between sea water and one-dimensionally anisotropic rock. *Journal of Applied Physics*, 58: 3963–3974.
- Pan WY (1986) Measurement of lateral waves along a three-layered medium. *IEEE Transactions on Antennas and Propagation*, AP-34(2): 267–277.
- Pan WY and Zhang HQ (2003) Electromagnetic field of a vertical electric dipole on the spherical conductor covered with a dielectric layer. *Radio Science*, 38(3), 1059, doi:10.1029/2002RS002689.
- Pan WY (2004) *LF VLF ELF Wave Propagation*. Chengdu, China: UESTC Press. (In Chinese)
- Pan WY, Li K, and Zhang HQ (2005) Lateral-wave electromagnetic field generated by a horizontal electric dipole below the spherical-earth surface. *Journal of Electromagnetic Waves and Applications*, 19(7): 953–972.
- Rahmat-Samii Y, Mittra R, and Parhami P (1981) Evaluation of Sommerfeld integrals for lossy half-space problems. *Electromagnetics*, 1: 1–28.
- Rolf B (1930) Graphs to Prof. Sommerfeld's attenuation formula for radio waves. *Proceeding of the IRE*, 18: 391–402.
- Sommerfeld A (1909) Propagation of waves in wireless telegraphy. *Annalen der Physik*, 28: 665–736.
- Sommerfeld A (1926) Propagation of waves in wireless telegraphy. *Annalen der Physik*, 81: 1135–1153.
- Sommerfeld AN (1935) *In die differential und integralgleichungen der mechanik und physik*, II: 932–933. Frank P and Mises RV (Eds.), Braunschweig, Germany: F. Vieweg and Son.
- Spies KP and Wait JR (1966) On the calculation of the groundwave attenuation factor at low frequencies. *IEEE Transactions on Antennas and Propagation*, AP-14: 515–517.
- Van der Pol B and Niessen KF (1930) The propagation of electromagnetic waves over a plane earth. *Annalen der Physik*, 6: 273–294.
- Van der Pol B (1935) Theory of the reflection of light from a point source by a finitely conducting flat mirror: with application to Radiotelegraphy. *Physics*, 2: 843–853.
- Van der Pol B and Bremmer H (1938) The propagation of radio waves over a finitely conducting spherical earth. *Philosophical Magazine*, 25: 817–834; Further note on above (1939), 27: 261–275.
- Vogler LE (1964) A note on the attenuation function for propagation over a flat layered ground. *IEEE Transactions on Antennas Propagation*, AP-12: 240–242.
- Wait JR (1953) Propagation of radio waves over a stratified ground. *Geophysics*, 18: 416–422.
- Wait JR (1956a) Low frequency radiation from a horizontal earth. *Canadian Journal of Physics*, 34: 586–595.
- Wait JR (1956b) Radiation from a vertical electric dipole over a curved stratified ground. *Journal of Research of the National Bureau of Standards*, 56: 232–239.
- Wait JR (1956c) Radiation and propagation from a vertical antenna over a spherical earth. *Journal of Research of National Bureau of Standards*, 56: 237–244.
- Wait JR (1957) The transient behavior of the electromagnetic ground wave on a spherical earth. *IRE Transactions on Antennas and Propagation*, AP-5: 198–202.

- Wait JR (1960) On the excitation of electromagnetic surface wave on a curved surface. *IRE Transactions on Antennas and Propagation*, AP-8: 445–449.
- Wait JR (1961) The electromagnetic fields of a horizontal dipole in the presence of a conducting half-space. *Canadian Journal of Physics*, 39: 1017–1027.
- Wait JR (1970) *Electromagnetic Waves in Stratified Media* (2nd, Ed.). New York, NY, USA: Pergamon Press.
- Wait JR (1964) Electromagnetic surface waves. In *Advanced in Radio Research*, 1: 157–217. New York, NY, USA: Academic Press.
- Wait JR and Hill DA (1979) Excitation of the HF surface wave by vertical and horizontal antennas. *Radio Science*, 14: 767–780.
- Wait JR (1998a) The ancient and modern history of EM ground-wave propagation. *IEEE Antennas Propagation Magazine*, 40(5): 7–24.
- Wait JR (1998b) Comment on “The electromagnetic field of a vertical electric dipole in the presence of a three-layered region” by Ronold W. P. King and Sheldon S. Sandler. *Radio Science*, 33(2): 251–253.
- Watson GN (1918) The diffraction of radio waves by the earth. *Proceedings of the Royal Society*, A95: 83–99.
- Weyl H (1919) The propagation of plane waves over a plane conductor. *Annalen der Physik*, 60: 481–500.
- Wu TT and King RWP (1984) Lateral waves: New formula for $E_{1\phi}$ and E_{1z} . *Radio Science*, 17: 532–538; (1984) Correction, 19: 1422.
- Wu TT and King RWP (1987) Lateral Electromagnetic pulses generated by a vertical electric dipole on the boundary between two dielectrics. *Journal of Applied Physics*, 62: 4543–4355.
- Zenneck J (1907) Propagation of plane electromagnetic waves along a plane conducting surface and its bearing on the theory of transmission in wireless telegraphy. *Annalen der Physik* (Leipzig), 23:846–866.
- Zhang HQ (2001) *Trapped surface wave and lateral wave along a planar conductor coated with a dielectric layer*. PhD dissertation, Xi’an, China: Chinese Academy of Science. (In Chinese)
- Zhang HQ, Pan WY, and Shen KX (2001) Electromagnetic field of a horizontal electric dipole over a perfect conductor covered with a dielectric layer. *Chinese Journal of Radio Science*, 16(3): 367–374. (In Chinese)
- Zhang HQ and Pan WY (2002) Electromagnetic field of a vertical electric dipole on a perfect conductor coated with a dielectric layer. *Radio Science*, 37(4), 1060, doi:1029/2000RS002348.
- Zhang HQ, Li K, and Pan WY (2004). The electromagnetic field of a vertical dipole on the dielectric-coated imperfect conductor. *Journal of Electromagnetic Waves and Applications*, 18(10): 1305–1320.
- Zhang HQ, Pan WY, Li K, and Shen KX (2005) Electromagnetic field for a horizontal electric dipole buried inside a dielectric layer coated high Lossy half space. *Progress In Electromagnetics Research*, PIER 50: 163–186. Cambridge, MA, USA: EMW Publishing.

Electromagnetic Field of a Vertical Electric Dipole in the Presence of a Three-Layered Region

In this chapter, the approximate formulas are derived for the electromagnetic field radiated by a vertical electric dipole in the presence of a three-layered region. In particular, both the trapped surface wave and the lateral wave are examined in detailed. Computations and discussions are carried out in several different cases. Furthermore, radiation patterns of the vertical dipole in the presence of a three-layered region are computed and discussed for a dielectric base with a wide range medium such as sea and lake water, wet and dry earth, and dry sand. When both the dipole and the observation point are on the surface of dielectric-coated Earth, the trapped surface wave is dominant.

2.1 Introduction

Almost a century ago, the electromagnetic field of a vertical electric dipole located in the boundary between two different media was first formulated by Sommerfeld (1909). The subsequent developments on the electromagnetic field of a dipole in layered region have been carried out by many investigators, especially including Wait and King. Many papers were published by Wait (1953; 1954; 1956; 1957) and well summarized in the book (Wait, 1970). In the early 1990's, King et al. obtained the approximate formulas for the electromagnetic fields radiated by vertical and horizontal electric dipoles in the presence of a three-layered region (King, 1991, 1993; King and Sandler, 1994).

In 1998, Wait wrote a comment on the paper by King and Sandler (1994) and it is claimed that the trapped surface wave, which varies as $\rho^{-1/2}$ in the far-field region, is missed in their solutions (Wait, 1998). Further works by Mahmoud (1999) and Collin (2004a; 2004b) support the conclusions reached by Wait (1998). To clarify the controversies on the trapped surface wave, the old problem was revisited again by several investigators in the past several years (Zhang and Pan, 2002; Zhang, Li, and Pan, 2004; Li and Lu, 2005; Liu and Li, 2007). It is demonstrated that the trapped surface wave can be

excited efficiently by vertical or horizontal electric dipole in the presence of a three-layered region.

In what follows, the electromagnetic field of a vertical electric dipole in the presence of a three-layered region is outlined in detail (Zhang and Pan, 2002; Zhang, Li, and Pan, 2004). The radiation patterns of the vertical dipole are obtained for the dielectric base with a wide range medium such as sea and lake water, wet and dry earth, and dry sand (Liu and Li, 2007).

2.2 The Integrated Formulas for Electromagnetic Field in Air

The relevant geometry and Cartesian coordinate system are shown in Fig. 2.1, where a vertical electric dipole in the \hat{z} direction is located at $(0, 0, d)$. Region 0 ($z \geq 0$) is the space above the dielectric layer with the air characterized by the permeability μ_0 and uniform permittivity ε_0 . Region 1 ($-l \leq z \leq 0$) is the dielectric layer characterized by the permeability μ_0 , relative permittivity ε_{r1} , and conductivity σ_1 . Region 2 ($z \leq -l$) is a perfect conductor or dielectric characterized by the permeability μ_0 , relative permittivity ε_{r2} , and conductivity σ_2 . The wave numbers in the three-layered region are

$$k_0 = \omega \sqrt{\mu_0 \varepsilon_0}, \quad (2.1)$$

$$k_j = \omega \sqrt{\mu_0 (\varepsilon_0 \varepsilon_{rj} + i\sigma_j/\omega)}; \quad j = 1, 2. \quad (2.2)$$

Maxwell's equations in the three-layered region are expressed by

$$\nabla \times \mathbf{E}_j = i\omega \mathbf{B}_j, \quad (2.3)$$

$$\nabla \times \mathbf{B}_j = \mu_0 (-i\omega \varepsilon_j \mathbf{E}_j + \hat{\mathbf{z}} J_z^e), \quad (2.4)$$

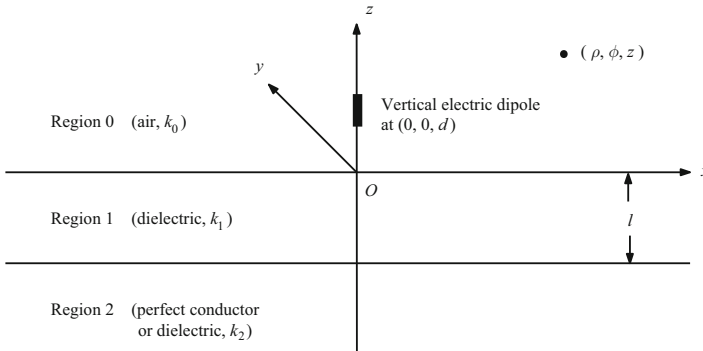


Fig. 2.1. The geometry of a vertical electric dipole on the surface of the perfect conductor or dielectric coated with a dielectric layer

where $j = 0, 1, 2$, and

$$J_z^e = \delta(x)\delta(y)\delta(z-d) \quad (2.5)$$

is the volume current density in the dipole.

Fourier transform of the form

$$\mathbf{E}(x, y, z) = \frac{1}{(2\pi)^2} \int_{-\infty}^{\infty} \int_{-\infty}^{\infty} e^{i(\xi x + \eta y)} \tilde{\mathbf{E}}(\xi, \eta, z) d\xi d\eta, \quad (2.6)$$

and similar transforms for $\mathbf{B}(x, y, z)$ and J_z^e are applied to Maxwell's equations. Thus,

$$\tilde{J}_z^e = \delta(z-d). \quad (2.7)$$

The transformed Maxwell's equations in Cartesian coordinates can be written in the following forms:

$$i\eta \tilde{E}_{jz} - \frac{\partial \tilde{E}_{jy}}{\partial z} = i\omega \tilde{B}_{jx}, \quad (2.8)$$

$$i\xi \tilde{E}_{jz} - \frac{\partial \tilde{E}_{jx}}{\partial z} = i\omega \tilde{B}_{jy}, \quad (2.9)$$

$$i\xi \tilde{E}_{jy} - i\eta \tilde{E}_{jx} = 0, \quad (2.10)$$

$$\frac{\partial \tilde{B}_{jy}}{\partial z} = i \frac{k_j^2}{\omega} \tilde{E}_{jx}, \quad (2.11)$$

$$\frac{\partial \tilde{B}_{jx}}{\partial z} = -i \frac{k_j^2}{\omega} \tilde{E}_{jy}, \quad (2.12)$$

$$i\xi \tilde{B}_{jy} - i\eta \tilde{B}_{jx} = -i \frac{k_j^2}{\omega} \tilde{E}_{jz} + \mu_0 \delta(z-d). \quad (2.13)$$

From Eqs. (2.8)~(2.10), it is seen that

$$\tilde{E}_{jy} = \frac{\eta}{\xi} \tilde{E}_{jx}, \quad (2.14)$$

$$\tilde{B}_{jy} = -\frac{\xi}{\eta} \tilde{B}_{jx}. \quad (2.15)$$

The substitution of Eqs. (2.14) and (2.15) into Eqs. (2.8) and (2.13) leads to the following ordinary equation for \tilde{B}_{jx} :

$$\left(\frac{d^2}{dz^2} + \gamma_j^2 \right) \tilde{B}_{jx} = -i\eta\mu_0\delta(z-d), \quad (2.16)$$

where

$$\gamma_j = \sqrt{k_j^2 - \xi^2 - \eta^2}; \quad j = 0, 1, 2. \quad (2.17)$$

It is noted that the imaginary part of the square root in Eq. (2.17) should be positive. The remaining components can be expressed in terms of \tilde{B}_{jx} . We write

$$\tilde{E}_{jx} = -i \frac{\omega}{k_j^2} \frac{\partial \tilde{B}_{jy}}{\partial z} = i \frac{\omega}{k_j^2} \frac{\xi}{\eta} \frac{\partial \tilde{B}_{jx}}{\partial z}, \quad (2.18)$$

$$\tilde{E}_{jy} = i \frac{\omega}{k_j^2} \frac{\partial \tilde{B}_{jx}}{\partial z}, \quad (2.19)$$

$$\tilde{E}_{jz} = \frac{\omega}{\eta k_j^2} \left(\frac{d^2}{dz^2} + k_j^2 \right) \tilde{B}_{jx}. \quad (2.20)$$

With the Sommerfeld radiation condition for $z \rightarrow \infty$, the solutions of Eq. (2.16) for \tilde{E}_{jx} ($j = 0, 1, 2$) are

$$\tilde{B}_{0x}(z) = C_1 e^{i\gamma_0 z} - \frac{\eta \mu_0}{2\gamma_0} e^{i\gamma_0 |z-d|}; \quad z \geq 0, \quad (2.21)$$

$$\tilde{B}_{1x}(z) = C_2 e^{-i\gamma_1 z} + C_3 e^{i\gamma_1 z}; \quad -l \leq z \leq 0, \quad (2.22)$$

$$\tilde{B}_{2x}(z) = C_4 e^{-i\gamma_2 z}; \quad z \leq -l. \quad (2.23)$$

On the boundary defined by $z = 0$, the conditions $\tilde{B}_{0x} = \tilde{B}_{1x}$ and $\tilde{E}_{0y} = \tilde{E}_{1y}$ obtain. With them, we write

$$C_1 - \frac{\eta \mu_0}{2\gamma_0} e^{-i\gamma_0 d} = C_2 + C_3, \quad (2.24)$$

$$\frac{\gamma_0}{k_0^2} \left(C_1 + \frac{\eta \mu_0}{2\gamma_0} e^{i\gamma_0 d} \right) = \frac{\gamma_1}{k_1^2} (-C_2 + C_3). \quad (2.25)$$

Similarly, on the boundary $z = -l$, $\tilde{B}_{1x} = \tilde{B}_{2x}$ and $\tilde{E}_{1y} = \tilde{E}_{2y}$. Thus,

$$C_2 e^{i\gamma_1 l} + C_3 e^{-i\gamma_1 l} = C_4 e^{i\gamma_2 l}, \quad (2.26)$$

$$\frac{\gamma_0}{k_0^2} \left(C_1 + \frac{\eta \mu_0}{2\gamma_0} e^{i\gamma_0 d} \right) = \frac{\gamma_1}{k_1^2} (-C_2 + C_3). \quad (2.27)$$

These equations with Eqs. (2.24) and (2.25) lead to

$$C_1 = \frac{\eta \mu_0}{2\gamma_0} e^{i\gamma_0 d} Q, \quad (2.28)$$

where

$$Q = - \frac{\frac{\gamma_0}{k_0^2} - \frac{\gamma_2}{k_2^2} - i \left(\frac{k_1^2 \gamma_0 \gamma_2}{k_0^2 k_2^2 \gamma_1} - \frac{\gamma_1}{k_1^2} \right) \tan(\gamma_1 l)}{\frac{\gamma_0}{k_0^2} + \frac{\gamma_2}{k_2^2} - i \left(\frac{k_1^2 \gamma_0 \gamma_2}{k_0^2 k_2^2 \gamma_1} + \frac{\gamma_1}{k_1^2} \right) \tan(\gamma_1 l)}. \quad (2.29)$$

Then, we have

$$\tilde{B}_{0x} = -\eta\mu_0 \frac{1}{2\gamma_0} \left[e^{i\gamma_0|z-d|} - Qe^{i\gamma_0(z+d)} \right], \quad (2.30)$$

$$\tilde{B}_{0y} = -\frac{\xi}{\eta} \tilde{B}_{0x} = \xi\mu_0 \frac{1}{2\gamma_0} \left[e^{i\gamma_0|z-d|} - Qe^{i\gamma_0(z+d)} \right], \quad (2.31)$$

$$\tilde{B}_{0z} = 0, \quad (2.32)$$

$$\tilde{E}_{0x} = -i \frac{\omega}{k_0^2} \frac{\partial \tilde{B}_{0y}}{\partial z} = \frac{\omega\xi\mu_0}{k_0^2} \left[\mp \frac{1}{2} e^{i\gamma_0|z-d|} + Qe^{i\gamma_0(z+d)} \right], \quad (2.33)$$

$$\tilde{E}_{0y} = \frac{\omega\eta\mu_0}{k_0^2} \left[\mp \frac{1}{2} e^{i\gamma_0|z-d|} + Qe^{i\gamma_0(z+d)} \right], \quad (2.34)$$

$$\tilde{E}_{0z} = \frac{\omega\mu_0(\xi^2 + \eta^2)}{2k_0^2} \frac{1}{\gamma_0} \left[e^{i\gamma_0|z-d|} - Qe^{i\gamma_0(z+d)} \right]. \quad (2.35)$$

These formulas can now be expressed in the cylindrical coordinates ρ, ϕ, z with the relations

$$x = \rho \cos \phi; \quad y = \rho \sin \phi; \quad \rho^2 = x^2 + y^2, \quad (2.36)$$

$$\xi = \lambda \cos \phi'; \quad \eta = \lambda \sin \phi'; \quad \lambda^2 = \xi^2 + \eta^2, \quad (2.37)$$

and the integral representations of the Bessel functions J_0 and J_1 , viz.,

$$J_0(\lambda\rho) = \frac{1}{2\pi} \int_0^{2\pi} e^{i\lambda\rho \cos(\phi-\phi')} d\phi', \quad (2.38)$$

$$J_1(\lambda\rho) = -\frac{i}{2\pi} \int_0^{2\pi} e^{i\lambda\rho \cos(\phi-\phi')} \cos(\phi-\phi') d\phi', \quad (2.39)$$

the final formulas are expressed in the following forms:

$$B_{0\phi}(\rho, z) = -\frac{i\mu_0}{4\pi} \int_0^\infty \left[e^{i\gamma_0|z-d|} - Qe^{i\gamma_0(z+d)} \right] J_1(\lambda\rho) \gamma_0^{-1} \lambda^2 d\lambda, \quad (2.40)$$

$$E_{0\rho}(\rho, z) = -\frac{i\omega\mu_0}{4\pi k_0^2} \int_0^\infty \left[\pm e^{i\gamma_0|z-d|} - Qe^{i\gamma_0(z+d)} \right] J_1(\lambda\rho) \lambda^2 d\lambda; \quad (2.41)$$

$$d < z \\ 0 \leq z \leq d,$$

$$E_{0z}(\rho, z) = -\frac{\omega\mu_0}{4\pi k_0^2} \int_0^\infty \left[e^{i\gamma_0|z-d|} - Qe^{i\gamma_0(z+d)} \right] J_1(\lambda\rho) \gamma_0^{-1} \lambda^3 d\lambda. \quad (2.42)$$

2.3 Field of Vertical Dipole over Dielectric-Coated Perfect Conductor

In this section, we will examine the electromagnetic field of a vertical electric dipole in air over a dielectric-coated perfect conductor.

2.3.1 Integrated Formulas of the Electromagnetic Field in Air

If Region 2 is occupied by a perfect conductor, $k_2 \rightarrow \infty$, the integrated formulas of the electromagnetic field due to a vertical electric dipole in the presence of a three-layered region are written in the forms

$$B_{0\phi} = \frac{i\mu_0}{4\pi} \int_0^\infty \left[e^{i\gamma_0|z-d|} + e^{i\gamma_0(z+d)} - (Q+1)e^{i\gamma_0(z+d)} \right] \gamma_0^{-1} J_1(\lambda\rho) \lambda^2 d\lambda, \quad (2.43)$$

$$E_{0\rho} = \frac{i\omega\mu_0}{4\pi k_0^2} \int_0^\infty \left[\pm e^{i\gamma_0|z-d|} + e^{i\gamma_0(z+d)} - (Q+1)e^{i\gamma_0(z+d)} \right] J_1(\lambda\rho) \lambda^2 d\lambda; \quad \begin{matrix} d < z \\ 0 \leq z \leq d \end{matrix}, \quad (2.44)$$

$$E_{0z} = \frac{-\omega\mu_0}{4\pi k_0^2} \int_0^\infty \left[e^{i\gamma_0|z-d|} + e^{i\gamma_0(z+d)} - (Q+1)e^{i\gamma_0(z+d)} \right] \gamma_0^{-1} J_0(\lambda\rho) \lambda^3 d\lambda, \quad (2.45)$$

where the reflection coefficient is expressed in the form

$$Q = -\frac{k_1^2\gamma_0 + ik_0^2\gamma_1 \tan(\gamma_1 l)}{k_1^2\gamma_0 - ik_0^2\gamma_1 \tan(\gamma_1 l)}, \quad (2.46)$$

and

$$\gamma_j = \sqrt{k_j^2 - \lambda^2}; \quad j = 0, 1. \quad (2.47)$$

The first and second terms in Eqs. (2.43)~(2.45) stand for the direct wave and the ideal reflected wave, respectively. The two terms have been evaluated in the book by King, Owens, and Wu (1992). Then, we write

$$B_{0\phi} = B_{0\phi}^{(1)} + B_{0\phi}^{(2)} + B_{0\phi}^{(3)}, \quad (2.48)$$

$$E_{0\rho} = E_{0\rho}^{(1)} + E_{0\rho}^{(2)} + E_{0\rho}^{(3)}, \quad (2.49)$$

$$E_{0z} = E_{0z}^{(1)} + E_{0z}^{(2)} + E_{0z}^{(3)}, \quad (2.50)$$

where

$$B_{0\phi}^{(1)} = -\frac{\mu_0}{4\pi} e^{ik_0 r_1} \left(\frac{\rho}{r_1} \right) \left(\frac{ik_0}{r_1} - \frac{1}{r_1^2} \right), \quad (2.51)$$

$$B_{0\phi}^{(2)} = -\frac{\mu_0}{4\pi} e^{ik_0 r_2} \left(\frac{\rho}{r_2} \right) \left(\frac{ik_0}{r_2} - \frac{1}{r_2^2} \right), \quad (2.52)$$

$$E_{0\rho}^{(1)} = -\frac{\omega\mu_0}{4\pi k_0} e^{ik_0 r_1} \left(\frac{\rho}{r_1} \right) \left(\frac{z-d}{r_1} \right) \left(\frac{ik_0}{r_1} - \frac{3}{r_1^2} - \frac{3i}{k_0 r_1^3} \right), \quad (2.53)$$

$$E_{0\rho}^{(2)} = -\frac{\omega\mu_0}{4\pi k_0} e^{ik_0 r_2} \left(\frac{\rho}{r_2} \right) \left(\frac{z+d}{r_2} \right) \left(\frac{ik_0}{r_2} - \frac{3}{r_2^2} - \frac{3i}{k_0 r_2^3} \right), \quad (2.54)$$

$$E_{0z}^{(1)} = \frac{\omega\mu_0}{4\pi k_0} e^{ik_0 r_1} \left[\frac{ik_0}{r_1} - \frac{1}{r_1^2} - \frac{i}{k_0 r_1^3} \left(\frac{z-d}{r_1} \right)^2 \left(\frac{ik_0}{r_1} - \frac{3}{r_1^2} - \frac{3i}{k_0 r_1^3} \right) \right], \quad (2.55)$$

$$E_{0z}^{(2)} = \frac{\omega\mu_0}{4\pi k_0} e^{ik_0 r_2} \left[\frac{ik_0}{r_2} - \frac{1}{r_2^2} - \frac{i}{k_0 r_2^3} \left(\frac{z+d}{r_2} \right)^2 \left(\frac{ik_0}{r_2} - \frac{3}{r_2^2} - \frac{3i}{k_0 r_2^3} \right) \right]. \quad (2.56)$$

In these formulas, $r_1 = \sqrt{\rho^2 + (z-d)^2}$ and $r_2 = \sqrt{\rho^2 + (z+d)^2}$. Since γ_0 and γ_1 are even functions of λ , and use is made of the relations between Bessel function and Hankel function

$$J_n(\lambda\rho) = \frac{1}{2} \left[H_n^{(1)}(\lambda\rho) + H_n^{(2)}(\lambda\rho) \right], \quad (2.57)$$

$$H_n^{(1)}(-\lambda\rho) = H_n^{(2)}(\lambda\rho)(-1)^{n+1}, \quad (2.58)$$

it follows that

$$B_{0\phi}^{(3)} = -\frac{k_0^2 \mu_0}{4\pi} \int_{-\infty}^{+\infty} \frac{\tan(\gamma_1 l) \gamma_1 H_1^{(1)}(\lambda\rho) e^{i\gamma_0(z+d)} \lambda^2}{[k_1^2 \gamma_0 - ik_0^2 \gamma_1 \tan(\gamma_1 l)] \gamma_0} d\lambda, \quad (2.59)$$

$$E_{0\rho}^{(3)} = -\frac{\omega\mu_0}{4\pi} \int_{-\infty}^{+\infty} \frac{\gamma_1 \tan(\gamma_1 l) H_1^{(1)}(\lambda\rho) e^{i\gamma_0(z+d)} \lambda^2}{k_1^2 \gamma_0 - ik_0^2 \gamma_1 \tan(\gamma_1 l)} d\lambda, \quad (2.60)$$

$$E_{0z}^{(3)} = -\frac{i\omega\mu_0}{4\pi} \int_{-\infty}^{+\infty} \frac{\gamma_1 \tan(\gamma_1 l) H_0^{(1)}(\lambda\rho) e^{i\gamma_0(z+d)} \lambda^3}{[k_1^2 \gamma_0 - ik_0^2 \gamma_1 \tan(\gamma_1 l)] \gamma_0} d\lambda. \quad (2.61)$$

Because of the high oscillatory of the Bessel functions $J_i(\lambda\rho)$ or Hankel functions $H_i^{(1)}(\lambda\rho)$ ($j = 0, 1$), the above three integrals converge very slowly. In what follows, we will evaluate the above three integrals by using analytical techniques.

2.3.2 Evaluations of Trapped Surface Wave and Lateral Wave

In order to evaluate the three integrals in Eqs. (2.59)~(2.61), it is necessary to shift the contour around the branch cuts at $\lambda = k_0$ and $\lambda = k_1$. The configuration of the poles and branch cuts is shown in Fig. 2.2. In the next step, it is necessary to determine the poles and to evaluate the integrations along the branch lines Γ_0 and Γ_1 . Let us examine the following equation:

$$q(\lambda) = k_1^2 \gamma_0 - i k_0^2 \gamma_1 \tan(\gamma_1 l) = 0. \quad (2.62)$$

Obviously, the roots of Eq. (2.62) are the poles of the integrand function.

Assuming that λ is real, and $k_0 < \lambda < k_1$, γ_0 is a positive imaginary number while γ_1 is a positive real number. Let

$$f(\lambda) = \frac{k_1^2 \sqrt{k_0^2 - \lambda^2}}{i k_0^2 \sqrt{k_1^2 - \lambda^2}}, \quad (2.63)$$

and

$$g(\lambda) = \tan \left(\sqrt{k_1^2 - \lambda^2} l \right), \quad (2.64)$$

it is seen that $f(\lambda)$ and $g(\lambda)$ are positive real numbers. We find $f(\lambda)|_{\lambda=k_0} = 0$ and $f(\lambda)|_{\lambda=k_1} = \infty$.

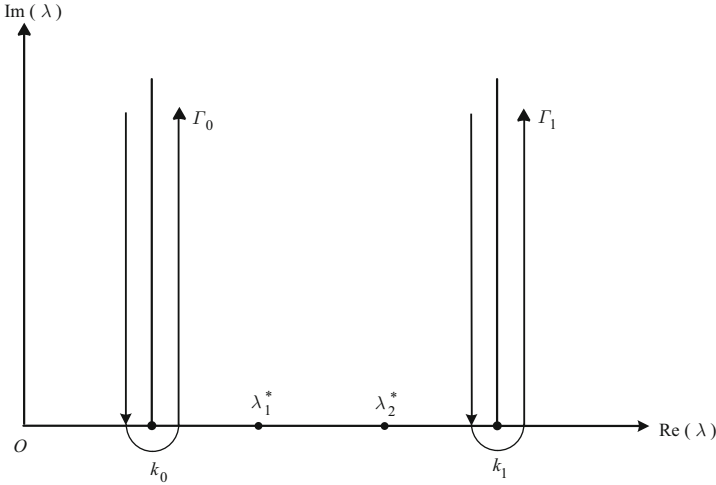


Fig. 2.2. The configuration of the poles and the branch lines

In the case of $\sqrt{k_1^2 - k_0^2} l < \pi/2$, $g(\lambda)$ decreases monotonously from $\tan(\sqrt{k_1^2 - \lambda^2} l)$ to zero as λ increases from k_0 to k_1 . As shown in Fig. 2.3, there is one intersection λ_1^* in the range of $k_0 < \lambda < k_1$ between the two functions $f(\lambda)$ and $g(\lambda)$. That is to say, Eq. (2.62) have only one root in the range of $k_0 < \lambda < k_1$.

In the case of $\pi/2 < \sqrt{k_1^2 - k_0^2} l < \pi$, if λ increases from k_0 to k_1 , $g(\lambda)$ decreases monotonously from a negative value $\tan \sqrt{k_1^2 - k_0^2} l$ to $-\infty$ in the beginning and from $+\infty$ to zero after $\gamma_1 l = \pi/2$. As shown in Fig. 2.4, there is also one intersection λ_1^* in the range of $k_0 < \lambda < k_1$ between $f(\lambda)$ and $g(\lambda)$. Obviously, Eq. (2.62) has only one root in the range of $\pi/2 < \sqrt{k_1^2 - k_0^2} l < \pi$.

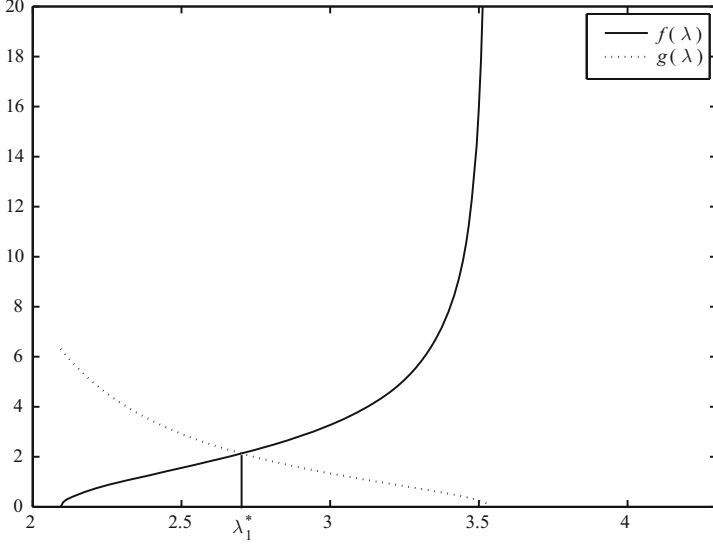


Fig. 2.3. Root of Eq. (2.62) for $f = 100$ MHz, $\varepsilon_{r1} = 2.85$, $\sqrt{k_1^2 - k_0^2}l = 0.45\pi$

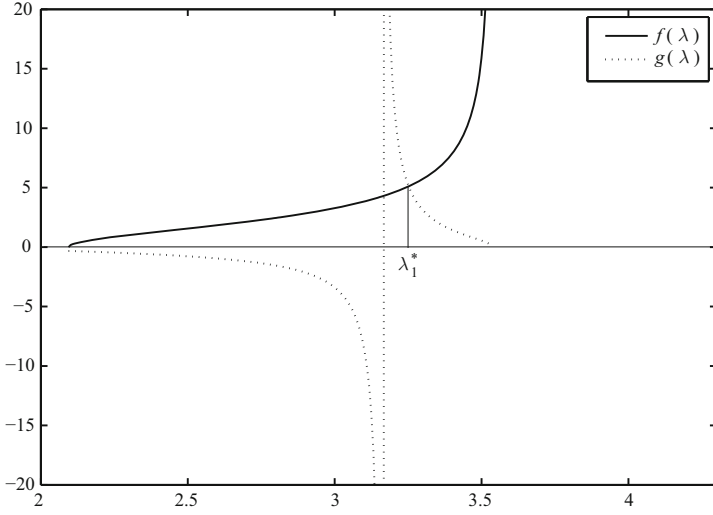


Fig. 2.4. Root of Eq. (2.62) for $f = 100$ MHz, $\varepsilon_{r1} = 2.85$, $\sqrt{k_1^2 - k_0^2}l = 0.90\pi$

When $\pi < \sqrt{k_1^2 - k_0^2}l < 2\pi$, Eq. (2.62) have two roots λ_1^* and λ_2^* , which are shown in Figs. 2.5 and 2.6, respectively. Generally, when $n\pi < \sqrt{k_1^2 - k_0^2}l < (n+1)\pi$, Eq. (2.62) will have $(n+1)$ roots. Correspondingly, there are $(n+1)$ poles for the integrand function.

As shown in Fig. 2.2, there are two branch cuts at $\lambda = k_0$ and $\lambda = k_1$. In the two sides of the branch line Γ_0 , the phase of γ_0 changes from $e^{-i\pi/4}$ to $e^{i3\pi/4}$, and γ_1 has the same values on the two sides of the branch line Γ_1 . It is easily verified that the evaluations of the integrals in Eqs. (2.59)~(2.61) along the branch line Γ_1 are zero. Then, we rewrite the integral in Eq. (2.59) in the following form:

$$B_{0\phi}^{(3)} = -\frac{2\pi i k_0^2 \mu_0}{4\pi} \sum_j \frac{\tan(\gamma_1(\lambda_j^*)l) \gamma_1(\lambda_j^*) \lambda_j^{*2}}{q'(\lambda_j^*) \gamma_0(\lambda_j^*)} e^{i\gamma_0(\lambda_j^*)(z+d)} H_1^{(1)}(\lambda_j^* \rho) - \frac{k_0^2 \mu_0}{4\pi} \int_{\Gamma_0} \frac{\tan(\gamma_1 l) \gamma_1 H_1^{(1)}(\lambda \rho) e^{i\gamma_0(z+d)}}{q(\lambda) \gamma_0} \lambda^2 d\lambda, \quad (2.65)$$

where

$$q(\lambda) = k_1^2 \gamma_0 - i k_0^2 \gamma_1 \tan(\gamma_1 l), \quad (2.66)$$

$$q'(\lambda) = -\frac{k_1^2 \lambda}{\gamma_0} + \frac{i k_0^2 \lambda}{\gamma_1} \tan(\gamma_1 l) + i k_0^2 \lambda l \sec^2(\gamma_1 l). \quad (2.67)$$

It is noted that the first term in Eq. (2.65) is the sum of residues of all poles. If the thickness of the dielectric layer satisfies the condition $n\pi < \sqrt{k_1^2 - k_0^2}l < (n+1)\pi$, there exists $n+1$ poles.

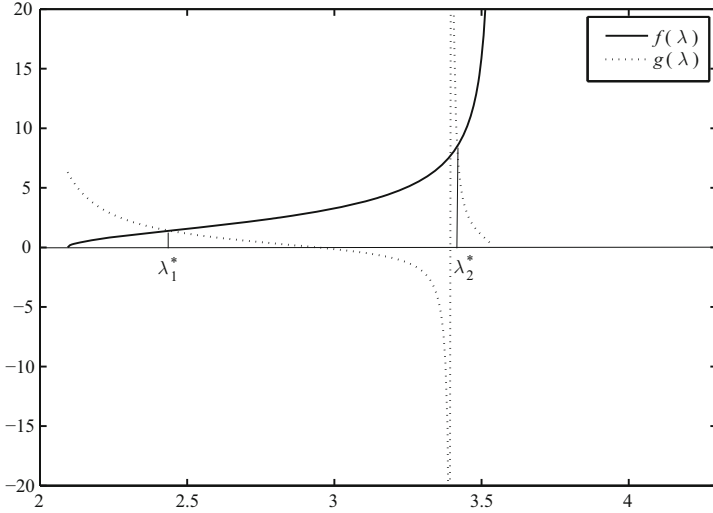


Fig. 2.5. Root of Eq. (2.62) for $f = 100$ MHz, $\varepsilon_{r1} = 2.85$, $\sqrt{k_1^2 - k_0^2}l = 1.4\pi$

Taking into account the far-field condition $k_0 \rho \gg 1$ and $(z+d) \ll \rho$, the dominant contribution of the integral along the branch line Γ_0 comes from the vicinity of k_0 . Let $\lambda = k_0(1 + i\tau^2)$, we have

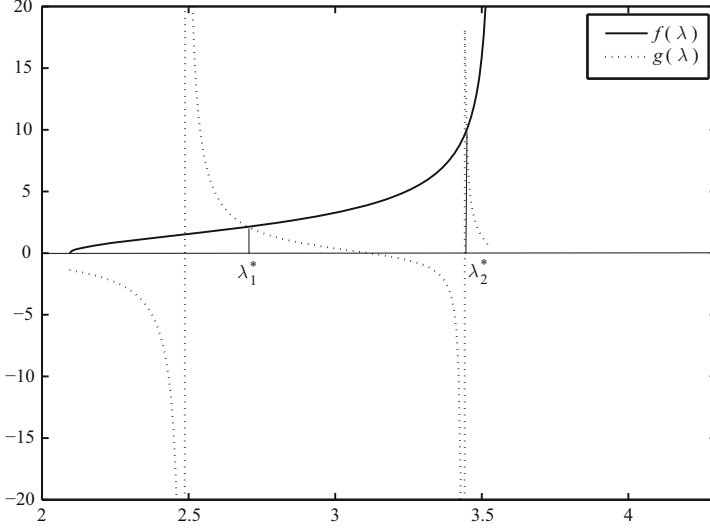


Fig. 2.6. Root of Eq. (2.62) for $f = 100$ MHz, $\varepsilon_{r1} = 2.85$, $\sqrt{k_1^2 - k_0^2}l = 1.7\pi$

$$\gamma_0 = \sqrt{k_0^2 - \lambda^2} \approx k_0 e^{i\frac{3}{4}\pi} \sqrt{2}\tau, \quad (2.68)$$

$$\gamma_1 = \sqrt{k_1^2 - \lambda^2} \approx \sqrt{k_1^2 - k_0^2}, \quad (2.69)$$

and

$$H_1^{(1)}(\lambda\rho) \approx \sqrt{\frac{2}{\pi k_0 \rho}} e^{i(k_0 \rho - \frac{3}{4}\pi)} e^{-k_0 \rho \tau^2}. \quad (2.70)$$

Then, the integral in Eq. (2.65) is written in the form

$$\begin{aligned} \int_{\Gamma_0} \frac{\tan \gamma_1 l \gamma_1 H_1^{(1)}(\lambda\rho) e^{i\gamma_0(z+d)}}{q(\lambda)\gamma_0} \lambda^2 d\lambda &\approx \frac{k_0 \sqrt{k_1^2 - k_0^2}}{k_1^2} \tan \sqrt{k_1^2 - k_0^2} l \sqrt{\frac{2}{\pi k_0 \rho}} \\ &\times e^{i(k_0 \rho + \frac{\pi}{4})} \int_{-\infty}^{+\infty} \frac{e^{-k_0 \rho t^2}}{t - e^{i\pi/4} \Delta} dt, \end{aligned} \quad (2.71)$$

where

$$\Delta = \frac{1}{\sqrt{2}} \left(\frac{z+d}{\rho} - i \frac{k_0 \sqrt{k_1^2 - k_0^2}}{k_1^2} \tan \sqrt{k_1^2 - k_0^2} l \right). \quad (2.72)$$

From Eq. (3.466) in the mathematics handbook by Gradshteyn and Ryzhik (1980), the integral in Eq. (2.71) is expressed in the form

$$\int_{-\infty}^{\infty} \frac{e^{-k_0 \rho t^2}}{t - e^{i\frac{\pi}{4}} \Delta} dt = i\pi e^{-i\Delta^2 k_0 \rho} \operatorname{erfc} \left(\sqrt{-i\Delta^2 k_0 \rho} \right). \quad (2.73)$$

Here the phase of $\sqrt{-i\Delta^2 k_0 \rho}$ in Eq. (2.73) should be satisfied by the condition

$$|\operatorname{Arg} \sqrt{-i\Delta^2 k_0 \rho}| \leq \frac{\pi}{4}, \quad (2.74)$$

and the error function is defined by

$$\operatorname{erfc}(x) = \frac{2}{\sqrt{\pi}} \int_x^\infty e^{-t^2} dt. \quad (2.75)$$

Let

$$p^* = \frac{k_0 \rho}{2} \left(\frac{z+d}{\rho} - i \frac{k_0 \sqrt{k_1^2 - k_0^2}}{k_1^2} \tan \sqrt{k_1^2 - k_0^2} l \right)^2, \quad (2.76)$$

we have

$$\operatorname{erfc}(\sqrt{-ip^*}) = \frac{2}{\sqrt{\pi}} \int_{\sqrt{-ip^*}}^\infty e^{-t^2} dt = \sqrt{2} e^{-i\frac{\pi}{4}} F(p^*), \quad (2.77)$$

where Fresnel integral is defined by

$$F(p^*) = \frac{1}{2}(1+i) - \int_0^{p^*} \frac{e^{it}}{\sqrt{2\pi t}} dt. \quad (2.78)$$

Therefore, the result becomes

$$\begin{aligned} B_{0\phi}^{(3)} = & \mu_0 k_0^2 \sqrt{\frac{1}{2\pi\rho}} e^{i\frac{3\pi}{4}} \sum_j \frac{\gamma_1(\lambda_j^*) \tan(\gamma_1(\lambda_j^*)l)}{q'(\lambda_j^*) \gamma_0(\lambda_j^*)} (\lambda_j^*)^{3/2} e^{i\gamma_0(\lambda_j^*)(z+d) + i\lambda_j^* \rho} \\ & - \frac{k_0^3 \mu_0 \sqrt{k_1^2 - k_0^2}}{2k_1^2} \sqrt{\frac{1}{\pi k_0 \rho}} \tan\left(\sqrt{k_1^2 - k_0^2} l\right) e^{i(k_0 r_2 + \frac{\pi}{2})} e^{-ip^*} F(p^*). \end{aligned} \quad (2.79)$$

With similar manner, it is obtained readily.

$$\begin{aligned} E_{0\rho}^{(3)} = & -\omega \mu_0 \sqrt{\frac{1}{2\pi\rho}} e^{i\frac{\pi}{4}} \sum_j \frac{\gamma_1(\lambda_j^*) \tan(\gamma_1(\lambda_j^*)l)}{q'(\lambda_j^*)} (\lambda_j^*)^{3/2} e^{i\gamma_0(\lambda_j^*)(z+d) + i\lambda_j^* \rho} \\ & + \frac{\omega k_0^2 \mu_0}{2k_1^2} \sqrt{\frac{1}{\pi k_0 \rho}} \sqrt{k_1^2 - k_0^2} \tan\left(\sqrt{k_1^2 - k_0^2} l\right) e^{ik_0 r_2} \\ & \times \left[\sqrt{\frac{\pi}{k_0 \rho}} + \frac{\pi k_0 \sqrt{k_1^2 - k_0^2}}{k_1^2} \tan\left(\sqrt{k_1^2 - k_0^2} l\right) e^{-ip^*} F(p^*) \right], \end{aligned} \quad (2.80)$$

and

$$\begin{aligned} E_{0z}^{(3)} = & -\omega \mu_0 \sqrt{\frac{1}{2\pi\rho}} e^{i\frac{3\pi}{4}} \sum_j \frac{\gamma_1(\lambda_j^*) \tan(\gamma_1(\lambda_j^*)l)}{q'(\lambda_j^*) \gamma_0(\lambda_j^*)} (\lambda_j^*)^{5/2} e^{i\gamma_0(\lambda_j^*)(z+d) + i\lambda_j^* \rho} \\ & + \frac{\omega k_0^2 \mu_0}{2k_1^2} \sqrt{\frac{1}{\pi k_0 \rho}} \sqrt{k_1^2 - k_0^2} \tan\left(\sqrt{k_1^2 - k_0^2} l\right) e^{i(k_0 r_2 + \frac{\pi}{2})} e^{-ip^*} F(p^*). \end{aligned} \quad (2.81)$$

2.3.3 Final Formulas for the Electromagnetic Field Components

By using the above obtained results and the available results of the direct wave and the ideal reflected wave in the book (King, Owen, and Wu, 1992), the final formulas of the three components $B_{0\phi}$, $E_{0\rho}$, and E_{0z} are obtained readily. They are

$$\begin{aligned}
 B_{0\phi}(\rho, z) = & -\frac{\mu_0}{4\pi} e^{ik_0 r_1} \left(\frac{\rho}{r_1} \right) \left(\frac{ik_0}{r_1} - \frac{1}{r_1^2} \right) - \frac{\mu_0}{4\pi} e^{ik_0 r_2} \left(\frac{\rho}{r_2} \right) \left(\frac{ik_0}{r_2} - \frac{1}{r_2^2} \right) \\
 & + \mu_0 k_0^2 \sqrt{\frac{1}{2\pi\rho}} e^{i\frac{3\pi}{4}} \sum_j \frac{\gamma_1(\lambda_j^*) \tan(\gamma_1(\lambda_j^*)l)}{q'(\lambda_j^*) \gamma_0(\lambda_j^*)} (\lambda_j^*)^{3/2} e^{i\gamma_0(\lambda_j^*)(z+d) + i\lambda_j^* \rho} \\
 & - \frac{k_0^3 \mu_0 \sqrt{k_1^2 - k_0^2}}{2k_1^2} \sqrt{\frac{1}{\pi k_0 \rho}} \tan\left(\sqrt{k_1^2 - k_0^2} l\right) e^{i(k_0 r_2 + \frac{\pi}{2})} e^{-ip^*} F(p^*), \quad (2.82)
 \end{aligned}$$

$$\begin{aligned}
 E_{0\rho}(\rho, z) = & -\frac{\omega\mu_0}{4\pi k_0} e^{ik_0 r_1} \left(\frac{\rho}{r_1} \right) \left(\frac{z-d}{r_1} \right) \left(\frac{ik_0}{r_1} - \frac{3}{r_1^2} - \frac{3i}{k_0 r_1^3} \right) \\
 & - \frac{\omega\mu_0}{4\pi k_0} e^{ik_0 r_2} \left(\frac{\rho}{r_2} \right) \left(\frac{z+d}{r_2} \right) \left(\frac{ik_0}{r_2} - \frac{3}{r_2^2} - \frac{3i}{k_0 r_2^3} \right) \\
 & - \omega\mu_0 \sqrt{\frac{1}{2\pi\rho}} e^{i\frac{\pi}{4}} \sum_j \frac{\gamma_1(\lambda_j^*) \tan(\gamma_1(\lambda_j^*)l)}{q'(\lambda_j^*)} (\lambda_j^*)^{3/2} e^{i\gamma_0(\lambda_j^*)(z+d) + i\lambda_j^* \rho} \\
 & + \frac{\omega k_0^2 \mu_0}{2k_1^2} \sqrt{\frac{1}{\pi k_0 \rho}} \sqrt{k_1^2 - k_0^2} \tan\left(\sqrt{k_1^2 - k_0^2} l\right) e^{ik_0 r_2} \\
 & \times \left[\sqrt{\frac{\pi}{k_0 \rho}} + \frac{\pi k_0 \sqrt{k_1^2 - k_0^2}}{k_1^2} \tan\left(\sqrt{k_1^2 - k_0^2} l\right) e^{-ip^*} F(p^*) \right], \quad (2.83)
 \end{aligned}$$

$$\begin{aligned}
 E_{0z}(\rho, z) = & \frac{\omega\mu_0}{4\pi k_0} e^{ik_0 r_1} \left[\frac{ik_0}{r_1} - \frac{1}{r_1^2} - \frac{i}{k_0 r_1^3} - \left(\frac{z-d}{r_1} \right)^2 \left(\frac{ik_0}{r_1} - \frac{3}{r_1^2} - \frac{3i}{k_0 r_1^3} \right) \right] \\
 & + \frac{\omega\mu_0}{4\pi k_0} e^{ik_0 r_2} \left[\frac{ik_0}{r_2} - \frac{1}{r_2^2} - \frac{i}{k_0 r_2^3} - \left(\frac{z+d}{r_2} \right)^2 \left(\frac{ik_0}{r_2} - \frac{3}{r_2^2} - \frac{3i}{k_0 r_2^3} \right) \right] \\
 & - \omega\mu_0 \sqrt{\frac{1}{2\pi\rho}} e^{i\frac{3\pi}{4}} \sum_j \frac{\gamma_1(\lambda_j^*) \tan(\gamma_1(\lambda_j^*)l)}{q'(\lambda_j^*) \gamma_0(\lambda_j^*)} (\lambda_j^*)^{5/2} e^{i\gamma_0(\lambda_j^*)(z+d) + i\lambda_j^* \rho} \\
 & + \frac{\omega k_0^2 \mu_0}{2k_1^2} \sqrt{\frac{1}{\pi k_0 \rho}} \sqrt{k_1^2 - k_0^2} \tan\left(\sqrt{k_1^2 - k_0^2} l\right) e^{i(k_0 r_2 + \frac{\pi}{2})} e^{-ip^*} F(p^*). \quad (2.84)
 \end{aligned}$$

From the above formulas, it is seen that the total field includes the following four modes: the direct wave, the ideal reflected wave, the trapped surface wave, and the lateral wave.

2.3.4 Computations and Discussions

From the final formulas Eqs. (2.82)~(2.84) of the electromagnetic field, it is seen that the term of the trapped surface wave is determined by the sum of residues of the poles. When $k_0 < \lambda_j^* < k_1$, $\gamma_0(\lambda_j^*) = i\sqrt{\lambda_j^{*2} - k_0^2}$ is always a positive imaginary number, the terms including the factor $e^{i\gamma_{0j}^* z}$ will attenuate exponentially as $e^{-\sqrt{\lambda_j^{*2} - k_0^2} z}$ in the \hat{z} direction. It is seen that the trapped-surface-wave terms in Eqs. (2.82)~(2.84) will decrease exponentially in the \hat{z} direction when the dipole or the observation point moves away the air-dielectric boundary. When both the dipole and the observation point are on or close to the boundary, the amplitude of the trapped surface wave attenuates as $\rho^{-1/2}$ in the $\hat{\rho}$ direction.

The wave numbers of the trapped surface waves, being in the range from k_0 to k_1 , depend on the operating frequency f , the relative permittivity ε_{r1} , and the thickness l of the dielectric layer. In Figs. 2.7 and 2.8, it is shown that the first pole λ_1^* varies with the thickness l of the dielectric layer. If the dielectric layer is a lossy medium, the wave number k_1 of the dielectric layer is not a pure real number, and it has a positive imaginary part. The roots of (2.62), which are not pure real numbers, can be obtained by using Newton's iteration method. The imaginary parts of λ_1^*/k_0 varying as the thickness l of the dielectric layer are computed and shown in Figs. 2.9 and 2.10.

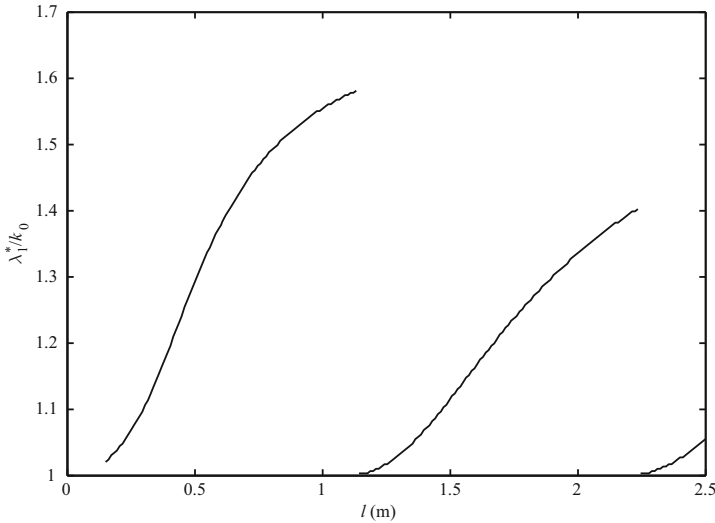


Fig. 2.7. The first root λ_1^* of Eq. (2.62) versus the thickness l of the dielectric layer: $f = 100$ MHz, $\varepsilon_{r1} = 2.85$

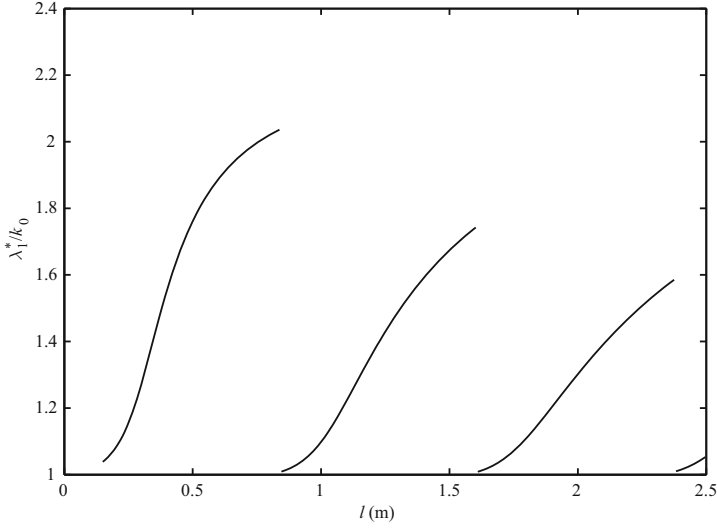


Fig. 2.8. The first root λ_1^* of Eq. (2.62) versus the thickness l of the dielectric layer: $f = 100$ MHz, $\varepsilon_{r1} = 4.85$

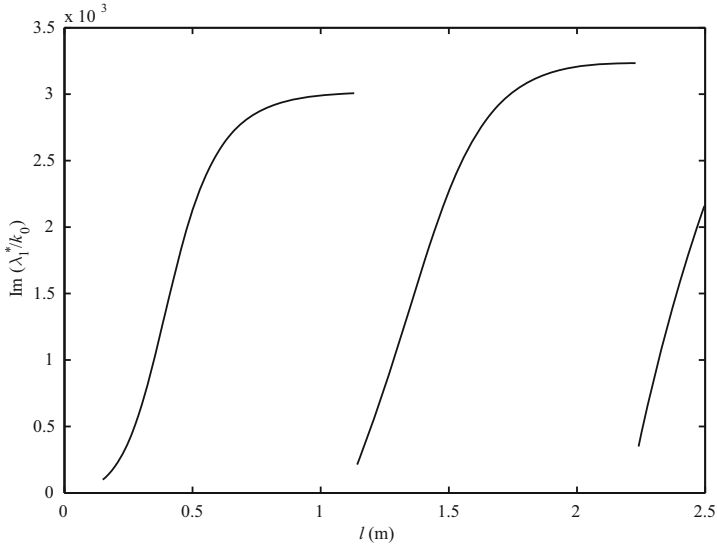


Fig. 2.9. The imaginary part of λ_1^*/k_0 versus the thickness l of the dielectric layer: $f = 100$ MHz, $\varepsilon_{r1} = 2.85 + 0.001i$

If the dielectric layer is thin, viz., $k_1 l \leq 0.6$, and subject to the condition $k_1^2 \gg k_0^2$, the second terms in Eqs. (2.79)~(2.81) coincide with the lateral-

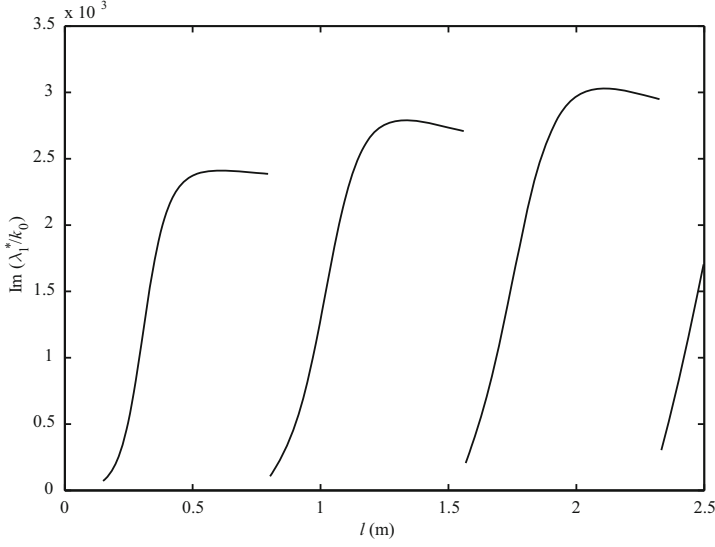


Fig. 2.10. The imaginary part of λ_1^*/k_0 versus the thickness l of the dielectric layer: $f = 100$ MHz, $\varepsilon_{r1} = 4.85 + 0.001i$

wave terms addressed in the paper by King and Sandler (1994). In this case, the parameter p^* can be simplified as

$$p^* \approx \frac{k_0 \rho}{2} \left(\frac{z+d}{\rho} - ik_0 l \right)^2 \approx \frac{k_0 r_2}{2} \left(\frac{z+d+\varepsilon r_2}{\rho} \right)^2 = p \quad (2.85)$$

where $\varepsilon = -ik_0 l$ and p are given in the paper by King and Sandler (1994). Then, the second term in Eq. (2.79) reduces to

$$\frac{-ik_0^3 l \mu_0}{2} \sqrt{\frac{1}{\pi k_0 \rho}} e^{ik_0 r_2} e^{-ip^*} \mathbf{F}(p^*). \quad (2.86)$$

It is seen that the corresponding term in the paper by King and Sandler (1994) is written in the form

$$\frac{k_0^2 \varepsilon \mu_0}{2\pi} \sqrt{\frac{\pi}{k_0 r_2}} e^{ik_0 r_2} e^{-ip} \mathbf{F}(p). \quad (2.87)$$

Obviously, r_2 equals approximately to ρ , Eq. (2.86) will coincide with Eq. (2.87). Similarly, the second terms in Eqs. (2.80) and (2.81) coincide with the corresponding lateral-wave terms in the paper by King and Sandler (1994).

With $f = 100$ MHz, $\varepsilon_{r1} = 2.85$, for the electric field E_{0z} , the total field, the trapped surface wave, and DRL waves, which include the direct wave, the ideal reflected wave, and the lateral wave, are computed for $k_1 l_1 = 0.4$ and $k_1 l_1 = 1.4$ at $z = d = 0$ m, and shown in Figs. 2.11 and 2.12, respectively. It is

concluded that the trapped surface wave is dominant in the far region when both the dipole and the observation point are on or near the air-dielectric boundary.

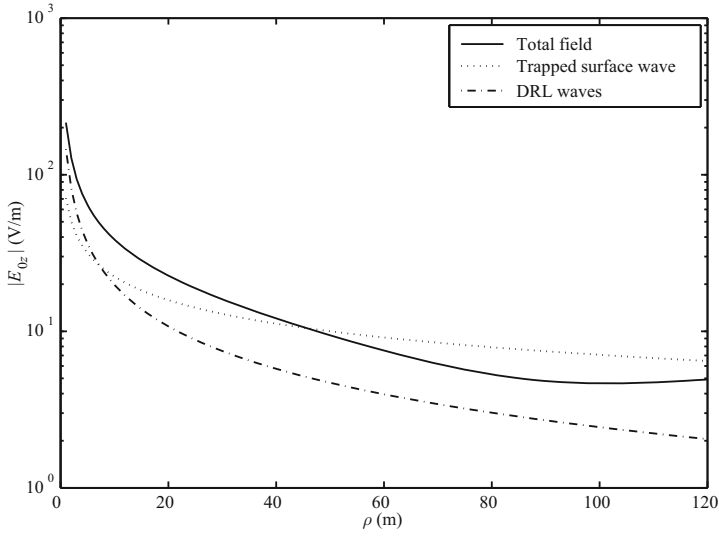


Fig. 2.11. The electric field $|E_{0z}|$ versus the propagation distance ρ at $k_1 l_1 = 0.4$

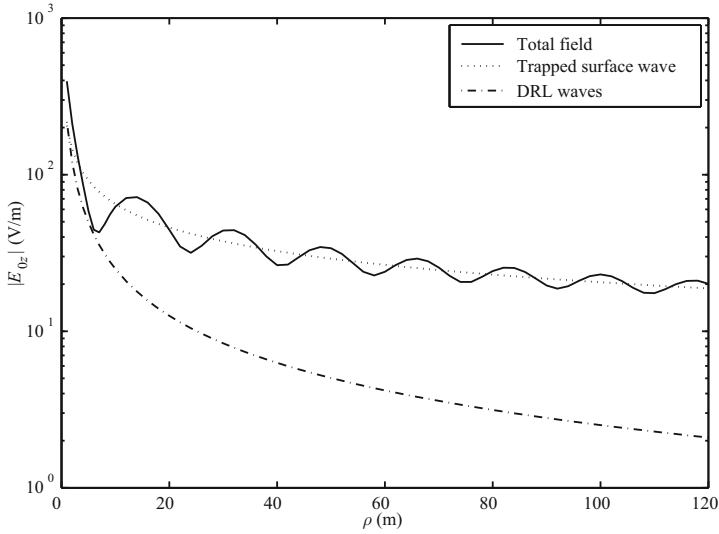


Fig. 2.12. The electric field $|E_{0z}|$ versus the propagation distance ρ at $k_1 l_1 = 1.4$

2.4 Field of Vertical Dipole over Dielectric-Coated Imperfect Conductor

In what follows, we will study the electromagnetic field of a vertical electric dipole in air over an imperfect conductor coated with a dielectric layer.

2.4.1 Statements of the Problem

If Region 2 is occupied by an imperfect conductor, as shown in Fig. 2.1, the integrated formulas of the electromagnetic field due to a vertical electric dipole in the presence of three-layered region can be written in the following forms:

$$B_{0\phi} = \frac{i\mu_0}{4\pi} \int_0^\infty \left[e^{i\gamma_0|z-d|} + e^{i\gamma_0(z+d)} - (Q+1)e^{i\gamma_0(z+d)} \right] \gamma_0^{-1} J_1(\lambda\rho) \lambda^2 d\lambda, \quad (2.88)$$

$$E_{0\rho} = \frac{i\omega\mu_0}{4\pi k_0^2} \int_0^\infty \left[\pm e^{i\gamma_0|z-d|} + e^{i\gamma_0(z+d)} - (Q+1)e^{i\gamma_0(z+d)} \right] J_1(\lambda\rho) \lambda^2 d\lambda; \quad (2.89)$$

$$\begin{aligned} d &< z \\ 0 &\leq z \leq d, \end{aligned}$$

$$E_{0z} = \frac{-\omega\mu_0}{4\pi k_0^2} \int_0^\infty \left[e^{i\gamma_0|z-d|} + e^{i\gamma_0(z+d)} - (Q+1)e^{i\gamma_0(z+d)} \right] \gamma_0^{-1} J_0(\lambda\rho) \lambda^3 d\lambda, \quad (2.90)$$

where the reflection coefficient is

$$-Q = \frac{\frac{\gamma_0}{k_0^2} - \frac{\gamma_2}{k_2^2} - i \left(\frac{\gamma_0}{k_0^2} \frac{\gamma_2}{k_2^2} \frac{k_1^2}{\gamma_1} - \frac{\gamma_1}{k_1^2} \right) \tan(\gamma_1 l)}{\frac{\gamma_0}{k_0^2} + \frac{\gamma_2}{k_2^2} - i \left(\frac{\gamma_0}{k_0^2} \frac{\gamma_2}{k_2^2} \frac{k_1^2}{\gamma_1} + \frac{\gamma_1}{k_1^2} \right) \tan(\gamma_1 l)}, \quad (2.91)$$

where

$$\gamma_j = \sqrt{k_j^2 - \lambda^2} \quad j = 0, 1, 2. \quad (2.92)$$

The first and second terms in Eqs. (2.88)~(2.90) stand for the direct wave and the ideal reflected wave, respectively. The evaluations for the two terms, which are carried out in the book by King, Owens, and Wu (2002), have been stated in the preceding chapter, and they are not repeated here. In what follows, the main tasks are to evaluate the following three integrals:

$$B_{0\phi}^{(3)} = \frac{-i\mu_0}{4\pi} \int_{-\infty}^\infty \frac{A(\lambda) H_1^{(1)}(\lambda\rho) e^{i\gamma_0(z+d)}}{q(\lambda) \gamma_0} \lambda^2 d\lambda, \quad (2.93)$$

$$E_{0\rho}^{(3)} = \frac{-i\omega\mu_0}{4\pi k_0^2} \int_{-\infty}^\infty \frac{A(\lambda) H_1^{(1)}(\lambda\rho) e^{i\gamma_0(z+d)}}{q(\lambda)} \lambda^2 d\lambda, \quad (2.94)$$

$$E_{0z}^{(3)} = \frac{-\omega\mu_0}{4\pi k_0^2} \int_{-\infty}^{\infty} \frac{A(\lambda)H_0^{(1)}(\lambda\rho)e^{i\gamma_0(z+d)}}{q(\lambda)\gamma_0} \lambda^3 d\lambda, \quad (2.95)$$

where

$$q(\lambda) = \frac{\gamma_0}{k_0^2} + \frac{\gamma_2}{k_2^2} - i \left(\frac{\gamma_0}{k_0^2} \frac{\gamma_2}{k_2^2} \frac{k_1^2}{\gamma_1} + \frac{\gamma_1}{k_1^2} \right) \tan(\gamma_1 l), \quad (2.96)$$

$$A(\lambda) = -\frac{\gamma_2}{k_2^2} + i \frac{\gamma_1}{k_1^2} \tan(\gamma_1 l), \quad (2.97)$$

$$r_1 = \sqrt{\rho^2 + (z-d)^2}, \quad (2.98)$$

$$r_2 = \sqrt{\rho^2 + (z+d)^2}. \quad (2.99)$$

2.4.2 The Trapped Surface Wave

In the preceding section, we outlined and analyzed the trapped surface wave radiated by a vertical electric dipole over the planar surface of a dielectric-coated perfect conductor ($k_2 \rightarrow \infty$). Along the research line, the investigations will be extended to the imperfect case. First, it is necessary to examine the following pole equation:

$$q(\lambda) = \frac{\gamma_0}{k_0^2} + \frac{\gamma_2}{k_2^2} - i \left(\frac{\gamma_0}{k_0^2} \frac{\gamma_2}{k_2^2} \frac{k_1^2}{\gamma_1} + \frac{\gamma_1}{k_1^2} \right) \tan(\gamma_1 l) = 0. \quad (2.100)$$

Let $s = k_0/k_2$, it is seen that the medium in Region 2 can be characterized by the parameter s . For the perfect conducting case, $s=0$; for the imperfect conducting case, s will be a complex number with its magnitude being less than 1 and its phase being from 0° to 45° .

Substitution $k_2 = k_0/s$ into Eq. (2.100) leads to

$$q(s, \lambda) = \frac{\gamma_0}{k_0^2} + \frac{s\sqrt{1-s^2\lambda^2/k_0^2}}{k_0} - i \tan(\gamma_1 l) \left(\frac{\gamma_0 s \sqrt{1-s^2\lambda^2/k_0^2} k_1^2}{\gamma_1 k_0^3} + \frac{\gamma_1}{k_1^2} \right) = 0. \quad (2.101)$$

Assuming that λ_i is the i -th root of Eq. (2.101), we write

$$\frac{dq(s, \lambda)}{ds} = g(\lambda, s) - f(\lambda, s) \frac{d\lambda}{ds} = 0, \quad (2.102)$$

where

$$g(\lambda, s) = \frac{\left(1 - \frac{2s^2\lambda^2}{k_0^2}\right) \left[1 - \frac{i\gamma_0 k_1^2}{k_0^2 \gamma_1} \tan(\gamma_1 l)\right]}{k_0 \sqrt{1-s^2\lambda^2/k_0^2}}, \quad (2.103)$$

$$f(\lambda, s) = \frac{\lambda}{k_0^2} \left(\frac{1}{\gamma_0} + \frac{s^3}{k_0 \sqrt{1-s^2\lambda^2/k_0^2}} \right) - \frac{i\lambda \tan(\gamma_1 l)}{\gamma_1}$$

$$\times \left[\frac{s^3 \gamma_0 k_1^2}{k_0^5 \sqrt{1 - s^2 \lambda^2 / k_0^2}} + \frac{1}{k_1^2} + \frac{s \sqrt{1 - s^2 \lambda^2 / k_0^2} k_1^2 (k_1^2 - k_0^2)}{\gamma_0 \gamma_1^2 k_0^3} \right] - \frac{i \lambda l}{\gamma_1} \sec^2(\gamma_1 l) \left[\frac{\gamma_1}{k_1^2} + \frac{\gamma_0 s \sqrt{1 - s^2 \lambda^2 / k_0^2} k_1^2}{\gamma_1 k_0^3} \right]. \quad (2.104)$$

Then, we get

$$\frac{d\lambda}{ds} = \frac{g(\lambda, s)}{f(\lambda, s)}. \quad (2.105)$$

When $k_2 \neq \infty$, from Eq. (2.105), the root λ_i is obtained readily.

$$\lambda_i = \lambda_i^* + \int_0^{k_0/k_2} \frac{g(\lambda, s)}{f(\lambda, s)} ds. \quad (2.106)$$

For the integral in (2.106), it is seen that the integral contour is in the fourth quadrant, and γ_0 , γ_1 , and $\sqrt{1 - s^2 \lambda^2 / k_0^2}$ have satisfied the following condition:

$$-\frac{\pi}{4} \leq \arg \gamma_i < \frac{3\pi}{4}. \quad (2.107)$$

The roots of Eq. (2.100) can be obtained from Eq. (2.106) by using numerical integration or from Eq. (2.100) by using Newton's iteration method. Therefore, the trapped-surface-wave terms of the electromagnetic field are expressed as follows:

$$\begin{aligned} B_{0\phi}^{sur} &= \frac{-\mu_0}{2} \sum_j \frac{A(\lambda_j) \lambda_j^2 e^{i\gamma_0(z+d)}}{q'(\lambda_j) \gamma_0(\lambda_j)} H_1^{(1)}(\lambda_j \rho) \\ &\approx \frac{\mu_0}{2} \sqrt{\frac{2}{\pi \rho}} e^{i\frac{\pi}{4}} \sum_j \frac{A(\lambda_j) \lambda_j^{3/2}}{q'(\lambda_j) \gamma_0(\lambda_j)} e^{i\gamma_0(\lambda_j)(z+d) + i\lambda_j \rho}, \end{aligned} \quad (2.108)$$

$$\begin{aligned} E_{0\rho}^{sur} &= \frac{-\omega \mu_0}{2k_0} \sum_j \frac{A(\lambda_j) \lambda_j^2 e^{i\gamma_0(\lambda_j)(z+d)}}{q'(\lambda_j)} H_1^{(1)}(\lambda_j \rho) \\ &\approx \frac{\omega \mu_0 e^{i\frac{\pi}{4}}}{2k_0^2} \sqrt{\frac{2}{\pi \rho}} \sum_j \frac{A(\lambda_j) \lambda_j^{3/2}}{q'(\lambda_j)} e^{i\gamma_0(\lambda_j)(z+d) + i\lambda_j \rho}, \end{aligned} \quad (2.109)$$

$$\begin{aligned} E_{0z}^{sur} &= \frac{-i\omega \mu_0}{2k_0^2} \sum_j \frac{A(\lambda_j) e^{i\gamma_0(\lambda_j)(z+d)}}{q'(\lambda_j) \gamma_0(\lambda_j)} \lambda_j^3 H_0^{(1)}(\lambda_j \rho) \\ &\approx \frac{-\omega \mu_0}{2k_0^2} e^{i\frac{\pi}{4}} \sqrt{\frac{2}{\pi \rho}} \sum_j \frac{A(\lambda_j) \lambda_j^{5/2}}{q'(\lambda_j) \gamma_0(\lambda_j)} e^{i\gamma_0(\lambda_j)(z+d) + i\lambda_j \rho}, \end{aligned} \quad (2.110)$$

where

$$q'(\lambda_0) = -\lambda \left(\frac{1}{k_0^2 \gamma_0} + \frac{1}{k_2^2 \gamma_2} \right) + i \frac{\lambda l}{\gamma_1} \sec^2(\gamma_1 l) \left(\frac{k_1^2}{k_0^2 k_2^2} \frac{\gamma_0 \gamma_2}{\gamma_1} + \frac{\gamma_1}{k_1^2} \right) + i \lambda \tan(\gamma_1 l) \left[\frac{1}{k_1^2 \gamma_1} + \frac{k_1^2}{k_0^2 k_2^2} \left(\frac{\gamma_2}{\gamma_1 \gamma_0} + \frac{\gamma_0}{\gamma_1 \gamma_2} - \frac{\gamma_0 \gamma_2}{\gamma_1^3} \right) \right]. \quad (2.111)$$

It is seen that the poles are determined by the wave numbers k_0 and k_1 and the thickness of the dielectric layer.

2.4.3 Lateral Wave

When $k_2 \neq \infty$, besides the poles λ_i , the integrands have the branch cuts at $\lambda = k_i$, ($i = 0, 1, 2$). The branch lines and the poles in the λ complex plane are shown in Fig. 2.13. Since both the integrands $q(\lambda)$ and $A(\lambda)$ are the even functions to γ_1 , it is easily verified that the evaluations of the integrals in Eqs. (2.93)~(2.95) along the branch line Γ_1 are zero. Considering that the wave number k_2 in the imperfect conductor has a positive imaginary part, the Hankel function $H_1^{(1)}(\lambda \rho)$ has a large attenuating factor along the branch line Γ_2 . Then, the integral along the branch line Γ_2 is regarded as the wave through the imperfect conductor from the dipole to the observation point and can be neglected in computations. Obviously, it is necessary to evaluate the contributions of the integration along the branch line Γ_0 . We write

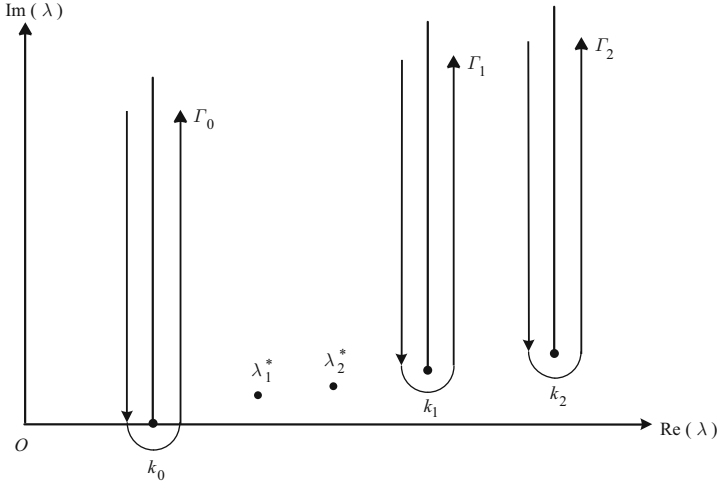


Fig. 2.13. The configuration of the poles and the branch lines

$$B_{0\phi}^l = \frac{i\mu_0}{4\pi} \int_{\Gamma_0} \frac{A(\lambda) e^{i\gamma_0(z+d)}}{q(\lambda) \gamma_0} H_1^{(1)}(\lambda \rho) \lambda^2 d\lambda, \quad (2.112)$$

where

$$H_1^{(1)}(\lambda\rho) \approx \sqrt{\frac{2}{\pi k_0 \rho}} e^{ik_0 \rho - i\frac{3\pi}{4}} e^{-k_0 \rho \tau^2}. \quad (2.113)$$

Considering the far-field condition $k_0 \rho \gg 1$ and $(z+d) \ll \rho$, the dominant contribution of the integral along the branch line Γ_0 comes from the vicinity of k_0 . Let $\lambda = k_0(1 + i\tau^2)$, γ_0 is approximated as

$$\gamma_0 = \sqrt{k_0^2 - \lambda^2} \approx k_0 \sqrt{2} e^{i\frac{3\pi}{4}} \tau. \quad (2.114)$$

On the left and right sides of the branch line Γ_0 , the phases of γ_0 are $e^{-i\pi/4}$ and $e^{i3\pi/4}$, respectively. Then, λ_1 and λ_2 are approximated as

$$\gamma_1 = \sqrt{k_1^2 - \lambda^2} \approx \sqrt{k_1^2 - k_0^2} = \gamma_1^*, \quad (2.115)$$

$$\gamma_2 = \sqrt{k_2^2 - \lambda^2} \approx \sqrt{k_2^2 - k_0^2} = \gamma_2^*. \quad (2.116)$$

Thus, the result becomes

$$\begin{aligned} B_{0\phi}^l &= \frac{i\mu_0}{4\pi} \exp \left\{ ik_0 \rho \left[1 + \frac{1}{2} \left(\frac{z+d}{\rho} \right)^2 \right] - i\frac{3\pi}{4} \right\} \sqrt{\frac{2}{\pi k_0 \rho}} k_0^2 \frac{A(k_0)}{q_0} \sqrt{2} e^{-i\frac{\pi}{4}} \\ &\times \int_{-\infty}^{\infty} \frac{\exp \left[-k_0 \rho \left(\tau + \frac{e^{i\pi/4}}{\sqrt{2}} \frac{z+d}{\rho} \right)^2 \right]}{\tau + c} d\tau, \end{aligned} \quad (2.117)$$

where

$$A(k_0) = \frac{-\gamma_2^*}{k_2^2} + i \frac{-\gamma_1^*}{k_1^2} \tan \gamma_1^* l, \quad (2.118)$$

$$q_0 = \frac{\sqrt{2} e^{i\frac{3\pi}{4}}}{k_0} \left(1 - i \frac{k_1^2 \gamma_2^*}{k_2^2 \gamma_1^*} \tan \gamma_1^* l \right), \quad (2.119)$$

$$c = -\frac{A(k_0)}{q_0}. \quad (2.120)$$

The integral in Eq. (2.117) can be evaluated analytically. It is

$$\begin{aligned} \int_{-\infty}^{\infty} \frac{\exp \left[-k_0 \rho \left(\tau + \frac{e^{i\pi/4}}{\sqrt{2}} \frac{z+d}{\rho} \right)^2 \right]}{\tau + c} d\tau &= i\pi \exp \left\{ -k_0 \rho \left(c - \frac{e^{i\pi/4}}{\sqrt{2}} \frac{z+d}{\rho} \right)^2 \right\} \\ &\times \operatorname{erfc} \left[\sqrt{-k_0 \rho \left(c - \frac{e^{i\pi/4}}{\sqrt{2}} \frac{z+d}{\rho} \right)^2} \right] \\ &= \sqrt{2} \pi e^{i\frac{\pi}{4}} e^{-iP^*} F(P^*), \end{aligned} \quad (2.121)$$

where

$$P^* = \frac{k_0 \rho}{2} \left(\frac{z+d}{\rho} + \frac{\frac{\gamma_2^* k_0}{k_2^2} - i \frac{\gamma_1^* k_0}{k_1^2} \tan \gamma_1^* l}{1 - i \frac{k_2^2 \gamma_2^*}{k_2^2 \gamma_1^*} \tan \gamma_1^* l} \right)^2, \quad (2.122)$$

and Fresnel integral is defined by

$$F(P^*) = \frac{1}{2}(1+i) - \int_0^{P^*} \frac{e^{it}}{(2\pi t)^{1/2}} dt. \quad (2.123)$$

Taking into account

$$r_2 = [\rho^2 + (z+d)^2]^{1/2} \approx \rho \left[1 + \frac{1}{2} \left(\frac{z+d}{\rho} \right)^2 \right], \quad (2.124)$$

the lateral-wave term is written in the form

$$B_{0\phi}^l = \frac{\mu_0 k_0^2}{2} \sqrt{\frac{1}{\pi k_0 \rho}} \varepsilon^* e^{ik_0 r_2} e^{-iP^*} F(P^*), \quad (2.125)$$

where

$$\varepsilon^* = \frac{\frac{k_0 \gamma_2^*}{k_2^2} - i \frac{k_0 \gamma_1^*}{k_1^2} \tan \gamma_1^* l}{1 - i \frac{k_2^2 \gamma_2^*}{k_2^2 \gamma_1^*} \tan \gamma_1^* l}. \quad (2.126)$$

Similarly, we have

$$E_{0\rho}^l = \frac{i\omega\mu_0 k_0}{2\pi} \varepsilon^* e^{ik_0 r_2} \left[\frac{1}{k_0 \rho} + i \sqrt{\frac{\pi}{k_0 \rho}} \varepsilon^* e^{-iP^*} F(P^*) \right], \quad (2.127)$$

$$E_{0z}^l = \frac{-\omega\mu_0 k_0}{2} \sqrt{\frac{1}{\pi k_0 \rho}} \varepsilon^* e^{ik_0 r_2} e^{-iP^*} F(P^*). \quad (2.128)$$

2.4.4 Final Formulas for the Electromagnetic Field Components

By using the above obtained results and the results of the direct wave and ideal reflected wave, the final formulas of the three components $B_{0\phi}$, $E_{0\rho}$, and E_{0z} are obtained readily.

$$\begin{aligned} B_{0\phi}(\rho, z) = & -\frac{\mu_0}{4\pi} \left[\left(\frac{\rho}{r_1} \right) \left(\frac{ik_0}{r_1} - \frac{1}{r_1^2} \right) e^{ik_0 r_1} + \left(\frac{\rho}{r_2} \right) \left(\frac{ik_0}{r_2} - \frac{1}{r_2^2} \right) e^{ik_0 r_2} \right] \\ & + \frac{\mu_0}{2} \sqrt{\frac{2}{\pi \rho}} e^{i\frac{\pi}{4}} \sum_j \frac{A(\lambda_j) \lambda_j^{3/2}}{q'(\lambda_j) \gamma_0(\lambda_j)} e^{i\gamma_0(\lambda_j)(z+d) + i\lambda_j \rho} \\ & + \frac{\mu_0 k_0^2}{2} \sqrt{\frac{1}{\pi k_0 \rho}} \varepsilon^* e^{ik_0 r_2} e^{-iP^*} F(P^*), \end{aligned} \quad (2.129)$$

$$E_{0\rho}(\rho, z) = -\frac{\omega\mu_0}{4\pi k_0} \left(\frac{\rho}{r_1} \right) \left(\frac{z-d}{r_1} \right) \left(\frac{ik_0}{r_1} - \frac{3}{r_1^2} - \frac{3i}{k_0 r_1^3} \right) e^{ik_0 r_1}$$

$$\begin{aligned}
& -\frac{\omega\mu_0}{4\pi k_0} \left(\frac{\rho}{r_2}\right) \left(\frac{z+d}{r_2}\right) \left(\frac{ik_0}{r_2} - \frac{3}{r_2^2} - \frac{3i}{k_0 r_2^3}\right) e^{ik_0 r_2} \\
& + \frac{\omega\mu_0 e^{i\frac{\pi}{4}}}{2k_0^2} \sqrt{\frac{2}{\pi\rho}} \sum_j \frac{A(\lambda_j) \lambda_j^{3/2}}{q'(\lambda_j)} e^{i\gamma_0(\lambda_j)(z+d) + i\lambda_j \rho} \\
& + \frac{i\omega\mu_0 k_0}{2\pi} \varepsilon^* e^{ik_0 r_2} \left[\frac{1}{k_0 \rho} + i \sqrt{\frac{\pi}{k_0 \rho}} \varepsilon^* e^{-iP^*} F(P^*) \right], \tag{2.130}
\end{aligned}$$

$$\begin{aligned}
E_{0z}(\rho, z) = & \frac{\omega\mu_0}{4\pi k_0} \left[\frac{ik_0}{r_1} - \frac{1}{r_1^2} - \frac{i}{k_0 r_1^3} - \left(\frac{z-d}{r_1}\right)^2 \left(\frac{ik_0}{r_1} - \frac{3}{r_1^2} - \frac{3i}{k_0 r_1^3}\right) \right] e^{ik_0 r_1} \\
& + \frac{\omega\mu_0}{4\pi k_0} \left[\frac{ik_0}{r_2} - \frac{1}{r_2^2} - \frac{i}{k_0 r_2^3} - \left(\frac{z+d}{r_2}\right)^2 \left(\frac{ik_0}{r_2} - \frac{3}{r_2^2} - \frac{3i}{k_0 r_2^3}\right) \right] e^{ik_0 r_2} \\
& - \frac{\omega\mu_0}{2k_0^2} e^{i\frac{\pi}{4}} \sqrt{\frac{2}{\pi\rho}} \sum_j \frac{A(\lambda_j) \lambda_j^{5/2}}{q'(\lambda_j) \gamma_0(\lambda_j)} e^{i\gamma_0(\lambda_j)(z+d) + i\lambda_j \rho} \\
& - \frac{\omega\mu_0 k_0}{2} \sqrt{\frac{1}{\pi k_0 \rho}} \varepsilon^* e^{ik_0 r_2} e^{-iP^*} F(P^*). \tag{2.131}
\end{aligned}$$

2.4.5 Computations and Discussions

Assuming that $k_0^2 \ll k_1^2 \ll k_2^2$ and $k_1 l \leq 0.6$, we have

$$\gamma_1^* = \sqrt{k_1^2 - k_0^2} \approx k_1, \tag{2.132}$$

$$\gamma_2^* = \sqrt{k_2^2 - k_0^2} \approx k_2, \tag{2.133}$$

$$\tan \gamma_1^* l \approx k_1 l. \tag{2.134}$$

Evidently, we obtain

$$\varepsilon^* = \frac{\frac{k_0 \gamma_2^*}{k_2^2} - i \frac{\gamma_1^* k_0}{k_1^2} \tan \gamma_1^* l}{1 - i \frac{k_1^2 \gamma_2^*}{k_2^2 \gamma_1^*} \tan \gamma_1^* l} \approx \frac{k_0}{k_2} - ik_0 l, \tag{2.135}$$

and

$$\begin{aligned}
P^* &= \frac{k_0 \rho}{2} \left(\frac{z+d}{\rho} + \frac{\frac{\gamma_2^* k_0}{k_2^2} - i \frac{\gamma_1^* k_0}{k_1^2} \tan \gamma_1^* l}{1 - i \frac{k_1^2 \gamma_2^*}{k_2^2 \gamma_1^*} \tan \gamma_1^* l} \right)^2 \\
&= \frac{k_0 \rho}{2} \left(\frac{z+d + \varepsilon \rho}{\rho} \right)^2 = P. \tag{2.136}
\end{aligned}$$

Here the above parameters ε^* and P^* are in agreement with ε and P in the paper by King and Sandler (1994). It is seen that when the dielectric layer

is satisfied by $k_0^2 \ll k_1^2 \ll k_2^2$ and $k_1 l \leq 0.6$, the present results for the lateral wave coincide with the corresponding results addressed by King and Sandler (1994).

Except for the lateral wave, the trapped surface wave is excited efficiently by a vertical electric dipole only when both the dipole and the observation point are on or close to the air-dielectric boundary. With $f = 100$ MHz, $\varepsilon_{r1} = 2.85$, $\varepsilon_{r2} = 80$, $\sigma_2 = 4$ S/m, the real and imaginary parts of λ_1^*/k_0 are computed and shown in Figs. 2.14 and 2.15, respectively. It is seen that the attenuation factor to the thickness of the dielectric layer is discontinuity in the case of $k_1 l \in (0, \pi/2)$.

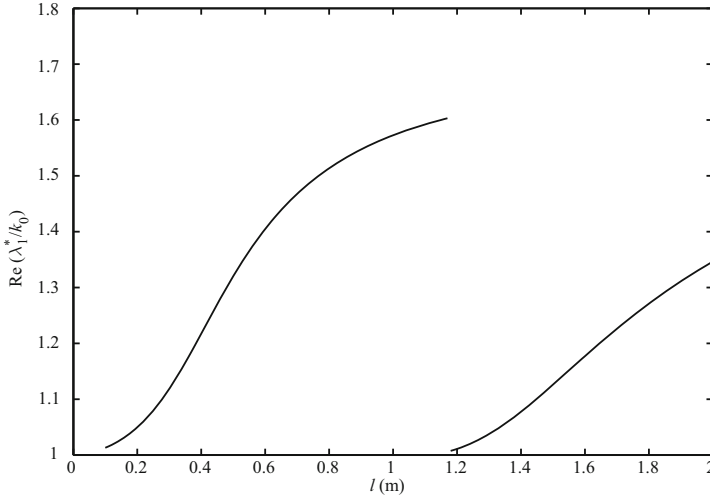


Fig. 2.14. The real part of λ_1^*/k_0 versus the thickness l of the dielectric layer: $f=100$ MHz, $\varepsilon_{r1} = 2.85$, $\varepsilon_{r2} = 80$, $\sigma_2 = 4$ S/m

With $f = 100$ MHz, $\varepsilon_{r1} = 2.85$, and $z = d = 0$ m, graphs of E_{0z} in V/m due to unit vertical electric dipole for the well conductor with $\varepsilon_{r2} = 80$, $\sigma = 4$ S/m are computed and shown in Figs. 2.16~2.18 at $k_1 l = 0.4$, $k_1 l = 0.9$, and $k_1 l = 1.4$, respectively. Compared with the corresponding results in the preceding section, it is seen that the trapped surface wave is affected significantly by the conductivity of the imperfect conductor and the attenuation will increase as the conductivity decreases.

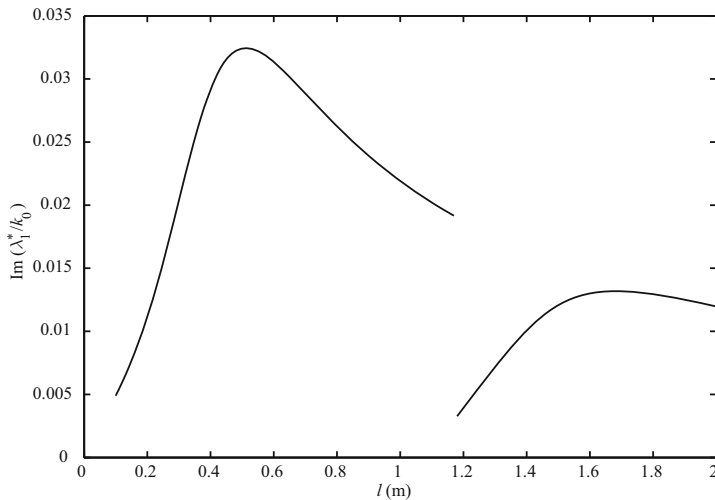


Fig. 2.15. The imaginary part of λ_1^*/k_0 versus the thickness l of the dielectric layer: $f=100\text{MHz}$, $\varepsilon_{r1} = 2.85$, $\varepsilon_{r2} = 80$, $\sigma_2 = 4 \text{ S/m}$

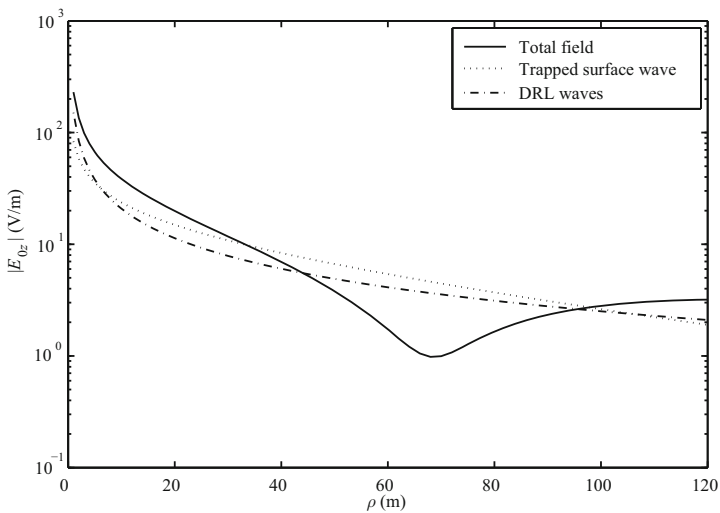


Fig. 2.16. Magnitude of E_{0z} in V/m due to unit vertical dipole versus the propagation distances ρ at $k_1 l = 0.4$

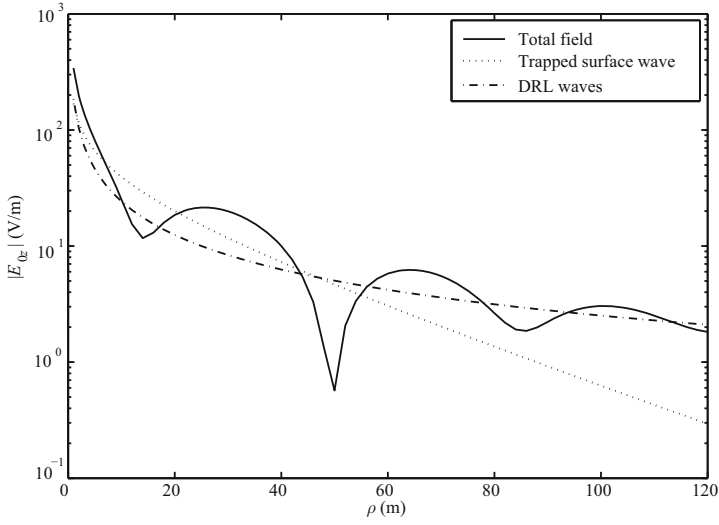


Fig. 2.17. Magnitude of E_{0z} in V/m due to unit vertical dipole versus the propagation distances ρ at $k_1 l = 0.9$

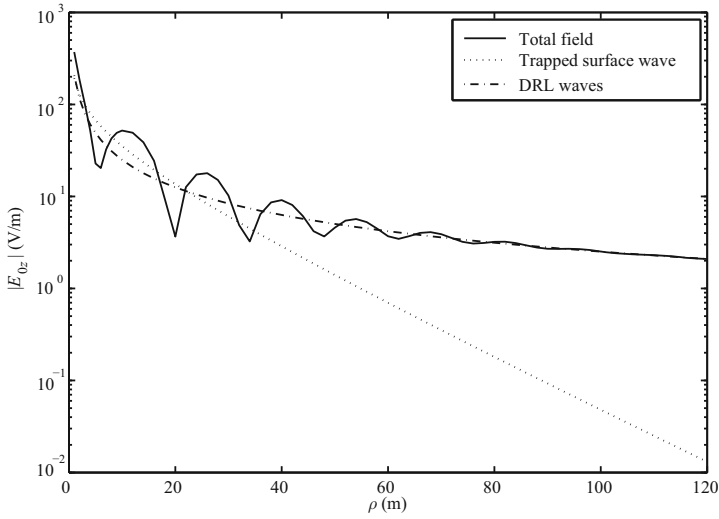


Fig. 2.18. Magnitude of E_{0z} in V/m due to unit vertical dipole versus the propagation distances ρ at $k_1 l = 1.4$

2.5 Radiation from Vertical Dipole in Three-Layered Region

In this section, based on the results obtained in Sec. 2.4, further developments for the radiation from a vertical electric dipole in the presence of a three-layered region will be carried out.

2.5.1 Field of Vertical Dipole in Three-Layered Region

When the condition $|P^*| \geq 4$ is satisfied, the Fresnel-integral term is approximated as the form with

$$P^* = \frac{k_0 \rho}{2} \left(\frac{z+d}{\rho} + \varepsilon^* \right)^2, \quad (2.137)$$

$$\begin{aligned} T^* &= k_0^2 \varepsilon^* \sqrt{\frac{\pi}{k_0 \rho}} e^{-iP^*} \mathbf{F}(P^*) \\ &\rightarrow \frac{ik_0 \rho}{\rho^2} \frac{\varepsilon^*}{\varepsilon^* + (z+d)/\rho} + \frac{\varepsilon^*}{\rho^2} \left[\frac{1}{\varepsilon^* + (z+d)/\rho} \right]^3. \end{aligned} \quad (2.138)$$

With Eqs. (2.137) and (2.138), Eqs. (2.129)~(2.131) have the following far-field forms:

$$\begin{aligned} B_{0\phi}^r(\rho, z) &= -\frac{\mu_0}{4\pi} \left[\frac{ik_0 \rho}{r_1^2} e^{ik_0 r_1} + \left(\frac{ik_0 \rho}{r_2^2} - 2T^* \right) e^{ik_0 r_2} \right] \\ &\quad + \frac{\mu_0}{2} \sqrt{\frac{2}{\pi \rho}} e^{i\frac{\pi}{4}} \sum_j \frac{A(\lambda_j) \lambda_j^{3/2}}{q'(\lambda_j) \gamma_0(\lambda_j)} e^{i\gamma_0(\lambda_j)(z+d) + i\lambda_j \rho}, \end{aligned} \quad (2.139)$$

$$\begin{aligned} E_{0\rho}^r(\rho, z) &= -\frac{\omega \mu_0}{4\pi k_0} \left\{ \left(\frac{ik_0 \rho}{r_1^2} \right) \left(\frac{z-d}{r_1} \right) e^{ik_0 r_1} \right. \\ &\quad \left. + \left[\frac{ik_0 \rho}{r_2^2} \left(\frac{z+d}{r_2} - 2\varepsilon^* \frac{r_2^2}{\rho^2} \right) + 2\varepsilon^* T^* \right] e^{ik_0 r_2} \right\} \\ &\quad + \frac{\omega \mu_0}{2k_0^2} e^{i\frac{\pi}{4}} \sqrt{\frac{2}{\pi \rho}} \sum_j \frac{A(\lambda_j) \lambda_j^{3/2}}{q'(\lambda_j)} e^{i\gamma_0(\lambda_j)(z+d) + i\lambda_j \rho}, \end{aligned} \quad (2.140)$$

$$\begin{aligned} E_{0z}^r(\rho, z) &= \frac{\omega \mu_0}{4\pi k_0} \left\{ \left(\frac{ik_0}{r_1} \right) \left(\frac{\rho}{r_1} \right)^2 e^{ik_0 r_1} + \left[\frac{ik_0}{r_2} \left(\frac{\rho}{r_2} \right)^2 - 2T^* \right] e^{ik_0 r_2} \right\} \\ &\quad - \frac{\omega \mu_0}{2k_0^2} e^{i\frac{\pi}{4}} \sqrt{\frac{2}{\pi \rho}} \sum_j \frac{A(\lambda_j) \lambda_j^{5/2}}{q'(\lambda_j) \gamma_0(\lambda_j)} e^{i\gamma_0(\lambda_j)(z+d) + i\lambda_j \rho}. \end{aligned} \quad (2.141)$$

It is possible to express the electromagnetic field in spherical coordinates with r_0 , Θ , Φ with substitutions

$$r_0 = \sqrt{\rho^2 + z^2}; \quad \sin \Theta = \frac{\rho}{r_0}; \quad \cos \Theta = \frac{z}{r_0}. \quad (2.142)$$

Taking into account $d^2 \ll r_0^2$, it is known that $r_1 \sim r_0 - d \cos \Theta$, $r_2 \sim r_0 + d \cos \Theta$ in phase and $r_1 \sim r_2 \sim r_0$ in amplitudes. It follows that

$$\frac{\rho}{r_1} \sim \frac{\rho}{r_2} \sim \frac{\rho}{r_0} = \sin \Theta, \quad (2.143)$$

$$\frac{z-d}{r_1} \sim \frac{z-d}{r_0} = \cos \Theta - \frac{d}{r_0}, \quad (2.144)$$

$$\frac{z+d}{r_2} \sim \frac{z+d}{r_0} = \cos \Theta + \frac{d}{r_0}. \quad (2.145)$$

With these simplifications, we write

$$\begin{aligned} B_{0\phi}^r(r_0, \Theta) = & \frac{-\mu_0}{2\pi} e^{ik_0 r_0} \left\{ \frac{ik_0 \sin \Theta}{r_0} \left[\frac{-i\varepsilon^* \sin(k_0 d \cos \Theta)}{\varepsilon^* \sin^2 \Theta + \sin \Theta (\cos \Theta + \frac{d}{r_0})} \right. \right. \\ & + \cos(k_0 d \cos \Theta) \frac{\sin \Theta (\cos \Theta + \frac{d}{r_0}) - \varepsilon^* \cos^2 \Theta}{\sin \Theta (\cos \Theta + \frac{d}{r_0}) + \varepsilon^* \sin^2 \Theta} \Big] \\ & \left. - \frac{\varepsilon^*}{r_0^2} \frac{\sin \Theta e^{ik_0 d \cos \Theta}}{(\varepsilon^* \sin \Theta + \cos \Theta + \frac{d}{r_0})^3} \right\} + \frac{\mu_0}{2} \sqrt{\frac{2}{\pi \rho}} e^{i\frac{\pi}{4}} \\ & \times \sum_j \frac{A(\lambda_j) \lambda_j^{3/2}}{q'(\lambda_j) \gamma_0(\lambda_j)} e^{i\gamma_0(\lambda_j) r_0 (\cos \Theta + \frac{d}{r_0}) + i\lambda_j r_0 \sin \Theta}, \end{aligned} \quad (2.146)$$

$$\begin{aligned} E_{0\rho}^r(r_0, \Theta) = & -\frac{\omega \mu_0}{2\pi k_0} e^{ik_0 r_0} \\ & \times \left\{ \left(\cos(k_0 d \cos \Theta) \left[(\sin^2 \Theta \cos \Theta - \varepsilon^*) \left(\cos \Theta + \frac{d}{r_0} \right) \right. \right. \right. \\ & \left. \left. \left. + \varepsilon^* \sin^3 \Theta \cos \Theta \right] + i \sin(k_0 d \cos \Theta) \right. \right. \\ & \left. \left. \times \left[\left(\frac{d \sin^2 \Theta}{r_0} - \varepsilon^* \right) \left(\frac{d}{r_0} + \cos \Theta \right) + \frac{d \varepsilon^* \sin^3 \Theta}{r_0} \right] \right) \right. \\ & \left. \times \frac{ik_0}{r_0 \sin \Theta (\varepsilon^* \sin \Theta + \cos \Theta + \frac{d}{r_0})} \right. \\ & \left. + \frac{\varepsilon^{*2}}{r_0^2} \frac{\sin \Theta e^{ik_0 d \cos \Theta}}{(\varepsilon^* \sin \Theta + \cos \Theta + \frac{d}{r_0})^3} \right\} + \frac{\omega \mu_0}{2k_0^2} e^{i\frac{\pi}{4}} \sqrt{\frac{2}{\pi r_0 \sin \Theta}} \end{aligned}$$

$$\times \sum_j \frac{A(\lambda_j) \lambda_j^{3/2}}{q'(\lambda_j)} e^{i\gamma_0(\lambda_j)(r_0 \cos \Theta + d) + i\lambda_j r_0 \sin \Theta}, \quad (2.147)$$

$$\begin{aligned} E_{0z}^r(\rho, z) &= \frac{\omega \mu_0}{2k_0 \pi} e^{ik_0 r_0} \\ &\times \left\{ \frac{ik_0}{r_0 \sin \Theta (\varepsilon^* \sin \Theta + \cos \Theta + \frac{d}{r_0})} \right. \\ &\quad \times \left[-i\varepsilon^* \sin \Theta \sin(k_0 d \cos \Theta) + \cos(k_0 d \cos \Theta) \sin \Theta \right. \\ &\quad \times \left(\varepsilon^* \sin^3 \Theta + \sin^2 \Theta \cos \Theta + \frac{d}{r_0} \sin^2 \Theta - \varepsilon^* \right) \left. \right] \\ &\quad \left. - \frac{\varepsilon^*}{r_0^2} \frac{\sin \Theta e^{ik_0 d \cos \Theta}}{(\varepsilon^* \sin \Theta + \cos \Theta + \frac{d}{r_0})^3} \right\} - \frac{\omega \mu_0}{2k_0^2} e^{i\frac{\pi}{4}} \sqrt{\frac{2}{\pi r_0 \sin \Theta}} \\ &\times \sum_j \frac{A(\lambda_j) \lambda_j^{5/2}}{q'(\lambda_j) \gamma_0(\lambda_j)} e^{i\gamma_0(\lambda_j)(r_0 \cos \Theta + d) + i\lambda_j r_0 \sin \Theta}. \end{aligned} \quad (2.148)$$

After considerable algebraic manipulation, the field components in spherical coordinates r_0, Θ, Φ can be expressed as follows:

$$\begin{aligned} E_{0\Theta}^r(r_0, \Theta) &= -\frac{\omega \mu_0}{2\pi k_0} e^{ik_0 r_0} \\ &\times \left\{ \frac{ik_0 \cos(k_0 d \cos \Theta)}{r_0 \sin \Theta (\varepsilon^* \sin \Theta + \cos \Theta + \frac{d}{r_0})} \right. \\ &\quad \times \left[(\varepsilon^* \sin^3 \Theta + \sin^2 \Theta \cos \Theta - \varepsilon^*) + \frac{d(\sin^2 \Theta - \varepsilon^* \cos \Theta)}{r_0} \right] \\ &\quad + \frac{ik_0 [i \sin(k_0 d \cos \Theta)]}{r_0 \sin \Theta (\varepsilon^* \sin \Theta + \cos \Theta + \frac{d}{r_0})} \left[\frac{d\varepsilon^* \cos \Theta \sin^3 \Theta}{r_0} \right. \\ &\quad + \frac{d \sin^2 \Theta \cos^2 \Theta}{r_0} + \left(\frac{d}{r_0} \right)^2 \sin^2 \Theta \cos \Theta - \varepsilon^* - \frac{d\varepsilon^* \cos \Theta}{r_0} \left. \right] \\ &\quad \left. + \frac{\varepsilon^*}{r_0^2} \frac{\sin \Theta (\varepsilon^* \cos \Theta - \sin \Theta) e^{ik_0 d \cos \Theta}}{(\varepsilon^* \sin \Theta + \cos \Theta + d/r_0)^3} \right\} \\ &+ \frac{\omega \mu_0}{2k_0^2} e^{i\frac{\pi}{4}} \sqrt{\frac{2}{\pi r_0 \sin \Theta}} \sum_j \frac{A(\lambda_j) \lambda_j^{3/2}}{q'(\lambda_j)} \\ &\times \left[\cos \Theta + \frac{\lambda_j}{\gamma_0(\lambda_j)} \sin \Theta \right] e^{i\gamma_0(\lambda_j)(r_0 \cos \Theta + d) + i\lambda_j r_0 \sin \Theta}. \end{aligned} \quad (2.149)$$

With Eqs. (2.147) and (2.148), the transverse component of the electric field in spherical coordinates is obtained. It is

$$\begin{aligned}
E_{0r}^r(r_0, \Theta) = & -\frac{\omega\mu_0}{2k_0\pi} e^{ik_0r_0} \\
& \times \left\{ -\frac{ik_0\varepsilon^* \frac{d}{r_0} \cos(k_0d \cos \Theta)}{r_0(\varepsilon^* \sin \Theta + \cos \Theta + \frac{d}{r_0})} \right. \\
& - \frac{k_0 \sin(k_0d \cos \Theta) \left[\frac{d\varepsilon^* \sin^3 \Theta}{r_0} + \left(\frac{d \sin^2 \Theta}{r_0} - \varepsilon^* \right) \cos \Theta - \frac{d\varepsilon^*}{r_0} \right]}{r_0(\varepsilon^* \sin \Theta + \cos \Theta + \frac{d}{r_0})} \\
& \left. + \frac{\varepsilon^* \sin \Theta (\varepsilon^* \sin \Theta + \cos \Theta)}{r_0^2 (\varepsilon^* \sin \Theta + \cos \Theta + \frac{d}{r_0})^3} e^{ik_0d \cos \Theta} \right\} \\
& + \frac{\omega\mu_0}{2k_0^2} e^{i\frac{\pi}{4}} \sqrt{\frac{2}{\pi r_0 \sin \Theta}} \sum_j \frac{A(\lambda_j) \lambda_j^{3/2}}{q'(\lambda_j)} \left[\sin \Theta - \frac{\lambda_j}{\gamma_0(\lambda_j)} \cos \Theta \right] \\
& \times e^{i\gamma_0(\lambda_j)(r_0 \cos \Theta + d) + i\lambda_j r_0 \sin \Theta}. \tag{2.150}
\end{aligned}$$

In practical applications the antenna is usually placed on the surface of the earth, either as a based-insulated dipole or a monopole base-driven against a buried ground system. In this case $d/r_0 \sim 0$, $k_0d \sim 0$, the expressions of the three components are simplified as the following forms:

$$\begin{aligned}
B_{0\Phi}^r(r_0, \Theta) = & -\frac{\mu_0}{2\pi} e^{ik_0r_0} \left[\frac{ik_0 \cos \Theta (\sin \Theta - \varepsilon^* \cos \Theta)}{r_0(\cos \Theta + \varepsilon^* \sin \Theta)} - \frac{\varepsilon^* \sin \Theta}{r_0^2 (\varepsilon^* \sin \Theta + \cos \Theta)^3} \right] \\
& + \frac{\mu_0}{2} \sqrt{\frac{2}{\pi \rho}} e^{i\frac{\pi}{4}} \sum_j \frac{A(\lambda_j) \lambda_j^{3/2}}{q'(\lambda_j) \gamma_0(\lambda_j)} e^{i\gamma_0(\lambda_j)r_0 \cos \Theta + i\lambda_j r_0 \sin \Theta}, \tag{2.151}
\end{aligned}$$

$$\begin{aligned}
E_{0\Theta}^r(r_0, \Theta) = & -\frac{\omega\mu_0}{2\pi k_0} e^{ik_0r_0} \left[\frac{ik_0 (\varepsilon^* \sin^3 \Theta + \sin^2 \Theta \cos \Theta - \varepsilon^*)}{r_0 \sin \Theta (\varepsilon^* \sin \Theta + \cos \Theta)} \right. \\
& \left. + \frac{\varepsilon^* \sin \Theta (\varepsilon^* \cos \Theta + \sin \Theta)}{r_0^2 (\varepsilon^* \sin \Theta + \cos \Theta)^3} \right] \\
& + \frac{\omega\mu_0}{2k_0^2} e^{i\frac{\pi}{4}} \sqrt{\frac{2}{\pi r_0 \sin \Theta}} \sum_j \frac{A(\lambda_j) \lambda_j^{3/2}}{q'(\lambda_j)} \\
& \times \left[\cos \Theta + \frac{\lambda_j}{\gamma_0(\lambda_j)} \sin \Theta \right] e^{i\gamma_0(\lambda_j)r_0 \cos \Theta + i\lambda_j r_0 \sin \Theta}, \tag{2.152}
\end{aligned}$$

$$\begin{aligned}
E_{0r}^r(r_0, \Theta) = & -\frac{\omega\mu_0}{2k_0\pi} e^{ik_0r_0} \frac{\varepsilon^* \sin \Theta (\varepsilon^* \cos \Theta + \sin \Theta)}{r_0^2 (\varepsilon^* \sin \Theta + \cos \Theta)^3} \\
& + \frac{\omega\mu_0}{2k_0^2} e^{i\frac{\pi}{4}} \sqrt{\frac{2}{r_0 \pi \sin \Theta}} \sum_j \frac{A(\lambda_j) \lambda_j^{3/2}}{q'(\lambda_j)}
\end{aligned}$$

$$\times \left[\sin \Theta - \frac{\lambda_j}{\gamma_0(\lambda_j)} \cos \Theta \right] e^{i\gamma_0(\lambda_j)r_0 \cos \Theta + i\lambda_j r_0 \sin \Theta}. \quad (2.153)$$

The electromagnetic field on the surface is given by $\Theta = \pi/2$, $r_0 = \rho$, so that

$$B_{0\Phi}^r(\rho, \pi/2) = \frac{\omega\mu_0}{2\pi k_0} \frac{e^{ik_0\rho}}{\varepsilon^* \rho^2} + \frac{\omega\mu_0}{2k_0^2} e^{i\frac{\pi}{4}} \sqrt{\frac{2}{\pi\rho}} \sum_j \frac{A(\lambda_j)\lambda_j^{3/2}}{q'(\lambda_j)\gamma_0(\lambda_j)} e^{i\lambda_j\rho}, \quad (2.154)$$

$$E_{0\Theta}^r(\rho, \pi/2) = \frac{\omega\mu_0}{2\pi k_0} \frac{e^{ik_0\rho}}{\varepsilon^* \rho^2} + \frac{\omega\mu_0}{2k_0^2} e^{i\frac{\pi}{4}} \sqrt{\frac{2}{\pi\rho}} \sum_j \frac{A(\lambda_j)\lambda_j^{5/2}}{q'(\lambda_j)\gamma_0(\lambda_j)} e^{i\lambda_j\rho}, \quad (2.155)$$

$$E_{0r}^r(\rho, \pi/2) = -\frac{\omega\mu_0}{2\pi k_0} \frac{e^{ik_0\rho}}{\varepsilon^* \rho^2} + \frac{\omega\mu_0}{2k_0^2} e^{i\frac{\pi}{4}} \sqrt{\frac{2}{\pi\rho}} \sum_j \frac{A(\lambda_j)\lambda_j^{3/2}}{q'(\lambda_j)} e^{i\lambda_j\rho}. \quad (2.156)$$

It is noted that these formulas consist of the lateral-wave and trapped-surface-wave terms. The direct and ideal reflected waves vanish along the boundary.

2.5.2 Graphical Representations of the Far Field

In the present study, it is of interest in the case when both the dipole point and the observation point are on, or close to, the boundary between the air and the dielectric layer coating on the Earth or sea. Obviously, in this case the radial distance ρ is very large compared with the heights d and z so that the conditions $d^2 \ll \rho^2$ and $z^2 \ll \rho^2$ are well satisfied. The parameters for Region 2 including the conductivity σ_2 , the relative permittivity ε_{r2} have a wide range for possible communication. The following values are chosen for graphical representations: (a) sea water with $\varepsilon_{r2} = 80$, $\sigma = 4$ S/m; (b) lake water with $\varepsilon_{r2} = 80$, $\sigma = 0.004$ S/m; (c) wet earth with $\varepsilon_{r2} = 12$, $\sigma = 0.4$ S/m; (d) dry earth with $\varepsilon_{r2} = 8$, $\sigma = 0.04$ S/m; (e) dry sand with $\varepsilon_{r2} = 2$, $\sigma = 0$ S/m.

The DRL waves, which include the direct wave, the ideal reflected wave, and the lateral wave, are computed and shown in Fig. 2.19. In contrast with King's results, the corresponding results are obtained in Chapter 8 of the book (King, Fikioris, and Mack, 2002) and also plotted in the same figure. As predicted, it is seen that the numerical results of the DRL waves in this section are in agreement with King's results. The total field, the lateral-wave and trapped-surface-wave terms for the electric field components $E_{0r}^r(r_0, \Theta)$ and $E_{0\Theta}^r(r_0, \Theta)$ versus the propagation distance ρ are computed and shown in Figs. 2.20 and 2.21, respectively. In Figs. 2.22 and 2.23, the similar numerical results for the electric field components $E_{0r}^r(r_0, \Theta)$ and $E_{0\Theta}^r(r_0, \Theta)$ versus the angular degrees of Θ are computed and shown, respectively.

The far-field patterns for the electric field components $E_{0r}^r(r_0, \Theta)$ and $E_{0\Theta}^r(r_0, \Theta)$ of vertical electric dipole over the dielectric-coated earth or sea

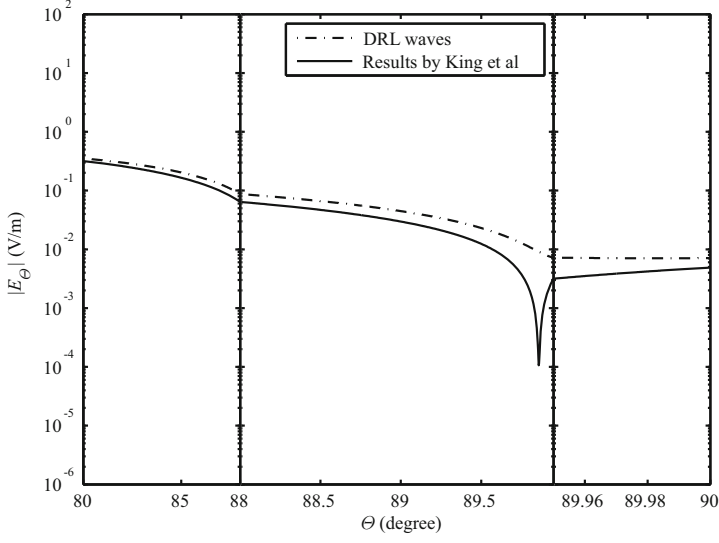


Fig. 2.19. Comparison between the DRL waves and King's results (Fig. 8.25 in [2]) for the electric field $E_{0r}(r_0, \Theta)$ in V/m with $f = 100$ MHz, $\varepsilon_{r1} = 2.65$, $\varepsilon_{r2} = 80$, $\sigma_2 = 4$ S/m, $r_0 = 200$ m, and $l = 0.45$ m

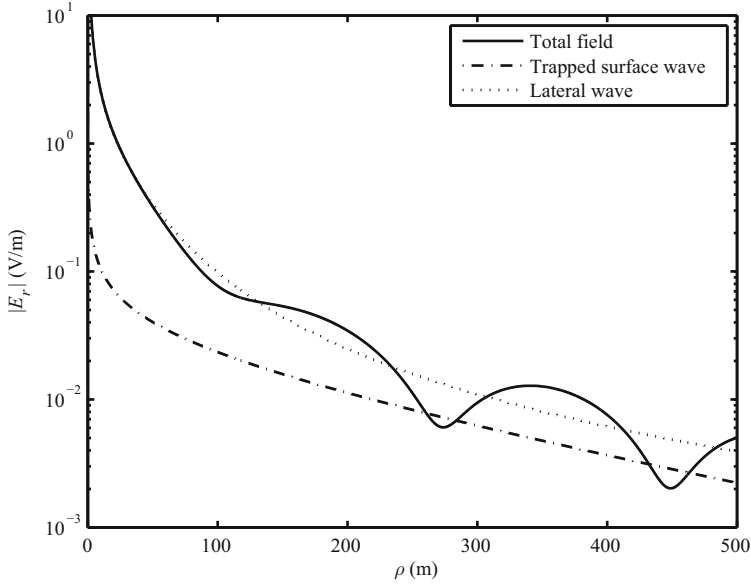


Fig. 2.20. The total field, the trapped surface wave, and the lateral wave for the electric field $E_{0r}(r_0, \Theta)$ in V/m versus the propagation distance ρ in m with $f = 100$ MHz, $\varepsilon_{r1} = 2.65$, $\varepsilon_{r2} = 80$, $\sigma_2 = 4$ S/m, $k_1 l = 0.45$, and $z = d = 0$ m

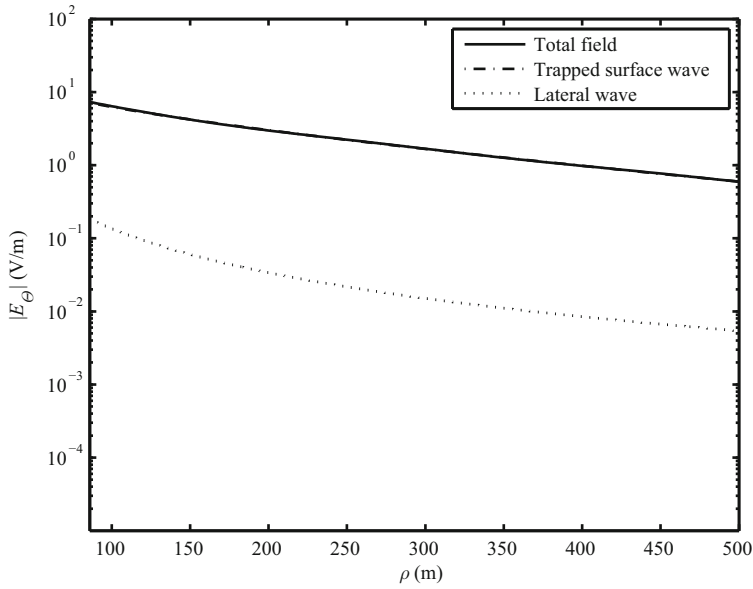


Fig. 2.21. The total field, the trapped surface wave, and the lateral wave for the electric field $E_{0\Theta}(r_0, \Theta)$ in V/m versus the propagation distances ρ in m with $f = 100$ MHz, $\varepsilon_{r1} = 2.65$, $\varepsilon_{r2} = 80$, $\sigma_2 = 4$ S/m, $k_1 l = 0.45$, and $z = d = 0$ m

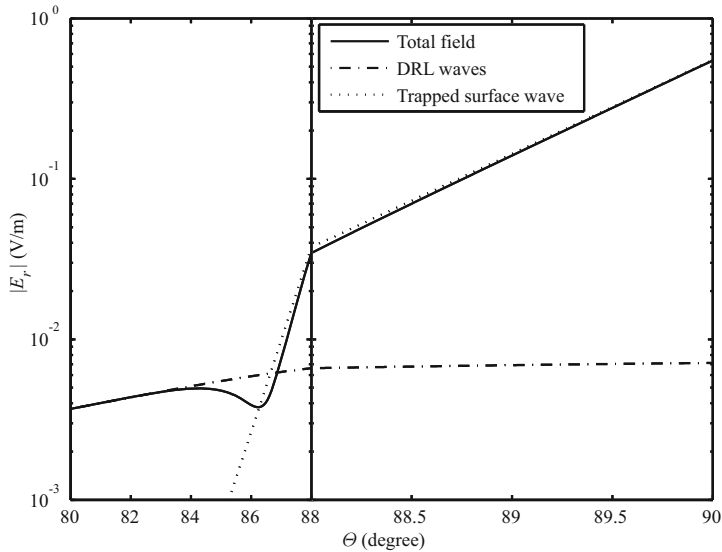


Fig. 2.22. The total field, the DRL waves, and the trapped surface for the electric field $E_{0r}(r_0, \Theta)$ in V/m with $f = 100$ MHz, $\varepsilon_{r1} = 2.65$, $\varepsilon_{r2} = 80$, $\sigma_2 = 4$ S/m, $d = 0$ m, $k_1 l = 0.45$, and $r_0 = 200$ m

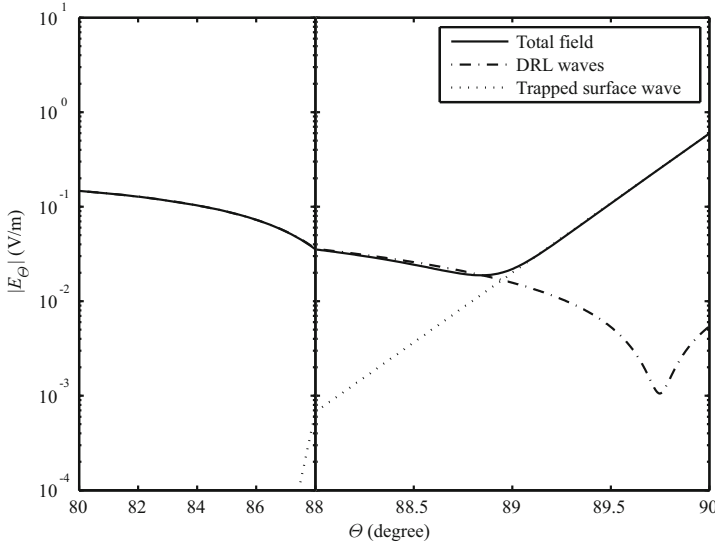


Fig. 2.23. The total field, the DRL waves, and the trapped surface for the electric field $E_{0\Theta}(r_0, \Theta)$ in V/m with $f = 100$ MHz, $\varepsilon_{r1} = 2.65$, $\varepsilon_{r2} = 80$, $\sigma_2 = 4$ S/m, $d = 0$ m, $k_1 l = 0.45$, and $r_0 = 500$ m

are computed and shown in Figs. 2.24~2.29 at the radial distances $r_0 = 200$ m, 500 m, and 1000 m, respectively, for sea and lake water, two types of earth, and dry sand. Specifically, Figs. 2.24, 2.26, and 2.28 show logarithmic graphs of $E_{0r}^r(r_0, \Theta)$ in the range of $80^\circ \leq \Theta \leq 90^\circ$. Similar graphs of $E_{0\Theta}^r(r_0, \Theta)$ are shown in Figs. 2.25, 2.27, and 2.29. In Figs. 2.24 and 2.25, all curves for sea and lake water and two types of earth with $r_0 = 200$ m have large peaks at $\Theta = 90^\circ$. The peaks in Figs. 2.26~2.29 for sea and lake water and wet earth with $r_0 = 500$ m and $r_0 = 1000$ m are much smaller. It is noted that the peaks for the dry earth in Figs. 2.26~2.29 do not appear.

From these figures, it is seen that there is a significant contribution from the trapped surface wave for all above-mentioned five kinds of media. When $\Theta \leq 88^\circ$, the dipole point or the observation point is away to the air-dielectric boundary, the term of trapped surface wave attenuates exponentially in the \hat{z} direction and the trapped surface wave can be neglected. Comparing Figs. 2.27 and 2.29 with Figs. 8.13 and 8.15 in the book by King, Fikioris, and Mack (2002), respectively, it is seen that when conditions $\Theta \leq 88^\circ$ and $k_0 l \leq 0.6$ are satisfied, the computed results are agreement with the available results in the book by King, Fikioris, and Mack (2002). When $\Theta > 88^\circ$, both the dipole and observation point are closed to the boundary, the term of trapped surface wave should be considered. When $\Theta = 90^\circ$, both the dipole and the observation point are on the air-dielectric boundary, the total field is determined primarily by the trapped surface wave.

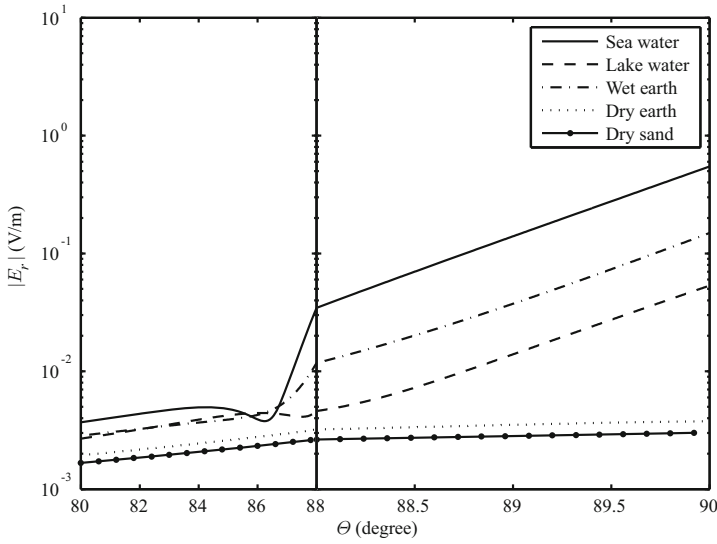


Fig. 2.24. The electric field $E_{0r}(r_0, \Theta)$ in V/m with $f = 100$ MHz, $\varepsilon_{r1} = 2.65$, $d = 0$ m, $k_1 l = 0.45$, and $r_0 = 200$ m. It is noted that Region 2 are sea and lake water, wet and dry earth, and dry sand, respectively

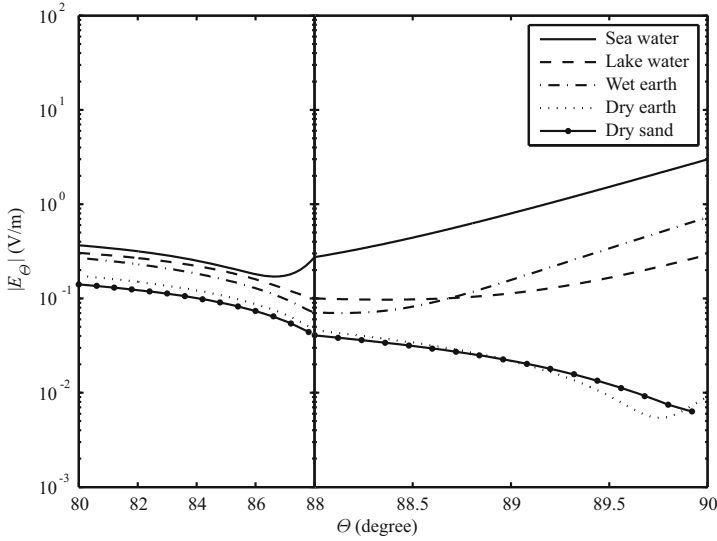


Fig. 2.25. The electric field $E_{0\Theta}(r_0, \Theta)$ in V/m with $f = 100$ MHz, $\varepsilon_{r1} = 2.65$, $d = 0$ m, $k_1 l = 0.45$, and $r_0 = 200$ m. It is noted that Region 2 are sea and lake water, wet and dry earth, and dry sand, respectively

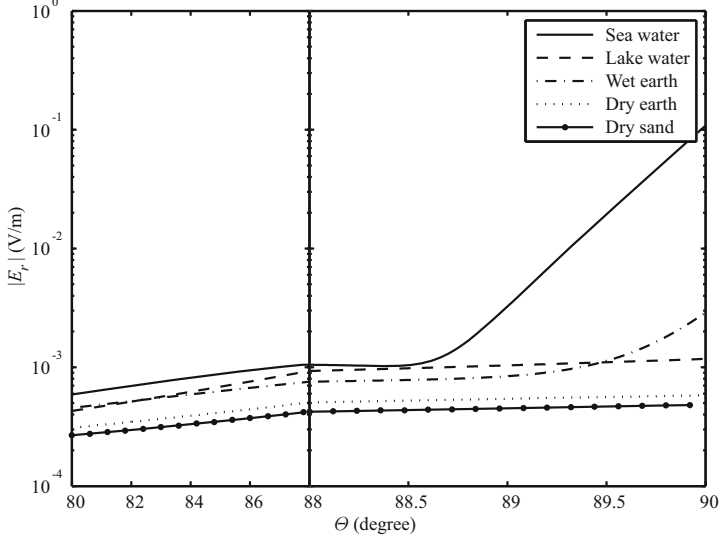


Fig. 2.26. The electric field $E_{0r}(r_0, \Theta)$ in V/m with $f = 100$ MHz, $\varepsilon_{r1} = 2.65$, $d = 0$ m, $k_1 l = 0.45$, and $r_0 = 500$ m. It is noted that Region 2 are sea and lake water, wet and dry earth, and dry sand, respectively

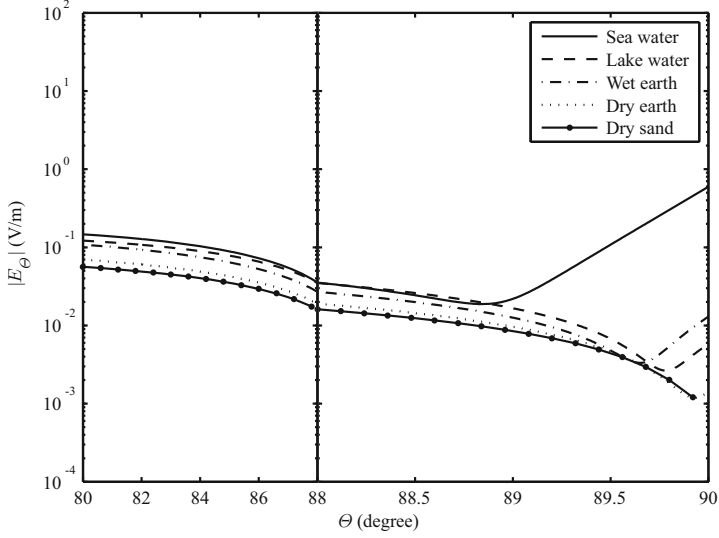


Fig. 2.27. The electric field $E_{0\Theta}(r_0, \Theta)$ in V/m with $f = 100$ MHz, $\varepsilon_{r1} = 2.65$, $d = 0$ m, $k_1 l = 0.45$, and $r_0 = 500$ m. It is noted that Region 2 are sea and lake water, wet and dry earth, and dry sand, respectively

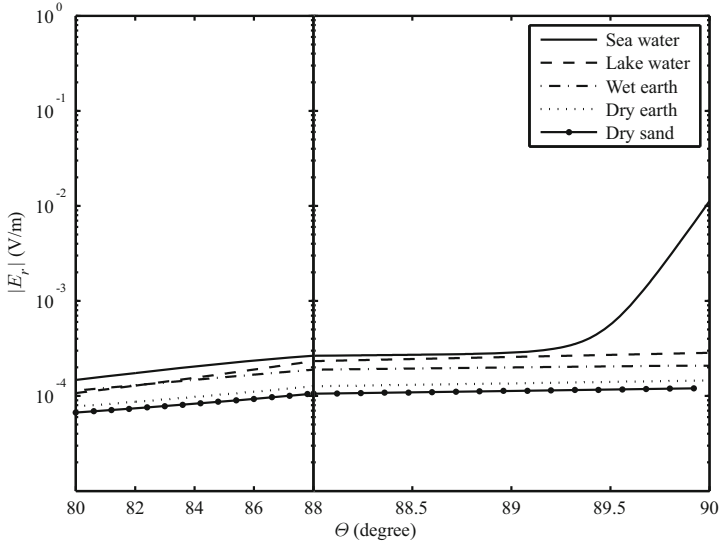


Fig. 2.28. The electric field $E_{0r}(r_0, \Theta)$ in V/m with $f = 100$ MHz, $\varepsilon_{r1} = 2.65$, $d = 0$ m, $k_1 l = 0.45$, and $r_0 = 1000$ m. It is noted that Region 2 are sea and lake water, wet and dry earth, and dry sand, respectively

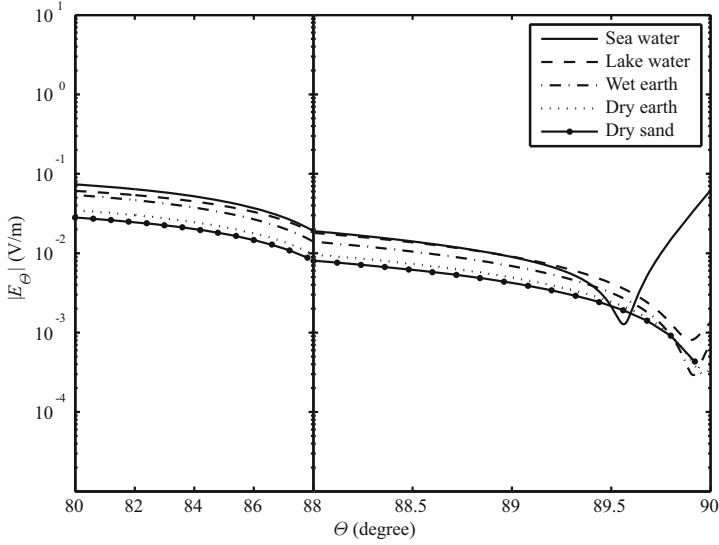


Fig. 2.29. The electric field $E_{0\theta}(r_0, \Theta)$ in V/m with $f = 100$ MHz, $\varepsilon_{r1} = 2.65$, $d = 0$ m, $k_1 l = 0.3$, and $r_0 = 1000$ m. It is noted that Region 2 are sea and lake water, wet and dry earth, and dry sand, respectively

References

- Collin RE (2004a) Some observations about the near zone electric field of a hertzian dipole above a lossy earth. *IEEE Transactions on Antennas and Propagation*, 52(11): 3133–3137.
- Collin RE (2004b) Hertzian Dipole Radiation Over a Lossy Earth or Sea: Some early and Late 20th Century Controversies. *IEEE Antennas and Propagation Magazine*, 46(2): 64–79.
- Fei T, Li LW, Yeo TS, Wang HL, and Wu Q (2007) A comparative study of radio wave propagation over the earth due to a vertical electric dipole. *IEEE Transactions on Antennas and Propagation*, 55(10): 2723–2732.
- Gradshteyn IS and Ryzhik IM (1980) *Table of Integrals, Series, and Products*. New York, NY, USA: Academic Press.
- King RWP (1991) The electromagnetic field of a horizontal electric dipole in the presence of a three-layered region. *Journal of Applied Physics*, 69(12): 7987–7995.
- King RWP, Owens M, and Wu TT (1992) *Lateral Electromagnetic Waves: Theory and Applications to Communications, Geophysical Exploration, and Remote Sensing*. New York, NY, USA: Springer-Verlag.
- King RWP (1993) The electromagnetic field of a horizontal electric dipole in the presence of a three-layered region: supplement. *Journal of Applied Physics*, 74(8): 4845–4548.
- King RWP and Sandler SS (1994) The electromagnetic field of a vertical electric dipole in the presence of a three-layered region. *Radio Science*, 29(1): 97–113.
- King RWP and Sandler SS (1998) Reply. *Radio Science*, 33(2): 255–256.
- King RWP, Fikioris GJ, and Mack RB (2002) *Cylindrical Antennas and Array*. Cambridge, UK: Cambridge University Press.
- Li K and Lu Y (2005) Electromagnetic field generated by a horizontal electric dipole near the surface of a planar perfect conductor coated with a uniaxial layer. *IEEE Transactions on Antennas and Propagation*, 53(10): 3191–3200.
- Liu L and Li K (2007) Radiation from a vertical electric dipole in the presence of a three-layered region. *IEEE Transactions on Antennas and Propagation*, 55(12): 3469–3475.
- Mahmoud SF (1999) Remarks on “The electromagnetic field of a vertical electric dipole over the earth or Sea”. *IEEE Transactions on Antennas and Propagation*, 46(12): 1745–1946.
- Sommerfeld A (1909) Propagation of waves in wireless telegraphy. *Annalen der Physik* (Leipzig), 28: 665–736.
- Sommerfeld A (1926) Propagation of waves in wireless telegraphy. *Annalen der Physik* (Leipzig), 81: 1135–1153.
- Wait JR (1953) Radiation from a vertical electric dipole over a stratified ground. *IRE Transactions on Antennas and Propagation*, AP-1: 9–12.
- Wait JR (1954) Radiation from a vertical electric dipole over a stratified ground. *IRE Transactions on Antennas and Propagation*, AP-2: 144–146.
- Wait JR (1956) Radiation from a vertical electric dipole over a curved stratified ground ground. *Journal of Research of the National Bureau of Standards*, 56: 232–239.

- Wait JR (1957) Excitation of surface waves on conducting dielectric clad and corrugated surfaces. *Journal of Research of the National Bureau of Standards*, 59(6): 365–377.
- Wait JR (1970) *Electromagnetic Waves in Stratified Media* (2nd, Ed.). New York, NY, USA: Pergamon Press.
- Wait JR (1990a) Radiation from a vertical electric dipole located over laterally anisotropic ground plane. *Electronics Letters*, 26(1): 74–76.
- Wait JR (1990b) Electromagnetic fields of a vertical electric dipole over a laterally anisotropic surface. *IEEE Transactions on Antennas and Propagation*, 38(10): 1719–1723.
- Wait JR (1998) Comment on “The electromagnetic field of a vertical electric dipole in the presence of a three-layered region” by Ronold, W. P. King and Sheldon S. Sandler. *Radio Science*, 33(2): 251–253.
- Zhang HQ and Pan WY (2002) Electromagnetic field of a vertical electric dipole on a perfect conductor coated with a dielectric layer. *Radio Science*, 37(4), 1060, doi:1029/2000RS002348.
- Zhang HQ, Li K, and Pan WY (2004) The electromagnetic field of a vertical dipole on the dielectric-coated imperfect conductor. *Journal of Electromagnetic Waves and Applications*, 18(10): 1305–1320.

Electromagnetic Field of a Horizontal Electric Dipole in the Presence of a Three-Layered Region

The approximate formulas are derived for the electromagnetic field generated by a horizontal electric dipole in the presence of a three-layered region. Especially, both the trapped surface wave and lateral wave are treated in detail. Further investigations on the far-field radiation in spherical coordinates and radiation patterns of a patch antenna with specific current distributions are carried out specifically.

3.1 Introduction

The electromagnetic field excited by a horizontal antenna over the planar boundary between two different media is well known to involve a surface wave of the lateral-wave type. When the boundary includes a layer of third material with intermediate properties, the electromagnetic field excited by the same horizontal antenna is in general much more complicated. Because of its many useful applications, especially in microstrip antenna, the electromagnetic field of a horizontal dipole in the presence of a three-layered region has been treated by many investigators.

In the early 1990's, the simple analytical formulas were derived for the electromagnetic field of a horizontal dipole in the presence of a three-layered region (King, 1991; 1993). In Chapter 12 of the book by King, Owens, and Wu (1992), it is explained that the trapped surface wave can be excited by a dipole in a three-layered region, but in their study the trapped surface wave is not considered. In the preceding chapter, it is concluded that the trapped surface wave can be excited efficiently by a vertical electric dipole in the presence of a three-layered region. Along this line of research, in this chapter we will examine the electromagnetic field of a horizontal electric dipole in the presence of a three-layered region in detail (Zhang, Pan, and Shen, 2001). Furthermore, the radiation of a horizontal dipole in spherical coordinates and the radiation patterns of a patch antenna are treated analytically (Liu, Li, and Xu, 2008).

3.2 Electromagnetic Field of Horizontal Electric Dipole

In this section, we will treat the electromagnetic field of a horizontal electric dipole in the presence of a three-layered region in detail. The region of interest consists of a perfect conductor, coated with a dielectric layer, and air above.

3.2.1 Integrated Formulas for Electromagnetic Field in Air

The relevant geometry and Cartesian coordinate system are shown in Fig. 3.1, where a horizontal electric dipole in the \hat{x} direction is located at $(0, 0, d)$. Region 0 ($z \geq 0$) is the space above the dielectric layer with the air characterized by the permeability μ_0 and uniform permittivity ε_0 , Region 1 ($-l \leq z \leq 0$) is the dielectric layer characterized by the permeability μ_0 , relative permittivity ε_{r1} , and conductivity σ_1 , and Region 2 ($z \leq 0$) is the rest space occupied by a perfect conductor. Then the wave numbers of the three layers are

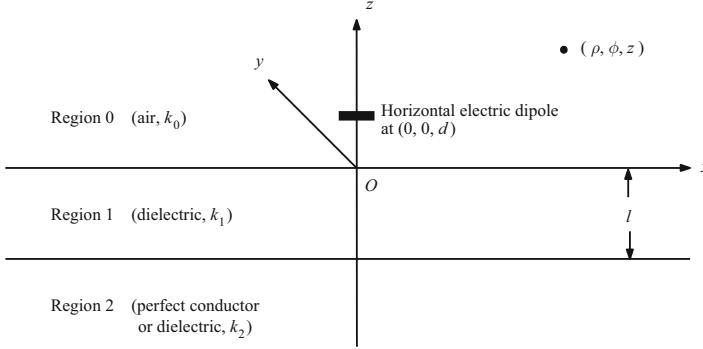


Fig. 3.1. Unit horizontal electric dipole at $(0, 0, d)$ over the air-dielectric boundary $z = 0$ in the presence of a three-layered region

$$k_0 = \omega \sqrt{\mu_0 \varepsilon_0}, \quad (3.1)$$

$$k_1 = \omega \sqrt{\mu_0 (\varepsilon_0 \varepsilon_{r1} + i\sigma_1/\omega)}, \quad (3.2)$$

$$k_2 \rightarrow \infty. \quad (3.3)$$

Maxwell's equations in Region 0 and Region 1 can be expressed by

$$\nabla \times \mathbf{E}_j = i\omega \mathbf{B}_j, \quad (3.4)$$

$$\nabla \times \mathbf{B}_j = \mu_0 (-i\omega \varepsilon_j \mathbf{E}_j + \hat{\mathbf{x}} J_x^e), \quad (3.5)$$

where

$$J_x^e = Idl\delta(x)\delta(y)\delta(z-d) \quad (3.6)$$

is the volume current density in the dipole.

Because the transforms of the tangential electric field components and the magnetic field continue on the interface, it follows that $\tilde{E}_{1x}(x, y, 0) = \tilde{E}_{0x}(x, y, 0)$, $\tilde{E}_{1y}(x, y, 0) = \tilde{E}_{0y}(x, y, 0)$, $k_1^2 \tilde{E}_{1z}(x, y, 0) = k_0^2 \tilde{E}_{0z}(x, y, 0)$, and $\tilde{B}_1(x, y, 0) = \tilde{B}_0(x, y, 0)$. Taking into account Region 2 being a perfect conductor, it yields the boundary conditions that $\tilde{E}_{1x}(x, y, -l) = \tilde{E}_{1y}(x, y, -l) = 0$. Similar to the manner addressed in the preceding chapter, the formulas for the six components of the electromagnetic field in air due to a horizontal electric dipole can be derived readily. They are

$$E_{0\rho}(\rho, \phi, z) = -\frac{\omega\mu_0 Idl}{4\pi k_0^2} \cos\phi [F_{\rho 0}(\rho, z-d) - F_{\rho 0}(\rho, z+d) + F_{\rho 1}(\rho, z+d)] \quad (3.7)$$

$$E_{0\phi}(\rho, \phi, z) = \frac{\omega\mu_0 Idl}{4\pi k_0^2} \sin\phi [F_{\phi 0}(\rho, z-d) - F_{\phi 0}(\rho, z+d) + F_{\phi 1}(\rho, z+d)] \quad (3.8)$$

$$E_{0z}(\rho, \phi, z) = \frac{i\omega\mu_0 Idl}{4\pi k_0^2} \cos\phi [F_{z0}(\rho, z-d) - F_{z0}(\rho, z+d) + F_{z1}(\rho, z+d)] \quad (3.9)$$

$$B_{0\rho}(\rho, \phi, z) = -\frac{\mu_0 Idl}{4\pi} \sin\phi [G_{\rho 0}(\rho, z-d) - G_{\rho 0}(\rho, z+d) + G_{\rho 1}(\rho, z+d)] \quad (3.10)$$

$$B_{0\phi}(\rho, \phi, z) = -\frac{\mu_0 Idl}{4\pi} \cos\phi [G_{\phi 0}(\rho, z-d) - G_{\phi 0}(\rho, z+d) + G_{\phi 1}(\rho, z+d)] \quad (3.11)$$

$$B_{0z}(\rho, \phi, z) = \frac{i\mu_0 Idl}{4\pi} \sin\phi [G_{z0}(\rho, z-d) - G_{z0}(\rho, z+d) + G_{z1}(\rho, z+d)]. \quad (3.12)$$

In these formulas, $F_{m0}(\rho, z-d)$ and $G_{m0}(\rho, z-d)$ ($m = \rho, \phi$ and z) represent the direct wave in Region 0 of the horizontal electric dipole at $(0, 0, d)$, and $F_{m0}(\rho, z+d)$ and $G_{m0}(\rho, z+d)$ represent the ideal reflected wave or the wave of a ideal image dipole at $(0, 0, -d)$. The evaluations of the integrals $F_{m0}(\rho, z-d)$ and $G_{m0}(\rho, z-d)$ ($m = \rho, \phi$ and z) have been obtained by King (1991; 1993), and will not be duplicated in this chapter.

Next, emphasis is placed on finding a solution to the last terms in the brackets in Eqs. (3.7)~(3.12) by using analytical techniques. The last terms are expressed in the following forms

$$F_{\rho 1}(\rho, z+d) = F_{\rho 2}(\rho, z+d) + F_{\rho 3}(\rho, z+d), \quad (3.13)$$

$$F_{\phi 1}(\rho, z+d) = F_{\phi 2}(\rho, z+d) + F_{\phi 3}(\rho, z+d), \quad (3.14)$$

$$G_{\rho 1}(\rho, z + d) = G_{\rho 2}(\rho, z + d) + G_{\rho 3}(\rho, z + d), \quad (3.15)$$

$$G_{\phi 1}(\rho, z + d) = G_{\phi 2}(\rho, z + d) + G_{\phi 3}(\rho, z + d), \quad (3.16)$$

where

$$\begin{aligned} F_{\rho 2}(\rho, z + d) &= \frac{1}{2} \int_0^\infty \gamma_0 (Q_3 + 1) [J_0(\lambda \rho) \mp J_2(\lambda \rho)] e^{i\gamma_0(z+d)} \lambda d\lambda, \\ F_{\phi 2}(\rho, z + d) &= \frac{1}{2} \int_0^\infty \gamma_0 (Q_3 + 1) [J_0(\lambda \rho) \mp J_2(\lambda \rho)] e^{i\gamma_0(z+d)} \lambda d\lambda, \end{aligned} \quad (3.17)$$

$$\begin{aligned} F_{\rho 3}(\rho, z + d) &= \frac{k_0^2}{2} \int_0^\infty \gamma_0^{-1} (P_3 - 1) [J_0(\lambda \rho) \pm J_2(\lambda \rho)] e^{i\gamma_0(z+d)} \lambda d\lambda, \\ F_{\phi 3}(\rho, z + d) &= \frac{k_0^2}{2} \int_0^\infty \gamma_0^{-1} (P_3 - 1) [J_0(\lambda \rho) \pm J_2(\lambda \rho)] e^{i\gamma_0(z+d)} \lambda d\lambda, \end{aligned} \quad (3.18)$$

$$\begin{aligned} G_{\rho 2}(\rho, z + d) &= -\frac{1}{2} \int_0^\infty (Q_3 + 1) [J_0(\lambda \rho) \pm J_2(\lambda \rho)] e^{i\gamma_0(z+d)} \lambda d\lambda, \\ G_{\phi 2}(\rho, z + d) &= -\frac{1}{2} \int_0^\infty (Q_3 + 1) [J_0(\lambda \rho) \pm J_2(\lambda \rho)] e^{i\gamma_0(z+d)} \lambda d\lambda, \end{aligned} \quad (3.19)$$

$$\begin{aligned} G_{\rho 3}(\rho, z + d) &= \frac{1}{2} \int_0^\infty (P_3 - 1) [J_0(\lambda \rho) \mp J_2(\lambda \rho)] e^{i\gamma_0(z+d)} \lambda d\lambda, \\ G_{\phi 3}(\rho, z + d) &= \frac{1}{2} \int_0^\infty (P_3 - 1) [J_0(\lambda \rho) \mp J_2(\lambda \rho)] e^{i\gamma_0(z+d)} \lambda d\lambda, \end{aligned} \quad (3.20)$$

$$F_{z1}(\rho, z + d) = \int_0^\infty (Q_3 + 1) J_1(\lambda \rho) e^{i\gamma_0(z+d)} \lambda^2 d\lambda, \quad (3.21)$$

$$G_{z1}(\rho, z + d) = - \int_0^\infty (P_3 - 1) \gamma_0^{-1} J_1(\lambda \rho) e^{i\gamma_0(z+d)} \lambda^2 d\lambda. \quad (3.22)$$

The integrals F_{z1} , $F_{\rho 2}$, $F_{\phi 2}$, $G_{\rho 2}$, and $G_{\phi 2}$ involving $(Q_3 + 1)$ are defined as the terms of the electric-type field, also known as the transverse magnetic (TM) field. The integrals G_{z1} , $F_{\rho 3}$, $F_{\phi 3}$, $G_{\rho 3}$, and $G_{\phi 3}$ involving $(P_3 - 1)$ are defined as the terms of the magnetic-type field, also known as the transverse electric (TE) field. The factors $(Q_3 + 1)$ and $(P_3 - 1)$ are expressed as follows:

$$\frac{\gamma_0}{2} (Q_3 + 1) = -i \frac{k_0^2 \gamma_0 \gamma_1 \tan(\gamma_1 l)}{k_1^2 \gamma_0 - i k_0^2 \gamma_1 \tan(\gamma_1 l)}, \quad (3.23)$$

$$\frac{k_0^2}{2\gamma_0} (P_3 - 1) = i \frac{k_0^2 \tan(\gamma_1 l)}{\gamma_1 - i \gamma_0 \tan(\gamma_1 l)}, \quad (3.24)$$

where

$$\gamma_1^2 = k_1^2 - \lambda^2; \quad \text{Im}\{\gamma_1\} \geq 0, \quad (3.25)$$

$$\gamma_0^2 = k_0^2 - \lambda^2; \quad \text{Im}\{\gamma_0\} \geq 0, \quad (3.26)$$

$$\lambda^2 = k_x^2 + k_y^2, \quad (3.27)$$

$$k_1^2 = k_0^2 \varepsilon_1, \quad (3.28)$$

$$k_0 = \omega \sqrt{\mu_0 \varepsilon_0} = 2\pi/\lambda_0, \quad (3.29)$$

$$\omega = 2\pi f, \quad (3.30)$$

where f is the frequency and λ_0 is the wavelength in air.

3.2.2 Evaluation for the Electric-Type Field

Because all integrands including Bessel functions $J_j(\lambda\rho)$ ($j = 0, 1, 2$) in Eqs. (3.17)~(3.22) are highly oscillatory, these integrals converge very slowly. This requires more sampling points in the numerical integration. In this section these integrals will be evaluated by using an analytical technique. Considering γ_0 , γ_1 , and γ_1 are even functions of λ , use is made of the following relations between a Bessel function and Hankel function

$$J_n(\lambda\rho) = \frac{1}{2} \left[H_n^{(1)}(\lambda\rho) + H_n^{(2)}(\lambda\rho) \right], \quad (3.31)$$

$$H_n^{(1)}(-\lambda\rho) = (-1)^{n+1} H_n^{(2)}(\lambda\rho), \quad (3.32)$$

Eq. (3.17) can be rewritten in the form

$$\frac{F_{\rho_2}}{F_{\phi_2}} = \frac{1}{4} \int_{-\infty}^{\infty} \gamma_0(Q_3 + 1) e^{i\gamma_0(z+d)} \left[H_0^{(1)}(\lambda\rho) \mp H_2^{(1)}(\lambda\rho) \right] \lambda d\lambda. \quad (3.33)$$

Substituting Eq. (3.23) into Eq. (3.33), we get

$$\frac{F_{\rho_2}}{F_{\phi_2}} = -\frac{ik_0^2}{2} \int_{-\infty}^{\infty} \frac{\gamma_1\gamma_0 \tan(\gamma_1 l) e^{i\gamma_0(z+d)}}{k_1^2\gamma_0 - ik_0^2\gamma_1 \tan(\gamma_1 l)} \left[H_0^{(1)}(\lambda\rho) \mp H_2^{(1)}(\lambda\rho) \right] \lambda d\lambda. \quad (3.34)$$

Following the similar manner as addressed in Chapter 2, the integrals in Eq. (3.34) can be evaluated readily. In order to evaluate the above integrals, we shift the contour around the branch cuts at $\lambda = k_0$ and $\lambda = k_1$. The poles of the integrands satisfy the following equation

$$q(\lambda) = k_1^2\gamma_0 - ik_0^2\gamma_1 \tan(\gamma_1 l) = 0. \quad (3.35)$$

It is seen that the pole equation is the same as that for the electromagnetic field of a vertical dipole over the dielectric-coated perfect conductor, as addressed in Sec. 2.3. Naturally, when the condition for the dielectric layer

$$n\pi < \sqrt{k_1^2 - k_0^2}l < (n+1)\pi, \quad (3.36)$$

is satisfied, Eq. (3.35) has $n+1$ roots. Correspondingly, the integrand in Eq. (3.34) has $n+1$ poles. Namely, the trapped surface wave includes $(n+1)$ modes. Assuming that λ_{jE}^* is the j -th root of Eq. (3.35), and

$$\gamma_{0E}^* = \sqrt{k_0^2 - \lambda_{jE}^{*2}}, \quad (3.37)$$

$$\gamma_{1E}^* = \sqrt{k_1^2 - \lambda_{jE}^{*2}}, \quad (3.38)$$

F_{ρ_2} and F_{ϕ_2} are rewritten in the forms

$$\begin{aligned}
\frac{F_{\rho_2}}{F_{\phi_2}} &= \pi k_0^2 \sum_j \frac{\gamma_0^* \gamma_{1E}^* \tan(\gamma_{1E}^* l)}{q'(\lambda_{jE}^*)} e^{i\gamma_{0E}^*(z+d)} \lambda_{jE}^* \left[H_0^{(1)}(\lambda_{jE}^* \rho) \mp H_2^{(1)}(\lambda_{jE}^* \rho) \right] \\
&\quad - \frac{ik_0^2}{2} \int_{\Gamma_0 + \Gamma_1} \frac{\gamma_1 \gamma_0 \tan(\gamma_1 l) e^{i\gamma_0(z+d)}}{k_1^2 \gamma_0 - ik_0^2 \gamma_1 \tan(\gamma_1 l)} \left[H_0^{(1)}(\lambda \rho) \mp H_2^{(1)}(\lambda \rho) \right] \lambda d\lambda,
\end{aligned} \tag{3.39}$$

where

$$q'(\lambda_{jE}^*) = -\frac{k_1^2 \lambda_{jE}^*}{\gamma_{0E}^*} + i \frac{k_0^2 \lambda_{jE}^*}{\gamma_{1E}^*} \left[\tan(\gamma_{1E}^* l) + \gamma_{1E}^* l \sec^2(\gamma_{1E}^* l) \right]. \tag{3.40}$$

In what follows we will evaluate the integrals along the branch lines Γ_0 and Γ_1 . Because the phase of the branch cut γ_1 remains the same value on both sides of Γ_1 , it is seen that the evaluation of the integrals in Eq. (3.39) along the branch line Γ_1 is zero. Taking into account the conditions of $k_0 \rho \gg 1$ and $z + d \ll \rho$, the dominant contribution of the integral in Eq. (3.39) along the branch line Γ_0 comes from the vicinity of k_0 . It is noted that the parameter $\lambda = k_0(1 + i\tau^2)$ is used for the integration. At the vicinity of k_0 , γ_0 and γ_1 are approximated by

$$\gamma_0 \approx \sqrt{2} k_0 e^{i\frac{3\pi}{4}} \tau, \tag{3.41}$$

$$\gamma_1 \approx \sqrt{k_1^2 - k_0^2}. \tag{3.42}$$

Let

$$A = \frac{k_0}{k_1^2} \sqrt{k_1^2 - k_0^2} \tan \left(\sqrt{k_1^2 - k_0^2} l \right), \tag{3.43}$$

the integral in Eq. (3.39) is evaluated readily.

$$\begin{aligned}
& -\frac{ik_0^2}{2} \int_{\Gamma_0} \frac{\gamma_1 \gamma_0 \tan(\gamma_1 l)}{k_1^2 \gamma_0 - ik_0^2 \gamma_1 \tan(\gamma_1 l)} e^{i\gamma_0(z+d)} \left[H_0^{(1)}(\lambda \rho) \mp H_2^{(1)}(\lambda \rho) \right] \lambda d\lambda \\
&= 2e^{-i\frac{\pi}{4}} k_0^3 A \sqrt{\frac{2}{\pi k_0 \rho}} e^{ik_0 r_2} \left(-\frac{1}{k_0 \rho} \right) \\
&\quad \times \left\{ -e^{i\frac{\pi}{4}} \sqrt{\frac{\pi}{2k_0 \rho}} \left(\frac{z+d}{\rho} + iA \right) + \frac{\pi}{2} A^2 \exp \left[-i \frac{k_0 \rho}{2} \left(\frac{z+d}{\rho} - iA \right)^2 \right] \right. \\
&\quad \left. \times \operatorname{erfc} \sqrt{-i \frac{k_0 \rho}{2} \left(\frac{z+d}{\rho} - iA \right)^2} \right\},
\end{aligned} \tag{3.44}$$

where the error function “erfc” is defined by

$$\operatorname{erfc}(x) = - \int_x^\infty e^{-t^2} dt. \tag{3.45}$$

Therefore, the final formula of Eq. (3.39) is obtained in the form

$$\begin{aligned}
 \frac{F_{\rho_2}}{F_{\phi_2}} &= \pi k_0^2 \sum_j \frac{\gamma_{0E}^* \gamma_{1E}^* \tan(\gamma_{1E}^* l)}{q'(\lambda_{jE}^*)} e^{i\gamma_{0E}^*(z+d)} \lambda_{jE}^* \left[H_0^{(1)}(\lambda_{jE}^* \rho) \mp H_2^{(1)}(\lambda_{jE}^* \rho) \right] \\
 &\quad + 2e^{-i\frac{\pi}{4}} k_0^3 A \sqrt{\frac{2}{\pi k_0 \rho}} e^{ik_0 r_2} \left(-\frac{1}{k_0 \rho} \right) \\
 &\quad \times \left\{ -e^{i\frac{\pi}{4}} \sqrt{\frac{\pi}{2k_0 \rho}} \left(\frac{z+d}{\rho} + iA \right) + \frac{\pi}{2} A^2 \exp \left[-i \frac{k_0 \rho}{2} \left(\frac{z+d}{\rho} - iA \right)^2 \right] \right. \\
 &\quad \left. \times \operatorname{erfc} \sqrt{-i \frac{k_0 \rho}{2} \left(\frac{z+d}{\rho} - iA \right)^2} \right\}. \tag{3.46}
 \end{aligned}$$

With similar steps, the remaining terms are expressed as follows:

$$\begin{aligned}
 \frac{G_{\rho_2}}{G_{\phi_2}} &= \pi k_0^2 \sum_j \frac{\gamma_{1E}^* \tan(\gamma_{1E}^* l)}{q'(\lambda_{jE}^*)} e^{i\gamma_{0E}^*(z+d)} \lambda_{jE}^* \left[H_0^{(1)}(\lambda_{jE}^* \rho) \pm H_2^{(1)}(\lambda_{jE}^* \rho) \right] \\
 &\quad - 2k_0^2 A \sqrt{\frac{1}{\pi k_0 \rho}} e^{ik_0 r_2} \left(-\frac{i}{k_0 \rho} \right) \\
 &\quad \times \left\{ \sqrt{\frac{\pi}{k_0 \rho}} + \frac{\pi}{\sqrt{2}} e^{i\frac{\pi}{4}} A \exp \left[-i \frac{k_0 \rho}{2} \left(\frac{z+d}{\rho} - iA \right)^2 \right] \right. \\
 &\quad \left. \times \operatorname{erfc} \sqrt{-i \frac{k_0 \rho}{2} \left(\frac{z+d}{\rho} - iA \right)^2} \right\}, \tag{3.47}
 \end{aligned}$$

$$\begin{aligned}
 F_{z_1} &= 2\pi k_0^2 \sum_j \frac{\gamma_{1E}^* \tan(\gamma_{1E}^* l)}{q'(\lambda_{jE}^*)} e^{i\gamma_{0E}^*(z+d)} \lambda_{jE}^{*2} H_1^{(1)}(\lambda_{jE}^* \rho) \\
 &\quad + 2ik_0^3 A \sqrt{\frac{1}{\pi k_0 \rho}} e^{ik_0 r_2} \left\{ \sqrt{\frac{\pi}{k_0 \rho}} + \frac{\pi e^{i\frac{\pi}{4}}}{\sqrt{2}} A \exp \left[-i \frac{k_0 \rho}{2} \left(\frac{z+d}{\rho} - iA \right)^2 \right] \right. \\
 &\quad \left. \times \operatorname{erfc} \sqrt{-i \frac{k_0 \rho}{2} \left(\frac{z+d}{\rho} - iA \right)^2} \right\}. \tag{3.48}
 \end{aligned}$$

It is seen that all first terms in Eqs. (3.46)~(3.48) are the sum of residues of the poles λ_{jE}^* . Taking into account $k_0 < \lambda_{jE}^* < k_1$, $\gamma_{0E}^* = \sqrt{k_0^2 - \lambda_{jE}^{*2}}$ has a positive imaginary part. When ε_1 is real, γ_{0E}^* is a positive imaginary number. Thus the factor $e^{i\gamma_{0E}^*(z+d)}$ will be an attenuation factor. When the dipole or observation point in the air moves away from the air-dielectric boundary, all terms which contain $e^{i\gamma_{0E}^*(z+d)}$ will decrease exponentially as $e^{\sqrt{\lambda_{jE}^{*2} - k_0^2}(z+d)}$ in the \hat{z} direction. In Eqs. (3.46)~(3.48), the approximate representations of three Hankel functions $H_0^{(1)}(\lambda_{jE}^* \rho)$, $H_1^{(1)}(\lambda_{jE}^* \rho)$, and $H_2^{(1)}(\lambda_{jE}^* \rho)$ include the

factor $e^{i\lambda_{jE}^*\rho}$, which is the propagation factor in the $\hat{\rho}$ direction with its wave number λ_{jE}^* in the range from k_0 to k_1 . Those terms attenuate as $\rho^{-1/2}$ in the $\hat{\rho}$ direction. From Eqs. (3.46)~(3.48), it is seen that the electric-type lateral wave results from the integration along the branch line Γ_0 and its wave number is k_0 .

3.2.3 Evaluation for the Magnetic-Type Field

The integrals for the magnetic-type field can be treated in a similar manner to the electric-type field. Then, the integral in Eq. (3.18) is rewritten as follows:

$$\frac{F_{\rho_3}}{F_{\phi_3}} = -\frac{ik_0^2}{2} \int_{-\infty}^{\infty} \frac{\tan(\gamma_1 l) e^{i\gamma_0(z+d)}}{\gamma_1 - i\gamma_0 \tan(\gamma_1 l)} \left[H_0^{(1)}(\lambda\rho) \pm H_2^{(1)}(\lambda\rho) \right] \lambda d\lambda. \quad (3.49)$$

These poles of the integrands in Eq. (3.49) satisfy the following equation:

$$p(\lambda) = \gamma_1 - i\gamma_0 \tan(\gamma_1 l) = 0. \quad (3.50)$$

It should be pointed out that $\lambda = k_1$ is a removable pole, because of both the denominator and numerator of the integrand in Eq. (3.49) being 0. In order to evaluate the integrals in Eq. (3.49), we shift the contour around the branch cuts at $\lambda = k_0$ and $\lambda = k_1$. In the case of positive real λ with $k_0 < \lambda < k_1$, γ_0 is a positive imaginary number and γ_1 is a positive real number. Then,

$$p(\lambda) = \sqrt{k_1^2 - \lambda^2} + \sqrt{\lambda^2 - k_0^2} \tan\left(\sqrt{k_1^2 - \lambda^2} l\right). \quad (3.51)$$

Let

$$A(\lambda) = -\frac{\sqrt{k_1^2 - \lambda^2}}{\sqrt{\lambda^2 - k_0^2}}; \quad (3.52)$$

$$B(\lambda) = \tan\left(\sqrt{k_1^2 - \lambda^2} l\right), \quad (3.53)$$

when $\lambda \rightarrow k_1$, $A(\lambda) \rightarrow 0$, and when $\lambda \rightarrow k_0$, $A(\lambda) \rightarrow -\infty$. If $\sqrt{k_1^2 - k_0^2} l < \frac{\pi}{2}$, $B(\lambda)$ is always positive at $k_0 < \lambda < k_1$, and there is no intersection between $A(\lambda)$ and $B(\lambda)$, as illustrated in Fig. 3.2. Thus, Eq. (3.50) has no root. When $\frac{\pi}{2} < \sqrt{k_1^2 - k_0^2} l < \frac{3\pi}{2}$, there is one intersection point between $A(\lambda)$ and $B(\lambda)$, namely, Eq. (3.50) has one root, as illustrated in Fig. 3.3. When $\frac{3\pi}{2} < \sqrt{k_1^2 - k_0^2} l < \frac{5\pi}{2}$, there are two intersection points between $A(\lambda)$ and $B(\lambda)$. So that Eq. (3.50) has two roots.

In general, when the condition for the dielectric layer

$$\left(n - \frac{1}{2}\right)\pi < \sqrt{k_1^2 - k_0^2} l < \left(n + \frac{1}{2}\right)\pi \quad (3.54)$$

is satisfied, Eq. (3.50) has n roots. Correspondingly, the integrand in Eq. (3.49) has n poles. Assuming that λ_{jB}^* is the j -th pole, Eq. (3.49) can be rewritten in the form

$$\begin{aligned} \frac{F_{\rho_3}}{F_{\phi_3}} = & \pi k_0^2 \sum_j \frac{\tan(\gamma_{1B}^* l) e^{i\gamma_{0B}^*(z+d)}}{p'(\lambda_{jB}^*)} \lambda_{jB}^* \left[H_0^{(1)}(\lambda_{jB}^* \rho) \pm H_2^{(1)}(\lambda_{jB}^* \rho) \right] \\ & - \frac{ik_0^2}{2} \int_{\Gamma_0 + \Gamma_1} \frac{\tan(\gamma_1 l) e^{i\gamma_0(z+d)}}{\gamma_1 - i\gamma_0 \tan(\gamma_1 l)} \left[H_0^{(1)}(\lambda \rho) \pm H_2^{(1)}(\lambda \rho) \right] \lambda d\lambda, \end{aligned} \quad (3.55)$$

where

$$p'(\lambda_{jB}^*) = -\frac{\lambda_{jB}^*}{\gamma_{1B}^*} + i\lambda_{jB}^* \left[\frac{\tan(\gamma_{1B}^* l)}{\gamma_{0B}^*} + \frac{\gamma_{0B}^* l}{\gamma_{1B}^*} \sec^2(\gamma_{1B}^* l) \right], \quad (3.56)$$

$$\gamma_{1B}^* = \sqrt{k_1^2 - \lambda_{jB}^{*2}}, \quad (3.57)$$

$$\gamma_{0B}^* = \sqrt{k_0^2 - \lambda_{jB}^{*2}}. \quad (3.58)$$

Next, we will evaluate the integral along the branch lines Γ_0 and Γ_1 . Similar to the evaluation of integrals along the branch line Γ_1 for the electric-type field, the evaluation of the integrals in Eq. (3.55) along the branch line Γ_1 is zero, too. Since $k_0 \rho \gg 1$ and $z + d \ll \rho$, it is seen evidently that the dominant contribution of the integral in Eq. (3.55) comes from the vicinity of k_0 . Assuming

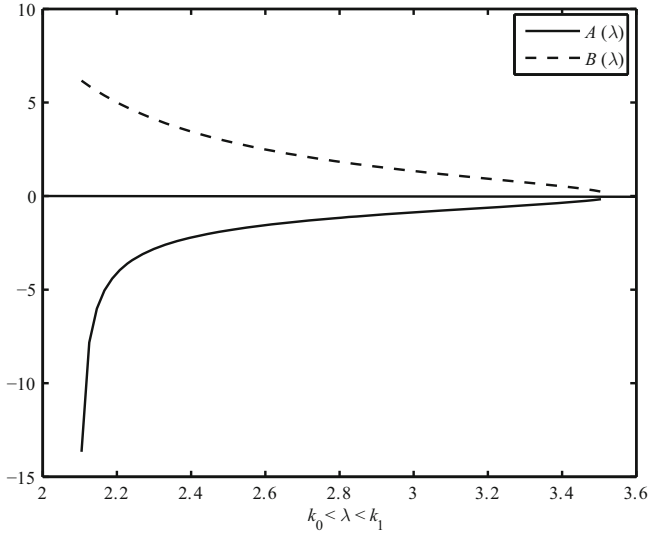


Fig. 3.2. Roots of Eq. (3.50) with $f = 100\text{MHz}$, $\varepsilon_1 = 2.85$, and $\sqrt{k_1^2 - k_0^2}l < \frac{\pi}{2}$

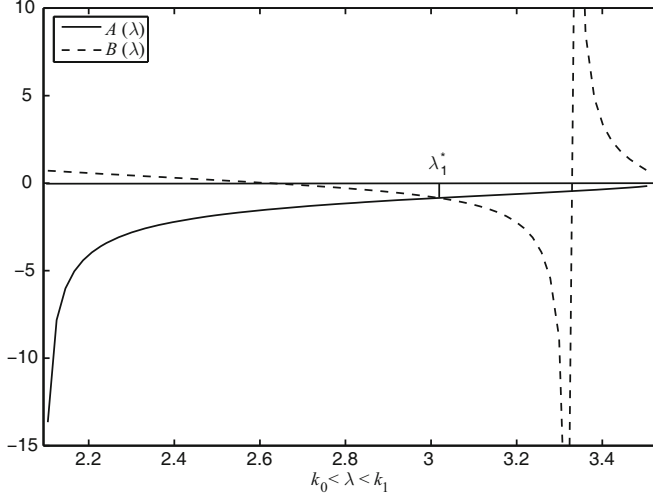


Fig. 3.3. Roots of Eq. (3.50) with $f = 100\text{MHz}$, $\varepsilon_1 = 2.85$, and $\frac{\pi}{2} < \sqrt{k_1^2 - k_0^2}l < \frac{3\pi}{2}$

$$T = \frac{\sqrt{k_1^2 - k_0^2}}{k_0 \tan\left(\sqrt{k_1^2 - k_0^2}l\right)}, \quad (3.59)$$

the integral in Eq. (3.55) is evaluated as follows:

$$\begin{aligned} & \frac{-ik_0^2}{2} \int_{\Gamma_0} \frac{\tan(\gamma_1 l) e^{i\gamma_0(z+d)}}{\gamma_1 - i\gamma_0 \tan(\gamma_1 l)} \left[H_0^{(1)}(\lambda\rho) \pm H_2^{(1)}(\lambda\rho) \right] \lambda d\lambda \\ &= -2ik_0^3 \sqrt{\frac{1}{\pi k_0 \rho}} e^{ik_0 r_2} \left\{ \sqrt{\frac{\pi}{k_0 \rho}} - \frac{i\pi e^{-i\frac{\pi}{4}}}{\sqrt{2}} T \exp \left[-i \frac{k_0 \rho}{2} \left(\frac{z+d}{\rho} + iT \right)^2 \right] \right. \\ & \quad \left. \times \operatorname{erfc} \left[\sqrt{-i \frac{k_0 \rho}{2} \left(\frac{z+d}{\rho} + iT \right)^2} \right] \right\} \begin{pmatrix} -\frac{i}{k_0 \rho} \\ 1 \end{pmatrix}. \end{aligned} \quad (3.60)$$

Then, we have

$$\begin{aligned} \frac{F_{\rho_3}}{F_{\phi_3}} &= \pi k_0^2 \sum_j \frac{\tan(\gamma_{1B}^* l) e^{i\gamma_{0B}^*(z+d)}}{p'(\lambda_{jB}^*)} \lambda_{jB}^* \left[H_0^{(1)}(\lambda_{jB}^* \rho) \pm H_2^{(1)}(\lambda_{jB}^* \rho) \right] \\ & \quad - 2ik_0^3 \sqrt{\frac{1}{\pi k_0 \rho}} e^{ik_0 r_2} \begin{pmatrix} -\frac{i}{k_0 \rho} \\ 1 \end{pmatrix} \\ & \quad \times \left\{ \sqrt{\frac{\pi}{k_0 \rho}} - \frac{\pi T}{\sqrt{2}} e^{i\frac{\pi}{4}} - 2ik_0^3 \sqrt{\frac{1}{\pi k_0 \rho}} e^{ik_0 r_2} \exp \left[-i \frac{k_0 \rho}{2} \left(\frac{z+d}{\rho} + iT \right)^2 \right] \right. \\ & \quad \left. \times \begin{pmatrix} -\frac{i}{k_0 \rho} \\ 1 \end{pmatrix} \operatorname{erfc} \sqrt{-\frac{ik_0 \rho}{2} \left(\frac{z+d}{\rho} + iT \right)^2} \right\}. \end{aligned} \quad (3.61)$$

Similarly, we get

$$\begin{aligned}
 \frac{G_{\rho_3}}{G_{\phi_3}} &= \pi \sum_j \frac{\gamma_{0B}^* \tan(\gamma_{1B}^* l) e^{i\gamma_{0B}^* (z+d)}}{p'(\lambda_{jB}^*)} \lambda_{jB}^* \left[H_0^{(1)}(\lambda_{jB}^* \rho) \mp H_2^{(1)}(\lambda_{jB}^* \rho) \right] \\
 &\quad + 2k_0^2 e^{i\frac{\pi}{4}} \sqrt{\frac{2}{\pi k_0 \rho}} e^{ik_0 r_2} \left(-\frac{1}{k_0 \rho} \right) \\
 &\quad \times \left\{ -\frac{e^{i\frac{\pi}{4}}}{\sqrt{2}} \left(\frac{z+d}{2} - iT \right) \sqrt{\frac{\pi}{k_0 \rho}} + \frac{\pi T^2}{2} \exp \left[-i \frac{k_0 \rho}{2} \left(\frac{z+d}{\rho} + iT \right)^2 \right] \right. \\
 &\quad \left. \times \operatorname{erfc} \sqrt{-i \frac{k_0 \rho}{2} \left(\frac{z+d}{\rho} + iT \right)^2} \right\}, \tag{3.62}
 \end{aligned}$$

$$\begin{aligned}
 G_{z_1} &= 2\pi \sum_j \frac{\tan(\gamma_{1B}^* l) e^{i\gamma_{0B}^* (z+d)}}{p'(\lambda_{jB}^*)} \lambda_{jB}^{*2} H_1^{(1)}(\lambda_{jB}^* \rho) \\
 &\quad - 2k_0^2 \sqrt{\frac{1}{\pi k_0 \rho}} \left\{ \sqrt{\frac{\pi}{k_0 \rho}} - \frac{\pi T}{\sqrt{2}} e^{i\frac{\pi}{4}} \exp \left[-i \frac{k_0 \rho}{2} \left(\frac{z+d}{\rho} + iT \right)^2 \right] \right. \\
 &\quad \left. \times \operatorname{erfc} \sqrt{-i \frac{k_0 \rho}{2} \left(\frac{z+d}{\rho} + iT \right)^2} \right\} e^{ik_0 r_2}. \tag{3.63}
 \end{aligned}$$

Similar to the electric-type trapped surface wave, the magnetic-type trapped surface wave decreases exponentially as $e^{\sqrt{\lambda_{jB}^{*2} - k_0^2} (z+d)}$ in the \hat{z} direction and attenuates as $\rho^{-1/2}$ in the $\hat{\rho}$ direction. The factor $e^{i\lambda_{jB}^* \rho}$ is the propagation factor in the $\hat{\rho}$ direction with its wave number λ_{jB}^* . From Eqs. (3.61)~(3.63), it is seen that the magnetic-type lateral wave results from the integration along the branch line Γ_0 and its wave number is k_0 .

3.2.4 New Techniques for Determining the Poles λ_E and λ_B

In this section we will analyze the pole equations for both electric-type and magnetic-type waves. From Eq. (3.35), it follows that

$$\frac{d\lambda}{dl} = \frac{k_0^2 (k_1^2 - \lambda^2) \sec^2(\sqrt{k_1^2 - \lambda^2} l)}{\frac{k_1 \lambda}{\sqrt{\lambda^2 - k_0^2}} + k_0^2 \tan(\sqrt{k_1^2 - \lambda^2} l) + k_0^2 l \lambda \sec^2(\sqrt{k_1^2 - \lambda^2} l)}, \tag{3.64}$$

and

$$\tan \left(\sqrt{k_1^2 - \lambda^2} l \right) = \frac{k_1^2 \sqrt{\lambda^2 - k_0^2}}{k_0^2 \sqrt{k_1^2 - \lambda^2}}. \tag{3.65}$$

Substituting Eq. (3.65) into Eq. (3.64), and considering that k_1 is a real number, it is seen that all the terms to the right of Eq. (3.64) are positive

because the poles λ_{jE} are between k_0 and k_1 . So $\sqrt{k_1^2 - \lambda^2}l$ is always positive, and it means that $\frac{d\lambda}{dl} > 0$. Then it is known that λ_{jE} increases as l in the interval $n\pi < \sqrt{k_1^2 - k_0^2}l < (n+1)\pi$. When the condition $\sqrt{k_1^2 - k_0^2}l < 0.6$ is satisfied, the approximate formula of the pole for the electric-type wave can be obtained readily.

$$\lambda_E = k_0 + \frac{\left[-k_1^2\sqrt{2k_0} + \sqrt{2k_1^4k_0 + 8k_0^5(k_1^2 - k_0^2)l^2}\right]^2}{16k_0^6l^2}. \quad (3.66)$$

Similarly, Eq. (3.50) can be rewritten in the form

$$\sqrt{k_1^2 - \lambda^2} \tan\left(\sqrt{k_1^2 - k_0^2}l - \frac{\pi}{2}\right) - \sqrt{\lambda^2 - k_0^2} = 0. \quad (3.67)$$

Then,

$$\frac{d\lambda}{dl} = \frac{\sqrt{k_1^2 - \lambda^2}\sqrt{\lambda^2 - k_0^2}\sec^2(\sqrt{k_1^2 - \lambda^2}l)}{\frac{\lambda}{\sqrt{k_1^2 - \lambda^2}} + \frac{\lambda l \sqrt{\lambda^2 - k_0^2}\sec^2(\sqrt{k_1^2 - \lambda^2}l)}{\sqrt{k_1^2 - \lambda^2}} - \frac{\lambda \tan(\sqrt{k_1^2 - \lambda^2}l)}{\sqrt{\lambda^2 - k_0^2}}}, \quad (3.68)$$

and

$$\tan\left(\sqrt{k_1^2 - k_0^2}l\right) = -\frac{\sqrt{k_1^2 - \lambda^2}}{\sqrt{\lambda^2 - k_0^2}}. \quad (3.69)$$

Substituting Eq. (3.69) into Eq. (3.68), and considering that k_1 is a real number, it is easily verified that $\frac{d\lambda}{dl} > 0$ in the case of $k_0 < \lambda < k_1$. When the condition $0 < \sqrt{k_1^2 - k_0^2}l - \pi/2 \ll 1$ is satisfied, we have

$$\tan\left(\sqrt{k_1^2 - k_0^2}l - \frac{\pi}{2}\right) \approx \sqrt{k_1^2 - k_0^2}l - \frac{\pi}{2}. \quad (3.70)$$

From Eq. (3.68), after algebraic manipulation, the approximate formula of the pole for the magnetic-type wave is obtained readily.

$$\lambda_B = k_0 + \frac{(\sqrt{2k_0} - \sqrt{2k_0 - 4A_bB_b})^2}{4B_b^2}, \quad (3.71)$$

where

$$A_b = \sqrt{k_1^2 - k_0^2} \left(\sqrt{k_1^2 - k_0^2}l - \frac{\pi}{2}\right), \quad (3.72)$$

$$B_b = \frac{\pi}{2} \frac{k_0}{\sqrt{k_1^2 - k_0^2}} - 2k_0l. \quad (3.73)$$

As shown in Fig. 3.4, it is seen that the approximate values of λ_E are agreement with the corresponding accurate values under the condition $\sqrt{k_1^2 - k_0^2}l < 0.6$ for the electric-type wave. Similarly, from Fig. 3.5, it is seen that the approximate values of λ_B are also agreement with the corresponding accurate values under the condition $0 < \sqrt{k_1^2 - k_0^2}l - \pi/2 \ll 1$ for the magnetic-type wave.

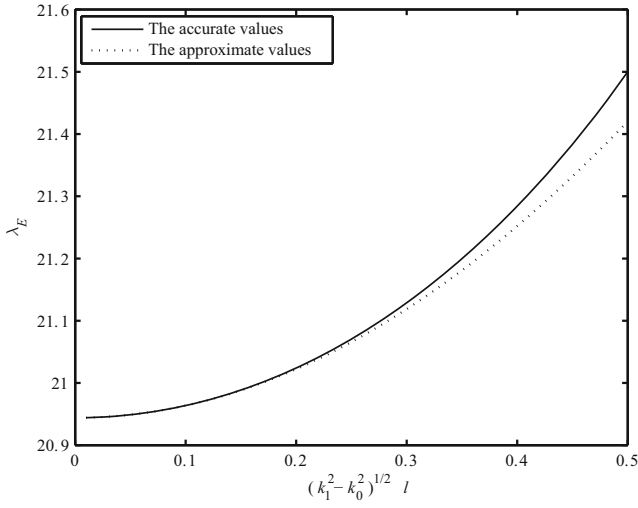


Fig. 3.4. The values of λ versus the thickness l of the dielectric layer for the electric-type wave with $f = 1$ GHz and $\varepsilon_{r1} = 4$

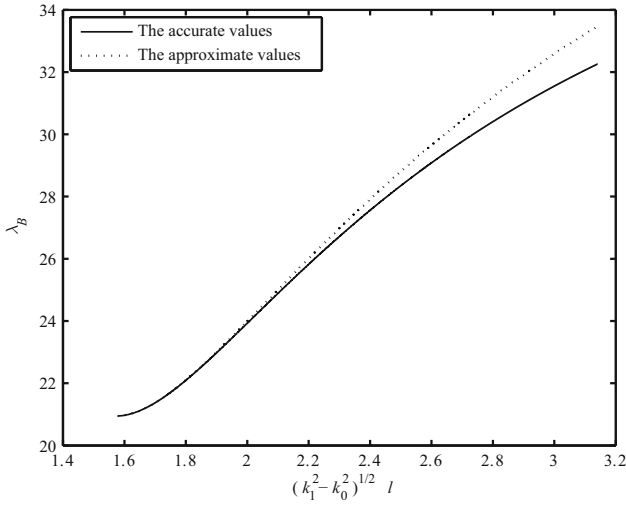


Fig. 3.5. The values of λ versus the thickness l of the dielectric layer for the magnetic-type wave with $f = 1$ GHz and $\varepsilon_{r1} = 4$

3.2.5 Final Formulas for Six Field Components

Using the above derivations for the terms of the trapped surface wave and lateral wave, and the results for the direct and ideal reflected waves addressed in the book (King, Owens, Wu, 1992), the final formulas for the six field components are obtained readily.

$$\begin{aligned}
 E_{0\rho}(\rho, \phi, z) = & -\frac{\omega\mu_0 Idl}{4\pi k_0^2} \cos \phi \\
 & \times \left\{ -\left[\frac{2k_0}{r_1^2} + \frac{2i}{r_1^3} + \left(\frac{z-d}{r_1} \right)^2 \left(\frac{ik_0^2}{r_1} - \frac{3k_0}{r_1^2} - \frac{3i}{r_1^3} \right) \right] e^{ik_0 r_1} \right. \\
 & + \left[\frac{2k_0}{r_2^2} + \frac{2i}{r_2^3} + \left(\frac{z+d}{r_2} \right)^2 \left(\frac{ik_0^2}{r_2} - \frac{3k_0}{r_2^2} - \frac{3i}{r_2^3} \right) \right] e^{ik_0 r_2} \\
 & \left. + F_{\rho 2} + F_{\rho 3} \right\}, \tag{3.74}
 \end{aligned}$$

$$\begin{aligned}
 E_{0\varphi}(\rho, \phi, z) = & -\frac{\omega\mu_0 Idl}{4\pi k_0^2} \sin \phi \\
 & \times \left[-\left(\frac{ik_0^2}{r_1} - \frac{k_0}{r_1^2} - \frac{i}{r_1^3} \right) e^{ik_0 r_1} + \left(\frac{ik_0^2}{r_2} - \frac{k_0}{r_2^2} - \frac{i}{r_2^3} \right) e^{ik_0 r_2} \right. \\
 & \left. + F_{\varphi 2} + F_{\varphi 3} \right], \tag{3.75}
 \end{aligned}$$

$$\begin{aligned}
 E_{0z}(\rho, \phi, z) = & \frac{i\omega\mu_0 Idl}{4\pi k_0^2} \cos \phi \\
 & \times \left[-\left(\frac{\rho}{r_1} \right) \left(\frac{z-d}{r_1} \right) \left(\frac{k_0^2}{r_1} + \frac{3ik_0}{r_1^2} - \frac{3}{r_1^3} \right) e^{ik_0 r_1} + \left(\frac{\rho}{r_2} \right) \right. \\
 & \left. \times \left(\frac{z+d}{r_2} \right) \left(\frac{k_0^2}{r_2} + \frac{3ik_0}{r_2^2} - \frac{3}{r_2^3} \right) e^{ik_0 r_2} + F_{z1} \right], \tag{3.76}
 \end{aligned}$$

$$\begin{aligned}
 B_{0\rho}(\rho, \phi, z) = & \frac{\mu_0 Idl}{4\pi} \sin \phi \\
 & \times \left[\left(\frac{z-d}{r_1} \right) \left(\frac{ik_0}{r_1} - \frac{1}{r_1^2} \right) e^{ik_0 r_1} - \left(\frac{z+d}{r_2} \right) \left(\frac{ik_0}{r_2} - \frac{1}{r_2^2} \right) e^{ik_0 r_2} \right. \\
 & \left. - G_{\rho 2} - G_{\rho 3} \right], \tag{3.77}
 \end{aligned}$$

$$B_{0\phi}(\rho, \phi, z) = \frac{\mu_0 Idl}{4\pi} \cos \phi$$

$$\times \left[\left(\frac{z-d}{r_1} \right) \left(\frac{ik_0}{r_1} - \frac{1}{r_1^2} \right) e^{ik_0 r_1} - \left(\frac{z+d}{r_2} \right) \left(\frac{ik_0}{r_2} - \frac{1}{r_2^2} \right) e^{ik_0 r_2} - G_{\varphi 2} - G_{\varphi 3} \right], \quad (3.78)$$

$$B_{0z}(\rho, \phi, z) = \frac{i\mu_0 I dl}{4\pi} \sin \phi \left[- \left(\frac{\rho}{r_1} \right) \left(\frac{k_0}{r_1} + \frac{i}{r_1^2} \right) e^{ik_0 r_1} + \left(\frac{\rho}{r_2} \right) \left(\frac{ik_0}{r_2} - \frac{1}{r_2^2} \right) e^{ik_0 r_2} + G_{z1} \right]. \quad (3.79)$$

From the above formulas, it is seen that the electromagnetic field includes the direct wave, ideal reflected wave, lateral wave, and trapped surface wave. Both the lateral-wave and trapped-surface-wave terms can be divided into the electric-type and magnetic-type terms.

3.2.6 Computations and Conclusions

With $f = 100$ MHz, $\varepsilon_{r1} = 2.85 + 0.01i$, $k_1 l_1 = 0.8$, and $z = d = 0$ m for the radical electric field components $E_{0\rho}(\rho, 0, z)$ and $E_{0\phi}(\rho, \pi/2, z)$, the total field, the lateral-wave term and trapped-surface-wave terms of electric type and magnetic type are computed and shown in Figs. 3.6 and 3.7, respectively. Similar to those shown in Figs. 3.6 and 3.7, the corresponding results at $z = d = 3$ m are shown in Figs. 3.8 and 3.9, respectively. The magnitudes of $E_{0\rho}(\rho, 0, z)$ and $E_{0\varphi}(\rho, \pi/2, z)$ in V/m at $k_1 l = 0.4\pi$ and $k_1 l = 0.8\pi$ are computed and plotted in Figs. 3.10 and 3.11, respectively.

From the above analysis and computations it is concluded as follows:

- The trapped surface waves of electric type and magnetic type attenuate exponentially as $e^{\sqrt{\lambda_{jE}^{*2} - k_0^2}(z+d)}$ and $e^{\sqrt{\lambda_{jB}^{*2} - k_0^2}(z+d)}$ in the \hat{z} direction, respectively. Therefore, the trapped surface wave can be neglected when the dipole or the observation point moves away and is not too close to the air-dielectric boundary. The wave numbers λ_{jE}^* and λ_{jB}^* of electric-type and magnetic-type trapped surface wave are between k_0 and k_1 and determined by the operating frequency, the permittivity ε_1 , and the thickness of the dielectric layer.
- For the component $E_{0\rho}$, the total field is determined primarily by the trapped surface wave of electric type, and for the component $E_{0\phi}$, the total field is determined primarily by the trapped surface wave of magnetic type.
- When the conditions $k_0 \rho \gg 1$ and $z+d \ll \rho$ are satisfied, both the electric-type and magnetic-type lateral waves with the wave numbers being k_0 can be excited efficiently.

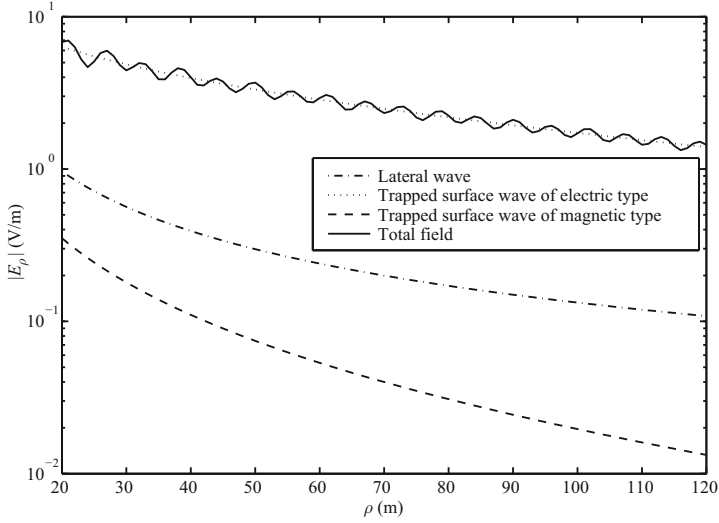


Fig. 3.6. Electric field component $E_{0\rho}(\rho, 0, z)$ in V/m with $f = 100$ MHz, $\varepsilon_{r1} = 2.85 + 0.01i$, $k_1 l_1 = 0.8$, and $z = d = 0$ m, and $\phi = 0$

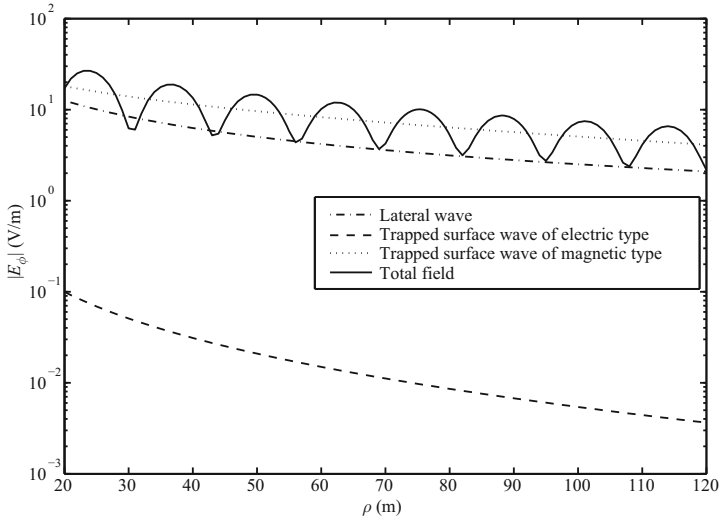


Fig. 3.7. Electric field component $E_{0\phi}(\rho, \pi/2, z)$ in V/m with $f = 100$ MHz, $\varepsilon_{r1} = 2.85 + 0.01i$, $k_1 l_1 = 0.8$, and $z = d = 0$ m, and $\phi = \pi/2$

- It is seen that the electromagnetic field due to a horizontal electric dipole is greatly affected by the thickness of the dielectric layer. When the condition $n\pi < \sqrt{k_1^2 - k_0^2}l < (n+1)\pi$ is satisfied, there are $n+1$ modes of the electric-type trapped surface wave to propagate along the air-dielectric boundary, and there are n modes of the magnetic-type trapped surface

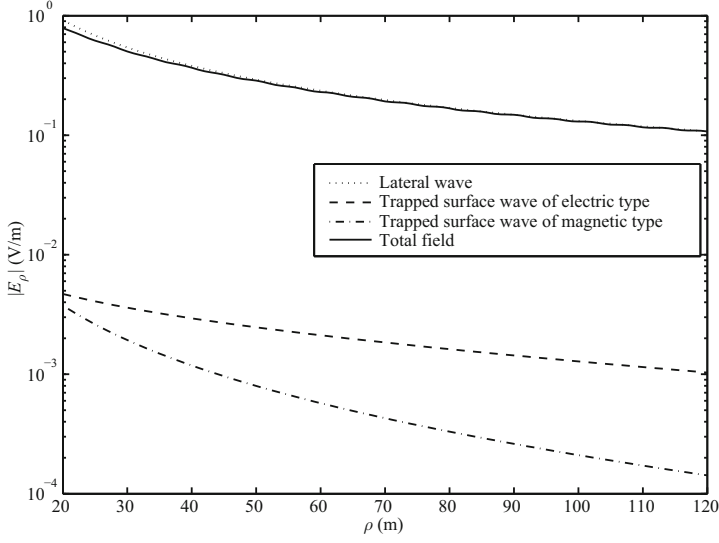


Fig. 3.8. Electric field component $E_{0\rho}(\rho, 0, z)$ in V/m with $f = 100$ MHz, $\varepsilon_{r1} = 2.85 + 0.01i$, $k_1 l_1 = 0.8$, and $z = d = 3$ m, and $\phi = 0$

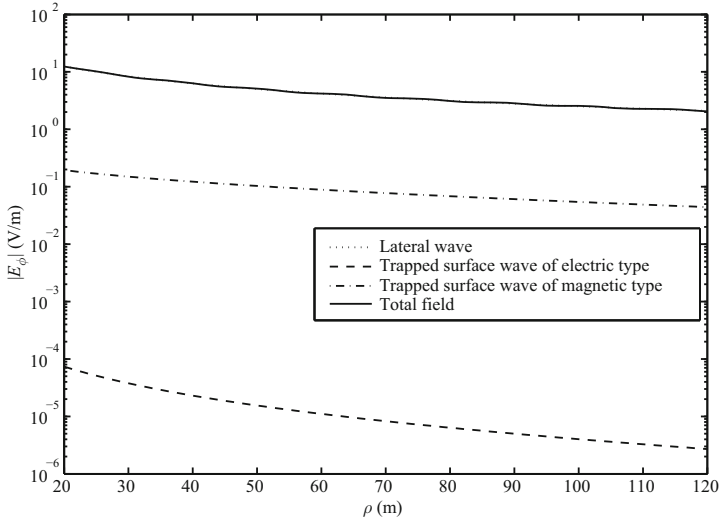


Fig. 3.9. Electric field component $E_{0\phi}(\rho, \pi/2, z)$ in V/m with $f = 100$ MHz, $\varepsilon_{r1} = 2.85 + 0.01i$, $k_1 l_1 = 0.8$, and $z = d = 3$ m, and $\phi = \pi/2$

wave to propagate along the boundary under the condition $(n - \frac{1}{2})\pi < \sqrt{k_1^2 - k_0^2}l < (n + \frac{1}{2})\pi$. It is seen that, in the thick-layer case, the variations of the total field will be more complex.

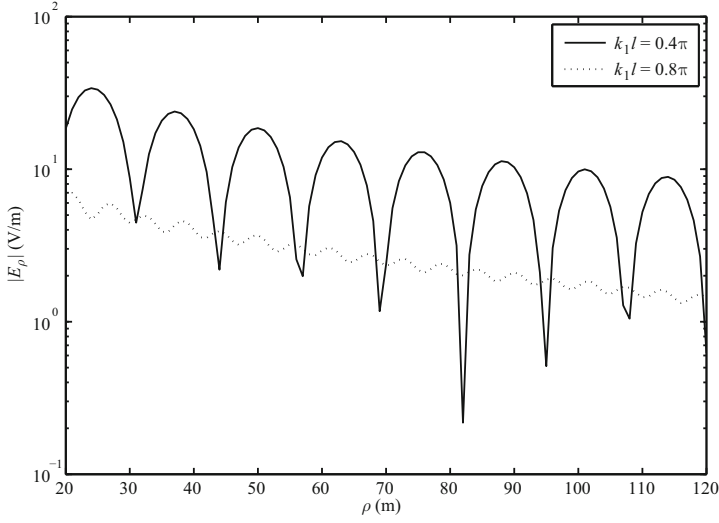


Fig. 3.10. Electric field component $E_{0\rho}(\rho, 0, z)$ in V/m at $k_1 l_1 = 0.4$ and $k_1 l_1 = 0.8$ with $f = 100$ MHz, $\varepsilon_{r1} = 2.85 + 0.01i$, $z = d = 0$ m, and $\phi = 0$

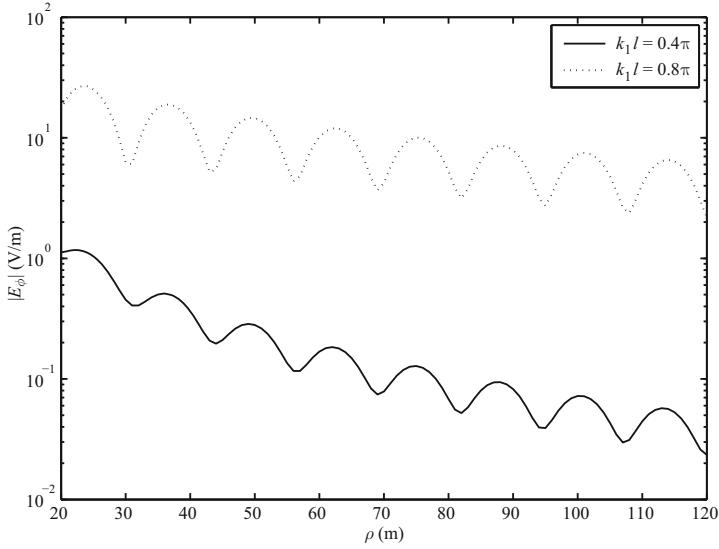


Fig. 3.11. Electric field component $E_{0\phi}(\rho, \pi/2, z)$ in V/m at $k_1 l_1 = 0.4$ and $k_1 l_1 = 0.8$ with $f = 100$ MHz, $\varepsilon_{r1} = 2.85 + 0.01i$, $z = d = 0$ m, and $\phi = \pi/2$

- The results obtained have useful applications in subsurface and close-to-the-surface communication, prospecting and diagnostics for the three-layered planar structure consisting of a perfect conductor coated with a dielectric layer and air above. Furthermore, the present formulas and com-

putations can be extended to the evaluation of the far field for the electrically narrow microstrip line on a uniaxial anisotropic substrate.

3.3 Radiation of Horizontal Electric Dipole and Microstrip Antenna

In this section, based on the results obtained in Sec. 3.2, further developments for the radiation from a horizontal electric dipole in the presence of a three-layered region will be outlined.

3.3.1 Radiation of a Horizontal Electric Dipole

The complete formulas for the electromagnetic field of a horizontal electric dipole in the three-layered region in a cylindrical coordinate system are obtained in this chapter. It is of particular interest when $z + d \ll \rho$. Then, it is known that $r_1 \sim r_0 - d \cos \Theta$, $r_2 \sim r_0 + d \cos \Theta$ in phases and $r_1 \sim r_2 \sim r_0$ in amplitudes. Taking into account the relations between cylindrical coordinates and spherical coordinates, and $\rho = r_0 \sin \Theta$, $z = r_0 \cos \Theta$, we write

$$E_{0r}(r_0, \Theta, \Phi) = E_{0\rho}(\rho, \phi, z) \sin \Theta + E_{0z}(\rho, \phi, z) \cos \Theta, \quad (3.80)$$

$$E_{0\Theta}(r_0, \Theta, \Phi) = E_{0\rho}(\rho, \phi, z) \cos \Theta + E_{0z}(\rho, \phi, z) \sin \Theta, \quad (3.81)$$

$$E_{0\Phi}(r_0, \Theta, \Phi) = E_{0\phi}(\rho, \phi, z), \quad (3.82)$$

$$B_{0r}(r_0, \Theta, \Phi) = B_{0\rho}(\rho, \phi, z) \sin \Theta + B_{0z}(\rho, \phi, z) \cos \Theta, \quad (3.83)$$

$$B_{0\Theta}(r_0, \Theta, \Phi) = B_{0\rho}(\rho, \phi, z) \cos \Theta - B_{0z}(\rho, \phi, z) \sin \Theta, \quad (3.84)$$

$$B_{0\Phi}(r_0, \Theta, \Phi) = B_{0\phi}(\rho, \phi, z). \quad (3.85)$$

When the far-field conditions $|p_1^*| \geq 4$ and $|p_2^*| \geq 4$ are satisfied, the Fresnel-integral terms can be written in the forms

$$iT k_0^2 \sqrt{\frac{\pi}{k_0 \rho}} e^{-ip_1^*} \mathbf{F}(p_1^*) = \frac{ik_0 \rho}{\rho^2} \frac{iT}{iT + (z + d)/\rho} + \frac{iT}{\rho^2} \left[\frac{1}{iT + (z + d)/\rho} \right]^3, \quad (3.86)$$

$$-iA k_0^2 \sqrt{\frac{\pi}{k_0 \rho}} e^{-ip_2^*} \mathbf{F}(p_2^*) = \frac{ik_0 \rho}{\rho^2} \frac{-iA}{-iA + (z + d)/\rho} + \frac{-iA}{\rho^2} \left[\frac{1}{-iA + (z + d)/\rho} \right]^3. \quad (3.87)$$

In practical applications the antenna is usually placed on the surface of the Earth, either as a based-insulated dipole or a monopole base-driven

against a buried ground system. Substituting Eqs. (3.74)~(3.79) into Eqs. (3.80)~(3.85), and considering the case $d/r_0 \sim 0$, $k_0 d \sim 0$, we can obtain the following simplified formulas:

$$\begin{aligned}
 E_{0r}(r_0, \Theta, \Phi) = & -\frac{\omega\mu_0 I dl \cos \Phi}{2\pi k_0^2} e^{ik_0 r_0} \\
 & \times \left\{ \frac{iTk_0 r_0 (\cos \Theta + iT \sin \Theta)^2 + T \sin \Theta}{r_0^3 (\cos \Theta + iT \sin \Theta)^3} - \frac{k_0 + ik_0^2 r_0 A^2 \sin \Theta}{r_0^2 \sin \Theta} \right. \\
 & + \frac{k_0^2 A^2 r_0 (-iA \sin \Theta + \cos \Theta)^2 (i \cos \Theta + A \sin \Theta)}{r_0^2 (-iA \sin \Theta + \cos \Theta)^3} \\
 & \left. + \frac{A^2 k_0 \sin \Theta \cos \Theta - ik_0 A^3 \sin^2 \Theta}{r_0^2 (-iA \sin \Theta + \cos \Theta)^3} \right\} - \frac{\omega\mu_0 I dl \cos \Phi}{4} \\
 & \times \left\{ \sum_j \frac{\gamma_{0E}^* \gamma_{1E}^* \sin \Theta \tan(\gamma_{1E}^* l)}{q'(\lambda_{jE}^*)} e^{i\gamma_{0E}^* r_0 \cos \Theta} \lambda_{jE}^* \right. \\
 & \times \left[H_0^{(1)}(\lambda_{jE}^* r_0 \sin \Theta) - H_2^{(1)}(\lambda_{jE}^* r_0 \sin \Theta) \right] \\
 & - \sum_j \frac{2i \cos \Theta \gamma_{1E}^* \tan(\gamma_{1E}^* l)}{q'(\lambda_{jE}^*)} e^{i\gamma_{0E}^* r_0 \cos \Theta} (\lambda_{jE}^*)^2 \\
 & \times H_1^{(1)}(\lambda_{jE}^* r_0 \sin \Theta) + \sum_j \frac{\tan(\gamma_{1B}^* l) \sin \Theta}{p'(\lambda_{jB}^*)} e^{i\gamma_{0B}^* r_0 \cos \Theta} \\
 & \left. \times \lambda_{jB}^* \left[H_0^{(1)}(\lambda_{jB}^* r_0 \sin \Theta) + H_2^{(1)}(\lambda_{jB}^* r_0 \sin \Theta) \right] \right\}, \quad (3.88)
 \end{aligned}$$

$$\begin{aligned}
 E_{0\Theta}(r_0, \Theta, \Phi) = & -\frac{\omega\mu_0 I dl \cos \Phi}{2\pi k_0^2} e^{ik_0 r_0} \\
 & \times \left\{ -\frac{k_0^2 A r_0 + k_0 \cos \Theta + ik_0^2 A^2 r_0 \sin \Theta \cos \Theta}{r_0^2 \sin^2 \Theta} \right. \\
 & + \frac{k_0^2 r_0 A^2 (\cos \Theta - iA \sin \Theta)^2 (A \cos \Theta - i \sin \Theta)}{r_0^2 (\cos \Theta - iA \sin \Theta)^3} \\
 & + \frac{iTk_0 r_0 \cos \Theta (\cos \Theta + iT \sin \Theta)^2 + T \sin \Theta \cos \Theta}{r_0^3 \sin \Theta (\cos \Theta + iT \sin \Theta)^3} \\
 & \left. - \frac{k_0 A^2 \sin^2 \Theta + iA^3 k_0 \sin \Theta \cos \Theta}{r_0^2 (\cos \Theta - iA \sin \Theta)^3} \right\} - \frac{\omega\mu_0 I dl \cos \Phi}{4} \\
 & \times \left\{ \sum_j \frac{\gamma_{0E}^* \gamma_{1E}^* \tan(\gamma_{1E}^* l)}{q'(\lambda_{jE}^*)} e^{i\gamma_{0E}^* r_0 \cos \Theta} \lambda_{jE}^* \cos \Theta \right.
 \end{aligned}$$

$$\begin{aligned}
 & \times \left[H_0^{(1)}(\lambda_{jE}^* r_0 \sin \Theta) - H_2^{(1)}(\lambda_{jE}^* r_0 \sin \Theta) \right] \\
 & + 2i \sin \Theta \sum_j \frac{\gamma_{1E}^* \tan(\gamma_{1E}^* l)}{q'(\lambda_{jE}^*)} e^{\gamma_{0E}^* r_0 \cos \Theta} (\lambda_{jE}^*)^2 \\
 & \times H_1^{(1)}(\lambda_{jE}^* r_0 \sin \Theta) + \cos \Theta \sum_j \frac{\tan(\gamma_{1B}^* l)}{p'(\lambda_{jB}^*)} e^{i\gamma_{0B}^* r_0 \cos \Theta} \\
 & \times \lambda_{jB}^* \left[H_0^{(1)}(\lambda_{jB}^* r_0 \sin \Theta) + H_2^{(1)}(\lambda_{jB}^* r_0 \sin \Theta) \right] \Bigg\}, \quad (3.89)
 \end{aligned}$$

$$\begin{aligned}
 E_{0\Phi}(r_0, \Theta, \Phi) &= -\frac{\omega \mu_0 I dl \sin \Phi}{2\pi k_0^2} e^{ik_0 r_0} \\
 & \times \left\{ -\frac{ik_0 A^3 r_0 (-iA \sin \Theta + \cos \Theta)^2 + A^3 \sin \Theta}{r_0^3 \sin \Theta (-iA \sin \Theta + \cos \Theta)^3} \right. \\
 & \quad - \frac{k_0^2 T r_0 (iT \sin \Theta + \cos \Theta)^2 - iT k_0 \sin \Theta}{r_0^2 (iT \sin \Theta + \cos \Theta)^3} \\
 & \quad \left. + \frac{k_0 A (i \cos \Theta - A \sin \Theta) - ik_0^2 r_0 \sin^2 \Theta}{r_0^2 \sin^3 \Theta} \right\} - \frac{\omega \mu_0 I dl \sin \Phi}{4} \\
 & \times \left\{ \sum_j \frac{\lambda_{jE}^* \gamma_{0E}^* \gamma_{1E}^* \tan(\gamma_{1E}^* l)}{q'(\lambda_{jE}^*)} e^{i\gamma_{0E}^* r_0 \cos \Theta} \right. \\
 & \quad \times \left[H_0^{(1)}(\lambda_{jE}^* r_0 \sin \Theta) + H_2^{(1)}(\lambda_{jE}^* r_0 \sin \Theta) \right] \\
 & \quad + \sum_j \frac{\lambda_{jB}^* \tan(\gamma_{1B}^* l)}{p'(\lambda_{jB}^*)} e^{\gamma_{0B}^* r_0 \cos \Theta} \\
 & \quad \left. \times \left[H_0^{(1)}(\lambda_{jB}^* r_0 \sin \Theta) - H_2^{(1)}(\lambda_{jB}^* r_0 \sin \Theta) \right] \right\}, \quad (3.90)
 \end{aligned}$$

$$\begin{aligned}
 B_{0r}(r_0, \Theta, \Phi) &= -\frac{\mu_0 I dl \sin \Phi}{2\pi} e^{ik_0 r_0} \\
 & \times \left\{ \frac{iA - k_0 r_0 (T \sin \Theta - i \cos \Theta + \frac{ir_0 \sin \Theta \cos \Theta}{2})}{r_0^2 \sin \Theta} \right. \\
 & \quad + \frac{k_0 T r_0 (iT \sin \Theta + \cos \Theta)^2 (\cos \Theta + iT \sin \Theta)}{r_0^2 (iT \sin \Theta + \cos \Theta)^3} \\
 & \quad + \frac{iA^2 \sin \Theta - k_0 A^2 r_0 (-iA \sin \Theta + \cos \Theta)^2}{k_0 r_0^3 (-iA \sin \Theta + \cos \Theta)^3} \\
 & \quad \left. + \frac{T \sin \Theta (T \sin \Theta - i \cos \Theta)}{r_0^2 (iT \sin \Theta + \cos \Theta)^3} \right\} - \frac{\mu_0 I dl \sin \Phi}{4}
 \end{aligned}$$

$$\begin{aligned}
& \times \left\{ \sum_j \frac{k_0^2 \lambda_{jE}^* \gamma_{1E}^* \sin \Theta \tan(\gamma_{1E}^* l)}{q'(\lambda_{jE}^*)} e^{i\gamma_{0E}^* r_0 \cos \Theta} \right. \\
& \quad \times \left[H_0^{(1)}(\lambda_{jE}^* r_0 \sin \Theta) + H_2^{(1)}(\lambda_{jE}^* r_0 \sin \Theta) \right] \\
& \quad + \sum_j \frac{\lambda_{jB}^* \gamma_{0B}^* \sin \Theta \tan(\gamma_{1B}^* l)}{p'(\lambda_{jB}^*)} e^{i\gamma_{0B}^* r_0 \cos \Theta} \\
& \quad \times \left[H_0^{(1)}(\lambda_{jB}^* r_0 \sin \Theta) - H_2^{(1)}(\lambda_{jB}^* r_0 \sin \Theta) \right] - 2i \cos \Theta \\
& \quad \times \sum_j \frac{\lambda_{jB}^{*2} \tan(\gamma_{1B}^* l)}{p'(\lambda_{jB}^*)} e^{i\gamma_{0B}^* r_0 \cos \Theta} H_1^{(1)}(\lambda_{jB}^* r_0 \sin \Theta) \left. \right\}, \tag{3.91}
\end{aligned}$$

$$\begin{aligned}
B_{0\Theta}(r_0, \Theta, \Phi) = & -\frac{\mu_0 I dl \sin \Phi}{2\pi} e^{ik_0 r_0} \\
& \times \left\{ \frac{iA \cos \Theta - k_0 r_0 \sin \Theta (T \cos \Theta + i \sin \Theta + \frac{ir_0 \cos^2 \Theta}{2})}{r_0^2 \sin^2 \Theta} \right. \\
& + \frac{k_0 T r_0 (iT \sin \Theta + \cos \Theta)^2 (iT \cos \Theta - \sin \Theta)}{r_0^2 (iT \sin \Theta + \cos \Theta)^3} \\
& + \frac{iA^2 \sin \Theta \cos \Theta - k_0 A^2 r_0 \cos \Theta (-iA \sin \Theta + \cos \Theta)^2}{k_0 r_0^3 \sin \Theta (-iA \sin \Theta + \cos \Theta)^3} \\
& \left. + \frac{T \sin \Theta (T \cos \Theta + i \sin \Theta)}{r_0^2 (iT \sin \Theta + \cos \Theta)^3} \right\} - \frac{\mu_0 I dl \sin \Phi}{4} \\
& \times \left\{ \sum_j \frac{k_0^2 \lambda_{jE}^* \gamma_{1E}^* \cos \Theta \tan(\gamma_{1E}^* l)}{q'(\lambda_{jE}^*)} e^{i\gamma_{0E}^* r_0 \cos \Theta} \right. \\
& \quad \times \left[H_0^{(1)}(\lambda_{jE}^* r_0 \sin \Theta) + H_2^{(1)}(\lambda_{jE}^* r_0 \sin \Theta) \right] \\
& \quad + \sum_j \frac{\lambda_{jB}^* \gamma_{0B}^* \cos \Theta \tan(\gamma_{1B}^* l)}{p'(\lambda_{jB}^*)} e^{i\gamma_{0B}^* r_0 \cos \Theta} \\
& \quad \times \left[H_0^{(1)}(\lambda_{jB}^* r_0 \sin \Theta) - H_2^{(1)}(\lambda_{jB}^* r_0 \sin \Theta) \right] \\
& \quad + \sum_j \frac{2i \lambda_{jB}^{*2} \sin \Theta \tan(\gamma_{1B}^* l)}{p'(\lambda_{jB}^*)} e^{i\gamma_{0B}^* r_0 \cos \Theta} \\
& \quad \times H_1^{(1)}(\lambda_{jB}^* r_0 \sin \Theta) \left. \right\}, \tag{3.92}
\end{aligned}$$

$$B_{0\Phi}(r_0, \Theta, \Phi) = -\frac{\mu_0 I dl \cos \Phi}{2\pi} e^{ik_0 r_0}$$

$$\begin{aligned}
& \times \left\{ -\frac{ik_0 A^2 r_0 (-iA \sin \Theta + \cos \Theta)^2 + A^2 \sin \Theta}{r_0^2 (-iA \sin \Theta + \cos \Theta)^3} \right. \\
& + \frac{k_0 T^2 r_0 (iT \sin \Theta + \cos \Theta)^2 - iT^2 \sin \Theta}{k_0 r_0^3 \sin \Theta (iT \sin \Theta + \cos \Theta)^3} e^{ik_0 d \cos \Theta} \\
& \left. - \frac{k_0 A r_0 \sin \Theta + \frac{r_0 \cos \Theta}{2} - iT}{r_0^2 \sin^2 \Theta} \right\} - \frac{\mu_0 I dl \cos \Phi}{4} \\
& \times \left\{ k_0^2 \sum_j \frac{\gamma_{1E}^* \tan(\gamma_{1E}^* l)}{q'(\lambda_{jE}^*)} e^{i\gamma_{0E}^* r_0 \cos \Theta} \lambda_{jE}^* \right. \\
& \times \left[H_0^{(1)}(\lambda_{jE}^* r_0 \sin \Theta) - H_2^{(1)}(\lambda_{jE}^* r_0 \sin \Theta) \right] \\
& + \sum_j \frac{\gamma_{0B}^* \tan(\gamma_{1B}^* l)}{p'(\lambda_{jB}^*)} \lambda_{jB}^* e^{i\gamma_{0B}^* r_0 \cos \Theta} \\
& \left. \times \left[H_0^{(1)}(\lambda_{jB}^* r_0 \sin \Theta) + H_2^{(1)}(\lambda_{jB}^* r_0 \sin \Theta) \right] \right\}. \quad (3.93)
\end{aligned}$$

3.3.2 Microstrip Antenna

The microstrip consists of strip transmission lines and antenna on the surface of a thin dielectric layer coating a highly conducting base, which can be regarded as a perfect conductor. The basic elements are horizontal electric dipoles. In this section we will treat a rectangular patch antenna end-driven by transmission lines, as illustrated in Fig. 3.12. The current-density distribution of a patch antenna with a width $2w$ and length $2h$ has the following form:

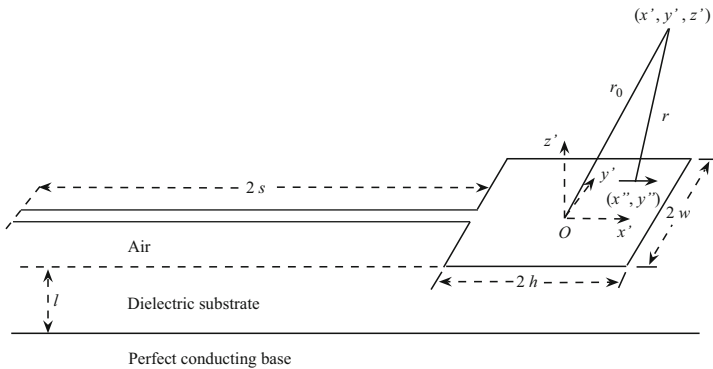


Fig. 3.12. Microstrip patch antenna end-driven by microstrip transmission line

$$J_x(x'', y'') = \frac{I_x(0)}{2w} \cos(k_1 x''); \quad \begin{cases} -h \leq x'' \leq h \\ -w \leq y'' \leq w \end{cases}, \quad (3.94)$$

where $k_1 = k_0 \sqrt{\varepsilon_{r1\text{eff}}}$ is the wave number that would characterize the patch as a segment of a microstrip transmission line for which $\varepsilon_{r1\text{eff}}$ is the relative effective permittivity at the operating frequency, $I_x(0)$ is the total current traversing the center line $x'' = 0$ of the patch. In the present study we assume that the transverse distribution of the \hat{x}' -directed current is uniform. Actually, there is a \hat{y}' -directed current with large peaks at the edges $|y''| = w$ and a minimum at the center $y'' = 0$. Since the impedance of the patch is very large when the driving-point current is small compared to $I_x(0)$, the assumed current in Eq. (3.94) should be a good approximation. The approximate formulas for the characteristic impedance Z_c of the microstrip transmission line and the relative effective permittivity $\varepsilon_{r1\text{eff}}$ were given in Eqs. (3.20)~(3.22) by Hoffman (1987). The relative permittivity $\varepsilon_{r1\text{eff}}$ is approximated as follows:

$$\varepsilon_{r1\text{eff}} = \frac{\varepsilon_{r1} + 1}{2} + \frac{\varepsilon_{r1} - 1}{2} \left(1 + \frac{5l}{w} \right)^{-1/2}. \quad (3.95)$$

In the far-field region, $r \sim r_0 = (x'^2 + y'^2 + z'^2)$ is adequate in amplitudes. In the phases, it is necessary to use the more accurate formula.

$$r \sim (r_0^2 - 2x'x'' - 2y'y'')^{1/2} = r_0 \left(1 - 2\frac{x'x''}{r_0^2} - 2\frac{y'y''}{r_0^2} \right)^{1/2}. \quad (3.96)$$

Following the similar steps addressed in Sec. 15.12 of the book (King, Owens, and Wu, 1992) or in Sec. 9.7 of the book (King, Fikioris, and Mack, 2002), and use is made of the above approximations, the field factor for the patch antenna is written in the following form:

$$\begin{aligned} P(\Theta, \Phi) &= \frac{I_x(0)}{2w} J(x'') J(y'') \\ &= I_x(0) \left[\frac{2k_1 \sin(k_1 h) \cos(k_0 h \sin \Theta \cos \Phi)}{-2k_0 \sin \Theta \cos \Phi \cos(k_1 h) \sin(k_0 h \sin \Theta \cos \Phi)} \right] \\ &\quad \times \left[\frac{\sin(k_0 w \sin \Phi \sin \Theta)}{k_0 w \sin \Phi \sin \Theta} \right]. \end{aligned} \quad (3.97)$$

If h is chosen as $k_1 h = \pi/2$, the field factor in Eq. (3.97) reduces to (15.12.14) in the book (King, Owens, and Wu, 1992) or Eq. (9.159) in the book (King, Fikioris, and Mack, 2002). Multiplying Eqs. (3.89), (3.90), (3.92), and (3.93) by the field factor in Eq. (3.97), the far-field components of the patch antenna are obtained readily.

$$[E_{0\Theta}^r(r_0, \Theta, \Phi)]_p = E_{0\Theta}(r_0, \Theta, \Phi)P(\Theta, \Phi), \quad (3.98)$$

$$[B_{0\Phi}^r(r_0, \Theta, \Phi)]_p = B_{0\Phi}(r_0, \Theta, \Phi)P(\Theta, \Phi), \quad (3.99)$$

$$[E_{0\Phi}^r(r_0, \Theta, \Phi)]_p = E_{0\Phi}(r_0, \Theta, \Phi)P(\Theta, \Phi), \quad (3.100)$$

$$[B_{0\Theta}^r(r_0, \Theta, \Phi)]_p = B_{0\Theta}(r_0, \Theta, \Phi)P(\Theta, \Phi). \quad (3.101)$$

It is noted that the above results are valid in the far-field region and not valid in the intermediate region.

3.3.3 Computations and Discussions

In this section, computations are carried out for high frequency of interest, $f = 1$ GHz. As shown in Figs. 3.13 and 3.14, the total field, both the trapped surface wave of electric type and that of magnetic type, and the lateral wave are calculated from Eq. (3.89) for $E_{0\Theta}^r(r_0, \Theta, \Phi)$ and from Eq. (3.90) for $E_{0\Phi}^r(r_0, \Theta, \Phi)$, respectively. Graphs of the amplitudes of the components $E_{0\Theta}^r(r_0, \Theta, \Phi)$ and $E_{0\Phi}^r(r_0, \Theta, \Phi)$ for a unit horizontal dipole versus the angular degrees of Θ are computed and shown in Figs. 3.15 and 3.16, respectively. It is noted that the DRL waves include the direct wave, ideal reflected wave, and lateral wave. From Figs. 3.13~3.16, it is seen that, for the component $E_{0\Theta}$, the total field is determined primarily by the trapped surface wave of electric type, and for the component $E_{0\Phi}$, the total field is determined primarily by the trapped surface wave of magnetic type when both the dipole and the observation point are located on the air-dielectric boundary.

Graphs of the amplitudes of the components $[E_{0\Theta}^r(r_0, \Theta, \Phi)]_p$ as calculated from Eq. (3.98) and $[E_{0\Phi}^r(r_0, \Theta, \Phi)]_p$ from Eq. (3.99) for the patch antenna versus the angular degrees of Φ are shown in Figs. 3.17 and 3.18, respectively. It is found that the amplitude of the total wave is approximately equal to that of the trapped surface wave under the conditions of $d = 0$ and $\Theta = \pi/2$. This also demonstrates that the total field is determined primarily by the trapped surface wave when both the dipole point and observation point are located on the air-dielectric boundary.

In Figs. 3.19 and 3.20, three-dimensional diagrams of the two components $[E_{0\Theta}^r(r_0, \Theta, \Phi)]_p$ and $[E_{0\Phi}^r(r_0, \Theta, \Phi)]_p$ for a patch antenna are shown, respectively. It is noted that the inner curves in Figs. 3.19 and 3.20 are for $\Theta = 86^\circ$ and the outer curves for $\Theta = 90^\circ$. It is seen that, for the component $[E_{0\Theta}^r(r_0, \Theta, \Phi)]_p$, the radiation of the greatly enlarged region is near $\Theta = \pi/2$ and $\Phi = 0$, or π . For the component $[E_{0\Phi}^r(r_0, \Theta, \Phi)]_p$, the radiation of the greatly enlarged region is near $\Theta = \pi/2$ and $\Phi = \pi/2$.

The field radiation from a patch antenna can be determined in the same manner for other types of load, such as resonant lines with impedance load and matched line with travelling-wave currents.

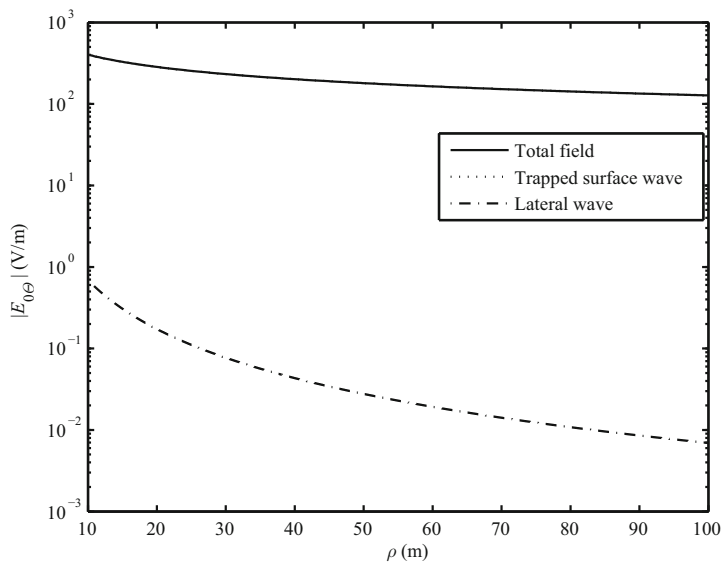


Fig. 3.13. Electric field component $E_{0\theta}$ in V/m with $f = 1$ GHz, $\varepsilon_{r1} = 2$, $l = 0.1$ m, $d = z = 0$ m, and $\Phi = 0$

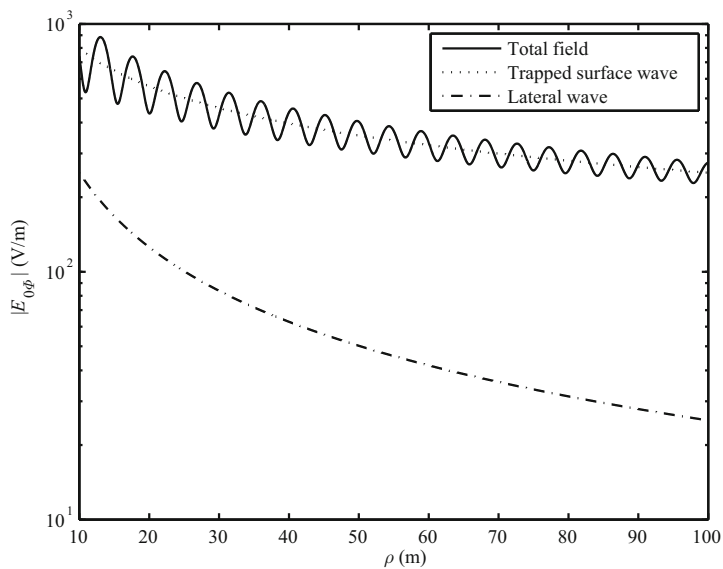


Fig. 3.14. Electric field component $E_{0\phi}$ in V/m with $f = 1$ GHz, $\varepsilon_{r1} = 2$, $l = 0.1$ m, $d = z = 0$ m, and $\Phi = \pi/2$

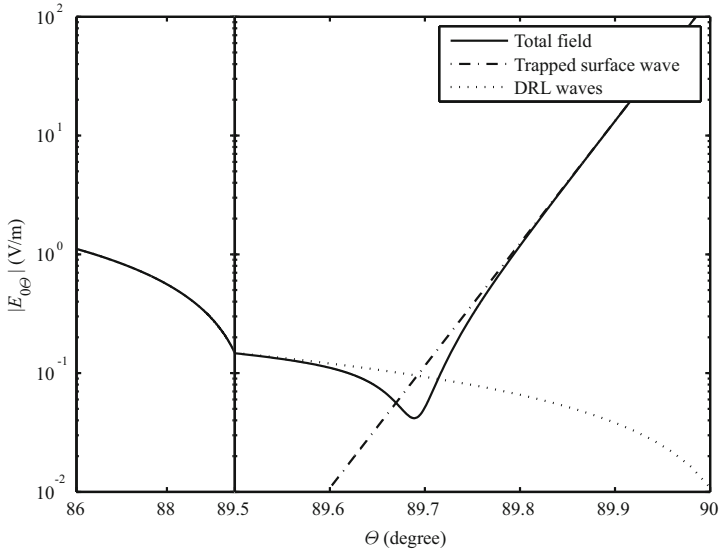


Fig. 3.15. Electric field component $E_{0\theta}$ in V/m versus θ with $f = 1$ GHz, $\varepsilon_{r1} = 2$, $r_0 = 80$ m, $l = 0.1$ m, $d = 0$ m, and $\Phi = 0$

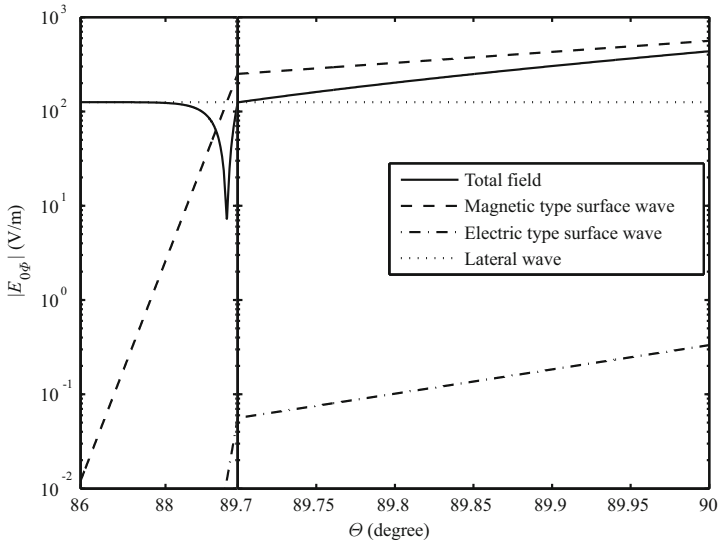


Fig. 3.16. Electric field component $E_{0\phi}$ in V/m versus θ with $f = 1$ GHz, $\varepsilon_{r1} = 2$, $r_0 = 20$ m, $l = 0.1$ m, $d = 0$ m, and $\Phi = \pi/2$

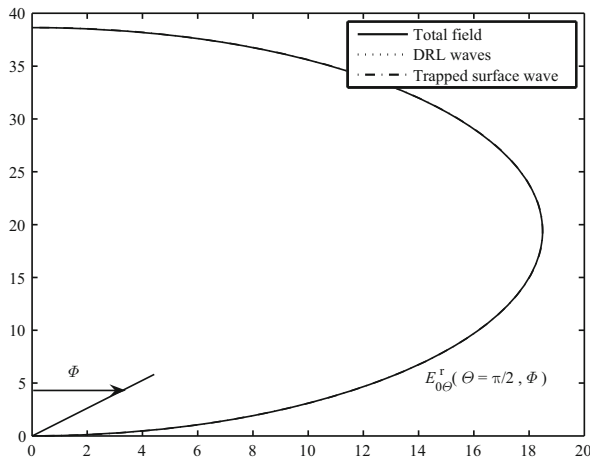


Fig. 3.17. Electric field component $[E_{0\Theta}^r(r_0, \Theta, \Phi)]_P$ radiated by a patch antenna versus Φ with $f = 1$ GHz, $\varepsilon_{r1} = 2$, $r_0 = 10$ m, $k_1 h = \pi/2$, $w = h$, $l = 0.05$ m, $d = 0$ m, $I_0 = 1$ A, and $\Theta = \pi/2$

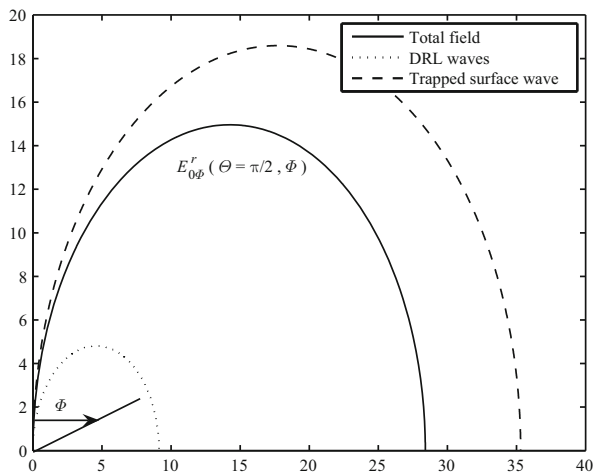


Fig. 3.18. $[E_{0\Phi}^r(r_0, \Theta, \Phi)]_P$ radiated by a patch antenna with $f = 1$ GHz, $\varepsilon_{r1} = 2$, $r_0 = 15$ m, $k_1 h = \pi/2$, $w = h$, $l = 0.1$ m, $d = 0$ m, $I_0 = 1$ A, and $\Theta = \pi/2$

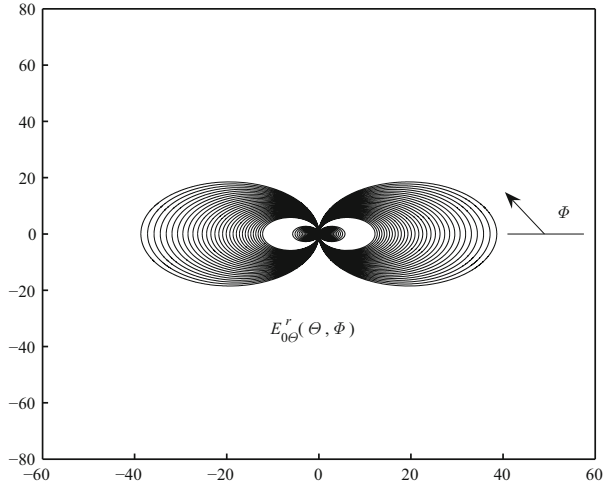


Fig. 3.19. Three-dimensional diagram of the component $[E_{0\Theta}^r(r_0, \Theta, \Phi)]_p$ radiated by a patch antenna with $f = 1$ GHz, $\varepsilon_{r1} = 2$, $r_0 = 10$ m, $k_1 h = \pi/2$, $w = h$, $l = 0.05$ m, $d = 0$ m, and $I_0 = 1$ A

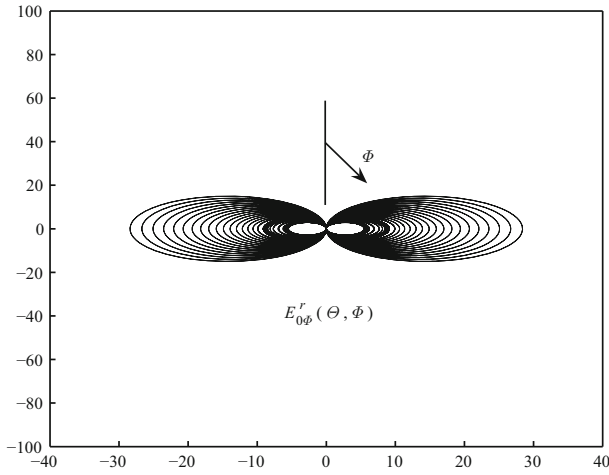


Fig. 3.20. Three-dimensional diagram of $[E_{0\Phi}^r(r_0, \Theta, \Phi)]_p$ of antenna with $f = 1$ GHz, $\varepsilon_{r1} = 2$, $r_0 = 15$ m, $k_1 h = \pi/2$, $w = h$, $l = 0.1$ m, $d = 0$ m, and $I_0 = 1$ A

3.4 Summary

In this chapter the electromagnetic field radiated by a horizontal electric dipole in the presence of a three-layered region is examined analytically. It is seen that both the trapped surface wave and the lateral wave can be separated into terms of electric type and those of magnetic type. Furthermore, the investigations and computations on the far-field radiation in spherical coordinates and radiation patterns of a patch antenna are carried out specifically. Analysis and computations show that, for the components $E_{0\rho}$ and $E_{0\theta}$, the total fields are determined primarily by the trapped surface wave of electric type and, for the components $E_{0\phi}$ and $E_{0\phi}$, the total fields are determined primarily by the trapped surface wave of magnetic type when both the dipole or the observation point are on the air-dielectric boundary.

When the dielectric layer in Region 1 is replaced by a uniaxially anisotropic medium or the conducting base in Region 2 is replaced by a dielectric base, the problem will be in general much more complicated. In these cases, the derivations and computations are also carried out (Li and Lu, 2005; Mei and Li, 2007; Zhang, et al., 2005) and they are not included because of using a similar method as addressed in this chapter.

References

- Collin RE (2004a) Some observations about the near zone electric field of a hertzian dipole above a lossy earth. *IEEE Transactions on Antennas and Propagation*, 52(11): 3133–3137.
- Collin RE (2004b) Hertzian dipole radiation over a lossy earth or sea: Some early and late 20th century controversies. *IEEE Antennas and Propagation Magazine*, 46(2): 64–79.
- Gradshteyn IS and Ryzhik IM (1980) *Table of Integrals, Series, and Products*. New York, NY, USA: Academic Press.
- Hoffman RK (1987) *Handbook of Microwave Integrated Circuits*. Norwood, MA, USA: Artech House.
- King RWP (1991) The electromagnetic field of a horizontal electric dipole in the presence of a three-layered region. *Journal of Applied Physics*, 69(12): 7987–7995.
- King RWP, Owens M, and Wu TT (1992) *Lateral Electromagnetic Waves: Theory and Applications to Communications, Geophysical Exploration, and Remote Sensing*. New York, NY, USA: Springer-Verlag.
- King RWP (1993) The electromagnetic field of a horizontal electric dipole in the presence of a three-layered region: supplement. *Journal of Applied Physics*, 74(8): 4845–4548.
- King RWP and Sandler SS (1994a) The electromagnetic field of a vertical electric dipole over the earth or Sea. *IEEE Transactions on Antennas and Propagation*, 42(3): 382–389.
- King RWP and Sandler SS (1994b) The electromagnetic field of a vertical electric dipole in the presence of a three-layered region. *Radio Science*, 29(1): 97–113.

- King RWP and Sandler SS (1998) Reply. *Radio Science*, 33(2): 255-256.
- King RWP, Fikioris GJ, and Mack RB (2002) *Cylindrical Antennas and Array*. Cambridge, UK: Cambridge University Press.
- Li K and Lu Y (2005) Electromagnetic field generated by a horizontal electric dipole near the surface of a planar perfect conductor coated with a uniaxial layer. *IEEE Transactions on Antennas and Propagation*, 53(10): 3191-3200.
- Liu L and Li K (2007) Radiation from a vertical electric dipole in the presence of a three-layered region. *IEEE Transactions on Antennas and Propagation*, 55(12): 3469-3475.
- Liu L, Li K, and Xu YH (2008) Radiation of a horizontal dipole in a three-layered region and microstrip antenna. *Progress In Electromagnetics Research*, PIER 86: 87-110. Cambridge, MA, USA: EMW Publishing.
- Mahmoud SF (1999) Remarks on "The electromagnetic field of a vertical electric dipole over the earth or Sea". *IEEE Transactions on Antennas and Propagation*, 46(12): 1745-1946.
- Sommerfeld A (1909) Propagation of waves in wireless telegraphy. *Annalen der Physik* (Leipzig), 28: 665-736.
- Sommerfeld A (1926) Propagation of waves in wireless telegraphy. *Annalen der Physik* (Leipzig), 81: 1135-1153.
- Wait JR (1953) Radiation from a vertical electric dipole over a stratified ground. *IRE Transactions on Antennas and Propagation*, AP-1: 9-12.
- Wait JR (1954) Radiation from a vertical electric dipole over a stratified ground. *IRE Transactions on Antennas and Propagation*, AP-2: 144-146.
- Wait JR (1956) Radiation from a vertical electric dipole over a curved stratified ground. *Journal of Research of the National Bureau of Standards*, 56: 232-239.
- Wait JR (1957) Excitation of surface waves on conducting dielectric clad and corrugated surfaces. *Journal of Research of the National Bureau of Standards*, 59(6): 365-377.
- Wait JR (1964) Electromagnetic surface waves. In *Advances in Radio Research* (pp.157-219). New York, NY, USA: Academic Press.
- Wait JR (1970) *Electromagnetic Waves in Stratified Media* (2nd, Ed.). New York, NY, USA: Pergamon Press.
- Wait JR (1990a) Radiation from a vertical electric dipole located over laterally anisotropic ground plane. *Electronics Letters*, 26(1): 74-76.
- Wait JR (1990b) Electromagnetic fields of a vertical electric dipole over a laterally anisotropic surface. *IEEE Transactions on Antennas and Propagation*, 38(10): 1719-1723.
- Wait JR (1998) Comment on "The electromagnetic field of a vertical electric dipole in the presence of a three-layered region" by Ronald, W. P. King and Sheldon S. Sandler. *Radio Science*, 33(2): 251-253.
- Zhang HQ and Pan WY (2002) Electromagnetic field of a vertical electric dipole on a perfect conductor coated with a dielectric layer. *Radio Science*, 37(4), 1060, doi:1029/2000RS002348.
- Zhang HQ, Li K, and Pan WY (2004) The electromagnetic field of a vertical dipole on the dielectric-coated imperfect conductor. *Journal of Electromagnetic Waves and Applications*, 18(10): 1305-1320.

- Zhang HQ, Pan WY, and Shen KX (2001) Electromagnetic field of a horizontal electric dipole over a perfect conductor covered with a dielectric layer. *Chinese Journal of Radio Science*, 16(3): 367–374. (In Chinese)
- Zhang HQ, Pan WY, Li K, and Shen KX (2005) Electromagnetic field for a horizontal electric dipole buried inside a dielectric layer coated high Lossy half space. *Progress In Electromagnetics Research*, PIER 50: 163–186. Cambridge, MA, USA: EMW Publishing.

Electromagnetic Field of a Vertical Electric Dipole in the Presence of a Four-Layered Region

The electromagnetic field radiated by a vertical electric dipole in the presence of a four-layered region is examined in detail. The region of interest consists of a perfect conductor, coated with two dielectric layers, and air above. It is noted that the properties of the electromagnetic field for the four-layered case are similar to those for the three-layered case. The wave numbers of the trapped surface waves, which are a contribution of the sum of the residues of poles, are between the wave numbers k_0 in the air and k_2 in the lower dielectric layer. Analysis and computations show that the trapped surface wave plays a major role in communication at large distances when both the dipole and the observation point are on or close to the boundary between the air and the upper dielectric layer.

4.1 Introduction

In pioneering works by Wait, extensive investigations were carried out for the electromagnetic field in a layered region by using asymptotic methods, contour integrations, and branch cuts (Wait, 1953; 1954; 1956; 1957; 1970). In the early 1990's, King et al. derived the complete formulas for the electromagnetic fields excited by vertical and horizontal electric dipoles in two- and three-layered regions (King, 1991, 1993; King, Owens, and Wu, 1992; King and Sandler, 1994). Lately, in a series of works by Li et al. (Li et al., 1998; 2004; Hoh et al., 1999), the dyadic Green's function technique was used to treat the electromagnetic field in a four-layered forest environment.

In Chapters 2 and 3, it is outlined the new developments on the electromagnetic field radiated by vertical and horizontal electric dipole in the presence of a three-layered region (Zhang and Pan, 2002; Zhang, Li, and Pan, 2004; Zhang et al., 2005; Li and Lu, 2005; Mei and Li, 2007; Liu and Li, 2007; Liu, Li, and Xu, 2008). It is concluded that the trapped surface wave, which are a contribution of the sum of the residues of poles, can be excited efficiently

by a dipole in the presence of a three-layered region. In the available references (Tsang et al., 2000; 2003), the term being a contribution of the sum of the residues of poles, which is named the surface wave, is included in their solutions and the electromagnetic field of a point source in a multi-layered region is examined in detail. These new developments, naturally, rekindle the interest extended to the four-layered case.

In this chapter, we will attempt to outline the trapped surface wave and lateral wave excited by a vertical electric dipole in the presence of a four-layered region when both the dipole and the observation point in the air are on or close to the boundary between the air and the upper dielectric layer.

4.2 Formulation of Problem

Consider the four-layered region as shown in Fig. 4.1. Region 0 ($z \geq 0$) is the space above the two dielectric layers occupied by the air. Region 1 ($-l_1 \leq z \leq 0$) is the upper dielectric layer characterized by the permeability μ_0 , relative permittivity ε_{r1} , and conductivity σ_1 . Region 2 ($-(l_1 + l_2) \leq z \leq -l_1$) is the lower dielectric layer characterized by the permeability μ_0 , relative permittivity ε_{r2} , and conductivity σ_2 . Region 3 ($z \leq -(l_1 + l_2)$) is the rest space occupied by a perfect conductor. Then, the wave numbers in the four-layered region are

$$k_0 = \omega \sqrt{\mu_0 \varepsilon_0}, \quad (4.1)$$

$$k_j = \omega \sqrt{\mu_0 (\varepsilon_0 \varepsilon_{rj} + i\sigma_j/\omega)}; \quad j = 1, 2, \quad (4.2)$$

$$k_3 \rightarrow \infty. \quad (4.3)$$

With the similar procedures as addressed in Chapter 2, the integrated formulas can be obtained for the electromagnetic field of a vertical electric dipole in the presence of a four-layered region from Maxwell's equations by using boundary conditions. From Eq. (11.5.1) to Eq. (11.5.3) in Chapter 11 of the book by King, Owens, and Wu (1992), the integrated formulas for the electromagnetic field can be written directly. They are

$$B_{0\phi} = \frac{i\mu_0}{4\pi} \int_0^\infty \gamma_0^{-1} \left[e^{i\gamma_0|z-d|} + e^{i\gamma_0(z+d)} - (Q+1)e^{i\gamma_0(z+d)} \right] J_1(\lambda\rho) \lambda^2 d\lambda, \quad (4.4)$$

$$E_{0\rho} = \frac{i\omega\mu_0}{4\pi k_0^2} \int_0^\infty \left[\pm e^{i\gamma_0|z-d|} + e^{i\gamma_0(z+d)} - (Q+1)e^{i\gamma_0(z+d)} \right] J_1(\lambda\rho) \lambda^2 d\lambda; \quad (4.5)$$

$$\begin{aligned} d &< z \\ 0 &\leq z \leq d \end{aligned}$$

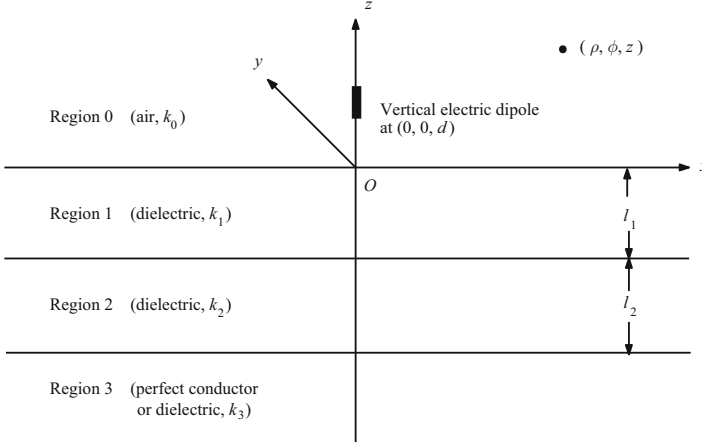


Fig. 4.1. Geometry of a vertical electric dipole in the four-layered region

$$E_{0z} = -\frac{\omega\mu_0}{4\pi k_0^2} \int_0^\infty \gamma_0^{-1} \left[e^{i\gamma_0|z-d|} + e^{i\gamma_0(z+d)} - (Q+1)e^{i\gamma_0(z+d)} \right] J_0(\lambda\rho) \lambda^3 d\lambda, \quad (4.6)$$

where

$$Q = -\frac{\gamma_0 + \frac{k_0^2}{\omega\mu_0} \frac{\gamma_1 k_2^2 \tan(\gamma_1 l_1) + \gamma_2 k_1^2 \tan(\gamma_2 l_2)}{k_1^2} \frac{\gamma_1 k_2^2 \tan(\gamma_1 l_1) + \gamma_2 k_1^2 \tan(\gamma_2 l_2)}{\gamma_1 k_2^2 - \gamma_2 k_1^2 \tan(\gamma_1 l_1) \tan(\gamma_2 l_2)}}{\gamma_0 - \frac{k_0^2}{\omega\mu_0} \frac{\gamma_1 k_2^2 \tan(\gamma_1 l_1) + \gamma_2 k_1^2 \tan(\gamma_2 l_2)}{k_1^2} \frac{\gamma_1 k_2^2 \tan(\gamma_1 l_1) + \gamma_2 k_1^2 \tan(\gamma_2 l_2)}{\gamma_1 k_2^2 - \gamma_2 k_1^2 \tan(\gamma_1 l_1) \tan(\gamma_2 l_2)}}, \quad (4.7)$$

$$\gamma_j = \sqrt{k_j^2 - \lambda^2}; \quad j = 0, 1, 2, \quad (4.8)$$

$$k_j = \omega\sqrt{\mu_0\epsilon_j}; \quad j = 0, 1, 2. \quad (4.9)$$

It is now convenient to rewrite Eqs. (4.4)~(4.6) in the following forms:

$$B_{0\phi} = B_{0\phi}^{(1)} + B_{0\phi}^{(2)} + B_{0\phi}^{(3)}, \quad (4.10)$$

$$E_{0\rho} = E_{0\rho}^{(1)} + E_{0\rho}^{(2)} + E_{0\rho}^{(3)}, \quad (4.11)$$

$$E_{0z} = E_{0z}^{(1)} + E_{0z}^{(2)} + E_{0z}^{(3)}, \quad (4.12)$$

where

$$B_{0\phi}^{(1)} = \frac{i\mu_0}{4\pi} \int_0^\infty \gamma_0^{-1} e^{i\gamma_0|z-d|} J_1(\lambda\rho) \lambda^2 d\lambda, \quad (4.13)$$

$$B_{0\phi}^{(2)} = \frac{i\mu_0}{4\pi} \int_0^\infty \gamma_0^{-1} e^{i\gamma_0(z+d)} J_1(\lambda\rho) \lambda^2 d\lambda, \quad (4.14)$$

$$E_{0\rho}^{(1)} = \frac{i\omega\mu_0}{4\pi k_0^2} \int_0^\infty \pm e^{i\gamma_0|z-d|} J_1(\lambda\rho) \lambda^2 d\lambda, \quad (4.15)$$

$$E_{0\rho}^{(2)} = \frac{i\omega\mu_0}{4\pi k_0^2} \int_0^\infty e^{i\gamma_0(z+d)} J_1(\lambda\rho) \lambda^2 d\lambda, \quad (4.16)$$

$$E_{0z}^{(1)} = -\frac{\omega\mu_0}{4\pi k_0^2} \int_0^\infty \gamma_0^{-1} e^{i\gamma_0|z-d|} J_0(\lambda\rho) \lambda^3 d\lambda, \quad (4.17)$$

$$E_{0z}^{(2)} = -\frac{\omega\mu_0}{4\pi k_0^2} \int_0^\infty \gamma_0^{-1} e^{i\gamma_0(z+d)} J_0(\lambda\rho) \lambda^3 d\lambda. \quad (4.18)$$

The first and second terms in Eqs. (4.4)~(4.6) represent the direct wave and the ideal reflected wave, respectively. The two terms have already been evaluated many years ago (King, Owens, and Wu, 1992). Next, the main tasks are to evaluate the third terms in Eqs. (4.10)~(4.12). Since γ_0 , γ_1 , and γ_2 are even functions, and use is made of the relations between Bessel function and Hankel function

$$J_n(\lambda\rho) = \frac{1}{2} \left[H_n^{(1)}(\lambda\rho) + H_n^{(2)}(\lambda\rho) \right], \quad (4.19)$$

$$H_n^{(1)}(-\lambda\rho) = H_n^{(2)}(\lambda\rho)(-1)^{n+1}, \quad (4.20)$$

the third terms in Eqs. (4.10)~(4.12) can be expressed in the following forms:

$$B_{0\phi}^{(3)} = -\frac{\mu_0 k_0^2}{4\pi} \int_{-\infty}^\infty \frac{\gamma_1 k_2^2 \tan(\gamma_1 l_1) + \gamma_2 k_1^2 \tan(\gamma_2 l_2)}{q(\lambda) \gamma_0} \gamma_1 e^{i\gamma_0(z+d)} H_1^{(1)}(\lambda\rho) \lambda^2 d\lambda, \quad (4.21)$$

$$E_{0\rho}^{(3)} = -\frac{\omega\mu_0}{4\pi} \int_{-\infty}^\infty \frac{\gamma_1 k_2^2 \tan(\gamma_1 l_1) + \gamma_2 k_1^2 \tan(\gamma_2 l_2)}{q(\lambda)} \gamma_1 e^{i\gamma_0(z+d)} H_1^{(1)}(\lambda\rho) \lambda^2 d\lambda, \quad (4.22)$$

$$E_{0z}^{(3)} = -\frac{i\omega\mu_0}{4\pi} \int_{-\infty}^\infty \frac{\gamma_1 k_2^2 \tan(\gamma_1 l_1) + \gamma_2 k_1^2 \tan(\gamma_2 l_2)}{q(\lambda) \gamma_0} \gamma_1 e^{i\gamma_0(z+d)} H_0^{(1)}(\lambda\rho) \lambda^3 d\lambda, \quad (4.23)$$

where

$$q(\lambda) = k_1^2 \gamma_0 [\gamma_1 k_2^2 - \gamma_2 k_1^2 \tan(\gamma_1 l_1) \tan(\gamma_2 l_2)] - ik_0^2 \gamma_1 [\gamma_1 k_2^2 \tan(\gamma_1 l_1) + \gamma_2 k_1^2 \tan(\gamma_2 l_2)]. \quad (4.24)$$

4.3 Evaluations of the Trapped Surface Wave and Lateral Wave

In this section, we will evaluate the integrals in Eqs. (4.21)~(4.23). We rewrite $B_{0\phi}^{(3)}$ in the form

$$B_{0\phi}^{(3)} = B_{0\phi}^{(3,1)} + B_{0\phi}^{(3,2)}, \quad (4.25)$$

where

$$B_{0\phi}^{(3,1)} = -\frac{\mu_0 k_0^2}{4\pi} \int_{-\infty}^{\infty} \frac{\gamma_1 \gamma_2 k_1^2 \tan(\gamma_2 l_2)}{q(\lambda) \gamma_0} e^{i\gamma_0(z+d)} H_1^{(1)}(\lambda \rho) \lambda^2 d\lambda, \quad (4.26)$$

$$B_{0\phi}^{(3,2)} = -\frac{\mu_0 k_0^2}{4\pi} \int_{-\infty}^{\infty} \frac{\gamma_1^2 k_2^2 \tan(\gamma_1 l_1)}{q(\lambda) \gamma_0} e^{i\gamma_0(z+d)} H_1^{(1)}(\lambda \rho) \lambda^2 d\lambda. \quad (4.27)$$

In order to evaluate the above two integrals, it is necessary to shift the contour around the branch cuts at $\lambda = k_0$, $\lambda = k_1$, and $\lambda = k_2$. The configuration of the poles and branch cuts is shown in Fig. 4.2. The next main tasks are to determine the poles and to evaluate the integrations along the branch lines Γ_0 , Γ_1 , and Γ_2 . First we consider the following pole equation:

$$\begin{aligned} q(\lambda) &= k_1^2 \gamma_0 [\gamma_1 k_2^2 - \gamma_2 k_1^2 \tan(\gamma_1 l_1) \tan(\gamma_2 l_2)] \\ &\quad - i k_0^2 \gamma_1 [\gamma_1 k_2^2 \tan(\gamma_1 l_1) + \gamma_2 k_1^2 \tan(\gamma_2 l_2)] = 0. \end{aligned} \quad (4.28)$$

Compared with the corresponding three-layered case in Chapter 2, the pole equation becomes much more complex. In the present study, the conditions $k_0 < k_1 < k_2$ and $k_3 \rightarrow \infty$ are satisfied. Obviously, it is seen that no pole exists in the case of $\lambda < k_0$ and $\lambda > k_2$. In the cases of $k_0 < \lambda < k_1$ and $k_1 < \lambda < k_2$, the poles may exist. As shown in Figs. 4.3 and 4.4, the poles are determined by using Newton's iteration method and it is found that the poles appear in the cases of $k_0 < \lambda < k_1$ and $k_1 < \lambda < k_2$. It is noted that k_1 is a removable pole.

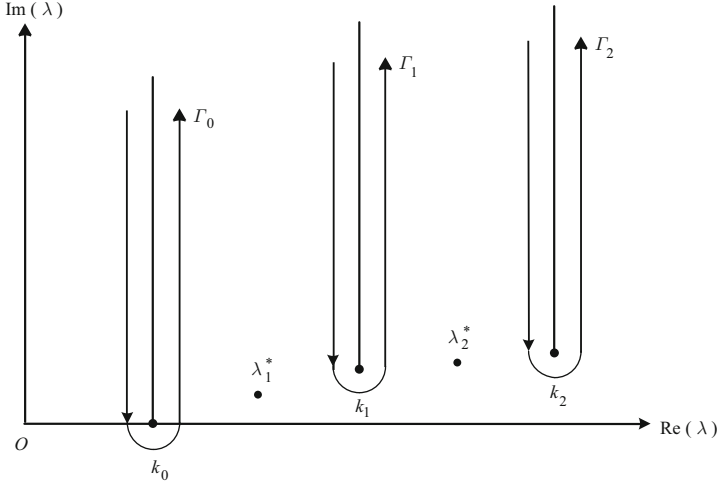


Fig. 4.2. The configuration of the poles and the branch lines

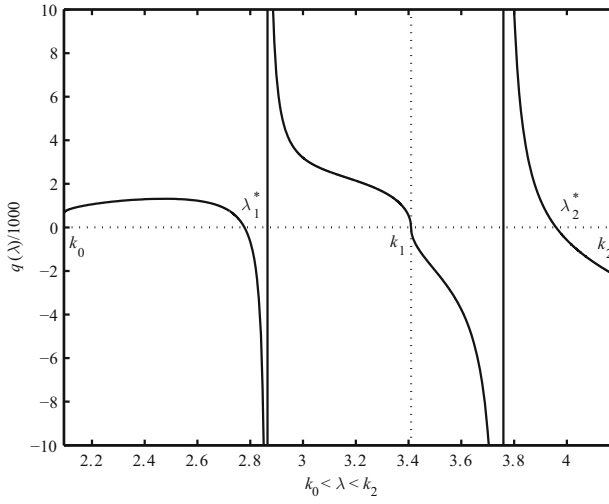


Fig. 4.3. Roots of Eq. (4.28) for $f = 100$ MHz, $\varepsilon_{r1} = 2.65$, $\varepsilon_{r2} = 4.0$, $l_1 = l_2 = 0.8$ m

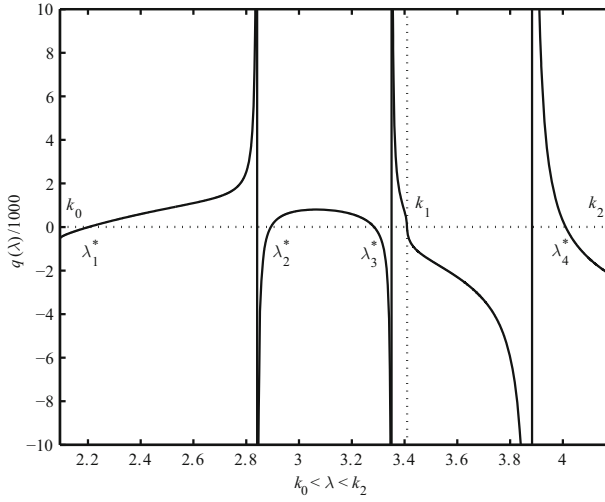


Fig. 4.4. Roots of Eq. (4.28) for $f = 100$ MHz, $\varepsilon_{r1} = 2.65$, $\varepsilon_{r2} = 4.0$, $l_1 = 3.0$ m, and $l_2 = 1.0$ m

On the two sides of the branch line Γ_0 , the phase of γ_0 changes by π , and γ_1 and γ_2 have the same values on the two sides of Γ_1 and Γ_2 . It is easily known that the evaluations of the integrals in Eqs. (4.26) and (4.27) along the branch lines Γ_1 and Γ_2 are zero. Therefore, the integral Eq. (4.26) is written in the form

$$B_{0\phi}^{(3,1)} = 2\pi i \frac{-\mu_0 k_0^2}{4\pi} \sum_j \frac{k_1^2 \gamma_1(\lambda_j^*) \gamma_2(\lambda_j^*) \tan(\gamma_2(\lambda_j^*) l_2)}{q'(\lambda_j^*) \gamma_0(\lambda_j^*)} e^{i\gamma_0(\lambda_j^*)(z+d)} H_1^{(1)}(\lambda_j^* \rho) \lambda_j^{*2} - \frac{\mu_0 k_0^2}{4\pi} \int_{\Gamma_0} \frac{\gamma_1 \gamma_2 k_1^2 \tan(\gamma_2 l_2)}{q(\lambda) \gamma_0} e^{i\gamma_0(z+d)} H_1^{(1)}(\lambda \rho) \lambda^2 d\lambda \quad (4.29)$$

where

$$\begin{aligned} q'(\lambda) = & -k_1^2 \frac{\lambda}{\gamma_0} [\gamma_1 k_2^2 - \gamma_2 k_1^2 \tan(\gamma_1 l_1) \tan(\gamma_2 l_2)] \\ & + i k_0^2 \frac{\lambda}{\gamma_1} [\gamma_1 k_2^2 \tan(\gamma_1 l_1) + \gamma_2 k_1^2 \tan(\gamma_2 l_2)] \\ & + k_1^2 \gamma_0 \left[-\frac{\lambda}{\gamma_1} k_2^2 + \frac{\lambda}{\gamma_2} k_1^2 \tan(\gamma_1 l_1) \tan(\gamma_2 l_2) \right. \\ & \left. + k_1^2 \gamma_2 \lambda \left(\frac{l_1}{\gamma_1} \sec^2 \gamma_1 l_1 \tan(\gamma_2 l_2) + \frac{l_2}{\gamma_2} \tan(\gamma_1 l_1) \sec^2 \gamma_2 l_2 \right) \right] \\ & + i k_0^2 \gamma_1 \lambda \left[\frac{k_2^2 \tan(\gamma_1 l_1)}{\gamma_1} + \frac{k_1^2 \tan(\gamma_2 l_2)}{\gamma_2} \right. \\ & \left. + k_2^2 l_1 \sec^2 \gamma_1 l_1 + k_1^2 l_2 \sec^2 \gamma_2 l_2 \right], \end{aligned} \quad (4.30)$$

$$\gamma_n(\lambda_j^*) = \sqrt{k_n^2 - \lambda_j^{*2}}; \quad n = 0, 1, 2. \quad (4.31)$$

Considering the far-field condition $k_0 \rho \gg 1$ and $(z+d) \ll \rho$, the dominant contribution of the integral along the branch line Γ_0 comes from the vicinity of k_0 . Let $\lambda = k_0(1 + i\tau^2)$, the following approximated formulas can be obtained readily.

$$\gamma_0 = \sqrt{k_0^2 - \lambda^2} \approx k_0 e^{i\frac{3}{4}\pi} \sqrt{2}\tau, \quad (4.32)$$

$$\gamma_1 = \sqrt{k_1^2 - \lambda^2} \approx \sqrt{k_1^2 - k_0^2} = \gamma_{10}, \quad (4.33)$$

$$\gamma_2 = \sqrt{k_2^2 - \lambda^2} \approx \sqrt{k_2^2 - k_0^2} = \gamma_{20}, \quad (4.34)$$

and

$$H_1^{(1)}(\lambda \rho) \approx \sqrt{\frac{2}{\pi k_0 \rho}} e^{i(k_0 \rho - \frac{3}{4}\pi)} e^{-k_0 \rho \tau^2}. \quad (4.35)$$

Then, we have

$$\begin{aligned}
 B_{0\phi}^{(3,1)} = & -\frac{\mu_0 k_0^2}{4\pi} \frac{\gamma_{10} \gamma_{20} \sqrt{\frac{2k_0}{\pi\rho}} \tan(\gamma_{20} l_2)}{\gamma_{10} k_2^2 - \gamma_{20} k_1^2 \tan(\gamma_{10} l_1) \tan(\gamma_{20} l_2)} \\
 & \times \exp \left[i \left(k_0 \rho + \frac{\pi}{4} \right) + i \frac{k_0 \rho}{2} \left(\frac{z+d}{\rho} \right)^2 \right] \\
 & \times \int_{-\infty}^{\infty} \frac{\exp \left[-k_0 \rho \left(\tau + \frac{e^{i\pi/4}}{\sqrt{2}} \frac{z+d}{\rho} \right)^2 \right]}{\tau - \Delta} d\tau, \quad (4.36)
 \end{aligned}$$

where

$$\Delta = -e^{-i\frac{\pi}{4}} \frac{k_0}{k_1^2} \frac{\gamma_{10}}{\sqrt{2}} \frac{\gamma_{10} k_2^2 \tan(\gamma_{10} l_1) + \gamma_{20} k_1^2 \tan(\gamma_{20} l_2)}{\gamma_{10} k_2^2 - \gamma_{20} k_1^2 \tan(\gamma_{10} l_1) \tan(\gamma_{20} l_2)}. \quad (4.37)$$

In terms of the variable $t = \tau + \frac{e^{i\pi/4}}{\sqrt{2}} \frac{z+d}{\rho}$, the integral in Eq. (4.36) becomes

$$\int_{-\infty}^{\infty} \frac{e^{-k_0 \rho t^2}}{t - e^{i\frac{\pi}{4}} \Delta'} dt = i\pi e^{-i\Delta'^2 k_0 \rho} \operatorname{erfc}(\sqrt{-i\Delta'^2 k_0 \rho}), \quad (4.38)$$

where

$$\Delta' = \frac{z+d}{\sqrt{2}\rho} + i \frac{k_0}{k_1^2} \frac{\gamma_{10}}{\sqrt{2}} \frac{\gamma_{10} k_2^2 \tan(\gamma_{10} l_1) + \gamma_{20} k_1^2 \tan(\gamma_{20} l_2)}{\gamma_{10} k_2^2 - \gamma_{20} k_1^2 \tan(\gamma_{10} l_1) \tan(\gamma_{20} l_2)}. \quad (4.39)$$

Here the phase of $\sqrt{-i\Delta'^2 k_0 \rho}$ in Eq. (4.38) requires to be satisfied by the condition

$$|\operatorname{Arg} \sqrt{-i\Delta'^2 k_0 \rho}| \leq \frac{\pi}{4}. \quad (4.40)$$

The error function and Fresnel integral are defined by

$$\operatorname{erfc}(x) = \frac{2}{\sqrt{\pi}} \int_x^{\infty} e^{-t^2} dt, \quad (4.41)$$

$$\mathbf{F}(p^*) = \frac{1}{2}(1+i) - \int_0^{p^*} \frac{e^{it}}{\sqrt{2\pi t}} dt, \quad (4.42)$$

where

$$p^* = \frac{k_0 \rho}{2} \left[\frac{z+d}{\rho} + i \frac{k_0}{k_1^2} \gamma_{10} \frac{\gamma_{10} k_2^2 \tan(\gamma_{10} l_1) + \gamma_{20} k_1^2 \tan(\gamma_{20} l_2)}{\gamma_{10} k_2^2 - \gamma_{20} k_1^2 \tan(\gamma_{10} l_1) \tan(\gamma_{20} l_2)} \right]^2, \quad (4.43)$$

and considering the relation between error function and Fresnel integral

$$\operatorname{erfc}(\sqrt{-ip^*}) = \sqrt{2} e^{-i\frac{\pi}{4}} \mathbf{F}(p^*), \quad (4.44)$$

the result becomes

$$\begin{aligned}
 B_{0\phi}^{(3,1)} = & \mu_0 k_0^2 k_1^2 \sqrt{\frac{1}{2\pi\rho}} e^{i\frac{3\pi}{4}} \\
 & \times \sum_j \left[\frac{\tan(\gamma_2(\lambda_j^*)l_2)}{q'(\lambda_j^*)\gamma_0(\lambda_j^*)} \gamma_1(\lambda_j^*)\gamma_2(\lambda_j^*)(\lambda_j^*)^{3/2} e^{i\gamma_0(\lambda_j^*)(z+d)+i\lambda_j^*\rho} \right] \\
 & - \frac{i\mu_0 k_0^3}{2} \sqrt{\frac{1}{\pi k_0 \rho}} e^{ik_0 r_2} \frac{\gamma_{10}\gamma_{20} \tan(\gamma_{20}l_2) e^{-ip^*} \mathbf{F}(p^*)}{\gamma_{10}k_2^2 - \gamma_{20}k_1^2 \tan(\gamma_{10}l_1) \tan(\gamma_{20}l_2)}, \quad (4.45)
 \end{aligned}$$

where

$$r_2 = \sqrt{\rho^2 + (z+d)^2} \approx \rho \left[1 + \frac{1}{2} \left(\frac{z+d}{\rho} \right)^2 \right]. \quad (4.46)$$

Similarly, we obtain

$$\begin{aligned}
 B_{0\phi}^{(3,2)} = & k_0^2 k_2^2 \mu_0 \sqrt{\frac{1}{2\pi\rho}} e^{i\frac{3\pi}{4}} \sum_j \left[\frac{\tan \gamma_1(\lambda_j^*)l_1}{q'(\lambda_j^*)\gamma_0(\lambda_j^*)} \gamma_1^2(\lambda_j^*)(\lambda_j^*)^{3/2} e^{i\gamma_0(\lambda_j^*)(z+d)+i\lambda_j^*\rho} \right] \\
 & - \frac{i\mu_0 k_0^3}{2} \frac{k_2^2}{k_1^2} \sqrt{\frac{1}{\pi k_0 \rho}} e^{ik_0 r_2} \frac{\gamma_{10}^2 \tan(\gamma_{10}l_1) e^{-ip^*} \mathbf{F}(p^*)}{\gamma_{10}k_2^2 - \gamma_{20}k_1^2 \tan(\gamma_{10}l_1) \tan(\gamma_{20}l_2)}. \quad (4.47)
 \end{aligned}$$

By using the above derivations and the results for the direct wave and ideal reflected wave (King, Owens, and Wu, 1992), the final formula for the magnetic field component $B_{0\phi}$ can be obtained readily. It is

$$\begin{aligned}
 B_{0\phi} = & -\frac{\mu_0}{4\pi} e^{ik_0 r_1} \left(\frac{\rho}{r_1} \right) \left(\frac{ik_0}{r_1} - \frac{1}{r_1^2} \right) - \frac{\mu_0}{4\pi} e^{ik_0 r_2} \left(\frac{\rho}{r_2} \right) \left(\frac{ik_0}{r_2} - \frac{1}{r_2^2} \right) \\
 & + \mu_0 k_0^2 \sqrt{\frac{1}{2\pi\rho}} e^{i\frac{3\pi}{4}} \sum_j \frac{(\lambda_j^*)^{3/2} e^{i\gamma_0(\lambda_j^*)(z+d)+i\lambda_j^*\rho}}{q'(\lambda_j^*)\gamma_0(\lambda_j^*)} \\
 & \times \left[k_2^2 \gamma_1^2(\lambda_j^*) \tan(\gamma_1(\lambda_j^*)l_1) + k_1^2 \gamma_1(\lambda_j^*)\gamma_2(\lambda_j^*) \tan(\gamma_2(\lambda_j^*)l_2) \right] \\
 & - \frac{i\mu_0 k_0^3}{2} \sqrt{\frac{1}{\pi k_0 \rho}} e^{ik_0 r_2} \frac{\gamma_{10}\gamma_{20} \tan(\gamma_{20}l_2) + \frac{k_2^2}{k_1^2} \gamma_{10}^2 \tan(\gamma_{10}l_1)}{\gamma_{10}k_2^2 - \gamma_{20}k_1^2 \tan(\gamma_{10}l_1) \tan(\gamma_{20}l_2)} e^{-ip^*} \mathbf{F}(p^*). \quad (4.48)
 \end{aligned}$$

With the similar procedures, the components $E_{0\rho}$ and E_{0z} are expressed as follows:

$$\begin{aligned}
 E_{0\rho} = & -\frac{\omega\mu_0}{4\pi k_0} e^{ik_0 r_1} \left(\frac{\rho}{r_1} \right) \left(\frac{z-d}{r_1} \right) \left(\frac{ik_0}{r_1} - \frac{3}{r_1^2} - \frac{3i}{k_0 r_1^3} \right) \\
 & - \frac{\omega\mu_0}{4\pi k_0} e^{ik_0 r_2} \left(\frac{\rho}{r_2} \right) \left(\frac{z+d}{r_2} \right) \left(\frac{ik_0}{r_2} - \frac{3}{r_2^2} - \frac{3i}{k_0 r_2^3} \right)
 \end{aligned}$$

$$\begin{aligned}
& -\omega\mu_0\sqrt{\frac{1}{2\pi\rho}}e^{-i\frac{\pi}{4}}\sum_j\frac{(\lambda_j^*)^{3/2}e^{i\gamma_0(\lambda_j^*)(z+d)+i\lambda_j^*\rho}}{q'(\lambda_j^*)} \\
& \times\left[k_1^2\gamma_1(\lambda_j^*)\gamma_2(\lambda_j^*)\tan(\gamma_2(\lambda_j^*)l_2)+k_2^2\gamma_1^2(\lambda_j^*)\tan(\gamma_1(\lambda_j^*)l_1)\right] \\
& +\frac{\omega\mu_0k_0^2}{2\pi}\sqrt{\frac{1}{\pi k_0\rho}}e^{ik_0r_2}\frac{\gamma_{10}\gamma_{20}\tan(\gamma_{20}l_2)+\frac{k_2^2}{k_1^2}\gamma_{10}^2\tan(\gamma_{10}l_1)}{\gamma_{10}k_2^2-\gamma_{20}k_1^2\tan(\gamma_{10}l_1)\tan(\gamma_{20}l_2)} \\
& \times\left[\sqrt{\frac{\pi}{k_0\rho}}+\pi\frac{k_0\gamma_{10}}{k_1^2}\frac{\gamma_{10}k_2^2\tan(\gamma_{10}l_1)+\gamma_{20}k_1^2\tan(\gamma_{20}l_2)}{\gamma_{10}k_2^2-\gamma_{20}k_1^2\tan(\gamma_{10}l_1)\tan(\gamma_{20}l_2)}e^{-ip^*}\mathbf{F}(p^*)\right],
\end{aligned} \tag{4.49}$$

$$\begin{aligned}
E_{0z} = & \frac{\omega\mu_0}{4\pi k_0}e^{ik_0r_1}\left[\frac{ik_0}{r_1}-\frac{1}{r_1^2}-\frac{i}{k_0r_1^3}-\left(\frac{z-d}{r_1}\right)^2\left(\frac{ik_0}{r_1}-\frac{3}{r_1^2}-\frac{3i}{k_0r_1^3}\right)\right] \\
& +\frac{\omega\mu_0}{4\pi k_0}e^{ik_0r_2}\left[\frac{ik_0}{r_2}-\frac{1}{r_2^2}-\frac{i}{k_0r_2^3}-\left(\frac{z+d}{r_2}\right)^2\left(\frac{ik_0}{r_2}-\frac{3}{r_2^2}-\frac{3i}{k_0r_2^3}\right)\right] \\
& +\omega\mu_0\sqrt{\frac{1}{2\pi\rho}}e^{-i\frac{\pi}{4}}\sum_j\frac{(\lambda_j^*)^{5/2}e^{i\gamma_0(\lambda_j^*)(z+d)+i\lambda_j^*\rho}}{q'(\lambda_j^*)\gamma_0(\lambda_j^*)} \\
& \times\left[k_1^2\gamma_1(\lambda_j^*)\gamma_2(\lambda_j^*)\tan(\gamma_2(\lambda_j^*)l_2)+k_2^2\gamma_1^2(\lambda_j^*)\tan(\gamma_1(\lambda_j^*)l_1)\right] \\
& +\frac{i\omega\mu_0k_0^2}{2}\sqrt{\frac{1}{\pi k_0\rho}}e^{ik_0r_2}\frac{\gamma_{10}\gamma_{20}\tan(\gamma_{20}l_2)+\frac{k_2^2}{k_1^2}\gamma_{10}^2\tan(\gamma_{10}l_1)}{\gamma_{10}k_2^2-\gamma_{20}k_1^2\tan(\gamma_{10}l_1)\tan(\gamma_{20}l_2)}e^{-ip^*}\mathbf{F}(p^*).
\end{aligned} \tag{4.50}$$

If Region 1 is made in the air by setting $k_1 = k_0$ or both Regions 2 and 3 are made in the same dielectric by setting $k_2 = k_1$, the above results reduce to the results for the three-layered case in Chapter 2.

4.4 Computations and Conclusions

Similar to the three-layered case, the electromagnetic field of a vertical electric dipole in the presence of a four-layered region, where both the dipole and observation point are located in the air, includes the following four modes: the direct wave, ideal reflected wave, trapped surface wave, and lateral wave. From the expressions of the three components $B_{0\phi}$, $E_{0\rho}$, and E_{0z} in Eqs. (4.48)~(4.50), it is seen that the term of the trapped surface wave is determined by the sum of residues of the poles. In the case of $k_0 < \lambda_j^* < k_2$, $\gamma_{0j}^* = i\sqrt{\lambda_j^{*2} - k_0^2}$ is always a positive imaginary number, the term including the factor $e^{i\gamma_{0j}^*z}$ attenuates exponentially as $e^{-\sqrt{\lambda_j^{*2} - k_0^2}z}$ in the \hat{z} direction.

The amplitude of the trapped surface wave attenuates as $\rho^{-1/2}$ in the $\hat{\rho}$ direction when both the dipole and the observation point are on or close to the boundary between the air and the upper dielectric layer. The wave numbers of the trapped surface waves, which are between k_0 and k_2 , can be evaluated by using Newton's iteration method.

With $f = 100$ MHz, $\varepsilon_{r1}=2.65$, and $\varepsilon_{r2}=4.0$, the total field, the trapped surface wave, and the DRL waves, for the component E_{0z} , are computed for $k_1l_1 = k_2l_2 = 0.4$ and $k_1l_1 = k_2l_2 = 1.4$ at $z = d = 0$, as shown in Figs. 4.5 and 4.6, respectively. It is noted that the DRL waves include the direct wave, ideal reflected wave, and lateral wave. Similarly, in the same four-layered region, the total field, the trapped surface wave, and the DRL waves are computed for $k_1l_1 = k_1l_2 = 0.4$ and $k_1l_1 = k_2l_2 = 1.4$ at $z = d = 3$ m and shown in Figs. 4.7 and 4.8, respectively.

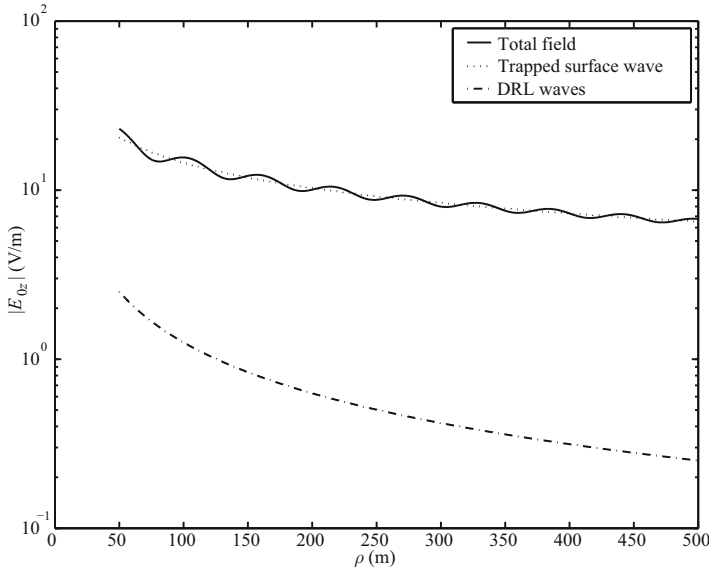


Fig. 4.5. The electric field $|E_z|$ in V/m with $f = 100$ MHz, $\varepsilon_{r1} = 2.65$, $\varepsilon_{r2} = 4$, $k_1l_1 = k_2l_2 = 0.4$, and $z = d = 0$ m

From Fig. 4.5 to Fig. 4.8, it is seen that the trapped surface wave plays a major role in communication at large distances when both the dipole and the observation point are on or close to the boundary between the air and the upper dielectric layer. The lateral wave, which is determined by the integrations along the branch lines, plays a major role when the dipole or the observation point is away from the boundary.

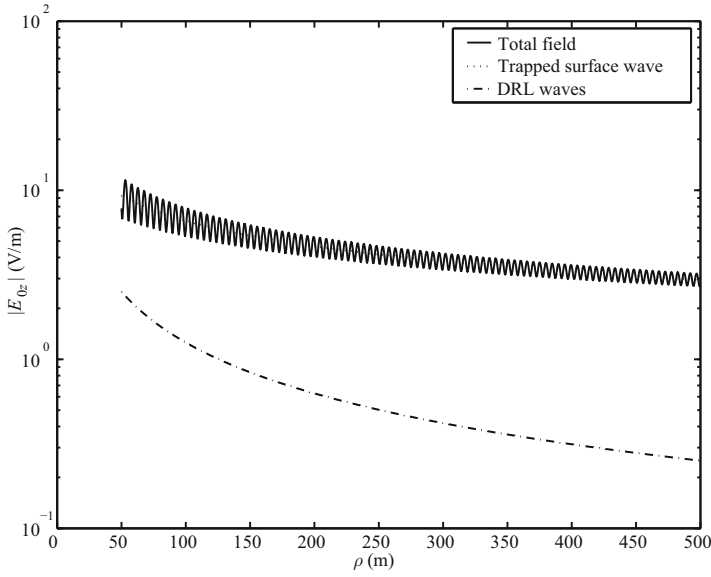


Fig. 4.6. The electric field $|E_z|$ in V/m with $f = 100$ MHz, $\varepsilon_{r1} = 2.65$, $\varepsilon_{r2} = 4$, $k_1 l_1 = k_2 l_2 = 1.4$, and $z = d = 0$ m

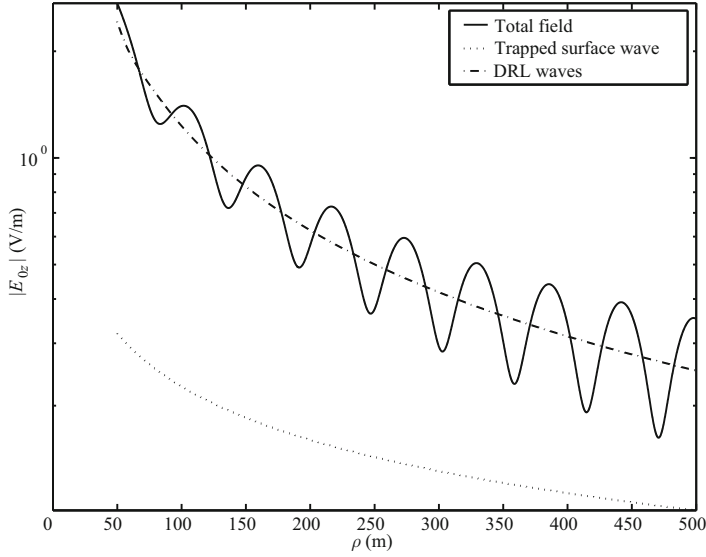


Fig. 4.7. The electric field $|E_z|$ in V/m with $f = 100$ MHz, $\varepsilon_{r1} = 2.65$, $\varepsilon_{r2} = 4$, $k_1 l_1 = k_2 l_2 = 0.4$, and $z = d = 3$ m

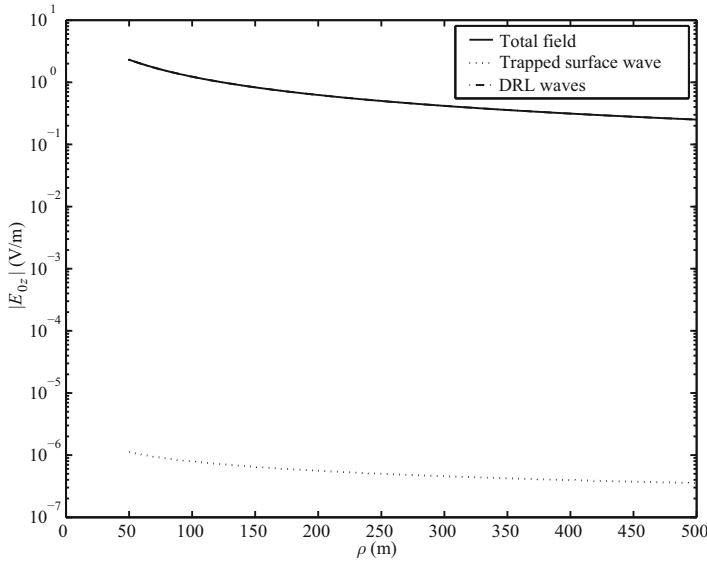


Fig. 4.8. The electric field $|E_z|$ in V/m with $f = 100$ MHz, $\varepsilon_{r1} = 2.65$, $\varepsilon_{r2} = 4$, $k_1 l_1 = k_2 l_2 = 1.4$, and $z = d = 3$ m

References

- Baños A Jr (1966) *Dipole Radiation in the Presence of a Conducting Half-Space*. Oxford, UK: Pergamon Press.
- Collin RE (2004a) Some observations about the near zone electric field of a hertzian dipole above a lossy earth. *IEEE Transactions on Antennas and Propagation*, 52(11): 3133–3137.
- Collin RE (2004b) Hertzian dipole radiation over a lossy earth or sea: Some early and late 20th century controversies. *IEEE Antennas and Propagation Magazine*, 46(2): 64–79.
- Dunn JM (1986) Lateral wave propagation in a three-layered medium. *Radio Science*, 21(5): 787–796.
- Gradshteyn IS and Ryzhik IM (1980) *Table of Integrals, Series, and Products*. New York, NY, USA: Academic Press.
- Hoh JH, Li LW, Kooi PS, Yeo TS, and Leong MS (1999) Dominant lateral waves in the canopy layer of a four-layered forest. *Radio Science*, 34(3): 681–691.
- King RWP (1982) New formulas for the electromagnetic field of a vertical electric dipole in a dielectric or conducting half-space near its horizontal interface. *Journal of Applied Physics*, 53: 8476–8482; (1984) Erratum, 56: 3366.
- King RWP (1991) The electromagnetic field of a horizontal electric dipole in the presence of a three-layered region. *Journal of Applied Physics*, 69(12): 7987–7995.

- King RWP, Owens M, and Wu TT (1992) *Lateral Electromagnetic Waves: Theory and Applications to Communications, Geophysical Exploration, and Remote Sensing*. New York, NY, USA: Springer-Verlag.
- King RWP (1993) The electromagnetic field of a horizontal electric dipole in the presence of a three-layered region: supplement. *Journal of Applied Physics*, 74(8): 4845–4548.
- King RWP and Sandler SS (1994a) The electromagnetic field of a vertical electric dipole over the earth or Sea. *IEEE Transactions on Antennas and Propagation*, 42(3): 382–389.
- King RWP and Sandler SS (1994b) The electromagnetic field of a vertical electric dipole in the presence of a three-layered region. *Radio Science*, 29(1): 97–113.
- King RWP and Sandler SS (1998) Reply. *Radio Science*, 33(2): 255–256.
- Li K and Lu Y (2005) Electromagnetic field generated by a horizontal electric dipole near the surface of a planar perfect conductor coated with a uniaxial layer. *IEEE Transactions on Antennas and Propagation*, 53(10): 3191–3200.
- Li LW, Yeo TS, Kooi PS, and Leong MS (1998) Radio wave propagation along mixed paths through a four-layered model of rain forest: an analytical approach. *IEEE Transactions on Antennas and Propagation*, 46(7): 1098–1111.
- Li LW, Lee CK, Yeo TS, and Leong MS (2004) Wave mode and path characteristics in four-layered anisotropic forest environment. *IEEE Transactions on Antennas and Propagation*, 52(9): 2445–2455.
- Liu L and Li K (2007) Radiation from a vertical electric dipole in the presence of a three-layered region. *IEEE Transactions on Antennas and Propagation*, 55(12): 3469–3475.
- Liu L, Li K, and Xu YH (2008) Radiation of a horizontal dipole in a three-layered region and microstrip antenna. *Progress In Electromagnetics Research*, PIER 86: 87–110. Cambridge, MA, USA: EMW Publishing.
- Mahmoud SF (1999) Remarks on “The electromagnetic field of a vertical electric dipole over the earth or Sea”. *IEEE Transactions on Antennas and Propagation*, 46(12): 1745–1946.
- Mei JP and Li K (2007) Electromagnetic field from a horizontal electric dipole on the surface of a high lossy medium coated with a uniaxial layer. *Progress In Electromagnetics Research*, PIER 73: 71–91. Cambridge, MA, USA: EMW Publishing.
- Wait JR (1953) Radiation from a vertical electric dipole over a stratified ground. *IRE Transactions on Antennas and Propagation*, AP-1: 9–12.
- Tsang L, Huang CC, and Chan CH (2000) Surface electromagnetic fields and impedance matrix elements of stratified media. *IEEE Transactions on Antennas and Propagation*, 48(10): 1533–1543.
- Tsang L, Ong CJ, Huang CC, and Jandhyala V (2003) Evaluation of the Green’s function for the mixed potential integral equation (MPIE) method in the time domain for layered media. *IEEE Transactions on Antennas and Propagation*, 51(7): 1559–1571.
- Wait JR (1954) Radiation from a vertical electric dipole over a stratified ground. *IRE Transactions on Antennas and Propagation*, 2: 144–146.
- Wait JR (1956) Radiation from a vertical electric dipole over a curved stratified ground ground. *Journal of Research of the National Bureau of Standards*, 56: 232–239.

- Wait JR (1957) Excitation of surface waves on conducting dielectric clad and corrugated surfaces. *Journal of Research of the National Bureau of Standards*, 59(6): 365–377.
- Wait JR (1970) *Electromagnetic Waves in Stratified Media* (2nd, Ed.). New York, NY, USA: Pergamon Press.
- Wait JR (1998) Comment on “The electromagnetic field of a vertical electric dipole in the presence of a three-layered region” by Ronold W. P. King and Sheldon S. Sandler. *Radio Science*, 33(2): 251–253.
- Xu YH, Ren W, Liu L, and Li K (2008a) Trapped surface wave and lateral wave in the presence of a four-layered region. *Progress In Electromagnetics Research*, PIER 82: 271–285. Cambridge, MA, USA: EMW Publishing.
- Xu YH, Li K, and Liu L (2008b) Electromagnetic field of a horizontal electric dipole in the presence of a four-layered region, *Progress In Electromagnetics Research*, PIER 81: 371–391. Cambridge, MA, USA: EMW Publishing.
- Zhang HQ and Pan WY (2002) Electromagnetic field of a vertical electric dipole on a perfect conductor coated with a dielectric layer. *Radio Science*, 37(4), 1060, doi:1029/2000RS002348.
- Zhang HQ, Li K, and Pan WY (2004) The electromagnetic field of a vertical dipole on the dielectric-coated imperfect conductor. *Journal of Electromagnetic Waves and Applications*, 18(10): 1305–1320.
- Zhang HQ, Pan WY, Li K, and Shen KX (2005) Electromagnetic field for a horizontal electric dipole buried inside a dielectric layer coated high lossy half space. *Progress In Electromagnetics Research*, PIER 50: 163–186. Cambridge, MA, USA: EMW Publishing.

Electromagnetic Field of a Horizontal Electric Dipole in the Presence of a Four-Layered Region

The electromagnetic field of a horizontal electric dipole in the presence of a four-layered region is examined in detail. Analysis and computations show that the properties for the electromagnetic field of a horizontal dipole in the presence of a four-layered region are similar to those for the corresponding three-layered case. It should be noted that both the trapped surface wave and the lateral wave are affected extensively by the thicknesses of the two dielectric layers. In practical applications, we can change the thicknesses of the upper and lower dielectric layers to fulfil the required results.

5.1 Integrated Formulas for the Electromagnetic Field

The relevant geometry and Cartesian coordinate system are shown in Fig. 5.1, where a horizontal electric dipole in the \hat{x} direction is located at $(0, 0, d)$. The region of interest is the same as that in Chapter 4, the wave numbers in the four-layered region are

$$k_0 = \omega \sqrt{\mu_0 \varepsilon_0}, \quad (5.1)$$

$$k_j = \omega \sqrt{\mu_0 (\varepsilon_0 \varepsilon_{rj} + \mathrm{i} \sigma_j / \omega)}; \quad j = 1, 2, \quad (5.2)$$

$$k_3 \rightarrow \infty. \quad (5.3)$$

When both the dipole and the observation point are on or near the air-dielectric boundary, the integrated formulas of the electromagnetic field of a horizontal electric dipole in the presence of a four-layered region can be obtained readily by using Eqs. (11.5.4)~(11.5.9) in the book by King, Owens, and Wu (1992). They are

$$E_{0\rho}(\rho, \phi, z) = \frac{\omega \mu_0}{4\pi k_0^2} \cos \phi$$

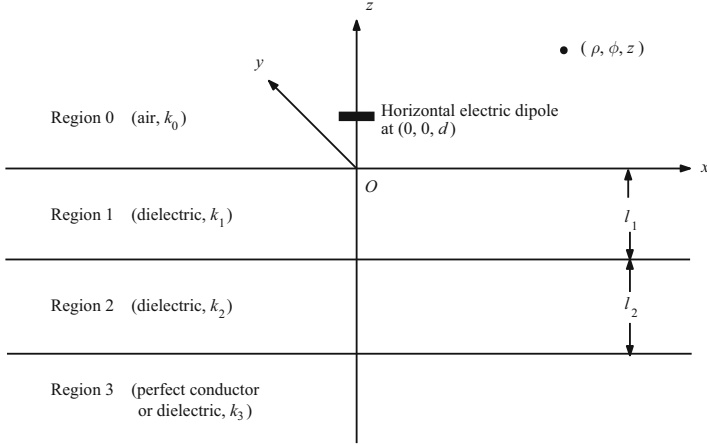


Fig. 5.1. Geometry of a horizontal dipole in the presence of a four-layered region

$$\begin{aligned} & \times \left\{ \int_0^\infty \left(k_0^2 J_0(\lambda \rho) - \frac{\lambda^2}{2} [J_0(\lambda \rho) - J_2(\lambda \rho)] \right) \gamma_0^{-1} e^{i\gamma_0|z-d|} \lambda d\lambda \right. \\ & \quad + \int_0^\infty \left(\frac{\gamma_0 Q}{2} [J_0(\lambda \rho) - J_2(\lambda \rho)] \right. \\ & \quad \left. \left. - \frac{k_0^2 P}{2\gamma_0} [J_0(\lambda \rho) + J_2(\lambda \rho)] \right) e^{i\gamma_0(z+d)} \lambda d\lambda \right\}, \quad (5.4) \end{aligned}$$

$$\begin{aligned} E_{0\phi}(\rho, \phi, z) &= \frac{\omega \mu_0}{4\pi k_0^2} \sin \phi \\ & \times \left\{ \int_0^\infty \left(k_0^2 J_0(\lambda \rho) - \frac{\lambda^2}{2} [J_0(\lambda \rho) + J_2(\lambda \rho)] \right) \gamma_0^{-1} e^{i\gamma_0|z-d|} \lambda d\lambda \right. \\ & \quad + \int_0^\infty \left(\frac{\gamma_0 Q}{2} [J_0(\lambda \rho) + J_2(\lambda \rho)] \right. \\ & \quad \left. \left. - \frac{k_0^2 P}{2\gamma_0} [J_0(\lambda \rho) - J_2(\lambda \rho)] \right) e^{i\gamma_0(z+d)} \lambda d\lambda \right\}, \quad (5.5) \end{aligned}$$

$$\begin{aligned} E_{0z}(\rho, \phi, z) &= \frac{i\omega \mu_0}{4\pi k_0^2} \cos \phi \int_0^\infty \left[\pm e^{i\gamma_0|z-d|} + Q e^{i\gamma_0(z+d)} \right] J_1(\lambda \rho) \lambda^2 d\lambda; \\ & \quad d < z \\ & \quad 0 \leq z \leq d, \quad (5.6) \end{aligned}$$

$$B_{0\rho}(\rho, \phi, z) = -\frac{\mu_0}{4\pi} \sin \phi$$

$$\times \left\{ \pm \int_0^\infty J_0(\lambda \rho) e^{i\gamma_0|z-d|} \lambda d\lambda + \int_0^\infty \left(\frac{Q}{2} [J_0(\lambda \rho) + J_2(\lambda \rho)] - \frac{P}{2} [J_0(\lambda \rho) - J_2(\lambda \rho)] \right) e^{i\gamma_0(z+d)} \lambda d\lambda \right\}; \quad \begin{matrix} d < z \\ 0 \leq z \leq d \end{matrix}, \quad (5.7)$$

$$B_{0\phi}(\rho, \phi, z) = -\frac{\mu_0}{4\pi} \cos \phi \times \left\{ \pm \int_0^\infty J_0(\lambda \rho) e^{i\gamma_0|z-d|} \lambda d\lambda + \int_0^\infty \left(\frac{Q}{2} [J_0(\lambda \rho) - J_2(\lambda \rho)] - \frac{P}{2} [J_0(\lambda \rho) + J_2(\lambda \rho)] \right) e^{i\gamma_0(z+d)} \lambda d\lambda \right\}; \quad \begin{matrix} d < z \\ 0 \leq z \leq d \end{matrix}, \quad (5.8)$$

$$B_{0z}(\rho, \phi, z) = \frac{i\mu_0}{4\pi} \sin \phi \int_0^\infty \left[e^{i\gamma_0|z-d|} - P e^{i\gamma_0(z+d)} \right] \gamma_0^{-1} J_1(\lambda \rho) \lambda^2 d\lambda, \quad (5.9)$$

where

$$Q = -\frac{k_1^2 \gamma_0 + i k_0^2 \gamma_1 \frac{\gamma_1 k_2^2 \tan(\gamma_1 l_1) + \gamma_2 k_1^2 \tan(\gamma_2 l_2)}{\gamma_1 k_2^2 - \gamma_2 k_1^2 \tan(\gamma_1 l_1) \tan(\gamma_2 l_2)}}{k_1^2 \gamma_0 - i k_0^2 \gamma_1 \frac{\gamma_1 k_2^2 \tan(\gamma_1 l_1) + \gamma_2 k_1^2 \tan(\gamma_2 l_2)}{\gamma_1 k_2^2 - \gamma_2 k_1^2 \tan(\gamma_1 l_1) \tan(\gamma_2 l_2)}}, \quad (5.10)$$

$$P = -\frac{\gamma_0 - i \gamma_1 \frac{\gamma_2 - \gamma_1 \tan(\gamma_1 l_1) \tan(\gamma_2 l_2)}{\gamma_1 \tan(\gamma_2 l_2) + \gamma_2 \tan(\gamma_1 l_1)}}{\gamma_0 + i \gamma_1 \frac{\gamma_2 - \gamma_1 \tan(\gamma_1 l_1) \tan(\gamma_2 l_2)}{\gamma_1 \tan(\gamma_2 l_2) + \gamma_2 \tan(\gamma_1 l_1)}}, \quad (5.11)$$

$$\gamma_j = \sqrt{k_j^2 - \lambda^2}; \quad j = 0, 1, 2, \quad (5.12)$$

$$k_j = \omega \sqrt{\mu_0 \varepsilon_j}; \quad j = 0, 1, 2. \quad (5.13)$$

It is convenient to rewrite Eqs. (5.4)~(5.9) in the following forms:

$$E_{0\rho}(\rho, \phi, z) = \frac{\omega \mu_0}{4\pi k_0^2} \cos \phi [F_{\rho 0}(\rho, z-d) - F_{\rho 0}(\rho, z+d) + F_{\rho 1}(\rho, z+d)], \quad (5.14)$$

$$E_{0\phi}(\rho, \phi, z) = \frac{\omega \mu_0}{4\pi k_0^2} \sin \phi [F_{\phi 0}(\rho, z-d) - F_{\phi 0}(\rho, z+d) + F_{\phi 1}(\rho, z+d)], \quad (5.15)$$

$$E_{0z}(\rho, \phi, z) = \frac{i\omega \mu_0}{4\pi k_0^2} \cos \phi [F_{z 0}(\rho, z-d) - F_{z 0}(\rho, z+d) + F_{z 1}(\rho, z+d)], \quad (5.16)$$

$$B_{0\rho}(\rho, \phi, z) = -\frac{\mu_0}{4\pi} \sin \phi [G_{\rho 0}(\rho, z-d) - G_{\rho 0}(\rho, z+d) + G_{\rho 1}(\rho, z+d)], \quad (5.17)$$

$$B_{0\phi}(\rho, \phi, z) = -\frac{\mu_0}{4\pi} \cos \phi [G_{\phi 0}(\rho, z-d) - G_{\phi 0}(\rho, z+d) + G_{\phi 1}(\rho, z+d)], \quad (5.18)$$

$$B_{0z}(\rho, \phi, z) = \frac{i\mu_0}{4\pi} \sin \phi [G_{z0}(\rho, z-d) - G_{z0}(\rho, z+d) + G_{z1}(\rho, z+d)]. \quad (5.19)$$

where

$$F_{\rho 0}(\rho, z-d) = \int_0^\infty \left\{ \frac{\gamma_0}{2} [J_0(\lambda\rho) - J_2(\lambda\rho)], \right. \\ \left. + \frac{k_0^2}{2\gamma_0} [J_0(\lambda\rho) + J_2(\lambda\rho)] \right\} e^{i\gamma_0|z-d|} \lambda d\lambda, \quad (5.20)$$

$$F_{\rho 0}(\rho, z+d) = \int_0^\infty \left\{ \frac{\gamma_0}{2} [J_0(\lambda\rho) - J_2(\lambda\rho)] \right. \\ \left. + \frac{k_0^2}{2\gamma_0} [J_0(\lambda\rho) + J_2(\lambda\rho)] \right\} e^{i\gamma_0(z+d)} \lambda d\lambda, \quad (5.21)$$

$$F_{\phi 0}(\rho, z-d) = \int_0^\infty \left\{ \frac{\gamma_0}{2} [J_0(\lambda\rho) + J_2(\lambda\rho)] \right. \\ \left. + \frac{k_0^2}{2\gamma_0} [J_0(\lambda\rho) - J_2(\lambda\rho)] \right\} e^{i\gamma_0|z-d|} \lambda d\lambda, \quad (5.22)$$

$$F_{\phi 0}(\rho, z+d) = \int_0^\infty \left\{ \frac{\gamma_0}{2} [J_0(\lambda\rho) + J_2(\lambda\rho)] \right. \\ \left. + \frac{k_0^2}{2\gamma_0} [J_0(\lambda\rho) - J_2(\lambda\rho)] \right\} e^{i\gamma_0(z+d)} \lambda d\lambda, \quad (5.23)$$

$$F_{z0}(\rho, z-d) = \pm \int_0^\infty J_1(\lambda\rho) e^{i\gamma_0|z-d|} \lambda^2 d\lambda; \quad \begin{matrix} d < z \\ 0 \leq z \leq d \end{matrix}, \quad (5.24)$$

$$F_{z0}(\rho, z+d) = \int_0^\infty J_1(\lambda\rho) e^{i\gamma_0(z+d)} \lambda^2 d\lambda, \quad (5.25)$$

$$G_{\rho 0}(\rho, z-d) = \pm \int_0^\infty J_0(\lambda\rho) e^{i\gamma_0|z-d|} \lambda d\lambda; \quad \begin{matrix} d < z \\ 0 \leq z \leq d \end{matrix}, \quad (5.26)$$

$$G_{\rho 0}(\rho, z+d) = \int_0^\infty J_0(\lambda\rho) e^{i\gamma_0(z+d)} \lambda d\lambda, \quad (5.27)$$

$$G_{\phi 0}(\rho, z-d) = G_{\rho 0}(\rho, z-d) \\ = \pm \int_0^\infty J_0(\lambda\rho) e^{i\gamma_0|z-d|} \lambda d\lambda; \quad \begin{matrix} d < z \\ 0 \leq z \leq d \end{matrix}, \quad (5.28)$$

$$G_{\phi 0}(\rho, z + d) = G_{\rho 0}(\rho, z + d) = \int_0^\infty J_0(\lambda \rho) e^{i\gamma_0(z+d)} \lambda d\lambda, \quad (5.29)$$

$$G_{z 0}(\rho, z - d) = \int_0^\infty J_1(\lambda \rho) \gamma_0^{-1} e^{i\gamma_0|z-d|} \lambda^2 d\lambda, \quad (5.30)$$

$$G_{z 0}(\rho, z + d) = \int_0^\infty J_1(\lambda \rho) \gamma_0^{-1} e^{i\gamma_0(z+d)} \lambda^2 d\lambda. \quad (5.31)$$

It is seen that the first and second terms in Eqs.(5.14)~(5.19), which have been evaluated many years ago (King, Owens, and Wu, 1992), stand for the direct wave and ideal reflected wave, respectively. In the next step, it is necessary to evaluate the remaining integrals. The third terms in Eqs.(5.14)~(5.19) can be separated into electric-type and magnetic-type terms. They are

$$F_{\rho 1}(\rho, z + d) = F_{\rho 2}(\rho, z + d) + F_{\rho 3}(\rho, z + d), \quad (5.32)$$

$$F_{\phi 1}(\rho, z + d) = F_{\phi 2}(\rho, z + d) + F_{\phi 3}(\rho, z + d), \quad (5.33)$$

$$G_{\rho 1}(\rho, z + d) = G_{\rho 2}(\rho, z + d) + G_{\rho 3}(\rho, z + d), \quad (5.34)$$

$$G_{\phi 1}(\rho, z + d) = G_{\phi 2}(\rho, z + d) + G_{\phi 3}(\rho, z + d), \quad (5.35)$$

where

$$F_{\rho 2}(\rho, z + d) = \int_0^\infty \frac{\gamma_0(Q+1)}{2} [J_0(\lambda \rho) - J_2(\lambda \rho)] e^{i\gamma_0(z+d)} \lambda d\lambda, \quad (5.36)$$

$$F_{\phi 2}(\rho, z + d) = \int_0^\infty \frac{\gamma_0(Q+1)}{2} [J_0(\lambda \rho) + J_2(\lambda \rho)] e^{i\gamma_0(z+d)} \lambda d\lambda, \quad (5.37)$$

$$G_{\rho 2}(\rho, z + d) = \int_0^\infty \frac{Q+1}{2} [J_0(\lambda \rho) + J_2(\lambda \rho)] e^{i\gamma_0(z+d)} \lambda d\lambda, \quad (5.38)$$

$$G_{\phi 2}(\rho, z + d) = \int_0^\infty \frac{Q+1}{2} [J_0(\lambda \rho) - J_2(\lambda \rho)] e^{i\gamma_0(z+d)} \lambda d\lambda, \quad (5.39)$$

$$F_{z 1}(\rho, z + d) = \int_0^\infty (Q+1) J_1(\lambda \rho) e^{i\gamma_0(z+d)} \lambda^2 d\lambda, \quad (5.40)$$

$$F_{\rho 3}(\rho, z + d) = - \int_0^\infty \frac{k_0^2(P-1)}{2\gamma_0} [J_0(\lambda \rho) + J_2(\lambda \rho)] e^{i\gamma_0(z+d)} \lambda d\lambda, \quad (5.41)$$

$$F_{\phi 3}(\rho, z + d) = - \int_0^\infty \frac{k_0^2(P-1)}{2\gamma_0} [J_0(\lambda \rho) - J_2(\lambda \rho)] e^{i\gamma_0(z+d)} \lambda d\lambda, \quad (5.42)$$

$$G_{\rho 3}(\rho, z + d) = - \int_0^\infty \frac{P-1}{2} [J_0(\lambda \rho) - J_2(\lambda \rho)] e^{i\gamma_0(z+d)} \lambda d\lambda, \quad (5.43)$$

$$G_{\phi 3}(\rho, z + d) = - \int_0^\infty \frac{P-1}{2} [J_0(\lambda \rho) + J_2(\lambda \rho)] e^{i\gamma_0(\rho, z+d)} \lambda d\lambda, \quad (5.44)$$

$$G_{z1}(\rho, z + d) = - \int_0^\infty (P - 1) J_1(\lambda \rho) \gamma_0^{-1} e^{i\gamma_0(z+d)} \lambda^2 d\lambda. \quad (5.45)$$

In this chapter, the integrals F_{z1} , $F_{\rho2}$, $F_{\phi2}$, $G_{\rho2}$, and $G_{\phi2}$ involving the factor $(Q+1)$ are defined as the electric-type terms, and the integrals G_{z1} , $F_{\rho3}$, $F_{\phi3}$, $G_{\rho3}$, and $G_{\phi3}$ involving the factor $(P-1)$ are defined as the magnetic-type terms.

5.2 Evaluation for the Electric-Type Field

Considering γ_0, γ_1 , and γ_2 are even functions of λ , and using the relations between Bessel function and Hankel function

$$J_n(\lambda \rho) = \frac{1}{2} \left[H_n^{(1)}(\lambda \rho) + H_n^{(2)}(\lambda \rho) \right], \quad (5.46)$$

$$H_n^{(1)}(-\lambda \rho) = H_n^{(2)}(\lambda \rho) (-1)^{n+1}, \quad (5.47)$$

$$J_0(\lambda \rho) + J_2(\lambda \rho) = \frac{2}{\lambda \rho} J_1(\lambda \rho). \quad (5.48)$$

Substitution Eqs. (5.46)~(5.48) into Eq. (5.36) yields to

$$\begin{aligned} F_{\rho2}(\rho, z + d) = & -\frac{i}{2} \int_{-\infty}^{\infty} \frac{k_0^2 \gamma_0 \gamma_1 \left[\gamma_1 k_2^2 \tan(\gamma_1 l_1) + \gamma_2 k_1^2 \tan(\gamma_2 l_2) \right]}{q(\lambda)} \\ & \times \left[H_0^{(1)}(\lambda \rho) - H_2^{(1)}(\lambda \rho) \right] e^{i\gamma_0(z+d)} \lambda d\lambda, \end{aligned} \quad (5.49)$$

where

$$\begin{aligned} q(\lambda) = & k_1^2 \gamma_0 \left[\gamma_1 k_2^2 - \gamma_2 k_1^2 \tan(\gamma_1 l_1) \tan(\gamma_2 l_2) \right] \\ & - i k_0^2 \gamma_1 \left[\gamma_1 k_2^2 \tan(\gamma_1 l_1) + \gamma_2 k_1^2 \tan(\gamma_2 l_2) \right]. \end{aligned} \quad (5.50)$$

It is convenient to decompose $F_{\rho2}$ into two terms $F_{\rho2}^{(1)}$ and $F_{\rho2}^{(2)}$. They are

$$F_{\rho2}^{(1)} = -\frac{i}{2} k_0^2 k_1^2 \int_{-\infty}^{\infty} \frac{\gamma_0 \gamma_1 \gamma_2 \tan(\gamma_2 l_2) \left[H_0^{(1)}(\lambda \rho) - H_2^{(1)}(\lambda \rho) \right]}{q(\lambda)} e^{i\gamma_0(z+d)} \lambda d\lambda, \quad (5.51)$$

$$F_{\rho2}^{(2)} = -\frac{i}{2} k_0^2 k_2^2 \int_{-\infty}^{\infty} \frac{\gamma_0 \gamma_1^2 \tan(\gamma_1 l_1) \left[H_0^{(1)}(\lambda \rho) - H_2^{(1)}(\lambda \rho) \right]}{q(\lambda)} e^{i\gamma_0(z+d)} \lambda d\lambda. \quad (5.52)$$

In order to evaluate the above two integrals, we shift the contour around the branch lines at $\lambda = k_0$, $\lambda = k_1$, and $\lambda = k_2$. The next main tasks are to

determine the poles and to evaluate the integrations along the branch lines Γ_0 , Γ_1 , and Γ_2 . The poles of the integrands satisfy the following equation:

$$q(\lambda) = k_1^2 \gamma_0 [\gamma_1 k_2^2 - \gamma_2 k_1^2 \tan(\gamma_1 l_1) \tan(\gamma_2 l_2)] - i k_0^2 \gamma_1 [\gamma_1 k_2^2 \tan(\gamma_1 l_1) + \gamma_2 k_1^2 \tan(\gamma_2 l_2)] = 0. \quad (5.53)$$

Compared with the vertical-dipole case as addressed in Chapter 4, it is seen that Eq. (5.53) is the same as that of the vertical-dipole case. Thus, $F_{\rho 2}^{(1)}$ can be written in the form

$$\begin{aligned} F_{\rho 2}^{(1)} = & 2\pi i \left(-\frac{i}{2} k_0^2 k_1^2 \right) \\ & \times \sum_j \frac{\gamma_{0E}^* \gamma_{1E}^* \gamma_{2E}^* \tan(\gamma_{2E}^* l_2) \left[H_0^{(1)}(\lambda_{jE}^* \rho) - H_2^{(1)}(\lambda_{jE}^* \rho) \right]}{q'(\lambda_{jE}^*)} e^{i\gamma_{0E}^*(z+d)} \lambda_{jE}^* \\ & - \frac{i}{2} k_0^2 k_1^2 \int_{\Gamma_0 + \Gamma_1 + \Gamma_2} \frac{\gamma_0 \gamma_1 \gamma_2 \tan(\gamma_2 l_2) \left[H_0^{(1)}(\lambda \rho) - H_2^{(1)}(\lambda \rho) \right]}{q(\lambda)} \\ & \times e^{i\gamma_0(z+d)} \lambda d\lambda, \end{aligned} \quad (5.54)$$

where λ_{jE}^* are poles of electric-type wave,

$$\begin{aligned} q'(\lambda) = & -k_1^2 \frac{\lambda}{\gamma_0} [\gamma_1 k_2^2 - \gamma_2 k_1^2 \tan(\gamma_1 l_1) \tan(\gamma_2 l_2)] \\ & + i k_0^2 \frac{\lambda}{\gamma_1} [\gamma_1 k_2^2 \tan(\gamma_1 l_1) + \gamma_2 k_1^2 \tan(\gamma_2 l_2)] \\ & + k_1^2 \gamma_0 \left\{ -\frac{\lambda}{\gamma_1} k_2^2 + \frac{\lambda}{\gamma_2} k_1^2 \tan(\gamma_1 l_1) \tan(\gamma_2 l_2) + k_1^2 \gamma_2 \lambda \right. \\ & \quad \times \left[\frac{l_1}{\gamma_1} \sec^2(\gamma_1 l_1) \tan(\gamma_2 l_2) + \frac{l_2}{\gamma_2} \tan(\gamma_1 l_1) \sec^2(\gamma_2 l_2) \right] \Big\} \\ & + i k_0^2 \gamma_1 \lambda \left[\frac{k_2^2 \tan(\gamma_1 l_1)}{\gamma_1} + \frac{k_1^2 \tan(\gamma_2 l_2)}{\gamma_2} + k_2^2 l_1 \sec^2(\gamma_1 l_1) \right. \\ & \quad \left. + k_1^2 l_2 \sec^2(\gamma_2 l_2) \right], \end{aligned} \quad (5.55)$$

$$\gamma_{nE}^* = \gamma_n^*(\lambda_{jE}^*) = \sqrt{k_n^2 - \lambda_{jE}^{*2}}; \quad n = 0, 1, 2. \quad (5.56)$$

Next, it is necessary to evaluate the integrals along the branch lines Γ_0 , Γ_1 , and Γ_2 . Similar to the three-layered case addressed in Chapter 3, it is easily verified that the integrations along the branch lines Γ_1 and Γ_2 are zero for the integrals in Eq. (5.54). Subject to the far-field condition of $k_0 \rho \gg 1$ and $z + d \ll \rho$, it is seen that the dominant contribution of the integration along Γ_0 comes from the vicinity of k_0 . Let $\lambda = k_0(1_i \tau^2)$, at the vicinity of k_0 , the values $H_n^{(1)}(\lambda \rho)$, γ_0 , γ_1 , and γ_2 are approximated as

$$H_n^{(1)}(\lambda\rho) \approx \sqrt{\frac{2}{\pi k_0 \rho}} e^{i(k_0 \rho - \frac{n}{2}\pi - \frac{1}{4}\pi)} e^{-k_0 \rho \tau^2}; \quad n = 0, 1, \quad (5.57)$$

$$\gamma_0 = \sqrt{k_0^2 - \lambda^2} \approx k_0 e^{i\frac{3}{4}\pi} \sqrt{2}\tau, \quad (5.58)$$

$$\gamma_1 = \sqrt{k_1^2 - \lambda^2} \approx \sqrt{k_1^2 - k_0^2} = \gamma_{10}, \quad (5.59)$$

$$\gamma_2 = \sqrt{k_2^2 - \lambda^2} \approx \sqrt{k_2^2 - k_0^2} = \gamma_{20}. \quad (5.60)$$

Then, with the change of variable $t = \tau + \frac{e^{i\pi/4}}{\sqrt{2}} \frac{z+d}{\rho}$, the integral along branch line Γ_0 in Eq. (5.54) is written in following form:

$$\begin{aligned} I_1 &= -\frac{i}{2} k_0^2 k_1^2 \int_{\Gamma_0} \frac{\gamma_0 \gamma_1 \gamma_2 \tan(\gamma_2 l_2) [H_0^{(1)}(\lambda\rho) - H_2^{(1)}(\lambda\rho)]}{q(\lambda)} e^{i\gamma_0(z+d)} \lambda d\lambda \\ &= \frac{2\sqrt{2} k_0^4 e^{-i\frac{\pi}{4}} \sqrt{\frac{1}{\pi k_0 \rho}} \gamma_{10} \gamma_{20} \tan(\gamma_{20} l_2) \exp \left[i k_0 \rho + i \frac{k_0 \rho}{2} \left(\frac{z+d}{\rho} \right)^2 \right]}{\gamma_{10} k_2^2 - \gamma_{20} k_1^2 \tan(\gamma_{10} l_1) \tan(\gamma_{20} l_2)} \\ &\quad \times \int_{-\infty}^{\infty} \frac{e^{-k_0 \rho t^2} \left(t - \frac{e^{i\frac{\pi}{4}}}{\sqrt{2}} \frac{z+d}{\rho} \right)^2}{t - e^{i\frac{\pi}{4}} \Delta'_1} dt, \end{aligned} \quad (5.61)$$

where

$$\Delta'_1 = \frac{z+d}{\sqrt{2}\rho} - i \frac{k_0 \gamma_{10} [\gamma_{10} k_2^2 \tan(\gamma_{10} l_1) + \gamma_{20} k_1^2 \tan(\gamma_{20} l_2)]}{\sqrt{2} k_1^2 [\gamma_{10} k_2^2 - \gamma_{20} k_1^2 \tan(\gamma_{10} l_1) \tan(\gamma_{20} l_2)]}. \quad (5.62)$$

The integral in Eq. (5.61) can be evaluated directly. The result becomes

$$\begin{aligned} \int_{-\infty}^{\infty} \frac{e^{-k_0 \rho t^2} \left(t - \frac{e^{i\frac{\pi}{4}}}{\sqrt{2}} \frac{z+d}{\rho} \right)^2}{t - e^{i\frac{\pi}{4}} \Delta'_1} dt &= e^{i\frac{\pi}{4}} \sqrt{\frac{\pi}{k_0 \rho}} \left(\Delta'_1 - \sqrt{2} \frac{z+d}{\rho} \right) \\ &\quad - \pi e^{-ip_1^*} \left(\Delta'_1 - \frac{1}{\sqrt{2}} \frac{z+d}{\rho} \right)^2 \operatorname{erfc}(\sqrt{-ip_1^*}), \end{aligned} \quad (5.63)$$

where $p_1^* = k_0 \rho \Delta_1'^2$, and the phase of $\sqrt{ik_0 \rho \Delta_1'^2}$ in Eq. (5.63) requires to be

$$\left| \operatorname{Arg} \sqrt{-i \Delta_1'^2 k_0 \rho} \right| \leq \frac{\pi}{4}. \quad (5.64)$$

Using the relation between the error function and the Fresnel integral, we have

$$\begin{aligned}
F_{\rho 2}^{(1)} = & \pi k_0^2 k_1^2 \\
& \times \sum_j \frac{\gamma_{0E}^* \gamma_{1E}^* \gamma_{2E}^* \tan(\gamma_{2E}^* l_2) \left[H_0^{(1)}(\lambda_{jE}^* \rho) - H_2^{(1)}(\lambda_{jE}^* \rho) \right]}{q'(\lambda_{jE}^*)} e^{i\gamma_{0E}^*(z+d)} \lambda_{jE}^* \\
& + \frac{2\sqrt{2}k_0^4 \gamma_{10} \gamma_{20} \tan(\gamma_{20} l_2)}{\gamma_{10} k_2^2 - \gamma_{20} k_1^2 \tan(\gamma_{10} l_1) \tan(\gamma_{20} l_2)} \sqrt{\frac{1}{\pi k_0 \rho}} e^{ik_0 r_2} \\
& \times \left[\sqrt{\frac{\pi}{k_0 \rho}} \left(\Delta'_1 - \sqrt{2} \frac{z+d}{\rho} \right) + i\sqrt{2}\pi \left(\Delta'_1 - \frac{1}{\sqrt{2}} \frac{z+d}{\rho} \right)^2 e^{-ip_1^* \mathbf{F}(p_1^*)} \right], \tag{5.65}
\end{aligned}$$

where $r_2 = \sqrt{\rho^2 + (z+d)^2} \approx \rho \left[1 + \frac{1}{2} \left(\frac{z+d}{\rho} \right)^2 \right]$.

Similarly, the integral in Eq. (5.52) can be evaluated readily.

$$\begin{aligned}
F_{\rho 2}^{(2)} = & \pi k_0^2 k_2^2 \\
& \times \sum_j \frac{\gamma_{0E}^* \gamma_1^2(\lambda_{jE}^*) \tan \gamma_{1E}^* l_1 \left[H_0^{(1)}(\lambda_{jE}^* \rho) - H_2^{(1)}(\lambda_{jE}^* \rho) \right]}{q'(\lambda_{jE}^*)} e^{i\gamma_{0E}^*(z+d)} \lambda_{jE}^* \\
& + \frac{2\sqrt{2}k_0^4 \frac{k_2^2}{k_1^2} \gamma_{10}^2 \tan(\gamma_{10} l_1)}{\gamma_{10} k_2^2 - \gamma_{20} k_1^2 \tan(\gamma_{10} l_1) \tan(\gamma_{20} l_2)} \sqrt{\frac{1}{\pi k_0 \rho}} e^{ik_0 r_2} \\
& \times \left[\sqrt{\frac{\pi}{k_0 \rho}} \left(\Delta'_1 - \sqrt{2} \frac{z+d}{\rho} \right) + i\sqrt{2}\pi \left(\Delta'_1 - \frac{1}{\sqrt{2}} \frac{z+d}{\rho} \right)^2 e^{-ip_1^* \mathbf{F}(p_1^*)} \right]. \tag{5.66}
\end{aligned}$$

Then, the final expression of $F_{\rho 2}(\rho, z+d)$ is written in the following form:

$$\begin{aligned}
F_{\rho 2} = & \pi k_0^2 \sum_j \frac{\gamma_{0E}^* \gamma_{1E}^* \left[k_2^2 \gamma_{1E}^* \tan(\gamma_{1E}^* l_1) + k_1^2 \gamma_{2E}^* \tan(\gamma_{2E}^* l_2) \right]}{q'(\lambda_{jE}^*)} \\
& \times \left[H_0^{(1)}(\lambda_{jE}^* \rho) - H_2^{(1)}(\lambda_{jE}^* \rho) \right] e^{i\gamma_{0E}^*(z+d)} \lambda_{jE}^* \\
& + \frac{2\sqrt{2}k_0^4 \gamma_{10} \left[\frac{k_2^2}{k_1^2} \gamma_{10} \tan(\gamma_{10} l_1) + \gamma_{20} \tan(\gamma_{20} l_2) \right]}{\gamma_{10} k_2^2 - \gamma_{20} k_1^2 \tan(\gamma_{10} l_1) \tan(\gamma_{20} l_2)} \sqrt{\frac{1}{\pi k_0 \rho}} e^{ik_0 r_2} \\
& \times \left[\sqrt{\frac{\pi}{k_0 \rho}} \left(\Delta'_1 - \sqrt{2} \frac{z+d}{\rho} \right) + i\sqrt{2}\pi \left(\Delta'_1 - \frac{1}{\sqrt{2}} \frac{z+d}{\rho} \right)^2 e^{-ip_1^* \mathbf{F}(p_1^*)} \right]. \tag{5.67}
\end{aligned}$$

Evidently, with similar procedures, the remaining terms of the electric-type field can also be evaluated. We write

$$\begin{aligned}
F_{\phi 2} = & \pi k_0^2 \sum_j \frac{\gamma_{0E}^* \gamma_{1E}^* [k_2^2 \gamma_{1E}^* \tan(\gamma_{1E}^* l_1) + k_1^2 \gamma_{2E}^* \tan(\gamma_{2E}^* l_2)]}{q'(\lambda_{jE}^*)} \\
& \times \left[H_0^{(1)}(\lambda_{jE}^* \rho) + H_2^{(1)}(\lambda_{jE}^* \rho) \right] e^{i\gamma_{0E}^*(z+d)} \lambda_{jE}^* \\
& - \frac{i2\sqrt{2}k_0^3 \gamma_{10} \left[\frac{k_2^2}{k_1^2} \gamma_{10} \tan(\gamma_{10} l_1) + \gamma_{20} \tan(\gamma_{20} l_2) \right]}{\rho [\gamma_{10} k_2^2 - \gamma_{20} k_1^2 \tan(\gamma_{10} l_1) \tan(\gamma_{20} l_2)]} \sqrt{\frac{1}{\pi k_0 \rho}} e^{ik_0 r_2} \\
& \times \left[\sqrt{\frac{\pi}{k_0 \rho}} \left(\Delta'_1 - \sqrt{2} \frac{z+d}{\rho} \right) + i\sqrt{2}\pi \left(\Delta'_1 - \frac{1}{\sqrt{2}} \frac{z+d}{\rho} \right)^2 e^{-ip_1^* \mathbf{F}(p_1^*)} \right], \tag{5.68}
\end{aligned}$$

$$\begin{aligned}
G_{\phi 2} = & -\pi k_0^2 \sum_j \frac{\gamma_{1E}^* [k_2^2 \gamma_{1E}^* \tan(\gamma_{1E}^* l_1) + k_1^2 \gamma_{2E}^* \tan(\gamma_{2E}^* l_2)]}{q'(\lambda_{jE}^*)} \\
& \times \left[H_0^{(1)}(\lambda_{jE}^* \rho) - H_2^{(1)}(\lambda_{jE}^* \rho) \right] e^{i\gamma_{0E}^*(z+d)} \lambda_{jE}^* \\
& - \frac{2k_0^3 \gamma_{10} \left[\frac{k_2^2}{k_1^2} \gamma_{10} \tan(\gamma_{10} l_1) + \gamma_{20} \tan(\gamma_{20} l_2) \right]}{\gamma_{10} k_2^2 - \gamma_{20} k_1^2 \tan \gamma_{10} l_1 \tan \gamma_{20} l_2} \sqrt{\frac{1}{\pi k_0 \rho}} e^{-k_0 r_2} \\
& \times \left[\sqrt{\frac{\pi}{k_0 \rho}} + i\sqrt{2}\pi \left(\Delta'_1 - \frac{z+d}{\sqrt{2}\rho} \right) e^{-ip_1^* \mathbf{F}(p_1^*)} \right], \tag{5.69}
\end{aligned}$$

$$\begin{aligned}
G_{\rho 2} = & -\pi k_0^2 \sum_j \frac{\gamma_{1E}^* [k_2^2 \gamma_{1E}^* \tan(\gamma_{1E}^* l_1) + k_1^2 \gamma_{2E}^* \tan(\gamma_{2E}^* l_2)]}{q'(\lambda_{jE}^*)} \\
& \times \left[H_0^{(1)}(\lambda_{jE}^* \rho) + H_2^{(1)}(\lambda_{jE}^* \rho) \right] e^{i\gamma_{0E}^*(z+d)} \lambda_{jE}^* \\
& + \frac{i2k_0^2 \gamma_{10} \left[\frac{k_2^2}{k_1^2} \gamma_{10} \tan(\gamma_{10} l_1) + \gamma_{20} \tan(\gamma_{20} l_2) \right]}{\rho [\gamma_{10} k_2^2 - \gamma_{20} k_1^2 \tan(\gamma_{10} l_1) \tan(\gamma_{20} l_2)]} \sqrt{\frac{1}{\pi k_0 \rho}} e^{ik_0 r_2} \\
& \times \left[\sqrt{\frac{\pi}{k_0 \rho}} + i\sqrt{2}\pi \left(\Delta'_1 - \frac{z+d}{\sqrt{2}\rho} \right) e^{-ip_1^* \mathbf{F}(p_1^*)} \right], \tag{5.70}
\end{aligned}$$

$$\begin{aligned}
F_{z1} = & 2\pi k_0^2 \sum_j \frac{\gamma_{1E}^* [k_2^2 \gamma_{1E}^* \tan(\gamma_{1E}^* l_1) + k_1^2 \gamma_{2E}^* \tan(\gamma_{2E}^* l_2)] \lambda_{jE}^{*2}}{q'(\lambda_{jE}^*)} \\
& \times H_1^{(1)}(\lambda_{jE}^* \rho) e^{i\gamma_{0E}^*(z+d)} \\
& + \frac{i2k_0^4 \gamma_{10} \left[\frac{k_2^2}{k_1^2} \gamma_{10} \tan(\gamma_{10} l_1) + \gamma_{20} \tan(\gamma_{20} l_2) \right]}{\gamma_{10} k_2^2 - \gamma_{20} k_1^2 \tan(\gamma_{10} l_1) \tan(\gamma_{20} l_2)} \sqrt{\frac{1}{\pi k_0 \rho}} e^{ik_0 r_2} \\
& \times \left[\sqrt{\frac{\pi}{k_0 \rho}} + i\sqrt{2}\pi \left(\Delta'_1 - \frac{z+d}{\sqrt{2}\rho} \right) e^{-ip_1^* \mathbf{F}(p_1^*)} \right]. \tag{5.71}
\end{aligned}$$

5.3 Evaluation for the Magnetic-Type Field

Substitution Eqs. (5.46)~(5.48) into Eq. (5.42) yields to

$$F_{\phi 3}(\rho, z + d) = \frac{k_0^2}{2} \int_{-\infty}^{\infty} \frac{[\gamma_1 \tan(\gamma_2 l_2) + \gamma_2 \tan(\gamma_1 l_1)] [H_0^{(1)}(\lambda \rho) - H_2^{(1)}(\lambda \rho)]}{p(\lambda)} \times e^{i\gamma_0(z+d)} \lambda d\lambda, \quad (5.72)$$

where

$$p(\lambda) = \gamma_0 \gamma_1 \tan(\gamma_2 l_2) + \gamma_0 \gamma_2 \tan(\gamma_1 l_1) + i\gamma_1 \gamma_2 - i\gamma_1^2 \tan(\gamma_1 l_1) \tan(\gamma_2 l_2). \quad (5.73)$$

It is convenient to decompose $F_{\phi 3}(\rho, z + d)$ into $F_{\phi 3}^{(1)}$ and $F_{\phi 3}^{(2)}$. They are expressed as follows:

$$F_{\phi 3}^{(1)} = \frac{k_0^2}{2} \int_{-\infty}^{\infty} \frac{\gamma_1 \tan(\gamma_2 l_2) [H_0^{(1)}(\lambda \rho) - H_2^{(1)}(\lambda \rho)]}{p(\lambda)} e^{i\gamma_0(z+d)} \lambda d\lambda, \quad (5.74)$$

$$F_{\phi 3}^{(2)} = \frac{k_0^2}{2} \int_{-\infty}^{\infty} \frac{\gamma_2 \tan(\gamma_1 l_1) [H_0^{(1)}(\lambda \rho) - H_2^{(1)}(\lambda \rho)]}{p(\lambda)} e^{i\gamma_0(z+d)} \lambda d\lambda. \quad (5.75)$$

In order to evaluate $F_{\phi 3}^{(1)}$ and $F_{\phi 3}^{(2)}$, it is necessary to examine the pole equation of the magnetic-type terms.

$$p(\lambda) = \gamma_0 \gamma_1 \tan(\gamma_2 l_2) + \gamma_0 \gamma_2 \tan(\gamma_1 l_1) + i\gamma_1 \gamma_2 - i\gamma_1^2 \tan(\gamma_1 l_1) \tan(\gamma_2 l_2) = 0. \quad (5.76)$$

Clearly, the poles may exist in the case of $k_0 < \lambda < k_2$, and k_1 is a removable pole. As illustrated in Figs. 5.2 and 5.3, the poles are determined by using Newton's iteration method. Then we have

$$F_{\phi 3}^{(1)} = 2\pi i \frac{k_0^2}{2} \sum_j \frac{\gamma_{1B}^* \tan(\gamma_{2B}^* l_2) [H_0^{(1)}(\lambda_{jB}^* \rho) - H_2^{(1)}(\lambda_{jB}^* \rho)]}{p'(\lambda_{jB}^*)} e^{i\gamma_{0B}^*(z+d)} \lambda_{jB}^* + \frac{k_0^2}{2} \int_{\Gamma_0 + \Gamma_1 + \Gamma_2} \frac{\gamma_1 \tan(\gamma_2 l_2) [H_0^{(1)}(\lambda \rho) - H_2^{(1)}(\lambda \rho)]}{p(\lambda)} e^{i\gamma_0(z+d)} \lambda d\lambda, \quad (5.77)$$

where λ_{jB}^* are the poles of the magnetic-type field.

$$p'(\lambda) = -\lambda \left[\frac{\gamma_1}{\gamma_0} \tan(\gamma_2 l_2) + \frac{\gamma_0}{\gamma_1} \tan(\gamma_2 l_2) + \frac{\gamma_0 \gamma_1 l_2}{\gamma_2} \sec^2(\gamma_2 l_2) \right]$$

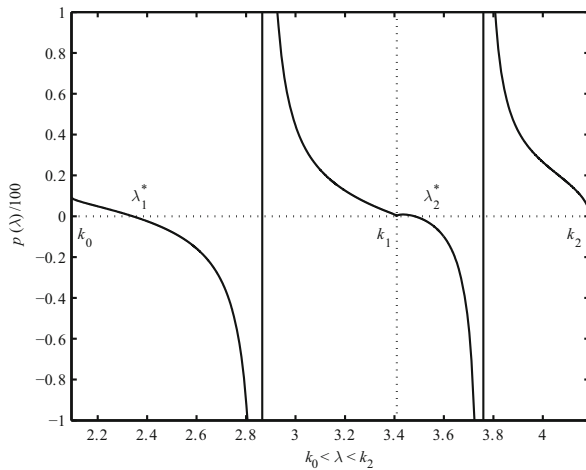


Fig. 5.2. Roots of Eq. (5.73) for $f = 100$ MHz, $\varepsilon_{r1} = 2.65$, $\varepsilon_{r2} = 4.0$, $l_1 = l_2 = 0.8$ m

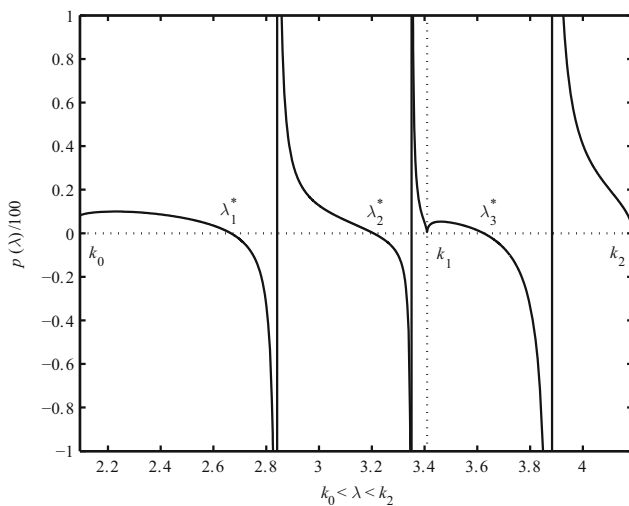


Fig. 5.3. Roots of Eq. (5.73) for $f = 100$ MHz, $\varepsilon_{r1} = 2.65$, $\varepsilon_{r2} = 4.0$, $l_1 = 3.0$ m, and $l_2 = 1.0$ m

$$\begin{aligned}
& + \frac{\gamma_2}{\gamma_0} \tan(\gamma_1 l_1) + \frac{\gamma_0}{\gamma_2} \tan(\gamma_1 l_1) + \frac{\gamma_0 \gamma_2 l_1}{\gamma_1} \sec^2(\gamma_1 l_1) \\
& + i \frac{\gamma_2}{\gamma_1} + i \frac{\gamma_1}{\gamma_2} - i 2 \tan(\gamma_1 l_1) \tan(\gamma_2 l_2) - i \gamma_1 l_1 \sec^2(\gamma_1 l_1) \tan(\gamma_2 l_2) \\
& - i \frac{\gamma_1^2 l_2}{\gamma_2} \tan(\gamma_1 l_1) \sec^2(\gamma_2 l_2) \Big], \tag{5.78}
\end{aligned}$$

$$\gamma_{nB}^* = \gamma_n^* (\lambda_{jB}^*) = \sqrt{k_n^2 - \lambda_{jB}^{*2}}, \quad n = 0, 1, 2. \tag{5.79}$$

Similar to the case of the electric-type field, it is seen that the integrations along the branch lines Γ_1 and Γ_2 are zero in Eq. (5.77). Subject to $k_0 \rho \gg 1$ and $z + d \ll \rho$, we have

$$\begin{aligned}
I_2 &= \frac{k_0^2}{2} \int_{\Gamma_0} \frac{\gamma_1 \tan(\gamma_2 l_2) [H_0^{(1)}(\lambda \rho) - H_2^{(1)}(\lambda \rho)]}{p(\lambda)} e^{i\gamma_0(z+d)} \lambda d\lambda \\
&= - \frac{i 2 k_0^3 \sqrt{\frac{1}{\pi k_0 \rho}} \gamma_{10} \tan(\gamma_{20} l_2) \exp \left[i k_0 \rho + i \frac{k_0 \rho}{2} \left(\frac{z+d}{\rho} \right)^2 \right]}{\gamma_{10} \tan(\gamma_{20} l_2) + \gamma_{20} \tan(\gamma_{10} l_1)} \\
&\quad \times \int_{-\infty}^{\infty} \frac{e^{-k_0 \rho t^2} \left(t - \frac{e^{i\frac{\pi}{4}}}{\sqrt{2}} \frac{z+d}{\rho} \right)}{t - e^{i\frac{\pi}{4}} \Delta'_2} dt, \tag{5.80}
\end{aligned}$$

where

$$\Delta'_2 = \frac{z+d}{\sqrt{2}\rho} + i \frac{\gamma_{10} \gamma_{20} - \gamma_{10}^2 \tan(\gamma_{10} l_1) \tan(\gamma_{20} l_2)}{\sqrt{2} k_0 [\gamma_{10} \tan(\gamma_{20} l_2) + \gamma_{20} \tan(\gamma_{10} l_1)]}. \tag{5.81}$$

Let $\lambda = k_0(1_i \tau^2)$, and using the notation $t = \tau + \frac{e^{i\frac{\pi}{4}}}{\sqrt{2}} \frac{z+d}{\rho}$, the integral along Γ_0 in Eq. (5.80) can be evaluated readily.

$$\begin{aligned}
I_2 &= - \frac{i 2 k_0^3 \sqrt{\frac{1}{\pi k_0 \rho}} \gamma_{10} \tan(\gamma_{20} l_2) \exp \left[i k_0 \rho + i \frac{k_0 \rho}{2} \left(\frac{z+d}{\rho} \right)^2 \right]}{\gamma_{10} \tan(\gamma_{20} l_2) + \gamma_{20} \tan(\gamma_{10} l_1)} \\
&\quad \times \left[\sqrt{\frac{\pi}{k_0 \rho}} + i \sqrt{2\pi} \left(\Delta'_2 - \frac{z+d}{\sqrt{2}\rho} \right) e^{-i p_2^* \mathbf{F}(i p_2^*)} \right]. \tag{5.82}
\end{aligned}$$

Then, we get

$$\begin{aligned}
F_{\phi 3}^{(1)} &= i \pi k_0^2 \sum_j \frac{\gamma_{1B}^* \tan(\gamma_{2B}^* l_2) [H_0^{(1)}(\lambda_{jB}^* \rho) - H_2^{(1)}(\lambda_{jB}^* \rho)]}{p'(\lambda_{jB}^*)} e^{i \gamma_{0B}^*(z+d)} \lambda_{jB}^* \\
&\quad - \frac{i 2 k_0^3 \gamma_{10} \tan(\gamma_{20} l_2)}{\gamma_{10} \tan(\gamma_{20} l_2) + \gamma_{20} \tan(\gamma_{10} l_1)} \sqrt{\frac{1}{\pi k_0 \rho}} e^{i k_0 r_2} \\
&\quad \times \left[\sqrt{\frac{\pi}{k_0 \rho}} + i \sqrt{2\pi} \left(\Delta'_2 - \frac{z+d}{\sqrt{2}\rho} \right) e^{-i p_2^* \mathbf{F}(i p_2^*)} \right]. \tag{5.83}
\end{aligned}$$

Similarly, we have

$$\begin{aligned}
 F_{\phi 3}^{(2)} = & i\pi k_0^2 \sum_j \frac{\gamma_{2B}^* \tan(\gamma_{1B}^* l_1) \left[H_0^{(1)}(\lambda_{jB}^* \rho) - H_2^{(1)}(\lambda_{jB}^* \rho) \right]}{p'(\lambda_{jB}^*)} e^{i\gamma_{0B}^*(z+d)} \lambda_{jB}^* \\
 & - \frac{i2k_0^3 \gamma_{20} \tan(\gamma_{10} l_1)}{\gamma_{10} \tan(\gamma_{20} l_2) + \gamma_{20} \tan(\gamma_{10} l_1)} \sqrt{\frac{1}{\pi k_0 \rho}} e^{ik_0 r_2} \\
 & \times \left[\sqrt{\frac{\pi}{k_0 \rho}} + i\sqrt{2}\pi \left(\Delta'_2 - \frac{z+d}{\sqrt{2}\rho} \right) e^{-ip_2^*} \mathbf{F}(ip_2^*) \right]. \quad (5.84)
 \end{aligned}$$

The final expression of $F_{\phi 3}(\rho, z+d)$ can be written as follows:

$$\begin{aligned}
 F_{\phi 3} = & i\pi k_0^2 \sum_j \frac{\gamma_{1B}^* \tan(\gamma_{2B}^* l_2) + \gamma_{2B}^* \tan(\gamma_{1B}^* l_1)}{p'(\lambda_{jB}^*)} \\
 & \times \left[H_0^{(1)}(\lambda_{jB}^* \rho) - H_2^{(1)}(\lambda_{jB}^* \rho) \right] e^{i\gamma_{0B}^*(z+d)} \lambda_{jB}^* - i2k_0^3 \sqrt{\frac{1}{\pi k_0 \rho}} e^{ik_0 r_2} \\
 & \times \left[\sqrt{\frac{\pi}{k_0 \rho}} + i\sqrt{2}\pi \left(\Delta'_2 - \frac{z+d}{\sqrt{2}\rho} \right) e^{-ip_2^*} \mathbf{F}(ip_2^*) \right]. \quad (5.85)
 \end{aligned}$$

Following similar procedures, it is obtained readily.

$$\begin{aligned}
 F_{\rho 3} = & i\pi k_0^2 \sum_j \frac{\gamma_{1B}^* \tan(\gamma_{2B}^* l_2) + \gamma_{2B}^* \tan(\gamma_{1B}^* l_1)}{p'(\lambda_{jB}^*)} \\
 & \times \left[H_0^{(1)}(\lambda_{jB}^* \rho) + H_2^{(1)}(\lambda_{jB}^* \rho) \right] e^{i\gamma_{0B}^*(z+d)} \lambda_{jB}^* - \frac{2k_0^2}{\rho} \sqrt{\frac{1}{\pi k_0 \rho}} e^{ik_0 r_2} \\
 & \times \left[\sqrt{\frac{\pi}{k_0 \rho}} + i\sqrt{2}\pi \left(\Delta'_2 - \frac{z+d}{\sqrt{2}\rho} \right) e^{-ip_2^*} \mathbf{F}(ip_2^*) \right], \quad (5.86)
 \end{aligned}$$

$$\begin{aligned}
 G_{\rho 3} = & i\pi \sum_j \frac{\gamma_{0B}^* [\gamma_{1B}^* \tan(\gamma_{2B}^* l_2) + \gamma_{2B}^* \tan(\gamma_{1B}^* l_1)]}{p'(\lambda_{jB}^*)} \\
 & \times \left[H_0^{(1)}(\lambda_{jB}^* \rho) - H_2^{(1)}(\lambda_{jB}^* \rho) \right] e^{i\gamma_{0B}^*(z+d)} \lambda_{jB}^* + i2\sqrt{2}k_0^2 \sqrt{\frac{1}{\pi k_0 \rho}} e^{ik_0 r_2} \\
 & \times \left[\sqrt{\frac{\pi}{k_0 \rho}} \left(\Delta'_2 - \sqrt{2} \frac{z+d}{\rho} \right) + i\sqrt{2}\pi \left(\Delta'_2 - \frac{z+d}{\sqrt{2}\rho} \right)^2 e^{-ip_2^*} \mathbf{F}(p_2^*) \right], \quad (5.87)
 \end{aligned}$$

$$\begin{aligned}
 G_{\phi 3} = & i\pi \sum_j \frac{\gamma_{0B}^* [\gamma_{1B}^* \tan(\gamma_{2B}^* l_2) + \gamma_{2B}^* \tan(\gamma_{1B}^* l_1)]}{p'(\lambda_{jB}^*)} \\
 & \times \left[H_0^{(1)}(\lambda_{jB}^* \rho) + H_2^{(1)}(\lambda_{jB}^* \rho) \right] e^{i\gamma_{0B}^*(z+d)} \lambda_{jB}^* + \frac{2\sqrt{2}k_0}{\rho} \sqrt{\frac{1}{\pi k_0 \rho}} e^{ik_0 r_2}
 \end{aligned}$$

$$\times \left[\sqrt{\frac{\pi}{k_0 \rho}} \left(\Delta'_2 - \sqrt{2} \frac{z+d}{\rho} \right) + i\sqrt{2}\pi \left(\Delta'_2 - \frac{z+d}{\sqrt{2}\rho} \right)^2 e^{-ip_2^* \mathbf{F}(p_2^*)} \right], \quad (5.88)$$

$$\begin{aligned} G_{z1} = 2\pi i \sum_j \frac{\gamma_{1B}^* \tan(\gamma_{2B}^* l_2) + \gamma_{2B}^* \tan(\gamma_{1B}^* l_1)}{p'(\lambda_{jB}^*)} \\ \times H_1^{(1)}(\lambda_{jB}^* \rho) e^{i\gamma_{0B}^*(z+d)} \lambda_{jB}^{*2} - 2k_0^2 \sqrt{\frac{1}{\pi k_0 \rho}} e^{ik_0 r_2} \\ \times \left[\sqrt{\frac{\pi}{k_0 \rho}} + i\sqrt{2}\pi \left(\Delta'_2 - \frac{z+d}{\sqrt{2}\rho} \right) e^{-ip_2^* \mathbf{F}(p_2^*)} \right]. \end{aligned} \quad (5.89)$$

5.4 Final Formulas for the Six-Field Components

With the above results for the trapped surface wave and lateral wave, and those for the direct wave and ideal reflected wave addressed in the book (King, Owens, and Wu, 1992), the final formulas for the six components of the electromagnetic field can be obtained readily.

$$\begin{aligned} E_{0\rho} = \frac{\omega\mu_0}{4\pi k_0^2} \cos \phi \left\{ - \left[\frac{2k_0}{r_1^2} + \frac{2i}{r_1^3} + \left(\frac{z-d}{r_1} \right)^2 \left(\frac{ik_0^2}{r_1} - \frac{3k_0}{r_1^2} - \frac{3i}{r_1^3} \right) \right] e^{ik_0 r_1} \right. \\ \left. + \left[\frac{2k_0}{r_2^2} + \frac{2i}{r_2^3} + \left(\frac{z+d}{r_2} \right)^2 \left(\frac{ik_0^2}{r_2} - \frac{3k_0}{r_2^2} - \frac{3i}{r_2^3} \right) \right] e^{ik_0 r_2} \right. \\ \left. + F_{\rho 2} + F_{\rho 3} \right\}, \end{aligned} \quad (5.90)$$

$$\begin{aligned} E_{0\phi} = \frac{\omega\mu_0}{4\pi k_0^2} \sin \phi \left[- \left(\frac{ik_0^2}{r_1} - \frac{k_0}{r_1^2} - \frac{i}{r_1^3} \right) e^{ik_0 r_1} + \left(\frac{ik_0^2}{r_2} - \frac{k_0}{r_2^2} - \frac{i}{r_2^3} \right) e^{ik_0 r_2} \right. \\ \left. + F_{\phi 2} + F_{\phi 3} \right], \end{aligned} \quad (5.91)$$

$$\begin{aligned} E_{0z} = \frac{i\omega\mu_0}{4\pi k_0^2} \cos \phi \left[- \left(\frac{\rho}{r_1} \right) \left(\frac{z-d}{r_1} \right) \left(\frac{k_0^2}{r_1} + \frac{3ik_0}{r_1^2} - \frac{3}{r_1^3} \right) e^{ik_0 r_1} + \left(\frac{\rho}{r_2} \right) \right. \\ \left. \times \left(\frac{z+d}{r_2} \right) \left(\frac{k_0^2}{r_2} + \frac{3ik_0}{r_2^2} - \frac{3}{r_2^3} \right) e^{ik_0 r_2} + F_{z1} \right], \end{aligned} \quad (5.92)$$

$$B_{0\rho} = -\frac{\mu_0}{4\pi} \sin \phi \left[- \left(\frac{z-d}{r_1} \right) \left(\frac{ik_0}{r_1} - \frac{1}{r_1^2} \right) e^{ik_0 r_1} \right.$$

$$+ \left(\frac{z+d}{r_2} \right) \left(\frac{ik_0}{r_2} - \frac{1}{r_2^2} \right) e^{ik_0 r_2} + G_{\rho 2} + G_{\rho 3} \Big], \quad (5.93)$$

$$B_{0\phi} = -\frac{\mu_0}{4\pi} \cos \phi \left[- \left(\frac{z-d}{r_1} \right) \left(\frac{ik_0}{r_1} - \frac{1}{r_1^2} \right) e^{ik_0 r_1} \right. \\ \left. + \left(\frac{z+d}{r_2} \right) \left(\frac{ik_0}{r_2} - \frac{1}{r_2^2} \right) e^{ik_0 r_2} + G_{\phi 2} + G_{\phi 3} \right], \quad (5.94)$$

$$B_{0z} = \frac{i\mu_0}{4\pi} \sin \phi \left[- \left(\frac{\rho}{r_1} \right) \left(\frac{k_0}{r_1} + \frac{i}{r_1^2} \right) e^{ik_0 r_1} \right. \\ \left. + \left(\frac{\rho}{r_2} \right) \left(\frac{ik_0}{r_2} - \frac{1}{r_2^2} \right) e^{ik_0 r_2} + G_{z1} \right]. \quad (5.95)$$

If Region 1 is made in the air by setting $k_1 = k_0$ or both Regions 1 and 2 are made in the same dielectric by setting $k_1 = k_2$, the above results reduce to the corresponding results for the three-layered case as addressed in Chapter 3.

5.5 Computations and Conclusions

From the above derivations and analysis, the complete formulas have been obtained for the electromagnetic field of a horizontal electric dipole in the presence of a four-layered region. It is seen that both the trapped surface wave and the lateral wave can be separated into electric-type and magnetic-type terms. The trapped surface wave with its wave number being between k_0 and k_2 , is determined by the sum of residues of the poles. The lateral wave with its wave number k_0 is determined by the integration of the branch line. For the radial electric field component $|E_{0\rho}(\rho, 0, z)|$ at $z = d = 0$ m, with $f = 100$ MHz, $\varepsilon_{r1} = 2.65$, and $\varepsilon_{r2} = 4.0$, the total field, the trapped surface wave, and the DRL waves are computed for $k_1 l_1 = k_2 l_2 = 0.8$ and $k_1 l_1 = k_2 l_2 = 1.6$, respectively. The results are shown in Figs. 5.4 and 5.5, respectively. It is noted that the DRL waves include the direct wave, ideal reflected wave, and lateral wave. Similarly, the corresponding results at $z = d = 3$ m are computed and shown in Figs. 5.6 and 5.7, respectively.

When both the dipole and the observation point are on or close to the boundary between the air and the upper dielectric layer, the total field is determined by the trapped surface wave. Once the dipole or the observation point is away from the boundary, the trapped surface wave attenuates rapidly and the total field is determined primarily by the lateral wave. In practical applications, we can change the thicknesses of the upper and lower dielectric layers to fulfil the required results.

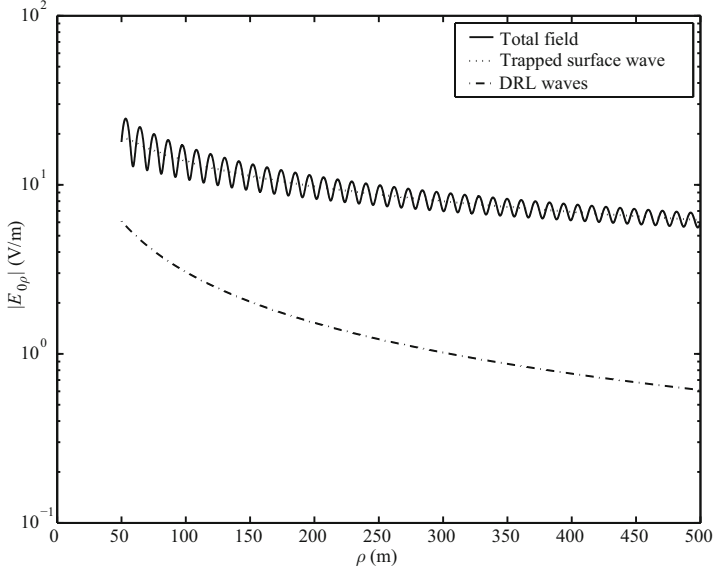


Fig. 5.4. The electric field $|E_\rho|$ in V/m with $f = 100$ MHz, $\varepsilon_{r1} = 2.65$, $\varepsilon_{r2} = 4$, $k_1 l_1 = k_2 l_2 = 0.8$, and $z = d = 0$ m

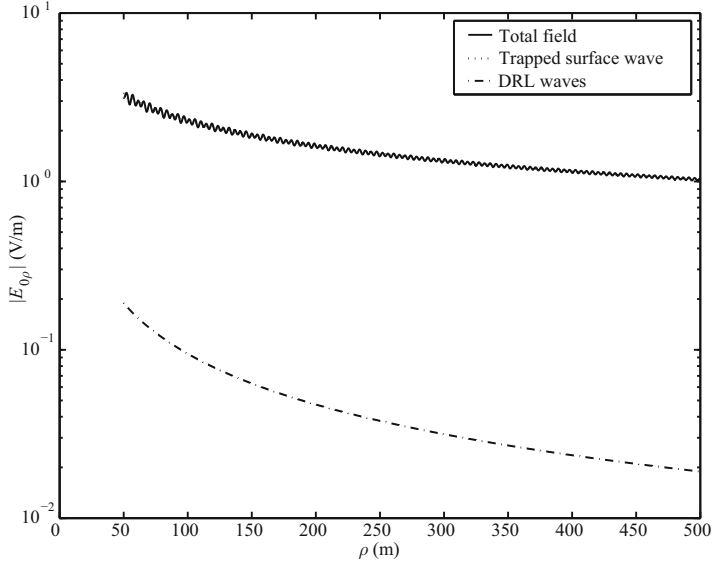


Fig. 5.5. The electric field $|E_\rho|$ in V/m with $f = 100$ MHz, $\varepsilon_{r1} = 2.65$, $\varepsilon_{r2} = 4$, $k_1 l_1 = k_2 l_2 = 1.6$, and $z = d = 0$ m

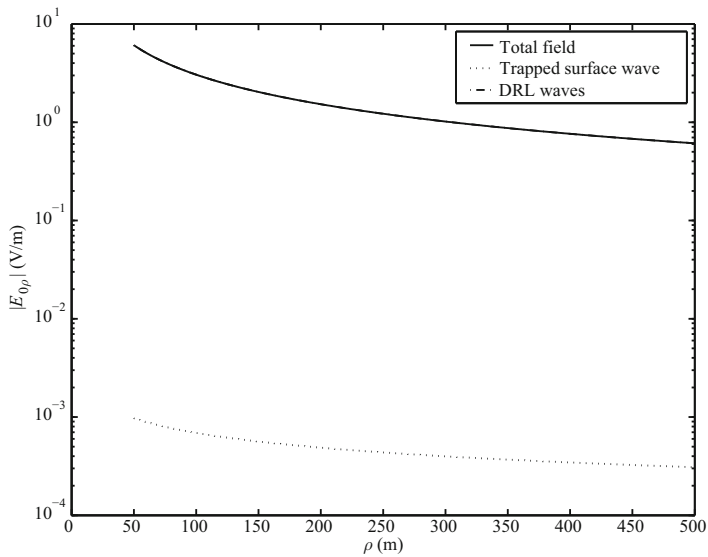


Fig. 5.6. The electric field $|E_\rho|$ in V/m with $f = 100$ MHz, $\varepsilon_{r1} = 2.65$, $\varepsilon_{r2} = 4$, $k_1 l_1 = k_2 l_2 = 0.8$, and $z = d = 3$ m

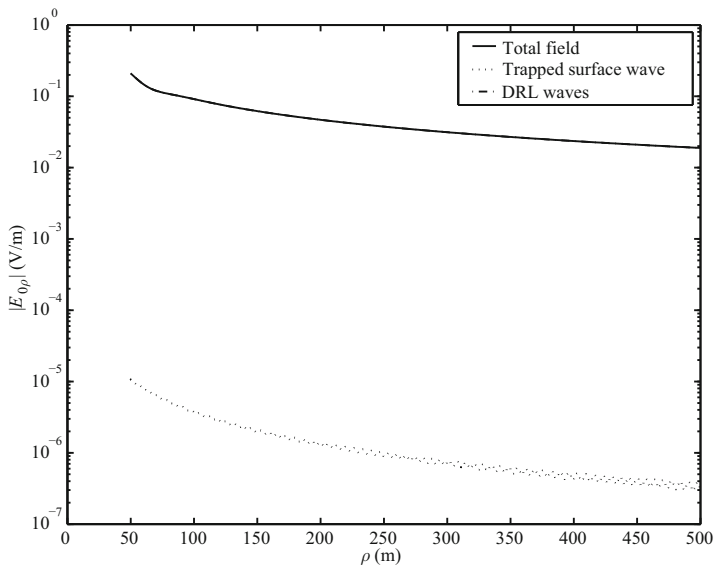


Fig. 5.7. The electric field $|E_\rho|$ in V/m with $f = 100$ MHz, $\varepsilon_{r1} = 2.65$, $\varepsilon_{r2} = 4$, $k_1 l_1 = k_2 l_2 = 1.6$, and $z = d = 3$ m

References

- Baños A Jr (1966) *Dipole Radiation in the Presence of a Conducting Half-Space*. Oxford, UK: Pergamon Press.
- Collin RE (2004a) Some observations about the near zone electric field of a hertzian dipole above a lossy earth. *IEEE Transactions on Antennas and Propagation*, 52(11): 3133–3137.
- Collin RE (2004b) Hertzian dipole radiation over a lossy earth or sea: Some early and late 20th century controversies. *IEEE Antennas and Propagation Magazine*, 46(2): 64–79.
- Dunn JM (1986) Lateral wave propagation in a three-layered medium. *Radio Science*, 21(5): 787–796.
- Gradshteyn IS and Ryzhik IM (1980) *Table of Integrals, Series, and Products*. New York, NY, USA: Academic Press.
- Hoh JH, Li LW, Kooi PS, Yeo TS, and Leong MS (1999) Dominant lateral waves in the canopy layer of a four-layered forest. *Radio Science*, 34(3): 681–691.
- King RWP (1982) New formulas for the electromagnetic field of a vertical electric dipole in a dielectric or conducting half-space near its horizontal interface. *Journal of Applied Physics*, 53: 8476–8482; (1984) Erratum, 56: 3366.
- King RWP (1991) The electromagnetic field of a horizontal electric dipole in the presence of a three-layered region. *Journal of Applied Physics*, 69(12): 7987–7995.
- King RWP, Owens M, and Wu TT (1992) *Lateral Electromagnetic Waves: Theory and Applications to Communications, Geophysical Exploration, and Remote Sensing*. New York, NY, USA: Springer-Verlag.
- King RWP (1993) The electromagnetic field of a horizontal electric dipole in the presence of a three-layered region: supplement. *Journal of Applied Physics*, 74(8): 4845–4548.
- King RWP and Sandler SS (1994a) The electromagnetic field of a vertical electric dipole over the earth or Sea. *IEEE Transactions on Antennas and Propagation*, 42(3): 382–389.
- King RWP and Sandler SS (1994b) The electromagnetic field of a vertical electric dipole in the presence of a three-layered region. *Radio Science*, 29(1): 97–113.
- King RWP and Sandler SS (1998) Reply. *Radio Science*, 33(2): 255–256.
- Li K and Lu Y (2005) Electromagnetic field generated by a horizontal electric dipole near the surface of a planar perfect conductor coated with a uniaxial layer. *IEEE Transactions on Antennas and Propagation*, 53(10): 3191–3200.
- Li LW, Yeo TS, Kooi PS, and Leong MS (1998) Radio wave propagation along mixed paths through a four-layered model of rain forest: an analytical approach. *IEEE Transactions on Antennas and Propagation*, 46(7): 1098–1111.
- Li LW, Lee CK, Yeo TS, and Leong MS (2004) Wave mode and path characteristics in four-layered anisotropic forest environment. *IEEE Transactions on Antennas and Propagation*, 52(9): 2445–2455.
- Liu L and Li K (2007) Radiation from a vertical electric dipole in the presence of a three-layered region. *IEEE Transactions on Antennas and Propagation*, 55(12): 3469–3475.

- Liu L, Li K, and Xu YH (2008) Radiation of a horizontal dipole in a three-layered region and microstrip antenna. *Progress In Electromagnetics Research*, PIER 86: 87–110. Cambridge, MA, USA: EMW Publishing.
- Mahmoud SF (1999) Remarks on “The electromagnetic field of a vertical electric dipole over the earth or Sea”. *IEEE Transactions on Antennas and Propagation*, 46(12): 1745–1946.
- Mei JP and Li K (2007) Electromagnetic field from a horizontal electric dipole on the surface of a high lossy medium coated with a uniaxial layer. *Progress In Electromagnetics Research*, PIER 73: 71–91. Cambridge, MA, USA: EMW Publishing.
- Wait JR (1953) Radiation from a vertical electric dipole over a stratified ground. *IRE Transactions on Antennas and Propagation*, AP-1: 9–12.
- Wait JR (1954) Radiation from a vertical electric dipole over a stratified ground. *IRE Transactions on Antennas and Propagation*, 2: 144–146.
- Wait JR (1956) Radiation from a vertical electric dipole over a curved stratified ground. *Journal of Research of the National Bureau of Standards*, 56: 232–239.
- Wait JR (1957) Excitation of surface waves on conducting dielectric clad and corrugated surfaces. *Journal of Research of the National Bureau of Standards*, 59(6): 365–377.
- Wait JR (1970) *Electromagnetic Waves in Stratified Media* (2nd, Ed.). New York, NY, USA: Pergamon Press.
- Wait JR (1998b) Comment on “The electromagnetic field of a vertical electric dipole in the presence of a three-layered region”, by Ronold W. P. King and Sheldon S. Sandler. *Radio Science*, 33(2): 251–253.
- Zhang HQ and Pan WY (2002) Electromagnetic field of a vertical electric dipole on a perfect conductor coated with a dielectric layer. *Radio Science*, 37(4), 1060, doi:1029/2000RS002348.
- Zhang HQ, Pan WY, Li K, and Shen KX (2005) Electromagnetic field for a horizontal electric dipole buried inside a dielectric layer coated high lossy half space. *Progress In Electromagnetics Research*, PIER 50: 163–186. Cambridge, MA, USA: EMW Publishing.
- Xu YH, Ren W, Liu L, and Li K (2008a) Trapped surface wave and lateral wave in the presence of a four-layered region. *Progress In Electromagnetics Research*, PIER 82: 271–285.
- Xu YH, Li K, and Liu L (2008b) Electromagnetic field of a horizontal electric dipole in the presence of a four-layered region, *Progress In Electromagnetics Research*, PIER 81: 371–391. Cambridge, MA, USA: EMW Publishing.

Electromagnetic Field Radiated by a Dipole Source over a Dielectric-Coated Spherical Earth

In this chapter, the region of interest consists of a spherical and electrically homogeneous Earth, coated with a dielectric layer, and air above. Both the dipole (vertical electric dipole, vertical magnetic dipole, or horizontal electric dipole) and the observation point are assumed to be located on or near the spherical surface of a dielectric-coated Earth. The approximate solution for the electromagnetic field at low frequencies is obtained. Analysis and computations are carried out specifically.

6.1 Introduction

The problem of the electromagnetic field radiated by a dipole over the spherical Earth has been intensively investigated since the early days of electromagnetic theory and radio practice because of its physical significance and mathematical challenges. Important work on the problem was carried out by Watson (1918), in the case of the Earth being a perfect conducting sphere. Lately, Watson's theory was extended to the case of a spherical and electrically homogeneous Earth. The remarkable progress has been made by many investigators, especially including several pioneers (Van der Pol and Bremmer, 1938; Bremmer, 1949; 1954; 1958; Wait, 1956; 1957; 1960; and Fock, 1965). Recently, exact solutions were carried out for the electromagnetic field radiated by vertical and horizontal electric dipoles over a spherical and electrically homogeneous Earth (Houdzoumis, 1999; 2000; Margetis, 2002).

In Chapters 2~5, the approximate formulas are derived for the electromagnetic field of a dipole in the presence of three- and four-layered region. These new developments naturally rekindled in the study on the electromagnetic field radiated by a dipole over the spherical surface of the dielectric-coated Earth. In a series recent works, the properties are treated analytically for the electromagnetic field radiated by dipole (vertical electric dipole, vertical magnetic dipole, or horizontal electric dipole) over the spherical surface of the

Earth coated with a dielectric layer and N-layered dielectric (Pan and Zhang, 2003; Li and Park, 2003; Li, Park, and Zhang, 2004a; 2004b; Li and Lu, 2005).

In this chapter, the approximate formulas are derived for the electromagnetic fields in the air when a dipole is located on or near the spherical surface of the dielectric-coated Earth. First we will attempt to derive for the formulas of the electromagnetic fields radiated by vertical electric and vertical magnetic dipoles. Next, based on these results, the approximate formulas are derived for the electromagnetic field of a horizontal electric dipole by using reciprocity theorem. Analysis and computations are carried out at low frequencies. These results obtained have useful applications in surface communications at low frequencies.

6.2 Electromagnetic Field due to Vertical Electric Dipole

In this section, we will attempt to treat the electromagnetic field of a vertical electric dipole in the presence of a three-layered spherical Earth.

6.2.1 Formulations of the Problem

The geometry under consideration is shown in Fig. 6.1. The air (Region 0, $r \geq a$) is characterized by the permeability μ_0 , uniform permittivity ε_0 , and conductivity $\sigma_0 = 0$. The dielectric layer (Region 1, $(a - l \leq r \leq a)$) with the uniform thickness l is characterized by the permeability μ_0 , relative permittivity ε_{r1} , and conductivity σ_1 . The Earth (Region 2, $r \leq a - l$) is the dielectric medium characterized by the permeability μ_0 , relative permittivity ε_{r2} , and conductivity σ_2 . Then, the wave numbers in the three regions are

$$k_0 = \omega \sqrt{\mu_0 \varepsilon_0}, \quad (6.1)$$

$$k_1 = \omega \sqrt{\mu_0 (\varepsilon_0 \varepsilon_{r1} + i\sigma_1/\omega)}, \quad (6.2)$$

$$k_2 = \omega \sqrt{\mu_0 (\varepsilon_0 \varepsilon_{r2} + i\sigma_2/\omega)}. \quad (6.3)$$

Assuming that the vertical electric dipole is represented by the current density $\hat{z}Idl\delta(x)\delta(y)\delta(z-b)$, where $b = z_s + a$, and $z_s > 0$ denotes the height of the dipole above the surface of the dielectric-coated Earth, the non-zero field components E_r , E_θ , and H_ϕ , where the electromagnetic field radiated by a vertical electric dipole is defined as the electric-type field, are expressed as follows:

$$E_r^{(j)} = \left(\frac{\partial^2}{\partial r^2} + k_j^2 \right) (U_j r), \quad (6.4)$$

$$E_\theta^{(j)} = \frac{1}{r} \frac{\partial^2}{\partial \theta \partial r} (U_j r), \quad (6.5)$$

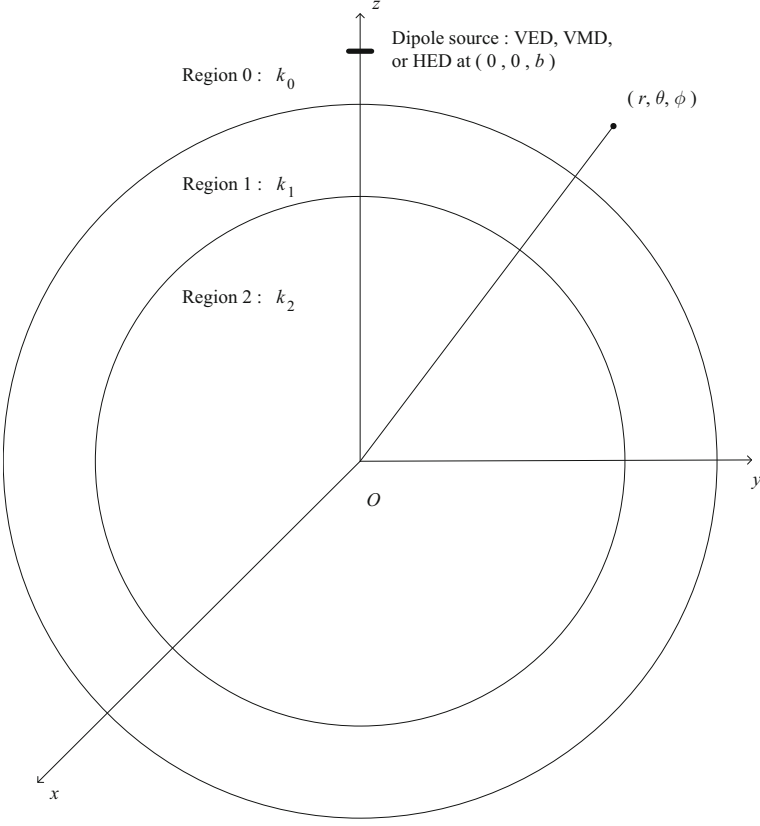


Fig. 6.1. Geometry of a dipole in the presence of a three-layered spherical region

$$H_{\phi}^{(j)} = -\frac{i\omega\epsilon_j}{r} \frac{\partial}{\partial \theta}(U_j r). \quad (6.6)$$

Here the potential function U_j is the solution of the scalar Helmholtz equation

$$(\nabla^2 + k_j^2)U_j = 0, \quad (6.7)$$

where $j = 0, 1, 2$.

In spherical coordinates, because of symmetry, the expanded form of Eq. (6.7) is written as

$$\frac{1}{r^2} \frac{\partial}{\partial r} \left(r^2 \frac{\partial U_j}{\partial r} \right) + \frac{1}{r^2 \sin \theta} \frac{\partial}{\partial \theta} \left(\sin \theta \frac{\partial U_j}{\partial \theta} \right) + k_j^2 U_j = 0. \quad (6.8)$$

The solution for U_j can be represented in the form

$$U_j = \frac{1}{r} Z_j(r) \Phi(\theta). \quad (6.9)$$

Then,

$$\frac{1}{\sin \theta} \frac{d}{d\theta} \left[\sin \theta \frac{d\Phi(\theta)}{d\theta} \right] + \nu(\nu + 1)\Phi(\theta) = 0, \quad (6.10)$$

$$\frac{d^2 Z_j(r)}{dr^2} + k_j^2 \left[1 - \frac{\nu(\nu + 1)}{k_j^2 r^2} \right] Z_j(r) = 0. \quad (6.11)$$

Eq. (6.10) can be transformed into the standard Legendre equation with the substitution $x = \cos(\pi - \theta)$. The solutions of Eq. (6.10) may be $P_\nu(\cos(\pi - \theta))$ or $Q_\nu(\cos(\pi - \theta))$. When ν is not an integer, the Legendre function of first kind $P_\nu(\cos(\pi - \theta))$ is singular only for $\theta = 0$, the second kind of Legendre function $Q_\nu(\cos(\pi - \theta))$ is singular both for $\theta = 0$ and π . But the dipole is located at $\theta = 0$, so that $Q_\nu(\cos(\pi - \theta))$ is not included in the solutions and the solution of Eq. (6.10) is taken as the Legendre functions of first kind.

$$\Phi(\theta) = P_\nu(\cos(\pi - \theta)). \quad (6.12)$$

Next, it is necessary to give the solution of Eq. (6.11).

Let $r = a + z_r$, $z_r > 0$ denotes the height of the observation point above the surface of the dielectric-coated Earth. It is assumed that both the dipole and the observation point are on or close to the spherical boundary between the air and the dielectric layer, namely, $z_s \ll a$ and $z_r \ll a$. Then, the following approximation is taken as

$$\frac{\nu(\nu + 1)}{k_0^2 r^2} \approx \frac{\nu(\nu + 1)}{k_0^2 a^2} \left(1 - \frac{2z_r}{a} \right). \quad (6.13)$$

Thus, Eq. (6.11) in Region 0 becomes

$$\frac{d^2 Z(z_r)}{dz_r^2} + k_0^2 \left[1 - \frac{\nu(\nu + 1)}{k_0^2 a^2} \left(1 - \frac{2z_r}{a} \right) \right] Z_0(z_r) = 0. \quad (6.14)$$

With the change of the variable,

$$y = \left[\frac{2\nu(\nu + 1)}{a^3} \right]^{1/3} z_r, \quad (6.15)$$

Eq. (6.14) is rewritten in the form

$$\frac{d^2 Z(y)}{dy^2} - (t - y)Z(y) = 0. \quad (6.16)$$

where

$$t = \left[\frac{a^3}{2\nu(\nu + 1)} \right]^{2/3} \left[\frac{\nu(\nu + 1)}{a^2} - k_0^2 \right]. \quad (6.17)$$

It is seen that Eq. (6.16) is a standard Stokes equation. When the condition $|t| \ll (k_0 a)^{2/3}$ is satisfied, the following approximation is obtained readily.

$$\begin{aligned}\nu(\nu+1) &= k_0^2 a^2 \left[1 + \frac{2^{2/3} t_n}{(k_0 a)^{2/3}} + \frac{4}{3} \frac{2^{1/3} t_n^2}{(k_0 a)^{4/3}} + \cdots \right] \\ &\approx k_0^2 a^2 \left[1 + \frac{2^{2/3} t_n}{(k_0 a)^{2/3}} \right] \approx k_0^2 a^2.\end{aligned}\quad (6.18)$$

Then, we have

$$y = \left[\frac{2\nu(\nu+1)}{a^3} \right]^{1/3} z_r \approx \left(\frac{2}{k_0 a} \right)^{1/3} k_0 z_r. \quad (6.19)$$

Taking into account the radiation condition, the solution of Eq. (6.16) is expressed in the form

$$Z_0(y) = A W_2(t - y), \quad (6.20)$$

where $W_2(t)$ is the Airy function of the second kind. When the variable t is a large negative value, $W_2(t)$ is approximated as

$$W_2(t) = (-t)^{-1/4} \exp \left[i \frac{2}{3} (-t)^{3/2} + i \frac{\pi}{4} \right]. \quad (6.21)$$

In Region 1, $a - l \leq r \leq a$, considering $l \ll a$, we take $r \approx a$. Then, Eq. (6.11) is simplified as

$$\frac{d^2 Z_1(r)}{dr^2} + (k_1^2 - k_0^2) Z_1(r) = 0. \quad (6.22)$$

The solution of Eq. (6.22) is written in the form

$$Z_1(r) = B e^{i\sqrt{k_1^2 - k_0^2}[r - (a-l)]} + C e^{-i\sqrt{k_1^2 - k_0^2}[r - (a-l)]}. \quad (6.23)$$

According to the impedance boundary condition at $r = a - l$, we write

$$\left. \frac{E_\theta^{(1)}}{\eta_1 H_\phi^{(1)}} \right|_{r=a-l} = -\Delta_g. \quad (6.24)$$

At low frequencies, the surface impedance Δ_g is approximated as

$$\Delta_g \approx \frac{k_1}{k_2} \sqrt{1 - \left(\frac{k_1}{k_2} \right)^2}. \quad (6.25)$$

Then,

$$\Delta_e = \frac{C}{B} = \frac{\sqrt{k_1^2 - k_0^2} - k_1 \Delta_g}{\sqrt{k_1^2 - k_0^2} + k_1 \Delta_g}. \quad (6.26)$$

At the boundary $r = a$, with the conditions $E_\theta^{(0)}|_{z=a} = E_\theta^{(1)}|_{z=a}$ and $H_\phi^{(0)}|_{z=a} = H_\phi^{(1)}|_{z=a}$, we have

$$-AW_2' \left(\frac{2}{k_0 a} \right)^{1/3} k_0 = iB \sqrt{k_1^2 - k_0^2} \left(e^{i\sqrt{k_1^2 - k_0^2} l} - \Delta_e e^{-i\sqrt{k_1^2 - k_0^2} l} \right), \quad (6.27)$$

$$Ak_0^2 W_2 = B k_1^2 \left(e^{i\sqrt{k_1^2 - k_0^2} l} + \Delta_e e^{-i\sqrt{k_1^2 - k_0^2} l} \right). \quad (6.28)$$

Then, the differential equation is obtained as follows:

$$W_2'(t) - qW_2(t) = 0, \quad (6.29)$$

where

$$q = \frac{-ik_0 \sqrt{k_1^2 - k_0^2}}{k_1^2} \left(\frac{k_0 a}{2} \right)^{1/3} \left(\frac{1 - \Delta_e e^{-i2\sqrt{k_1^2 - k_0^2} l}}{1 + \Delta_e e^{-i2\sqrt{k_1^2 - k_0^2} l}} \right). \quad (6.30)$$

In the case of the Earth being a perfect conducting sphere, $\Delta_g \rightarrow 0$, then, $\Delta_e = 1$, the above formula reduces to

$$q = \frac{k_0 \sqrt{k_1^2 - k_0^2}}{k_1^2} \left(\frac{k_0 a}{2} \right)^{1/3} \tan \left(\sqrt{k_1^2 - k_0^2} l \right). \quad (6.31)$$

If t_s ($s = 1, 2, 3, \dots$) are the roots of Eq. (6.29), the potential function U_0 in the air is represented in the form

$$U_0 = \frac{1}{r} \sum_s A_s F_s(z_r) P_\nu(\cos(\pi - \theta)), \quad (6.32)$$

where the normalized “height-gain” function $F_s(z_r)$ is

$$F_s(z_r) = \frac{W_2(t_s - y)}{W_2(t_s)}. \quad (6.33)$$

In the next step, it is necessary to determine the coefficient A_s ($s = 1, 2, 3, \dots$) in Eq. (6.32).

6.2.2 Determination of the Coefficient A_s

The coefficient A_s ($s = 1, 2, 3, \dots$) in Eq. (6.32) stands for the amplitude of the s -th mode of the electromagnetic wave, which is determined by the excitation condition in the source region. In order to determine the coefficient, we consider the following integral

$$N_{sn} = \int_0^\infty \frac{W_2(t_s - y)}{W_2(t_s)} \frac{W_2(t_n - y)}{W_2(t_n)} dz, \quad (6.34)$$

where t_s and t_n are the solutions of Eq. (6.29). Obviously, the integral can be simplified as

$$N_{sn} = \begin{cases} 0; & s \neq n, \\ \left(\frac{k_0 a}{2}\right)^{1/3} \frac{(t_s - q^2)}{k_0}; & s = n. \end{cases} \quad (6.35)$$

Multiplying the factor $r \frac{W_2(t_n - y)}{W_2(t_n)}$ on both sides of Eq. (6.32), and integrating it from 0 to ∞ for z , it follows that

$$\begin{aligned} \int_0^\infty r U_0 \frac{W_2(t_n - y)}{W_2(t_n)} dz &= \int_0^\infty \sum_{s=1}^\infty A_s \frac{W_2(t_s - y)}{W_2(t_s)} \frac{W_2(t_n - y)}{W_2(t_n)} P_\nu(\cos(\pi - \theta)) dz \\ &= A_n \frac{1}{k_0} \left(\frac{k_0 a}{2}\right)^{1/3} (t_n - q^2) P_\nu(\cos(\pi - \theta)). \end{aligned} \quad (6.36)$$

Then, we have

$$A_n = \left(\frac{2}{k_0 a}\right)^{1/3} \frac{k_0}{(t_n - q^2) P_\nu(\cos(\pi - \theta))} \int_0^\infty r U_0 \frac{W_2(t_n - y)}{W_2(t_n)} dz. \quad (6.37)$$

It is noted that Eq. (6.37) is satisfied for θ at any angular degree. On the nearby of the source, the integral can be rewritten as

$$\begin{aligned} \int_0^\infty r U_0 \frac{W_2(t_n - y)}{W_2(t_n)} dz &= \int_0^{z_s - \delta} r U_0 \frac{W_2(t_n - y)}{W_2(t_n)} dz \\ &\quad + \int_{z_s - \delta}^{z_s + \delta} r U_0 \frac{W_2(t_n - y)}{W_2(t_n)} dz \\ &\quad + \int_{z_s + \delta}^\infty r U_0 \frac{W_2(t_n - y)}{W_2(t_n)} dz, \end{aligned} \quad (6.38)$$

where z_s is the height of the dipole and δ is a finite small value. On the right side of Eq. (6.38), there are three integrals. Obviously, the first and third integrals are finite because their paths do not approach the dipole. The second integral will approach infinite when $\theta \rightarrow 0$, so that the first and third integrals can be neglected compared with the second one.

In the region of $|z - z_s| \leq \delta$, when δ is very small and $\theta \rightarrow 0$, the influence of the field by the Earth can be neglected. Then, when the conditions $|z - z_s| \leq \delta$ and $\theta \rightarrow 0$ are satisfied, the potential function U_0 is approximated as

$$U_0 \longrightarrow 4\pi\omega\varepsilon_0 r_s R \approx \frac{i I dl}{4\pi\omega\varepsilon_0 r_0 R}, \quad (6.39)$$

where R is the distance from the dipole and the observation point, $r_0 = a + z_s$, and

$$R \approx \sqrt{(r_0 \theta)^2 + (z - z_s)^2}. \quad (6.40)$$

Because of

$$\begin{aligned}
\int_{z_s-\delta}^{z_s+\delta} \frac{dz}{R} &\approx \int_{z_s-\delta}^{z_s+\delta} \frac{dz}{\sqrt{(r_0\theta)^2 + (z - z_s)^2}} \\
&= \ln \left[(z - z_s) + \sqrt{(r_0\theta)^2 + (z - z_s)^2} \right] \Big|_{z_s-\delta}^{z_s+\delta} \\
&= \ln \frac{\sqrt{\delta^2 + (r_0\theta)^2} + \delta}{\sqrt{\delta^2 + (r_0\theta)^2} - \delta} \\
&\approx -\ln \theta^2; \quad \theta \rightarrow 0 \text{ and } \delta \gg r_0\theta,
\end{aligned} \tag{6.41}$$

it is obtained readily.

$$\int_0^\infty r U_0 \frac{W_2(t_n - y)}{W_2(t_n)} dz \approx \frac{-i I dl}{4\pi\omega\varepsilon_0} \frac{W_2(t_n - y_s)}{W_2(t_n)} \ln \theta^2, \tag{6.42}$$

where

$$y_s = \left(\frac{2}{k_0 a} \right)^{1/3} k_0 z_s. \tag{6.43}$$

When $\theta \rightarrow 0$, the Legendre function $P_\nu(\cos(\pi - \theta))$ is approximated as

$$P_\nu(\cos(\pi - \theta)) \longrightarrow \frac{\sin \nu\pi}{\pi} \ln \theta^2. \tag{6.44}$$

Therefore,

$$A_n = \left(\frac{2}{k_0 a} \right)^{1/3} k_0 \frac{-I dl}{4\pi\omega\varepsilon_0} \frac{W_2(t_n - y_s)}{W_2(t_n)} \frac{1}{t_n - q^2} \frac{\pi}{\sin \nu\pi}. \tag{6.45}$$

Generally, ν has a large positive imaginary part. It follows that

$$\sin \nu\pi \approx \frac{i}{2} e^{-i\nu\pi}. \tag{6.46}$$

Then, the following approximation is obtained readily.

$$A_n = - \left(\frac{2}{k_0 a} \right)^{1/3} k_0 \frac{I dl}{2\omega\varepsilon_0} e^{i\nu\pi} \frac{W_2(t_n - y_s)}{W_2(t_n)} \frac{1}{t_n - q^2}. \tag{6.47}$$

It is rewritten that

$$A_s = - \left(\frac{2}{k a} \right)^{1/3} \frac{k_0 I dl}{2\omega\varepsilon_0} \frac{F_s(z_s) e^{i\nu\pi}}{t_s - q^2}. \tag{6.48}$$

6.2.3 Final Formulas of the Electromagnetic Field

When ν is very large and θ is not close to 0 and π , the Legendre function $P_\nu(\cos(\pi - \theta))$ is approximated as

$$P_\nu(\cos(\pi - \theta)) = \sqrt{\frac{1}{2\pi k_0 a \sin \theta}} \exp[i(k_0 a \theta + t_s x)] \exp\left[i\left(\nu + \frac{1}{4}\right)\pi\right], \quad (6.49)$$

where

$$x = \left(\frac{k_0 a}{2}\right)^{1/3} \theta. \quad (6.50)$$

Then, the complete formulas for the components E_r , E_θ and ηH_ϕ of the electromagnetic field radiated by a vertical electric dipole at $(a + z_s, 0, 0)$ over the spherical surface of the dielectric-coated Earth are expressed in the following forms:

$$\begin{aligned} \begin{bmatrix} E_r(a + z_r, \theta, \phi) \\ E_\theta(a + z_r, \theta, \phi) \\ \eta_0 H_\phi(a + z_r, \theta, \phi) \end{bmatrix} &= \frac{i I d l \eta}{\lambda a} \frac{e^{i(k_0 a \theta + \frac{\pi}{4})}}{\sqrt{\theta \sin \theta}} \sqrt{\pi x} \\ &\times \begin{bmatrix} \sum_s \frac{F_s(z_s) F_s(z_r)}{t_s - q^2} e^{i t_s x} \\ \sum_s \frac{i F_s(z_s) \frac{\partial F_s(z)}{\partial z} \Big|_{z=z_r}}{k_0 (t_s - q^2) \left[1 + \frac{t_s}{2} \left(\frac{2}{k_0 a}\right)^{2/3}\right]} e^{i t_s x} \\ - \sum_{s'} \frac{F_{s'}(z_s) F_{s'}(z_r)}{(t_{s'} - q^2) \left[1 + \frac{t_{s'}}{2} \left(\frac{2}{k_0 a}\right)^{2/3}\right]} e^{i t_{s'} x} \end{bmatrix}. \end{aligned} \quad (6.51)$$

6.2.4 Computations for Parameters t_s

Let $t_s = t_s(q)$ denoting the roots of Eq. (6.29), it is noted that the roots $t_s(q)$ are functions of the complex parameter q . For the value $q = 0$ they reduce to the root $t'_s = t_s(0)$ and for the value $q = \infty$ they reduce to the roots $t_s^0 = t_s(\infty)$. The roots t'_s and t_s^0 are given in the book by Fock (1965).

$$t'_1 = 1.01879e^{i\frac{\pi}{3}}; \quad t_1^0 = 2.33811e^{i\frac{\pi}{3}}, \quad (6.52)$$

$$t'_2 = 3.24820e^{i\frac{\pi}{3}}; \quad t_2^0 = 4.08795e^{i\frac{\pi}{3}}, \quad (6.53)$$

$$t'_3 = 4.82010e^{i\frac{\pi}{3}}; \quad t_3^0 = 5.52056e^{i\frac{\pi}{3}}, \quad (6.54)$$

$$t'_4 = 6.16331e^{i\frac{\pi}{3}}; \quad t_4^0 = 6.78671e^{i\frac{\pi}{3}}, \quad (6.55)$$

$$t'_5 = 7.37218e^{i\frac{\pi}{3}}; \quad t_5^0 = 7.94417e^{i\frac{\pi}{3}}. \quad (6.56)$$

If $s \geq 6$, the roots t'_s and t_s^0 are approximated as

$$t'_s = \left(\frac{3X'_s}{2} \right)^{3/2} e^{i\frac{\pi}{3}}, \quad t_s^0 = \left(\frac{3X_s^0}{2} \right)^{3/2} e^{i\frac{\pi}{3}}, \quad (6.57)$$

where

$$X'_s = \left(s - \frac{3}{4} \right) \pi + \frac{0.123787}{4s-1} - \frac{0.7758}{(4s-1)^3} + \frac{0.389}{(4s-1)^5}; \quad s = 6, 7, 8, \dots, \quad (6.58)$$

$$X_s^0 = \left(s - \frac{1}{4} \right) \pi + \frac{0.088419}{4s-1} - \frac{0.08328}{(4s-1)^3} + \frac{0.4065}{(4s-1)^5}; \quad s = 6, 7, 8, \dots. \quad (6.59)$$

It is convenient to calculate the roots $t_s(q)$ for finite values q by using a numerical method from the differential equation:

$$\frac{dt_s}{dq} = \frac{1}{t_s - q^2}, \quad (6.60)$$

where the initial value is taken as t_s' for $q = 0$.

With large finite values q , noting $p = 1/q$, Eq. (6.29) can be written in the form

$$W_2(t) - pW'_2(t) = 0. \quad (6.61)$$

Then, we have

$$\frac{dt_s}{dp} = \frac{1}{1 - t_s p^2}. \quad (6.62)$$

The roots $t_s(q) = t_s(p)$ can be easily calculated from Eq. (6.61) by using the initial value t_s^0 for $p = 0$ or $q = \infty$.

Employing the above-mentioned numerical method, the parameters t_s can be calculated readily. We assume that the radius of the Earth is taken as $a = 6370$ km, the dielectric layer $a - l < r < a$ (Region 1) is characterized by the relative permittivity $\varepsilon_{r1} = 12$, and conductivity $\sigma_1 = 10^{-5}$ S/m, the Earth in the region $r < a - l$ (Region 2) is characterized by the relative permittivity $\varepsilon_{r2} = 80$, and conductivity $\sigma_2 = 4$ S/m. Fig. 6.2 shows both the real and imaginary parts of q . Figs. 6.3 and 6.4 show both the real parts and the imaginary parts of t_{s1} and $t_{s2} - t_{s5}$, respectively. It is noted that q is a positive parameter and will increase with the thickness l from zero when the thickness l of the dielectric layer satisfies the condition $0 < \sqrt{k_1^2 - k_0^2} l < \frac{\pi}{2}$. From Fig. 6.3, it is seen that the imaginary part of t_{s1} approaches zero when the thickness l of the dielectric layer is larger than 45 m or so. It means that the first mode will attenuate very slowly along the surface of the spherical Earth when the thickness l is larger than 45 m and the condition $0 < \sqrt{k_1^2 - k_0^2} l < \frac{\pi}{2}$ is satisfied.

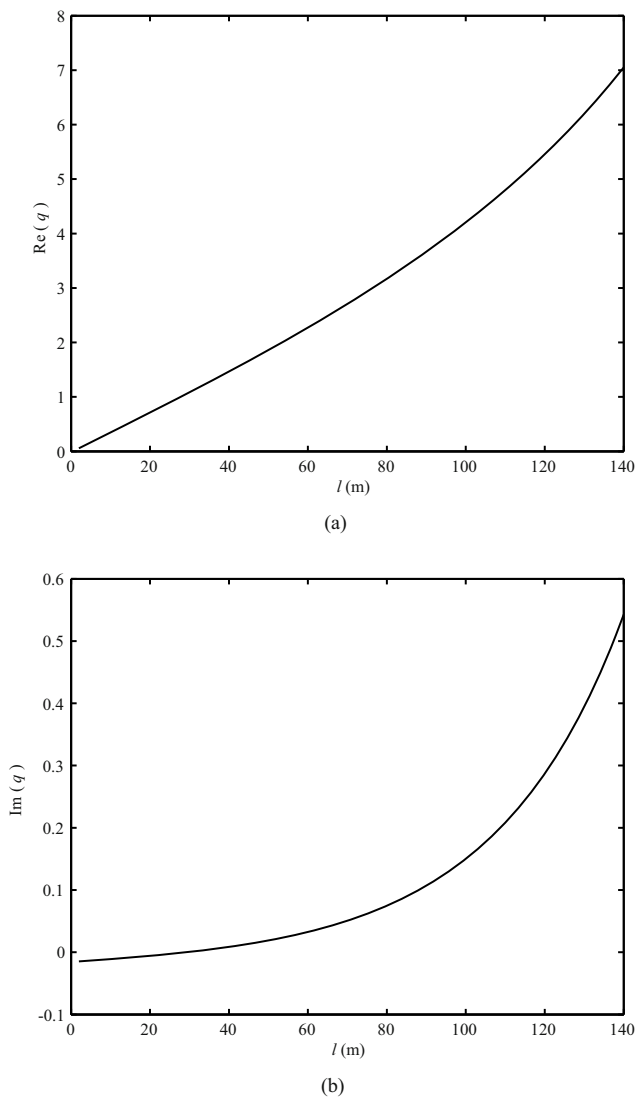
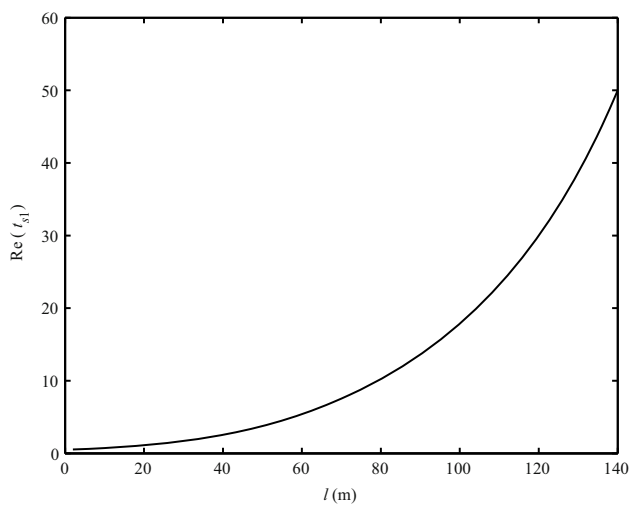
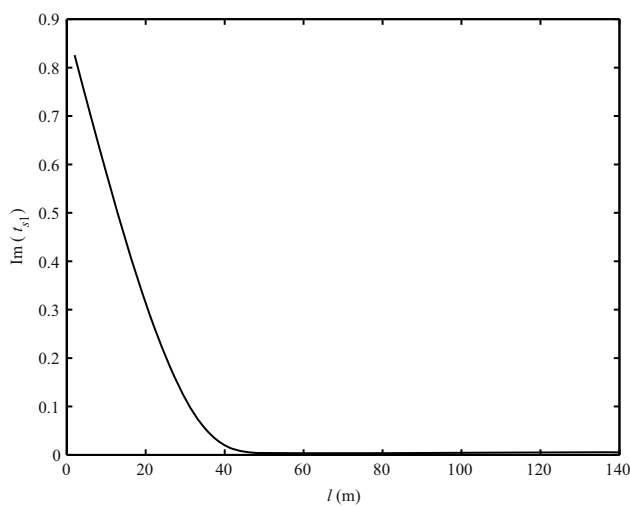


Fig. 6.2. The parameter q versus the thickness of the dielectric layer l



(a)



(b)

Fig. 6.3. The parameter t_{s1} versus the thickness of the dielectric layer l

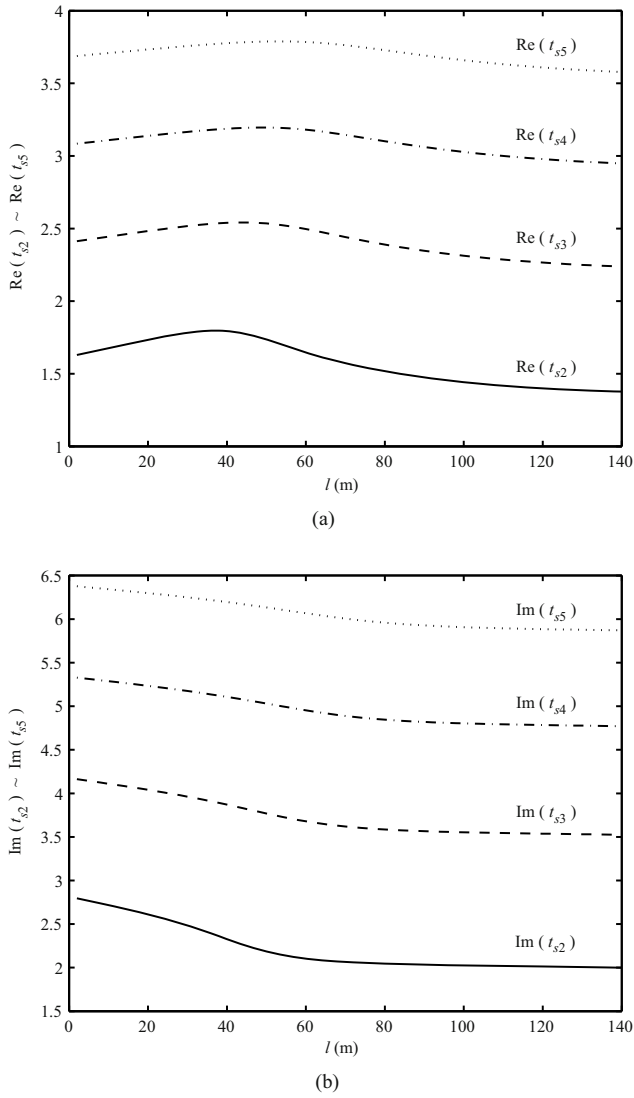


Fig. 6.4. The parameters $t_{s2} \sim t_{s5}$ versus the thickness of the dielectric layer l

6.2.5 Analysis and Computations

For the asphalt- and cement-coated spherical Earth or ice-coated spherical seawater at low frequencies, it is not too difficult to compute the electromagnetic field versus the propagating distances at different thicknesses of the dielectric layer.

Assumed that all the parameters of the dielectric layer (Region 1, $a - l < r < a$) and the Earth (Region 2, $r < a - l$) are the same as those in Figs. 6.2~6.4, and $z_r = z_s = 0$ m, $|E_r|$ in V/m and $|H_\phi|$ in A/m due to unit vertical electric dipole at $l = 0$ m, $l = 60$ m, and $l = 120$ m are computed and plotted in Figs. 6.5 and 6.6, respectively. From Figs. 6.5 and 6.6, it is concluded that the interference occurs when the thickness of the dielectric layer is larger than a certain value. Compared with the computations in the case of the Earth being a perfect conductor (Pan and Zhang, 2003), it is seen the attenuation of the electromagnetic field in the case of the perfect conducting Earth is larger than that in the case of the Earth being an electrical medium with finite conductivity.

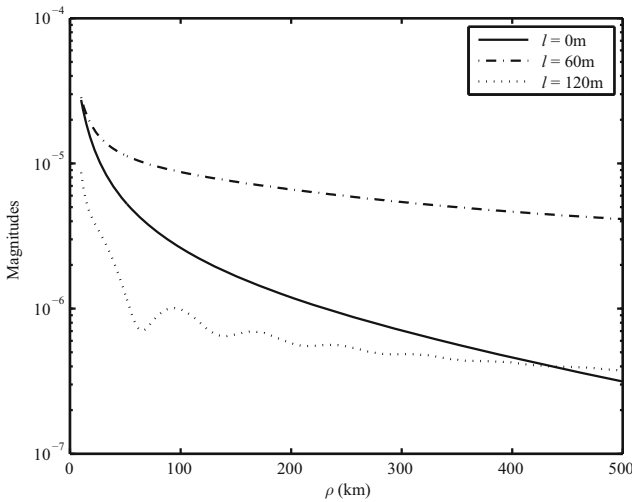


Fig. 6.5. $|E_r|$ in V/m due to unit vertical electric dipole versus the propagating distance ρ at $l = 0$ m, $l = 60$ m, and $l = 120$ m, respectively: $f = 100$ kHz, $a = 6370$ km, $\varepsilon_{r1} = 12$, $\varepsilon_{r2} = 80$, $\sigma_1 = 10^{-5}$ S/m, $\sigma_2 = 4$ S/m, and $z_r = z_s = 0$ m

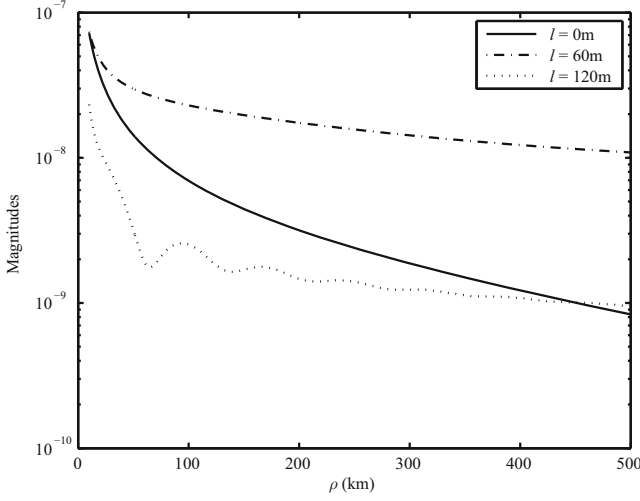


Fig. 6.6. $|H_\phi|$ in A/m due to unit vertical electric dipole versus the propagating distance ρ at $l = 0$ m, $l = 60$ m, and $l = 120$ m, respectively: $f = 100$ kHz, $a = 6370$ km, $\varepsilon_{r1} = 12$, $\varepsilon_{r2} = 80$, $\sigma_1 = 10^{-5}$ S/m, $\sigma_2 = 4$ S/m, and $z_r = z_s = 0$ m

6.3 Electromagnetic Field due to Vertical Magnetic Dipole

If the excitation source is replaced by a vertical magnetic dipole with its moment $M = Ida$, and da is the area of the loop, the non-zero components E_ϕ , H_r , and H_θ , where the electromagnetic field radiated by a vertical magnetic dipole is defined as the magnetic-type field, are represented in the following forms:

$$E_\phi^{(j)} = \frac{-i\omega\mu_0}{r} \frac{\partial}{\partial\theta}(V_j r), \quad (6.63)$$

$$H_r^{(j)} = \left(\frac{\partial^2}{\partial r^2} + k^2 \right) (V_j r), \quad (6.64)$$

$$H_\theta^{(j)} = \frac{1}{r} \frac{\partial^2}{\partial\theta\partial r}(V_j r). \quad (6.65)$$

where the potential function V_j is the solution of the scalar Helmholtz equation

$$(\nabla^2 + k_j^2)V_j = 0, \quad j = 0, 1. \quad (6.66)$$

It is noted that the surface impedance of magnetic type is expressed by

$$\left. \frac{E_\phi^{(1)}}{\eta_1 H_\theta^{(1)}} \right|_{r=a-l} = \Delta_g. \quad (6.67)$$

Following the same procedures in the preceding section, we will obtain the formulas of the components E_ϕ , H_r , and H_θ in the air generated by a vertical magnetic dipole over the dielectric-coated Earth.

$$\begin{bmatrix} E_\phi(a + z_r, \theta, \phi) \\ \eta_0 H_r(a + z_r, \theta, \phi) \\ \eta_0 H_\theta(a + z_r, \theta, \phi) \end{bmatrix} = \frac{\omega \mu_0 I da}{\lambda a} \frac{e^{i(k_0 a \theta + \frac{\pi}{4})}}{\sqrt{\theta \sin \theta}} \sqrt{\pi x} \begin{bmatrix} \sum_s \frac{G_s(z_s) G_s(z_r)}{t_s - (q^h)^2} e^{i t'_s x} \\ \sum_s \frac{G_s(z_s) G_s(z_r)}{t_s - (q^h)^2} e^{i t'_s x} \\ i \sum_s \frac{G_s(z_s)}{t_s - (q^h)^2} \frac{\partial G_s(z)}{\partial z} \Big|_{z=z_r} e^{i t'_s x} \end{bmatrix}, \quad (6.68)$$

where

$$q^h = \frac{-i \sqrt{k_1^2 - k_0^2}}{k_0} \left(\frac{k_0 a}{2} \right)^{1/3} \left(\frac{1 - \Delta_m e^{-i2\sqrt{k_1^2 - k_0^2}l}}{1 + \Delta_m e^{-i2\sqrt{k_1^2 - k_0^2}l}} \right), \quad (6.69)$$

$$\Delta_m = \frac{\sqrt{k_1^2 - k_0^2} \Delta_g + k_1}{\sqrt{k_1^2 - k_0^2} \Delta_g - k_1}. \quad (6.70)$$

In the case of the perfectly spherical conducting Earth, $\Delta_g \rightarrow 0$, then, $\Delta_m = -1$, the above formula reduces to

$$q^h = - \left(\frac{k_0 a}{2} \right)^{1/3} \frac{\sqrt{k_1^2 - k_0^2}}{k_0 \tan \left[\sqrt{k_1^2 - k_0^2}l \right]}. \quad (6.71)$$

Here t'_s ($s = 1, 2, \dots$) are the roots of the following differential equation:

$$W_2'(t'_s) - q^h W_2(t'_s) = 0, \quad (6.72)$$

where $W_2(t'_s)$ is the Airy function of the second kind. The normalized “height-gain” function $G_s(z_r)$ is

$$G_s(z_r) = \frac{W_2(t'_s - y)}{W_2(t'_s)}. \quad (6.73)$$

It noted that q is always negative and will increase from negative infinite to zero with the thickness l when the condition $0 < \sqrt{k_1^2 - k_0^2}l < \frac{\pi}{2}$ is satisfied. When $\frac{\pi}{2} < \sqrt{k_1^2 - k_0^2}l < \pi$, q is always positive and increases from zero to infinite with the thickness l . In fact, when the thickness l of the dielectric layer such as ice or permafrost is less than 200 m, the above condition $\frac{\pi}{2} < \sqrt{k_1^2 - k_0^2}l < \pi$ cannot be satisfied.

In contrast with the effects on $|E_\phi|$ and $|H_r|$ by the thickness l , we will compute $|E_\phi|$ and $|H_r|$ at different thicknesses l . Assuming that all the parameters of the dielectric layer $a - l < r < a$ (Region 1) and the Earth in the region $r < a - l$ (Region 2) are the same as those in the preceding section in this chapter, and $z_r = z_s = 0$ m, $|E_\phi|$ in V/m and $|H_r|$ in A/m due to unit

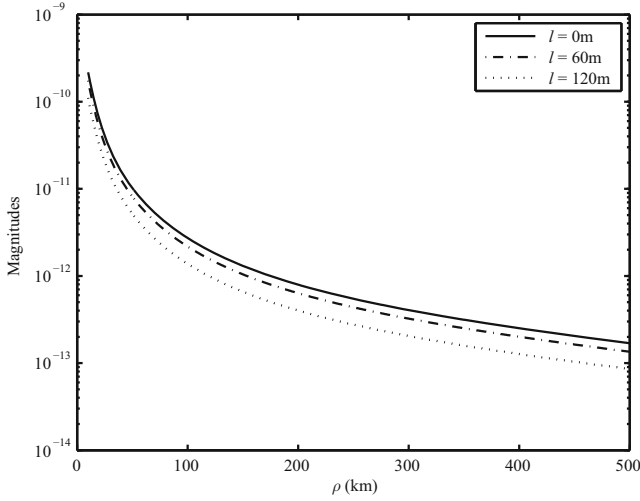


Fig. 6.7. $|E_\phi|$ in V/m due to unit vertical magnetic dipole versus the propagating distance ρ at $l = 0$ m, $l = 60$ m, and $l = 120$ m, respectively: $f = 100$ kHz, $a = 6370$ km, $\varepsilon_{r1} = 12$, $\varepsilon_{r2} = 80$, $\sigma_1 = 10^{-5}$ S/m, $\sigma_2 = 4$ S/m, and $z_r = z_s = 0$ m

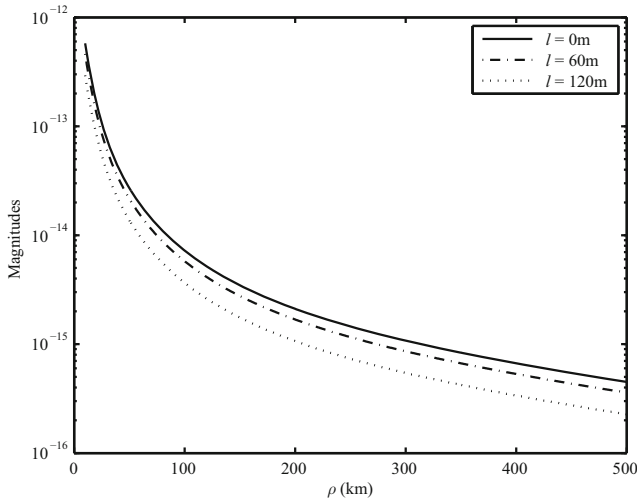


Fig. 6.8. $|H_r|$ in A/m due to unit vertical magnetic dipole versus the propagating distance ρ at $l = 0$ m, $l = 60$ m, and $l = 120$ m, respectively: $f = 100$ kHz, $a = 6370$ km, $\varepsilon_{r1} = 12$, $\varepsilon_{r2} = 80$, $\sigma_1 = 10^{-5}$ S/m, $\sigma_2 = 4$ S/m, and $z_r = z_s = 0$ m

vertical electric dipole at $l = 0$ m, $l = 60$ m, and $l = 120$ m are computed and plotted in Figs. 6.7 and 6.8, respectively.

From Fig. 6.5 to Fig. 6.8, it is seen that the excitation efficiency of a vertical electric dipole in the presence of a three-layered spherical region is much greater than that of a vertical magnetic dipole.

6.4 Electromagnetic Field due to Horizontal Electric Dipole

From the above representations of the electromagnetic field in the air radiated by the vertical electric dipole and those of the vertical magnetic dipole, using a reciprocity theorem, the approximate and complete formulas for the vertical components E_r^{he} and H_r^{he} of the electromagnetic field in the air radiated by a horizontal electric dipole on or near the spherical surface of the dielectric-coated Earth can be derived readily.

$$E_r^{he}(a + z_r, \theta, \phi) = -\frac{i\eta Ids^{he} e^{i(k_0 a \theta + \frac{\pi}{4})}}{\lambda a \sqrt{\theta \sin \theta}} \sqrt{\pi x} \cos \phi \\ \times \sum_s \frac{iF_s(z_r) \frac{\partial F_s(z)}{k_0 \partial z} \Big|_{z=z_s}}{(t_s - q^2) [1 + \frac{t_s}{2} (\frac{2}{k_0 a})^{2/3}]} e^{it_s x}, \quad (6.74)$$

$$H_r^{he}(a + z_r, \theta, \phi) = -\frac{i Ids^{he} e^{i(k_0 a \theta + \frac{\pi}{4})}}{\lambda a \sqrt{\theta \sin \theta}} \sqrt{\pi x} \sin \phi \sum_s \frac{G_s(z_s) G_s(z_r)}{t'_s - (q^h)^2} e^{it'_s x}. \quad (6.75)$$

In spherical coordinates, from Maxwell's equations, it is convenient to express the remaining four components E_θ^{he} , E_ϕ^{he} , H_θ^{he} and H_ϕ^{he} in terms of E_r^{he} and H_r^{he} .

$$\left(\frac{\partial^2}{\partial r^2} + k^2 \right) (r H_\phi^{he}) = i\omega \varepsilon_0 \frac{\partial E_r^{he}}{\partial \theta} + \frac{1}{\sin \theta} \frac{\partial^2 H_r^{he}}{\partial r \partial \phi}, \quad (6.76)$$

$$\left(\frac{\partial^2}{\partial r^2} + k^2 \right) (r E_\theta^{he}) = \frac{\partial^2 E_r^{he}}{\partial r \partial \theta} + \frac{i\omega \mu_0}{\sin \theta} \frac{\partial H_r^{he}}{\partial \phi}, \quad (6.77)$$

$$\left(\frac{\partial^2}{\partial r^2} + k^2 \right) (r H_\theta^{he}) = -\frac{i\omega \varepsilon_0}{\sin \theta} \frac{\partial E_r^{he}}{\partial \phi} + \frac{\partial^2 H_r^{he}}{\partial r \partial \theta}, \quad (6.78)$$

$$\left(\frac{\partial^2}{\partial r^2} + k^2 \right) (r E_\phi^{he}) = \frac{1}{\sin \theta} \frac{\partial^2 E_r^{he}}{\partial r \partial \phi} - i\omega \mu_0 \frac{\partial H_r^{he}}{\partial \theta}. \quad (6.79)$$

From Eq. (6.76), we get

$$\frac{\nu(\nu+1)}{r} H_\phi^{he} = i\omega\epsilon_0 \frac{\partial E_r^{he}}{\partial \theta} + \frac{1}{\sin \theta} \frac{\partial^2 H_r^{he}}{\partial r \partial \phi}. \quad (6.80)$$

Taking into account the relation $\nu(\nu+1)/r \approx k^2 a$, the component H_ϕ^{he} is formulated as follows:

$$\begin{aligned} H_\phi^{he}(a+z_r, \theta, \phi) = & -\frac{i I d s^{he}}{\lambda a} \frac{e^{i(k_0 a \theta + \frac{\pi}{4})}}{\sqrt{\theta \sin \theta}} \sqrt{\pi x} \cos \phi \\ & \times \left[\sum_s \frac{i F_s(z_r) \frac{\partial F_s(z)}{k_0 \partial z} \Big|_{z=z_s}}{t_s - q^2} e^{i t_s x} \right. \\ & \left. + \frac{1}{k_0 a \sin \theta} \sum_s \frac{\frac{\partial G_s(z)}{k_0 \partial z} \Big|_{z=z_r} G_s(z_s)}{t'_s - (q^h)^2} e^{i t'_s x} \right]. \quad (6.81) \end{aligned}$$

Similarly, the remaining three components E_θ^{he} , H_θ^{he} , and E_ϕ^{he} are written in the following forms:

$$\begin{aligned} H_\theta^{he}(a+z_r, \theta, \phi) = & \frac{I d s^{he}}{\lambda a} \frac{e^{i(k_0 a \theta + \frac{\pi}{4})}}{\sqrt{\theta \sin \theta}} \sqrt{\pi x} \sin \phi \\ & \times \left[\frac{i}{k_0 a \sin \theta} \sum_s \frac{F_s(z_r) \frac{\partial F_s(z)}{k_0 \partial z} \Big|_{z=z_s}}{(t_s - q^2) \left[1 + \frac{t_s}{2} \left(\frac{2}{k_0 a} \right)^{2/3} \right]} e^{i t_s x} \right. \\ & \left. - \sum_s \frac{\frac{\partial G_s(z)}{k_0 \partial z} \Big|_{z=z_r} G_s(z_s)}{t'_s - (q^h)^2} e^{i t'_s x} \right], \quad (6.82) \end{aligned}$$

$$\begin{aligned} E_\theta^{he}(a+z_r, \theta, \phi) = & \frac{\eta I d s^{he}}{\lambda a} \frac{e^{i(k_0 a \theta + \frac{\pi}{4})}}{\sqrt{\theta \sin \theta}} \sqrt{\pi x} \cos \phi \\ & \times \left[-i \sum_s \frac{\frac{\partial F_s(z)}{k_0 \partial z} \Big|_{z=z_r} \frac{\partial F_s(z)}{k_0 \partial z} \Big|_{z=z_s}}{t_s - q^2} e^{i t_s x} \right. \\ & \left. + \frac{1}{k_0 a \sin \theta} \sum_s \frac{G_s(z_r) G_s(z_s)}{t'_s - (q^h)^2} e^{i t'_s x} \right], \quad (6.83) \end{aligned}$$

$$\begin{aligned} E_\phi^{he}(a+z_r, \theta, \phi) = & \frac{i \eta I d s^{he}}{\lambda a} \frac{e^{i(k_0 a \theta + \frac{\pi}{4})}}{\sqrt{\theta \sin \theta}} \sqrt{\pi x} \sin \phi \\ & \times \left[\frac{i}{k_0 a \sin \theta} \sum_s \frac{\frac{\partial F_s(z)}{k_0 \partial z} \Big|_{z=z_r} \frac{\partial F_s(z)}{k_0 \partial z} \Big|_{z=z_s}}{(t_s - q^2) \left[1 + \frac{t_s}{2} \left(\frac{2}{k_0 a} \right)^{2/3} \right]} e^{i t_s x} \right. \\ & \left. + \sum_s \frac{G_s(z_r) G_s(z_s)}{t'_s - (q^h)^2} e^{i t'_s x} \right], \quad (6.84) \end{aligned}$$

where the superscripts *he* designate the horizontal electric dipole.

From the above derivations, it is seen that the electromagnetic field radiated by a horizontal electric dipole includes the terms of electric type and those of magnetic type. The electric field $|E_r|$ in V/m and magnetic field $|H_\phi|$ in A/m due to unit horizontal electric dipole at $l = 0$ m, $l = 60$ m, and $l = 120$ m are computed and shown in Figs. 6.9 and 6.10, respectively.

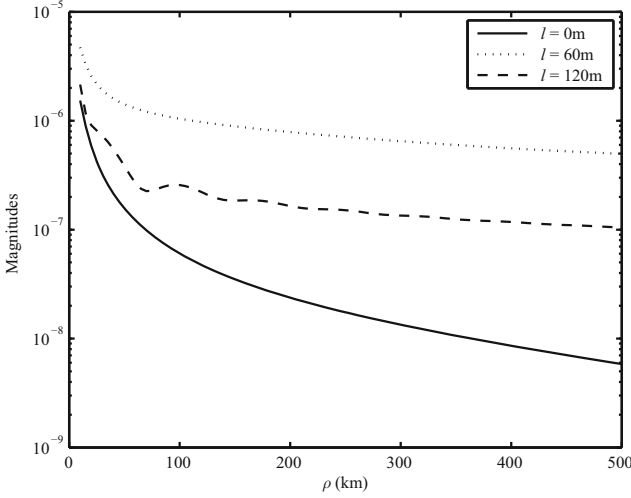


Fig. 6.9. The electric field $|E_r|$ in V/m at $l = 0$ m, $l = 60$ m, and $l = 120$ m due to unit horizontal electric dipole versus the propagating distance ρ ; $f = 100$ kHz, $a = 6370$ km, $\varepsilon_{r1} = 12$, $\varepsilon_{r2} = 80$, $\sigma_1 = 10^{-5}$ S/m, $\sigma_2 = 4$ S/m, $z_r = z_s = 1$ m, and $\phi = 0$

In order to discuss the convergence of the series of the field components, the number N of the required terms for accurate calculation of the electric field E_r due to a horizontal electric dipole is defined by

$$\frac{|E_N|}{\left| \sum_{n=1}^N E_n \right|} \leq 0.01. \quad (6.85)$$

If x is small, namely the observation point is close to the dipole, the series in Eqs. (6.51), (6.68), (6.74), (6.75), and (6.81)~(6.84) converge slowly and to calculate the sum large terms may be required. In Table 6.1, the required terms N to calculate the sum in Eq. (6.74) are listed at several different frequencies and different distances when $l = 0$ m. In order to illustrate the effect on the convergence of the thickness of the dielectric layer, the required terms N to calculate the sum in Eq. (6.74) are listed at several different frequencies

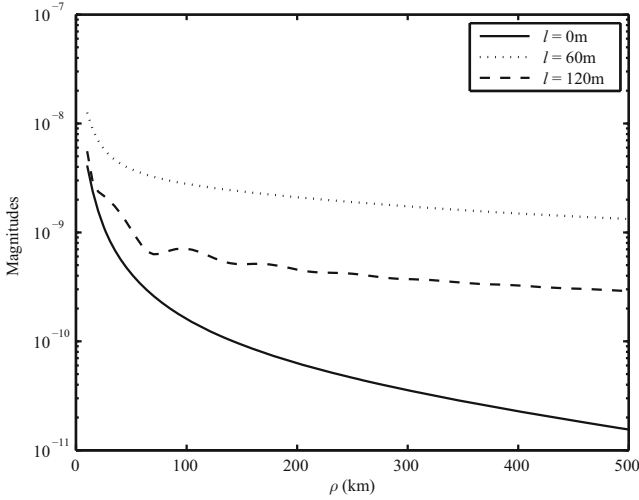


Fig. 6.10. The magnetic field $|H_\phi|$ in A/m at $l = 0$ m, $l = 60$ m, and $l = 120$ m due to unit horizontal electric dipole versus the propagating distance ρ ; $f = 100$ kHz, $a = 6370$ km, $\varepsilon_{r1} = 12$, $\varepsilon_{r2} = 80$, $\sigma_1 = 10^{-5}$ S/m, $\sigma_3 = 4$ S/m, $z_r = z_s = 1$ m, and $\phi = 0$

and different distances when $l = 120$ m in Table 6.2. In the computations in Tables 6.1 and 6.2, it is assumed that $a = 6370$ km, $f = 100$ kHz, $\varepsilon_{r1} = 12$, $\sigma_1 = 10^{-5}$ S/m, $\sigma_2 \rightarrow \infty$, and $z_r = z_s = 0$ m. Obviously, when the distance between the observation point and the dipole is not too large, the thickness of the dielectric layer largely affects the convergence, and to calculate the sum more terms may be required. In calculating the electromagnetic field, the Planar-Earth formulas are good approximations when $x < 0.2$ and the Spherical-Earth formulas are good approximations when $x > 0.2$.

Table 6.1. The terms N to compute the electric field $|E_r|$ when $l = 0$ m

ρ	100 kHz	200 kHz	300 kHz	1 MHz	2 MHz
1 km	61	61	60	58	57
10 km	41	38	36	29	26
50 km	17	14	13	9	8
100 km	10	8	7	5	4
200 km	6	5	4	3	3
300 km	4	4	3	3	3
500 km	3	3	2	2	2

Table 6.2. The terms N to calculate the electric field $|E_r|$ when $l = 120$ m

ρ	100 kHz	200 kHz	300 kHz	1 MHz	2 MHz
1 km	93	123	103	95	87
10 km	71	75	73	58	38
50 km	20	28	17	19	7
100 km	7	14	10	9	3
200 km	3	7	6	5	2
300 km	2	5	4	3	2
500 km	2	3	3	3	2

6.5 Summary

In this chapter, the approximate formulas are derived for the electromagnetic field in the air over the spherical surface of the dielectric-coated Earth when a dipole (vertical electric dipole, vertical magnetic dipole, or horizontal electric dipole) in the air is on or close to the surface. In the case where both the dipole and the observation point are located in the electrical Earth, the derivations and computations are carried out by Li and Park (2003) and they are not included in this chapter because they use a similar method to that addressed here.

References

- Bremmer H (1949) *Terrestrial Radio Waves*. New York, NY, USA: Elsevier.
- Bremmer H (1954) The extension of Sommerfeld's formula for the propagation of radio waves over a flat earth to different conductivities of the soil. *Physica*, 20: 441–460.
- Bremmer H (1958) Applications of operational calculus to groundwave propagation, particularly for long waves. *IRE Transactions on Antennas and Propagation*, AP-6: 267–274.
- Fock VA (1965) *Electromagnetic Diffraction and Propagation Problems*. Oxford, UK: Pergamon Press.
- Gradshteyn IS and Ryzhik IM (1980) *Table of Integrals, Series, and Products*. New York, NY, USA: Academic Press.
- Hill DA and Wait JR (1980) Ground wave attenuation function for a spherical earth with arbitrary surface impedance. *Radio Science*, 15(3): 637–643.
- Houdzoumis VA (1999) Vertical electric dipole radiation over a sphere: character of the waves that propagate through the sphere. *Journal of Applied Physics*, 86: 3939–3942.
- Houdzoumis VA (2000) Two modes of wave propagation manifested in vertical electric dipole radiation over a sphere. *Radio Science*, 35(1): 19–29.
- Li K and Park SO (2003) Electromagnetic field in the air generated by a horizontal electric dipole located in the spherical electrically earth coated with a dielectric layer. *Journal of Electromagnetic Waves and Applications*, 17(10): 1399–1417.

- Li K, Park SO, and Zhang HQ (2004a) Electromagnetic field in the presence of a three-layered spherical region. *Progress In Electromagnetics Research*, PIER 45: 103–121, Cambridge, MA, USA: EMW Publishing.
- Li K, Park SO, and Zhang HQ (2004b) Electromagnetic field over the spherical earth coated with N-layered dielectric. *Radio Science*, 39, RS2008, doi:10.1029/2002RS002771.
- Li K and Lu Y (2005) Electromagnetic Field from a Horizontal Electric Dipole in the spherical electrically earth Coated with N-layered dielectrics. *Progress In Electromagnetics Research*, PIER 54: 221–244. Cambridge, MA, USA: EMW Publishing.
- Margetis D (2002) Radiation of horizontal electric dipole on large dielectric sphere. *Journal of Mathematical Physics*, 43: 3162–3201.
- North KA (1941) The calculations of ground-wave field intensity over a finitely conducting spherical earth. *Proceedings of the IRE*, 29: 623–639.
- Pan WY and Zhang HQ (2003) Electromagnetic field of a vertical electric dipole on the spherical conductor covered with a dielectric layer. *Radio Science*, 38(3), 1061, doi:10.1029/2002RS002689.
- Spies KP and Wait JR (1966) On the calculation of the groundwave attenuation factor at low frequencies. *IEEE Transactions on Antennas and Propagation*, AP-14: 515–517.
- Van der Pol B and Bremmer H (1938) The propagation of radio waves over a finitely conducting spherical earth. *Philosophical Magazine*, 25: 817–834; Further note on above (1939), 27: 261–275.
- Watson GN (1918) The diffraction of radio waves by the earth. *Proceedings of the Royal Society*, A95: 83–99.
- Wait JR (1956) Radiation and propagation from a vertical antenna over a spherical earth. *Journal of Research of the National Bureau of Standards*, 56: 237–244.
- Wait JR (1957). The transient behavior of the electromagnetic ground wave on a spherical earth. *IEEE Transactions on Antennas and Propagation*, AP5: 198–202.
- Wait JR (1960) On the excitation of electromagnetic surface wave on a curved surface. *IRE Transactions on Antennas and Propagation*, AP-8: 445–449.

Electromagnetic Field of a Dipole Source over the Spherical Surface of Multi-Layered Earth

The analytical solution is carried out for the electromagnetic field in the air of a dipole over the spherical surface of the multi-layered Earth. The region of interest consists of a spherical dielectric Earth, coated with the dielectric layer composed of a succession of n spherically bounded layer under air. The surface impedance for the electric-type field is presented and the formulas are obtained for the electromagnetic field in the air radiated by a vertical electric dipole. Similarly, the surface admittance for the magnetic-type field is presented and the formulas are obtained for the electromagnetic field radiated by a vertical magnetic dipole. Based on the above results, the formulas are derived readily for the six components of the electromagnetic field of a horizontal electric dipole by using a reciprocity theorem.

7.1 Introduction

In the preceding chapter, the approximate formulas were derived for the electromagnetic field radiated by a dipole in air over a conducting or electrically spherical Earth coated with a dielectric layer. A more general case of spherical layering is when the dielectric layer is composed of successive n spherically bounded layers, each with arbitrary thickness l_j , $j = 1, 2, \dots, n$, as shown in Fig. 7.1. The center of the sphere is the origin of a spherical coordinate system (r, θ, ϕ) . The air (Region 0, $r \geq a$) is characterized by the permeability μ_0 , uniform permittivity ε_0 , and conductivity $\sigma_0 = 0$. The dielectric layer with the uniform thickness l consists of n spherical layers, e.g. $l = l_1 + l_2 + \dots + l_n$. The dielectric medium in Region j ($a - l'_j \leq r \leq a - l'_{j-1}$, $l'_j = l_1 + l_2 + \dots + l_j$) is characterized by the permeability μ_0 , relative permittivity ε_{rj} , and conductivity σ_j . The Earth (Region $n + 1$, $r \leq a - l'_n$, $l'_n = l_n$) is the dielectric medium characterized by the permeability μ_0 , relative permittivity $\varepsilon_{r(n+1)}$, and conductivity σ_{n+1} . Then, the wave numbers of those regions are

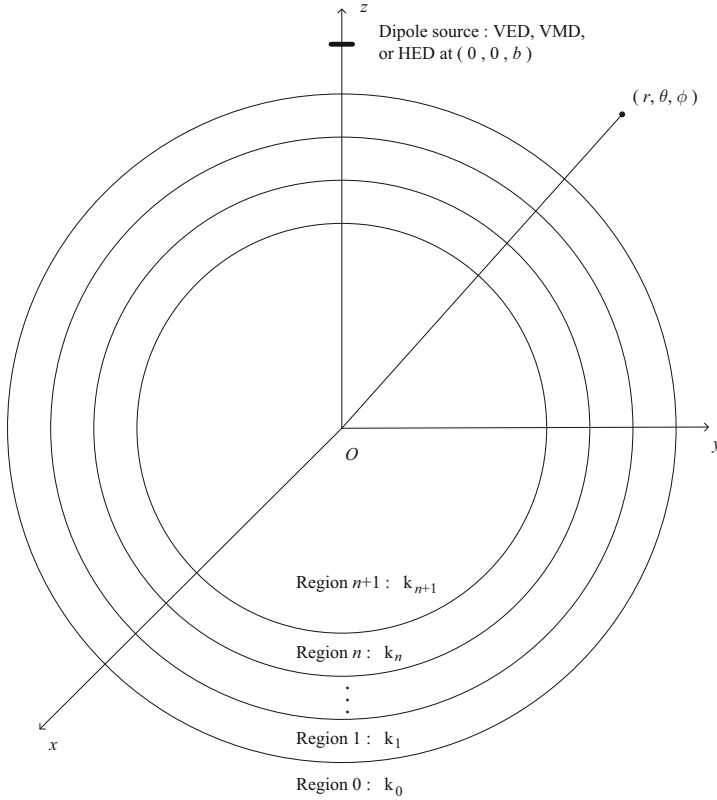


Fig. 7.1. The dipole at the height z_s over the spherical Earth coated with n -layered dielectric

$$k_0 = \omega \sqrt{\mu_0 \varepsilon_0}, \quad (7.1)$$

$$k_j = \omega \sqrt{\mu_0 (\varepsilon_0 \varepsilon_{rj} + i\sigma_j/\omega)}, \quad j = 1, 2, \dots, n, \quad (7.2)$$

$$k_{n+1} = \omega \sqrt{\mu_0 (\varepsilon_0 \varepsilon_{r(n+1)} + i\sigma_{n+1}/\omega)}. \quad (7.3)$$

In this chapter, the approximate formulas are derived for the electromagnetic field radiated by a dipole (a vertical electric dipole, vertical magnetic dipole, or horizontal electric dipole) in air over the spherical surface of an Earth coated with N -layered dielectric. To illustrate the applications of the general expressions obtained, the computations are carried out when the dielectric layer is composed of successive 2 spherically bounded layers, each with the thickness $l/2$. The present studies were addressed in a recent paper (Li, Park, and Zhang, 2004b).

7.2 Electromagnetic Field due to Vertical Electric Dipole

First, we will attempt to treat the electromagnetic field radiated by a vertical electric dipole over the spherical Earth coated with a dielectric layer composed of a succession of n spherically bounded layers. Assume that the vertical electric dipole is represented by the current density $\hat{z}Idl\delta(x)\delta(y)\delta(z-b)$, where $b = z_s + a$, and $z_s > 0$ denotes the height of the dipole above the spherical surface. The non-zero components E_r , E_θ , and H_ϕ are expressed as follows:

$$E_r^{(j)} = \left(\frac{\partial^2}{\partial r^2} + k_j^2 \right) (U_j r), \quad (7.4)$$

$$E_\theta^{(j)} = \frac{1}{r} \frac{\partial^2}{\partial \theta \partial r} (U_j r), \quad (7.5)$$

$$H_\phi^{(j)} = -\frac{i\omega\epsilon_j}{r} \frac{\partial}{\partial \theta} (U_j r). \quad (7.6)$$

Here the potential function U_j is the solution of the scalar Helmholtz equation

$$(\nabla^2 + k_j^2)U_j = 0, \quad (7.7)$$

where $j = 0, 1, 2, \dots, n+1$. In spherical coordinates, because of symmetry, a solution for U_j is written in the form of

$$U_j = \frac{1}{r} R_j(r) \Phi(\theta). \quad (7.8)$$

The azimuthal field variations may be expressed by the Legendre functions of first kind $P_\nu(\cos(\pi - \theta))$ and their derivatives (Pan and Zhang, 2003). The radial field variations are determined by the following differential equation:

$$\frac{d^2 R_j(r)}{dr^2} + k_j^2 \left[1 - \frac{\nu(\nu+1)}{k_j^2 r^2} \right] R_j(r) = 0. \quad (7.9)$$

In Region 0, the solution of Eq. (7.9) can be expressed in terms of Airy function of the second kind, which has been addressed specifically in the preceding chapter.

In Region j ($j = 1, 2, \dots, n$), $a - l'_j \leq r \leq a - l'_{j-1}$, taking into account $l'_j \ll a$, we take $r \approx a$. Then, Eq. (7.9) is simplified as

$$\frac{d^2 R_j(r)}{dr^2} + (k_j^2 - k_0^2) R_j(r) = 0. \quad (7.10)$$

The solution of Eq. (7.10) is

$$R_j(r) = B_j e^{i\gamma_j[r-(a-l'_j)]} + C_j e^{-i\gamma_j[r-(a-l'_j)]}, \quad (7.11)$$

where $\gamma_j = \sqrt{k_j^2 - k_0^2}$, $j = 1, 2, \dots, n$. The surface impedance at any point in the j st layer for the electric-type field is defined by

$$Z_j(r) = \frac{E_\theta^{(j)}}{H_\phi^{(j)}}. \quad (7.12)$$

Taking into account the impedance boundary condition at $r = a - l'_n$, we have

$$Z_n(r)|_{r=a-l'_n} = \frac{E_\theta^{(n)}}{H_\phi^{(n)}} \bigg|_{r=a-l'_n} = -\eta_n \Delta_g. \quad (7.13)$$

where $\eta_n = \sqrt{\mu_0/\varepsilon_n}$, $l'_n = l_1 + l_2 + \dots + l_n = l$. At low frequencies, the normalized surface impedance Δ_g at the boundary $z = r - l$ is approximated by

$$\Delta_g \approx \frac{k_n}{k_{n+1}} \sqrt{1 - \left(\frac{k_n}{k_{n+1}} \right)^2}. \quad (7.14)$$

The quantity $Z_n(r)$ with $a - l'_n \leq r \leq a - l'_{n-1}$ is

$$\begin{aligned} Z_n(r) &= -\frac{\omega\mu_0\gamma_n}{k_n^2} \frac{B_n e^{i\gamma_n[r-(a-l'_n)]} - C_n e^{-i\gamma_n[r-(a-l'_n)]}}{B_n e^{i\gamma_n[r-(a-l'_n)]} + C_n e^{-i\gamma_n[r-(a-l'_n)]}} \\ &= -\frac{\omega\mu_0\gamma_n}{k_n^2} \frac{\frac{B_n}{C_n} e^{i\gamma_n[r-(a-l'_n)]} - e^{-i\gamma_n[r-(a-l'_n)]}}{\frac{B_n}{C_n} e^{i\gamma_n[r-(a-l'_n)]} + e^{-i\gamma_n[r-(a-l'_n)]}} \\ &= -\frac{\omega\mu_0\gamma_n}{k_n^2} \tanh \left[\ln \left(\frac{B_n}{C_n} \right)^{\frac{1}{2}} + i\gamma_n[r-(a-l'_n)] \right]. \end{aligned} \quad (7.15)$$

With Eq. (7.15) at $r = a - l'_n$, the surface impedance in Region n is written readily.

$$Z_n(r) = -\frac{\omega\mu_0\gamma_n}{k_n^2} \tanh \left\{ i\gamma_n [r-(a-l'_n)] + \tanh^{-1} \left(\frac{k_n \Delta_g}{\gamma_n} \right) \right\}. \quad (7.16)$$

With the identity

$$\tanh(a + \tanh^{-1} b) = \coth(a + \coth^{-1} b), \quad (7.17)$$

Eq. (7.16) is expressed in the form

$$Z_n(r) = -\frac{\omega\mu_0\gamma_n}{k_n^2} \coth \left\{ i\gamma_n [r-(a-l'_n)] + \coth^{-1} \left(\frac{k_n \Delta_g}{\gamma_n} \right) \right\}. \quad (7.18)$$

The subtraction of 1 from the index n in Eq. (7.15) gives, for the $(n-1)$ st layer,

$$Z_{n-1}(r) = -\frac{\omega\mu_0\gamma_{n-1}}{k_{n-1}^2} \tanh \left\{ \ln \left(\frac{B_{n-1}}{C_{n-1}} \right)^{1/2} + i\gamma_{n-1} \left[r - (a - l'_{n-1}) \right] \right\};$$

$$(a - l'_{n-1} \leq r \leq a - l'_{n-2}). \quad (7.19)$$

With the required continuity relation,

$$Z_{n-1}(r)|_{r=a-l'_{n-1}} = Z_n(r)|_{r=a-l'_{n-1}}, \quad (7.20)$$

it follows that

$$\ln \left(\frac{B_{n-1}}{C_{n-1}} \right)^{1/2} = \tanh^{-1} \left\{ \frac{\gamma_n k_{n-1}^2}{\gamma_{n-1} k_n^2} \tanh \left[i\gamma_n l_n + \tanh^{-1} \left(\frac{k_n \Delta_g}{\gamma_n} \right) \right] \right\}, \quad (7.21)$$

and

$$Z_{n-1}(r) = -\frac{\omega\mu_0\gamma_{n-1}}{k_{n-1}^2} \left\{ i\gamma_{n-1} \left[r - (a - l'_{n-1}) \right] + \tanh^{-1} \left[\frac{\gamma_n k_{n-1}^2}{\gamma_{n-1} k_n^2} \right. \right. \\ \left. \left. \times \tanh \left[i\gamma_n l_n + \tanh^{-1} \left(\frac{k_n \Delta_g}{\gamma_n} \right) \right] \right] \right\}, \quad (7.22)$$

where $l_n = l'_n - l'_{n-1}$ is the thickness of the n -st layer.

If the procedure is continued to the boundary at $r = a - l'_1$ between 1 and 2, the desired surface impedance is obtained. It is represented as

$$Z_1(r) = -\frac{\omega\mu_0\gamma_1}{k_1^2} \tanh \left\{ i\gamma_1 \left[r - (a - l'_1) \right] + \tanh^{-1} \left[\frac{\gamma_2 k_1^2}{\gamma_1 k_2^2} \tanh \left[i\gamma_2 l_2 \right. \right. \right. \\ \left. \left. + \tanh^{-1} \left[\frac{\gamma_3 k_2^2}{\gamma_2 k_3^2} \tanh \left[i\gamma_3 l_3 + \dots \right. \right. \right. \right. \\ \left. \left. + \tanh^{-1} \left[\frac{\gamma_n k_{n-1}^2}{\gamma_{n-1} k_n^2} \tanh \left[i\gamma_n l_n \right. \right. \right. \right. \\ \left. \left. + \tanh^{-1} \left(\frac{k_n \Delta_g}{\gamma_n} \right) \right] \right] \dots \right] \right] \right\}. \quad (7.23)$$

With the required continuity relation

$$Z_0(r)|_{r=a} = Z_1(r)|_{r=a}, \quad (7.24)$$

it follows that

$$\begin{aligned}
\begin{bmatrix} E_r(a + z_r, \theta, \phi) \\ E_\theta(a + z_r, \theta, \phi) \\ \eta H_\phi(a + z_r, \theta, \phi) \end{bmatrix} &= \frac{iIdl\eta}{\lambda a} \frac{e^{i(k_0 a \theta + \frac{\pi}{4})}}{\sqrt{\theta \sin \theta}} \sqrt{\pi x} \\
&\times \begin{bmatrix} \sum_s \frac{F_s(z_s) F_s(z_r)}{t_s - q^2} e^{it_s x} \\ \sum_s \frac{i F_s(z_s) \left. \frac{\partial F_s(z)}{\partial z} \right|_{z=z_r}}{k_0(t_s - q^2) \left[1 + \frac{t_s}{2} \left(\frac{2}{k_0 a} \right)^{2/3} \right]} e^{it_s x} \\ \sum_s \frac{F_s(z_s) F_s(z_r)}{(t_s - q^2) \left[1 + \frac{t_s}{2} \left(\frac{2}{k_0 a} \right)^{2/3} \right]} e^{it_s x} \end{bmatrix}, \quad (7.31)
\end{aligned}$$

where t_s are the roots of Eq. (7.29), which correspond to propagation modes. z_r denotes the height of the observation point, and

$$x = \left(\frac{k_0 a}{2} \right)^{1/3} \theta. \quad (7.32)$$

The normalized “height-gain” function $F_s(z)$ is defined by

$$F_s(z) = \frac{W_2(t_s - y)}{W_2(t_s)}, \quad (7.33)$$

where

$$y = \left[\frac{2\nu(\nu + 1)}{a^3} \right]^{1/3} z \approx \left(\frac{2}{k_0 a} \right)^{1/3} k_0 z. \quad (7.34)$$

In Eq. (7.34), $z \ll a$, $z > 0$ denotes the height above the surface. In the above formulas, it is assumed that both the dipole and the point of observation are close to the spherical interface between the air and the dielectric layer.

7.3 Electromagnetic Field due to Vertical Magnetic Dipole

If the excitation source is replaced by a vertical magnetic dipole with its moment $M = Ida$, and da is the area of the loop, because of symmetry, the non-zero components $E_\phi^{(j)}$, $H_r^{(j)}$, and $H_\theta^{(j)}$ of the magnetic-type field are expressed as follows:

$$E_\phi^{(j)} = \frac{-i\omega\mu_0}{r} \frac{\partial}{\partial \theta} (V_j r), \quad (7.35)$$

$$H_r^{(j)} = \left(\frac{\partial^2}{\partial r^2} + k_j^2 \right) (V_j r), \quad (7.36)$$

$$H_\theta^{(j)} = \frac{1}{r} \frac{\partial^2}{\partial \theta \partial r} (V_j r). \quad (7.37)$$

where the potential function V_j is the solution of in the scalar Helmholtz equation

$$(\nabla^2 + k_j^2)V_j = 0. \quad (7.38)$$

It is necessary to define the surface admittance in the j st layer for the magnetic-type field.

$$Y_j(r) = \frac{H_\theta^{(j)}}{E_\phi^{(j)}}. \quad (7.39)$$

According to the admittance boundary condition at $r = a - l'_n$, we have

$$Y_n(r)|_{r=a-l'_n} = \frac{H_\theta^{(n)}}{E_\phi^{(n)}} \bigg|_{r=a-l'_n} = \frac{1}{\eta_n \Delta_g}. \quad (7.40)$$

The quantity $Y_n(r)$ with $a - l'_n \leq r \leq a - l'_{n-1}$ is

$$Y_n(r) = -\frac{\gamma_n}{\omega\mu_0} \frac{B_n e^{i\gamma_n[r-(a-l'_n)]} - C_n e^{-i\gamma_n[r-(a-l'_n)]}}{B_n e^{i\gamma_n[r-(a-l'_n)]} + C_n e^{-i\gamma_n[r-(a-l'_n)]}}. \quad (7.41)$$

Following the same steps in the preceding section, it follows that

$$\begin{aligned} Y_0(r)|_{r=a} = & -\frac{\gamma_1}{\omega\mu_0} \left\{ i\gamma_1 l_1 + \tanh^{-1} \left[\frac{\gamma_2}{\gamma_1} \tanh \left[i\gamma_2 l_2 \right. \right. \right. \\ & + \tanh^{-1} \left[\frac{\gamma_3}{\gamma_2} \tanh \left[i\gamma_3 l_3 + \cdots + \tanh^{-1} \left[\frac{\gamma_n}{\gamma_{n-1}} \right. \right. \right. \\ & \times \tanh \left[i\gamma_n l_n + \tanh^{-1} \left(-\frac{k_n}{\gamma_n \Delta_g} \right) \right] \cdots \left. \left. \left. \right] \right] \right] \right\}. \end{aligned} \quad (7.42)$$

Note that if $l_1 = l, l_2 = l_3 = \cdots = l_n = 0$, Eq. (7.42) reduces to

$$Y_0(r)|_{r=a} = -\frac{\gamma_1}{\omega\mu_0} \tanh \left[i\gamma_1 l + \tanh^{-1} \left(-\frac{k_1}{\gamma_1 \Delta_g} \right) \right]. \quad (7.43)$$

At $r = a$, with the boundary conditions

$$\frac{E_\phi^{(0)}}{H_\theta^{(0)}} \bigg|_{z=a} = Y_0(r)|_{z=a} = Y_0(a), \quad (7.44)$$

we get

$$\frac{W'_2 k_0 \left(\frac{2}{k_0 a} \right)^{1/3}}{i\omega\mu_0 W_2} = Y_0(a). \quad (7.45)$$

Then, the differential equation is obtained readily as follows:

$$W_2'(t') - q^h W_2(t') = 0, \quad (7.46)$$

where t'_s are the roots of the above differential equation and $W_2(t'_s)$ is the Airy function of the second kind,

$$q^h = \frac{i\omega\mu_0}{k_0} \left(\frac{k_0 a}{2} \right)^{1/3} Y_0(a). \quad (7.47)$$

With the same manner addressed in the preceding chapter, the complete formulas are derived for the components E_ϕ , H_r , and H_θ of the electromagnetic field generated by a vertical magnetic dipole at $(a + z_s, 0, 0)$ over the spherical Earth coated by the N-layered dielectric. We write

$$\begin{aligned} \begin{bmatrix} E_\phi(a + z_r, \theta, \phi) \\ \eta H_r(a + z_r, \theta, \phi) \\ \eta H_\theta(a + z_r, \theta, \phi) \end{bmatrix} &= \frac{\omega\mu_0 I da}{\lambda a} \frac{e^{i(k_0 a \theta + \frac{\pi}{4})}}{\sqrt{\theta \sin \theta}} \sqrt{\pi x} \\ &\times \begin{bmatrix} \sum_s \frac{G_s(z_s) G_s(z_r)}{t_s - (q^h)^2} e^{it_s x} \\ \sum_s \frac{G_s(z_s) G_s(z_r)}{t_s - (q^h)^2} e^{it_s x} \\ i \sum_s \frac{G_s(z_s) \frac{\partial G_s(z)}{\partial z} \Big|_{z=z_r}}{t_s - (q^h)^2} e^{it_s x} \end{bmatrix}, \end{aligned} \quad (7.48)$$

where the normalized “height-gain” function $G_s(z)$ is

$$G_s(z) = \frac{W_2(t'_s - y)}{W_2(t'_s)}. \quad (7.49)$$

7.4 Electromagnetic Field due to Horizontal Electric Dipole

From the above formulas of the electromagnetic field of the vertical electric dipole and those of the vertical magnetic dipole, using the reciprocity theorem, the complete formulas are derived readily for the vertical components E_r^{he} and H_r^{he} radiated by a horizontal electric dipole.

$$\begin{aligned} E_r^{he}(a + z_r, \theta, \phi) &= -\frac{i\eta I ds^{he}}{\lambda a} \frac{e^{i(k_0 a \theta + \frac{\pi}{4})}}{\sqrt{\theta \sin \theta}} \sqrt{\pi x} \cos \phi \\ &\times \sum_s \frac{i F_s(z_r) \frac{\partial F_s(z)}{\partial z} \Big|_{z=z_s}}{(t_s - q^2) \left[1 + \frac{t_s}{2} \left(\frac{2}{k_0 a} \right)^{2/3} \right]} e^{it_s x}, \end{aligned} \quad (7.50)$$

$$H_r^{he}(a + z_r, \theta, \phi) = -\frac{i I d s^{he} e^{i(k_0 a \theta + \frac{\pi}{4})}}{\lambda a \sqrt{\theta \sin \theta}} \sqrt{\pi x} \sin \phi \sum_s \frac{G_s(z_s) G_s(z_r)}{t'_s - (q^h)^2} e^{i t'_s x}. \quad (7.51)$$

From Maxwell's equations, it is known that the remaining four components E_θ^{he} , E_ϕ^{he} , H_θ^{he} and H_ϕ^{he} can be expressed in terms of E_r^{he} and H_r^{he} . We write

$$\begin{aligned} H_\phi^{he}(a + z_r, \theta, \phi) = & -\frac{i I d s^{he} e^{i(k_0 a \theta + \frac{\pi}{4})}}{\lambda a \sqrt{\theta \sin \theta}} \sqrt{\pi x} \cos \phi \\ & \times \left[\sum_s \frac{i F_s(z_r) \frac{\partial F_s(z)}{k_0 \partial z} \Big|_{z=z_s}}{t_s - q^2} e^{i t_s x} \right. \\ & \left. + \frac{1}{k_0 a \sin \theta} \sum_s \frac{\frac{\partial G_s(z)}{k_0 \partial z} \Big|_{z=z_r} G_s(z_s)}{t'_s - (q^h)^2} e^{i t'_s x} \right], \quad (7.52) \end{aligned}$$

$$\begin{aligned} H_\theta^{he}(a + z_r, \theta, \phi) = & \frac{I d s^{he} e^{i(k_0 a \theta + \frac{\pi}{4})}}{\lambda a \sqrt{\theta \sin \theta}} \sqrt{\pi x} \sin \phi \\ & \times \left[\frac{i}{k_0 a \sin \theta} \sum_s \frac{F_s(z_r) \frac{\partial F_s(z)}{k_0 \partial z} \Big|_{z=z_s}}{(t_s - q^2) \left[1 + \frac{t_s}{2} \left(\frac{2}{k_0 a} \right)^{2/3} \right]} e^{i t_s x} \right. \\ & \left. - \sum_s \frac{\frac{\partial G_s(z)}{k_0 \partial z} \Big|_{z=z_r} G_s(z_s)}{t'_s - (q^h)^2} e^{i t'_s x} \right], \quad (7.53) \end{aligned}$$

$$\begin{aligned} E_\theta^{he}(a + z_r, \theta, \phi) = & \frac{\eta I d s^{he} e^{i(k_0 a \theta + \frac{\pi}{4})}}{\lambda a \sqrt{\theta \sin \theta}} \sqrt{\pi x} \cos \phi \\ & \times \left[-i \sum_s \frac{\frac{\partial F_s(z)}{k_0 \partial z} \Big|_{z=z_r} \frac{\partial F_s(z)}{k_0 \partial z} \Big|_{z=z_s}}{t_s - q^2} e^{i t_s x} \right. \\ & \left. + \frac{1}{k_0 a \sin \theta} \sum_s \frac{G_s(z) G_s(z_s)}{t'_s - (q^h)^2} e^{i t'_s x} \right], \quad (7.54) \end{aligned}$$

$$\begin{aligned} E_\phi^{he}(a + z_r, \theta, \phi) = & \frac{i \eta I d s^{he} e^{i(k_0 a \theta + \frac{\pi}{4})}}{\lambda a \sqrt{\theta \sin \theta}} \sqrt{\pi x} \sin \phi \\ & \times \left[\frac{i}{k_0 a \sin \theta} \sum_s \frac{\frac{\partial F_s(z)}{k_0 \partial z} \Big|_{z=z_r} \frac{\partial F_s(z)}{k_0 \partial z} \Big|_{z=z_s}}{(t_s - q^2) \left[1 + \frac{t_s}{2} \left(\frac{2}{k_0 a} \right)^{2/3} \right]} e^{i t_s x} \right. \\ & \left. + \sum_s \frac{G_s(z_r) G_s(z_s)}{t'_s - (q^h)^2} e^{i t'_s x} \right]. \quad (7.55) \end{aligned}$$

Here and the superscripts *he* designate the horizontal electric dipole. It is seen that the electromagnetic field radiated by a horizontal electric dipole over the electrically spherical Earth coated with a N-layered dielectric consists of electric-type and magnetic-type terms.

7.5 Computations and Conclusions

To illustrate the general formulas for the electromagnetic field components, the computations are carried out when the dielectric layer is composed of a succession of 2 spherically bounded layers, each with the thickness $l/2$. Assuming that the thickness of the dielectric layer is $l = 120$ m, namely both the thickness of the first layer and that of the second layer are 60 m, the radius of the Earth is taken as $a = 6370$ km, the first dielectric layer (Region 1, $a - l/2 < r < a$) is characterized by the relative permittivity $\varepsilon_{r1} = 8$ and conductivity $\sigma_1 = 10^{-5}$ S/m, the second dielectric layer (Region 2, $a - l < r < a - l/2$) is characterized by the relative permittivity $\varepsilon_{r1} = 12$ and conductivity $\sigma_1 = 10^{-5}$ S/m, and the Earth in Region 3 ($r < a - l$) is characterized by the relative permittivity $\varepsilon_{r2} = 80$ and conductivity $\sigma_2 = 4$ S/m, and both the dipole and observation point are placed on the surface of the dielectric-coated Earth, $z_r = z_s = 0$ m, the electric field $|E_r|$ in V/m and the magnetic field $|H_\phi|$ in A/m due to unit vertical electric dipole at $f = 100$ kHz, and $f = 200$ kHz are computed and plotted in Figs. 7.2 and 7.3, respectively. In this chapter, the electromagnetic field due to a vertical electric dipole is defined as the electric-type field. It is seen that the interference occurs when the thickness of the dielectric layer is larger than a certain value.

Assuming that all parameters are the same as those in Figs. 7.2 and 7.3, the electric field $|E_\phi|$ in V/m and the magnetic field $|H_r|$ in A/m due to unit vertical magnetic dipole at $f = 100$ kHz and $f = 200$ kHz are computed and plotted in Figs. 7.4 and 7.5, respectively. The electromagnetic field of a vertical magnetic dipole is defined as the magnetic-type field. From Figs. 7.2~7.5, it is seen that the excitation efficiency of a vertical electric dipole is much higher than that of a vertical magnetic dipole. Therefore, the vertical magnetic dipole is not employed in practice for communication over the asphalt- and cement-coated planar and spherical Earth.

At low frequencies, the electromagnetic fields generated by electrically short and long horizontal antennas have useful applications in communications over the dielectric-coated Earth. Assuming that all parameters of the dielectric layers and the Earth are the same as those in Figs. 7.2 and 7.3, and the heights of the dipole and the observation point are $z_s = z_r = 1$ m, the electric field $|E_r|$ in V/m and the magnetic field $|H_\phi|$ in A/m due to unit horizontal electric dipole at $f = 100$ kHz and $f = 200$ kHz are computed and plotted in Figs. 7.6 and 7.7, respectively. Graphs for the electric field $|E_r|$ and the magnetic field $|H_\phi|$ of unit horizontal electric dipole at $l = 60$ m, $l = 120$ m, and $l = 180$ m are shown in Figs. 7.8 and 7.9, respectively.

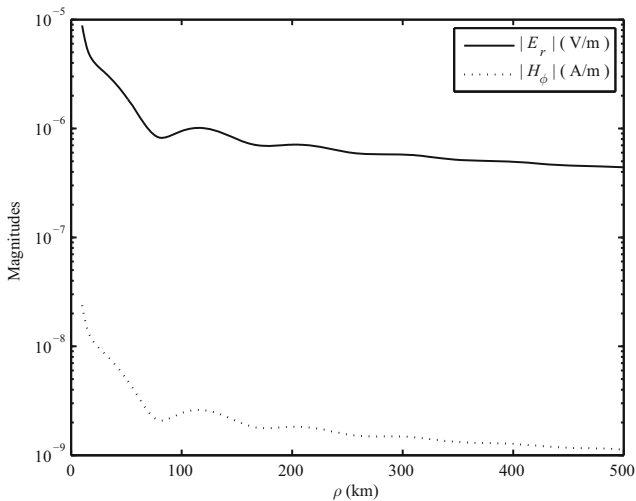


Fig. 7.2. The electric field $|E_r|$ in V/m and the magnetic field $|H_\phi|$ in A/m at $f = 100$ kHz due to unit vertical electric dipole versus the propagating distance ρ with $l = 120$ m, $a = 6370$ km, $\varepsilon_{r1} = 8$, $\varepsilon_{r2} = 12$, $\varepsilon_{r3} = 80$, $\sigma_1 = \sigma_2 = 10^{-5}$ S/m, $\sigma_3 = 4$ S/m, and $z_r = z_s = 0$ m

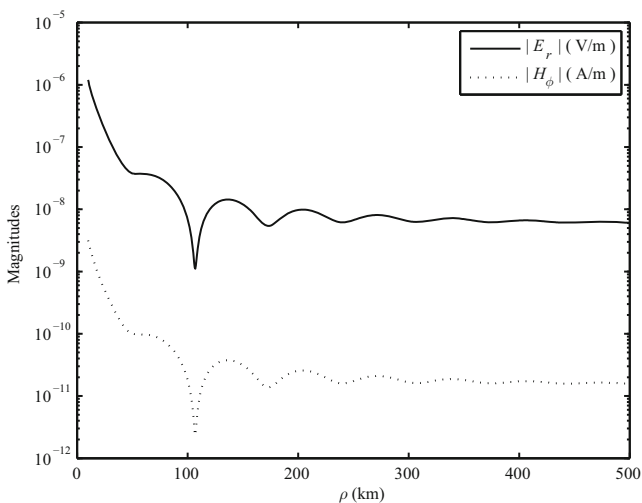


Fig. 7.3. The electric field $|E_r|$ in V/m and the magnetic field $|H_\phi|$ in A/m at $f = 200$ kHz due to unit vertical electric dipole versus the propagating distance ρ with $l = 120$ m, $a = 6370$ km, $\varepsilon_{r1} = 8$, $\varepsilon_{r2} = 12$, $\varepsilon_{r3} = 80$, $\sigma_1 = \sigma_2 = 10^{-5}$ S/m, $\sigma_3 = 4$ S/m, and $z_r = z_s = 0$ m

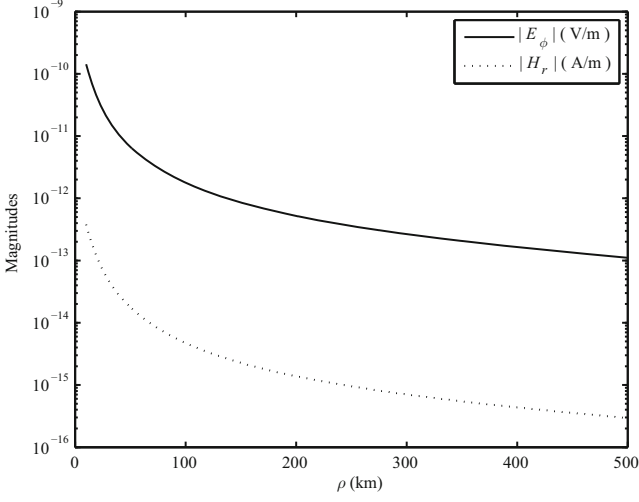


Fig. 7.4. The electric field $|E_\phi|$ in V/m and the magnetic field $|H_r|$ in A/m at $f = 100$ kHz due to unit vertical magnetic dipole versus the propagating distance ρ with $l = 120$ m, $a = 6370$ km, $\varepsilon_{r1} = 8$, $\varepsilon_{r2} = 12$, $\varepsilon_{r3} = 80$, $\sigma_1 = \sigma_2 = 10^{-5}$ S/m, $\sigma_3 = 4$ S/m, and $z_r = z_s = 0$ m

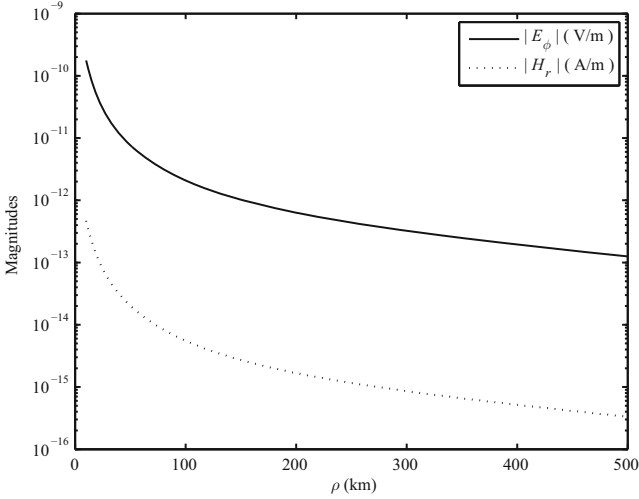


Fig. 7.5. The electric field $|E_\phi|$ in V/m and the magnetic field $|H_r|$ in A/m at $f = 200$ kHz due to unit vertical magnetic dipole versus the propagating distance ρ with $l = 120$ m, $a = 6370$ km, $\varepsilon_{r1} = 8$, $\varepsilon_{r2} = 12$, $\varepsilon_{r3} = 80$, $\sigma_1 = \sigma_2 = 10^{-5}$ S/m, $\sigma_3 = 4$ S/m, and $z_r = z_s = 0$ m

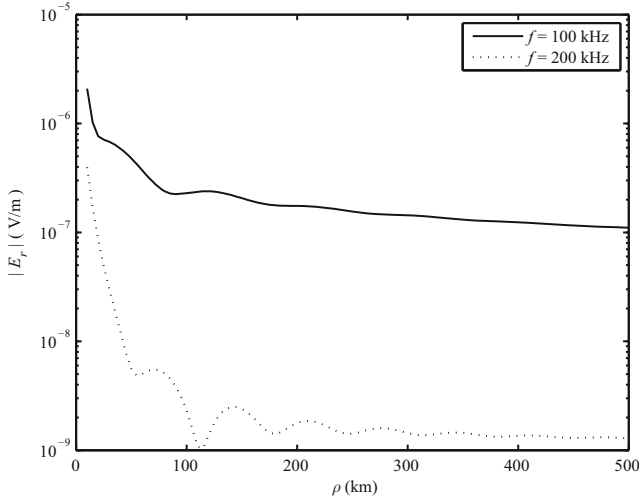


Fig. 7.6. The electric field $|E_r|$ in V/m at $f = 100$ kHz and $f = 200$ kHz due to unit horizontal electric dipole versus the propagating distance ρ with $l = 120$ m, $a = 6370$ km, $\varepsilon_{r1} = 8$, $\varepsilon_{r2} = 12$, $\varepsilon_{r3} = 80$, $\sigma_1 = \sigma_2 = 10^{-5}$ S/m, $\sigma_3 = 4$ S/m, $z_r = z_s = 1$ m, and $\phi = 0$

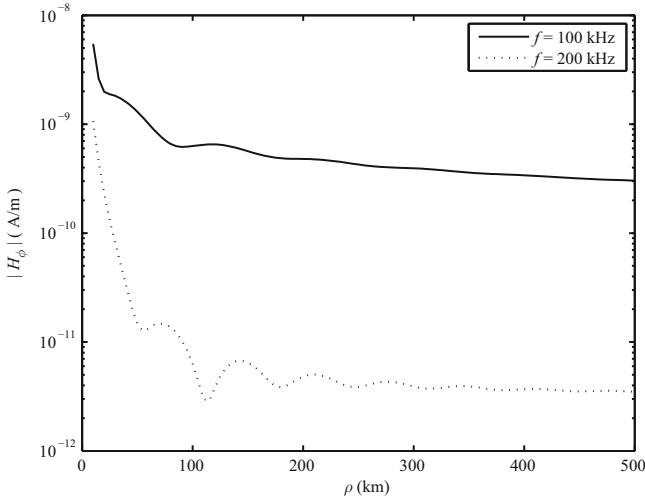


Fig. 7.7. The magnetic field $|H_\phi|$ in A/m at $f = 100$ kHz and $f = 200$ kHz due to unit horizontal electric dipole versus the propagating distance ρ with $l = 120$ m, $a = 6370$ km, $\varepsilon_{r1} = 8$, $\varepsilon_{r2} = 12$, $\varepsilon_{r3} = 80$, $\sigma_1 = \sigma_2 = 10^{-5}$ S/m, $\sigma_3 = 4$ S/m, $z_r = z_s = 1$ m, and $\phi = 0$

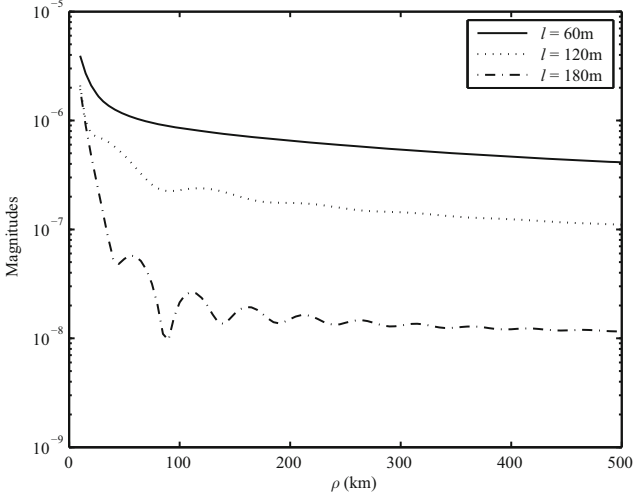


Fig. 7.8. The electric field $|E_r|$ in V/m at $l = 60$ m, $l = 120$ m, and $l = 180$ m due to unit horizontal electric dipole versus the propagating distance ρ with $f = 100$ kHz, $a = 6370$ km, $\varepsilon_{r1} = 8$, $\varepsilon_{r2} = 12$, $\varepsilon_{r3} = 80$, $\sigma_1 = \sigma_2 = 10^{-5}$ S/m, $\sigma_3 = 4$ S/m, $z_r = z_s = 1$ m, and $\phi = 0$

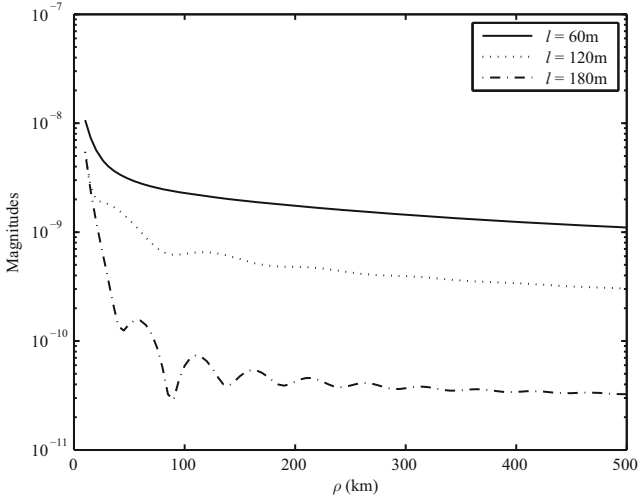


Fig. 7.9. The magnetic field $|H_\phi|$ in A/m at $l = 60$ m, $l = 120$ m, and $l = 180$ m due to unit horizontal electric dipole versus the propagating distance ρ with $f = 100$ kHz, $a = 6370$ km, $\varepsilon_{r1} = 8$, $\varepsilon_{r2} = 12$, $\varepsilon_{r3} = 80$, $\sigma_1 = \sigma_2 = 10^{-5}$ S/m, $\sigma_3 = 4$ S/m, $z_r = z_s = 1$ m, and $\phi = 0$

From Figs. 7.6~7.9, it is seen that the field components in the far-field region are quite different at different frequencies and different thicknesses of dielectric layer. Obviously, the interference occurs when the thickness of the dielectric layer is larger than a certain value and the conductivity of the dielectric layer should be considered.

References

- Bremmer H (1949) *Terrestrial Radio Waves*. New York, NY, USA: Elsevier.
- Bremmer H (1954) The extension of Sommerfeld's formula for the propagation of radio waves over a flat earth to different conductivities of the soil. *Physica*, 20: 441–460.
- Bremmer H (1958) Applications of operational calculus to groundwave propagation, particularly for long waves. *IRE Transactions on Antennas and Propagation*, AP-6: 267–274.
- Fock VA (1965) *Electromagnetic Diffraction and Propagation Problems*. Oxford, UK: Pergamon Press.
- Gradshteyn IS and Ryzhik IM (1980) *Table of Integrals, Series, and Products*. New York, NY, USA: Academic Press.
- Hill DA and Wait JR (1980) Ground wave attenuation function for a spherical earth with arbitrary surface impedance. *Radio Science*, 15(3): 637–643.
- Houdzoumis VA (1999) Vertical electric dipole radiation over a sphere: character of the waves that propagate through the sphere. *Journal of Applied Physics*, 86: 3939–3942.
- Houdzoumis VA (2000) Two modes of wave propagation manifested in vertical electric dipole radiation over a sphere. *Radio Science*, 35(1): 19–29.
- King RWP, Owens M, and Wu TT (1992) *Lateral Electromagnetic Waves: Theory and Applications to Communications, Geophysical Exploration, and Remote Sensing*. New York, NY, USA: Springer-Verlag.
- King RWP (1998) Electromagnetic ground-wave field of vertical antennas for communication at 1 to 30 MHz. *IEEE Transactions on Electromagnetic compatibility*, 40(4): 337–342.
- Li K, Park SO, and Zhang HQ (2004a) Electromagnetic field in the presence of a three-layered spherical region. *Progress In Electromagnetics Research*, PIER 45: 103–121. Cambridge, MA, USA: EMW Publishing.
- Li K, Park SO, and Zhang HQ (2004b) Electromagnetic field over the spherical earth coated with N-layered dielectric. *Radio Science*, 39, RS2008, doi:10.1029/2002RS002771.
- Margetis D (2002) Radiation of horizontal electric dipole on large dielectric sphere. *Journal of Mathematical Physics*, 43: 3162–3201.
- North KA (1941) The calculations of ground-wave field intensity over a finitely conducting spherical earth. *Proceedings of the IRE*, 29: 623–639.
- Pan WY and Zhang HQ (2003) Electromagnetic field of a vertical electric dipole on the spherical conductor covered with a dielectric layer. *Radio Science*, 38(3), 1059, doi:10.1029/2002RS002689.

- Spies KP and Wait JR (1966) On the calculation of the groundwave attenuation factor at low frequencies. *IEEE Transactions on Antennas and Propagation*, AP-14: 515–517.
- Van der Pol B and Bremmer H (1938) The propagation of radio waves over a finitely conducting spherical earth. *Philosophical Magazine*, 25: 817–834; Further note on above (1939), 27: 261–275.
- Wait JR (1956). Radiation and propagation from a vertical antenna over a spherical earth. *Journal of Research of the National Bureau of Standards*, 56: 237–244.
- Wait JR (1957) The transient behavior of the electromagnetic ground wave on a spherical earth. *IRE Transactions on Antennas and Propagation*, AP-5: 198–202.
- Wait JR (1960) On the excitation of electromagnetic surface wave on a curved surface. *IRE Transactions on Antennas and Propagation*, AP-8: 445–449.
- Watson GN (1918) The diffraction of radio waves by the earth. *Proceedings of the Royal Society*, A95: 83–99.

Exact Transient Field of a Horizontal Electric Dipole on the Boundary Between Two Dielectrics

In this chapter, the exact formulas are derived for the transient fields generated by a horizontal electric dipole with delta function excitation and Gaussian excitation on the plane boundary between two dielectrics. With the delta function excitation, the tangential electric fields consist of a delta function pulse travelling in the air with the velocity c , the oppositely directed delta function pulse travelling in the dielectric with the velocity $c/\varepsilon^{1/2}$ for the component E_ρ and the velocity $c\varepsilon^{1/2}$ for the component E_ϕ , and the final static electric field due to the charge left on the dipole. The appearance of the vertical magnetic field is similar to that of the tangential electric field. It is pointed out that the amplitude of the pulsed field along the boundary is $1/\rho^2$, which is characteristic of the lateral pulse. With the Gaussian excitation, the final exact formulas for the transient field are expressed in terms of several fundamental functions and finite integrals, which can be evaluated easily.

8.1 Introduction

The frequency-domain properties of lateral electromagnetic waves radiated by a dipole on or near the plane boundary between two different media has been investigated in the past century (Zenneck, 1907; Sommerfeld, 1909; 1926; Wait, 1970; Baños, 1966; King, 1982; 1986; Margetis, 2001). A historical account and extensive list of references can be found in the book by King, Owens and Wu (1992). In addition, the transient field of a dipole source near or on the boundary between two dielectrics was treated analytically by many investigators (Van der Pol, 1956; Wait, 1957; 1981; Frankena 1960; De Hoop and Frankena, 1960; Ezzeddine, Kong, and Tsang, 1981a; 1981b; Wu and King, 1987; Cicchetti, 1991; Dai and Young, 1997; Xia et al., 2004).

Over fifty years ago, the transient field was examined in detail by evaluating the Hertz potential of a delta function current in a vertical electric dipole on the boundary between two half-spaces (Van der Pol, 1956). Unfortunately, as pointed out in the Chapter 13 of the book by King, Owens, and Wu (1992),

the electric field components E_ρ and E_z cannot be obtained by evaluating the Hertz potential in the time domain. The important work for the exact solution of the components E_z and B_ϕ of the transient field radiated by a vertical electric dipole with delta function current on the boundary between two dielectrics was carried out by Wu and King (1987). Correspondingly, the exact formulas for the transient field of a vertical dipole with Gaussian excitation were obtained (King, 1989).

In this chapter, with the extension of the works by King and Wu (Wu and King, 1987; King, 1989), we will attempt to outline the exact formulas in terms of elementary function for three time-dependent components $E_{2z}(\rho, 0; t)$, $B_{2\rho}(\rho, \pi/2; t)$, and $B_{2\phi}(\rho, \pi/2; t)$ from a horizontal electric dipole with delta function excitation and Gaussian excitation on the boundary $z = 0$ between two dielectrics, which are addressed in our recent two papers (Li, Lu, and Pan, 2005a; 2005b).

8.2 Exact Transient Field with Delta Function Excitation

In this section, we will derive the exact formulas for the transient field of a horizontal electric dipole with delta function excitation on the plane boundary between two dielectrics.

8.2.1 Formal Representations of Time-independent Field due to Horizontal Electric Dipole

The geometry under consideration is shown in Fig. 8.1, where a unit horizontal

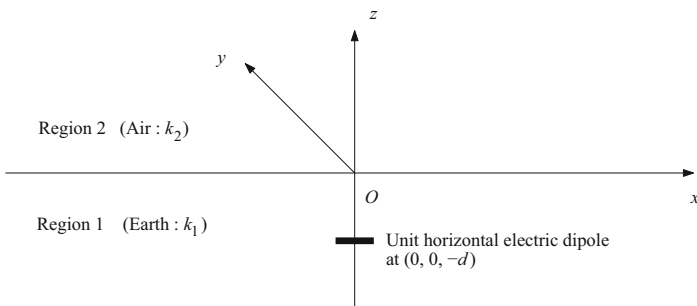


Fig. 8.1. Geometry of a \hat{x} -directed horizontal electric dipole on the boundary between two dielectrics like air and Earth

electric dipole in the \hat{x} direction is located at $(0, 0, -d)$. When the dipole and the observation point approach the boundary from below ($d \rightarrow 0^+$) and

from above ($z \rightarrow 0^+$), respectively, the frequency-domain formulas for the electromagnetic field in the cylindrical coordinates (ρ, ϕ, z) with $x = \rho \cos \phi$ and $y = \rho \sin \phi$ ($0 \leq \phi < 2\pi$) are readily derived (King, Owens, and Wu, 1992). They are

$$\begin{aligned}\tilde{E}_{2\rho}(\rho, \phi; \omega) &= \tilde{E}_{1\rho}(\rho, \phi; \omega) \\ &= -\frac{\omega\mu_0}{4\pi} \int_0^\infty \left\{ \frac{\sqrt{k_1^2 - \lambda^2} \sqrt{k_2^2 - \lambda^2}}{k_2^2 \sqrt{k_1^2 - \lambda^2} + k_1^2 \sqrt{k_2^2 - \lambda^2}} \right. \\ &\quad \times [J_0(\lambda\rho) - J_2(\lambda\rho)] + \frac{1}{\sqrt{k_2^2 - \lambda^2} + \sqrt{k_1^2 - \lambda^2}} \\ &\quad \left. \times [J_0(\lambda\rho) + J_2(\lambda\rho)] \right\} \cos \phi \lambda d\lambda, \quad (8.1)\end{aligned}$$

$$\begin{aligned}\tilde{E}_{2\phi}(\rho, \phi; \omega) &= \tilde{E}_{1\phi}(\rho, \phi; \omega) \\ &= \frac{\omega\mu_0}{4\pi} \int_0^\infty \left\{ \frac{\sqrt{k_1^2 - \lambda^2} \sqrt{k_2^2 - \lambda^2}}{k_2^2 \sqrt{k_1^2 - \lambda^2} + k_1^2 \sqrt{k_2^2 - \lambda^2}} \right. \\ &\quad \times [J_0(\lambda\rho) + J_2(\lambda\rho)] + \frac{1}{\sqrt{k_2^2 - \lambda^2} + \sqrt{k_1^2 - \lambda^2}} \\ &\quad \left. \times [J_0(\lambda\rho) - J_2(\lambda\rho)] \right\} \sin \phi \lambda d\lambda, \quad (8.2)\end{aligned}$$

$$\begin{aligned}\tilde{E}_{2z}(\rho, \phi; \omega) &= \frac{k_1^2}{k_2^2} \tilde{E}_{1z}(\rho, \phi; \omega) \\ &= \frac{i\omega\mu_0}{4\pi k_2^2} \int_0^\infty \frac{k_2^2 \sqrt{k_1^2 - \lambda^2} - k_1^2 \sqrt{k_2^2 - \lambda^2}}{k_2^2 \sqrt{k_1^2 - \lambda^2} + k_1^2 \sqrt{k_2^2 - \lambda^2}} J_1(\lambda\rho) \cos \phi \lambda^2 d\lambda; \quad (8.3)\end{aligned}$$

$$\begin{aligned}\tilde{B}_{2\rho}(\rho, \phi; \omega) &= \tilde{B}_{1\rho}(\rho, \phi; \omega) \\ &= -\frac{\mu_0}{8\pi} \int_0^\infty \left\{ \frac{k_2^2 \sqrt{k_1^2 - \lambda^2} - k_1^2 \sqrt{k_2^2 - \lambda^2}}{k_2^2 \sqrt{k_1^2 - \lambda^2} + k_1^2 \sqrt{k_2^2 - \lambda^2}} \right. \\ &\quad \times [J_0(\lambda\rho) + J_2(\lambda\rho)] + \frac{\sqrt{k_2^2 - \lambda^2} - \sqrt{k_1^2 - \lambda^2}}{\sqrt{k_2^2 - \lambda^2} + \sqrt{k_1^2 - \lambda^2}} \\ &\quad \left. \times [J_0(\lambda\rho) - J_2(\lambda\rho)] \right\} \sin \phi \lambda d\lambda, \quad (8.4)\end{aligned}$$

$$\begin{aligned}\tilde{B}_{2\phi}(\rho, \phi; \omega) &= \tilde{B}_{1\phi}(\rho, \phi; \omega) \\ &= -\frac{\mu_0}{8\pi} \int_0^\infty \left\{ \frac{k_2^2 \sqrt{k_1^2 - \lambda^2} - k_1^2 \sqrt{k_2^2 - \lambda^2}}{k_2^2 \sqrt{k_1^2 - \lambda^2} + k_1^2 \sqrt{k_2^2 - \lambda^2}} \right.\end{aligned}$$

$$\begin{aligned} & \times [J_0(\lambda\rho) - J_2(\lambda\rho)] + \frac{\sqrt{k_2^2 - \lambda^2} - \sqrt{k_1^2 - \lambda^2}}{\sqrt{k_2^2 - \lambda^2} + \sqrt{k_1^2 - \lambda^2}} \\ & \times [J_0(\lambda\rho) + J_2(\lambda\rho)] \Big\} \cos \phi \lambda d\lambda, \end{aligned} \quad (8.5)$$

$$\begin{aligned} \tilde{B}_{2z}(\rho, \phi; \omega) &= \tilde{B}_{1z}(\rho, \phi; \omega) \\ &= \frac{i\mu_0}{2\pi} \int_0^\infty \frac{1}{\sqrt{k_2^2 - \lambda^2} + \sqrt{k_1^2 - \lambda^2}} J_1(\lambda\rho) \sin \phi \lambda^2 d\lambda, \end{aligned} \quad (8.6)$$

where k_j ($j = 1, 2$) is the wave number in medium j , J_0 , J_1 , and J_2 are the Bessel functions of orders 0, 1, and 2, respectively.

For mathematical convenience, it is necessary to express the components in terms of ω instead of the wave number. With $\phi = 0$, $k_1 = \omega\varepsilon^{1/2}/c$, $k_2 = \omega/c$, $\lambda' = c\lambda$, and $\rho' = \rho/c$, where $c = (\mu_0\varepsilon_0)^{-1/2}$ is the velocity of light and $\varepsilon = \varepsilon_1/\varepsilon_0$ is the relative permittivity, and taking into account the following relations:

$$J_0(\lambda\rho) + J_2(\lambda\rho) = \frac{2}{\lambda\rho} J_1(\lambda\rho), \quad (8.7)$$

$$J_0(\lambda\rho) - J_2(\lambda\rho) = 2J_0(\lambda\rho) - \frac{2}{\lambda\rho} J_1(\lambda\rho), \quad (8.8)$$

the formulas for the six components can be expressed in the explicit forms.

$$\begin{aligned} \tilde{E}_{2\rho}(\rho', 0; \omega) &= \tilde{E}_{1\rho}(\rho', 0; \omega) \\ &= -\frac{\omega\mu_0}{2\pi c} \int_0^\infty \left\{ \frac{\sqrt{\omega^2\varepsilon - \lambda'^2} \sqrt{\omega^2 - \lambda'^2}}{\omega^2 \sqrt{\omega^2\varepsilon - \lambda'^2} + \omega^2\varepsilon \sqrt{\omega^2 - \lambda'^2}} \right. \\ &\quad \times \left[J_0(\lambda'\rho') - \frac{J_1(\lambda'\rho')}{\lambda'\rho'} \right] + \frac{J_1(\lambda'\rho')}{\lambda'\rho'} \\ &\quad \times \frac{1}{\sqrt{\omega^2 - \lambda'^2} + \sqrt{\omega^2\varepsilon - \lambda'^2}} \Big\} \lambda' d\lambda', \end{aligned} \quad (8.9)$$

$$\begin{aligned} \tilde{E}_{2\phi}(\rho', \pi/2; \omega) &= \tilde{E}_{1\phi}(\rho', \pi/2; \omega) \\ &= \frac{\omega\mu_0}{2\pi c} \int_0^\infty \left\{ \frac{\sqrt{\omega^2\varepsilon - \lambda'^2} \sqrt{\omega^2 - \lambda'^2}}{\omega^2 \sqrt{\omega^2\varepsilon - \lambda'^2} + \omega^2\varepsilon \sqrt{\omega^2 - \lambda'^2}} \frac{J_1(\lambda'\rho')}{\lambda'\rho'} \right. \\ &\quad + \left[J_0(\lambda'\rho') - \frac{J_1(\lambda'\rho')}{\lambda'\rho'} \right] \\ &\quad \times \frac{1}{\sqrt{\omega^2 - \lambda'^2} + \sqrt{\omega^2\varepsilon - \lambda'^2}} \Big\} \lambda' d\lambda', \end{aligned} \quad (8.10)$$

$$\tilde{E}_{2z}(\rho', 0; \omega) = \varepsilon \tilde{E}_{1z}(\rho', 0; \omega)$$

$$= \frac{i\mu_0}{4\pi\omega c} \int_0^\infty \frac{\omega^2 \sqrt{\omega^2 \varepsilon - \lambda'^2} - \omega^2 \varepsilon \sqrt{\omega^2 - \lambda'^2}}{\omega^2 \sqrt{\omega^2 \varepsilon - \lambda'^2} + \omega^2 \varepsilon \sqrt{\omega^2 - \lambda'^2}} J_1(\lambda' \rho') \lambda'^2 d\lambda', \quad (8.11)$$

$$\begin{aligned} \tilde{B}_{2\rho}(\rho', \pi/2; \omega) &= \tilde{B}_{1\rho}(\rho', \pi/2; \omega) \\ &= -\frac{\mu_0}{4\pi c^2} \int_0^\infty \left\{ \frac{\omega^2 \sqrt{\omega^2 \varepsilon - \lambda'^2} - \omega^2 \varepsilon \sqrt{\omega^2 - \lambda'^2}}{\omega^2 \sqrt{\omega^2 \varepsilon - \lambda'^2} + \omega^2 \varepsilon \sqrt{\omega^2 - \lambda'^2}} \frac{J_1(\lambda' \rho')}{\lambda' \rho'} \right. \\ &\quad \left. + \left[J_0(\lambda' \rho') - \frac{J_1(\lambda' \rho')}{\lambda' \rho'} \right] \right. \\ &\quad \left. \times \frac{\sqrt{\omega^2 - \lambda'^2} - \sqrt{\omega^2 \varepsilon - \lambda'^2}}{\sqrt{\omega^2 - \lambda'^2} + \sqrt{\omega^2 \varepsilon - \lambda'^2}} \right\} \lambda' d\lambda', \quad (8.12) \end{aligned}$$

$$\begin{aligned} \tilde{B}_{2\phi}(\rho', 0; \omega) &= \tilde{B}_{1\phi}(\rho', 0; \omega) \\ &= -\frac{\mu_0}{4\pi c^2} \int_0^\infty \left\{ \frac{\omega^2 \sqrt{\omega^2 \varepsilon - \lambda'^2} - \omega^2 \varepsilon \sqrt{\omega^2 - \lambda'^2}}{\omega^2 \sqrt{\omega^2 \varepsilon - \lambda'^2} + \omega^2 \varepsilon \sqrt{\omega^2 - \lambda'^2}} \right. \\ &\quad \times \left[J_0(\lambda' \rho') - \frac{1}{\lambda' \rho'} J_1(\lambda' \rho') \right] + \frac{J_1(\lambda' \rho')}{\lambda' \rho'} \\ &\quad \left. \times \frac{\sqrt{\omega^2 - \lambda'^2} - \sqrt{\omega^2 \varepsilon - \lambda'^2}}{\sqrt{\omega^2 - \lambda'^2} + \sqrt{\omega^2 \varepsilon - \lambda'^2}} \right\} \lambda' d\lambda', \quad (8.13) \end{aligned}$$

$$\begin{aligned} \tilde{B}_{2z}(\rho', \pi/2; \omega) &= \tilde{B}_{1z}(\rho', \pi/2; \omega) \\ &= \frac{i\mu_0}{2\pi c^2} \int_0^\infty \frac{1}{\sqrt{\omega^2 - \lambda'^2} + \sqrt{\omega^2 \varepsilon - \lambda'^2}} J_1(\lambda' \rho') \lambda'^2 d\lambda'. \quad (8.14) \end{aligned}$$

8.2.2 Time-Dependent Component $E_{2\rho}$

In this section, the time-dependent component $E_{2\rho}$ is evaluated analytically.

8.2.2.1 The Integrated Formula for Time-Dependent Component $E_{2\rho}$

If the exciting current in a horizontal dipole is a delta function current with a unit amplitude, the time-dependent component $E_{2\rho}$ is obtained by using a Fourier transform.

$$E_{2\rho}(\rho', 0; t) = \frac{1}{\pi} \text{Re} \int_0^\infty e^{-i\omega t} \tilde{E}_{2\rho}(\rho', 0; \omega) d\omega. \quad (8.15)$$

Substituting Eq. (8.9) into Eq. (8.15), it becomes

$$\begin{aligned}
E_{2\rho}(\rho', 0; t) = & -\frac{\mu_0}{2\pi^2 c} \int_0^\infty e^{-i\omega t} \omega d\omega \\
& \times \operatorname{Re} \int_0^\infty \left\{ \frac{\sqrt{\omega^2 \varepsilon - \lambda'^2} \sqrt{\omega^2 - \lambda'^2}}{\omega^2 \sqrt{\omega^2 \varepsilon - \lambda'^2} + \omega^2 \varepsilon \sqrt{\omega^2 - \lambda'^2}} \right. \\
& \times \left[J_0(\lambda' \rho') - \frac{1}{\lambda' \rho'} J_1(\lambda' \rho') \right] + \frac{J_1(\lambda' \rho')}{\lambda' \rho'} \\
& \left. \times \frac{1}{\sqrt{\omega^2 \varepsilon - \lambda'^2} + \sqrt{\omega^2 - \lambda'^2}} \right\} \lambda' d\lambda'. \quad (8.16)
\end{aligned}$$

The evaluation of the integral in Eq. (8.16) is a very difficult task. With the definition $\lambda' = \omega \xi$, $d\lambda' = \omega d\xi$, Eq. (8.16) reads as

$$\begin{aligned}
E_{2\rho}(\rho', 0; t) = & \frac{\mu_0}{2\pi^2 c} \operatorname{Re} \left\{ \int_0^\infty \frac{\sqrt{\varepsilon - \xi^2} \sqrt{1 - \xi^2}}{\sqrt{\varepsilon - \xi^2} + \varepsilon \sqrt{1 - \xi^2}} \xi d\xi \right. \\
& \times \left[\frac{\partial^2}{\partial t^2} \int_0^\infty e^{-i\omega t} J_0(\omega \xi \rho') d\omega + \frac{i}{\xi \rho'} \frac{\partial}{\partial t} \int_0^\infty e^{-i\omega t} J_1(\omega \xi \rho') d\omega \right] \\
& \left. - \frac{1}{\sqrt{\varepsilon - \xi^2} + \sqrt{1 - \xi^2}} \frac{i}{\xi \rho'} \frac{\partial}{\partial t} \int_0^\infty e^{-i\omega t} J_1(\omega \xi \rho') d\omega \right\}. \quad (8.17)
\end{aligned}$$

The integrals in Eq. (8.17) with respect to ω can be reduced readily by using the infinite integral in Eq. (6.611-1) of the handbook by Gradshteyn and Ryzhik (1980). When $t > \xi \rho'$,

$$\int_0^\infty e^{-i\omega t} J_0(\omega \xi \rho') d\omega = -\frac{i}{\sqrt{t^2 - \xi^2 \rho'^2}}, \quad (8.18)$$

$$\int_0^\infty e^{-i\omega t} J_1(\omega \xi \rho') d\omega = \frac{1}{\xi \rho'} \left(1 - \frac{t}{\sqrt{t^2 - \xi^2 \rho'^2}} \right). \quad (8.19)$$

Thus, we can write

$$E_{2\rho}(\rho', 0; t) = \frac{\mu_0}{2\pi^2 \rho' c} (I_1 + I_2 + I_3). \quad (8.20)$$

where

$$I_1 = \frac{\partial^2}{\partial t^2} \operatorname{Im} \int_0^\infty \frac{\sqrt{\varepsilon - \xi^2} \sqrt{1 - \xi^2}}{\sqrt{\varepsilon - \xi^2} + \varepsilon \sqrt{1 - \xi^2}} \frac{1}{\sqrt{t^2/\rho'^2 - \xi^2}} \xi d\xi, \quad (8.21)$$

$$I_2 = -\frac{\partial}{\partial t} \operatorname{Im} \int_0^\infty \frac{\sqrt{\varepsilon - \xi^2} \sqrt{1 - \xi^2}}{\sqrt{\varepsilon - \xi^2} + \varepsilon \sqrt{1 - \xi^2}} \frac{1}{\xi^2 \rho'} \left(1 - \frac{t}{\sqrt{t^2 - \xi^2 \rho'^2}} \right) \xi d\xi, \quad (8.22)$$

$$I_3 = \frac{\partial}{\partial t} \operatorname{Im} \int_0^\infty \frac{1}{\sqrt{\varepsilon - \xi^2} + \sqrt{1 - \xi^2}} \frac{1}{\xi^2 \rho'} \left(1 - \frac{t}{\sqrt{t^2 - \xi^2 \rho'^2}} \right) \xi d\xi. \quad (8.23)$$

Next, we should evaluate the above three integrals.

8.2.2.2 Evaluation of I_1

Following the similar manner used for the evaluation of $E_{2z}(\rho, t)$ due to the vertical dipole in the paper by Wu and King (1987), the evaluation of I_1 can be carried out readily. With the branch-cut structure in Fig. 8.2, it follows that

$$I_1 = 0; \quad t/\rho' < 1, \quad (8.24)$$

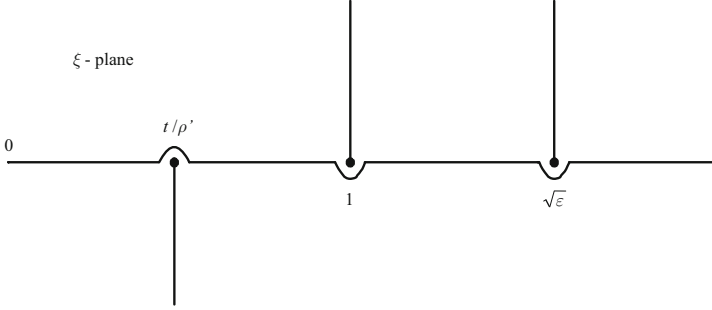


Fig. 8.2. Branch-cut structure for the integrals in Eqs. (8.21)~(8.23)

and

$$I_1 = \frac{\partial^2}{\partial t^2} \operatorname{Im} \left\{ \int_0^1 \left[\frac{\sqrt{\varepsilon - \xi^2} \sqrt{1 - \xi^2}}{(\sqrt{\varepsilon - \xi^2} + \varepsilon \sqrt{1 - \xi^2}) \sqrt{t^2/\rho'^2 - \xi^2}} - \frac{\sqrt{\varepsilon - \xi^2} \sqrt{1 - \xi^2}}{(\sqrt{\varepsilon - \xi^2} + \varepsilon \sqrt{1 - \xi^2})(-\sqrt{t^2/\rho'^2 - \xi^2})} \right] \xi d\xi \right. \\ \left. + \int_1^{t/\rho'} \left[\frac{i\sqrt{\varepsilon - \xi^2} \sqrt{\xi^2 - 1}}{(\sqrt{\varepsilon - \xi^2} + i\varepsilon \sqrt{\xi^2 - 1}) \sqrt{t^2/\rho'^2 - \xi^2}} - \frac{i\sqrt{\varepsilon - \xi^2} \sqrt{\xi^2 - 1}}{(\sqrt{\varepsilon - \xi^2} + i\varepsilon \sqrt{\xi^2 - 1})(-\sqrt{t^2/\rho'^2 - \xi^2})} \right] \xi d\xi \right\}; \quad (8.25)$$

$$1 < t/\rho' < \sqrt{\varepsilon}.$$

Because the integrand of the first integral is *real*, there is no contribution to the imaginary part.

$$I_1 = \frac{\partial^2}{\partial t^2} \operatorname{Im} \int_1^{t/\rho'} \frac{i2\sqrt{\varepsilon - \xi^2} \sqrt{\xi^2 - 1}}{(\sqrt{\varepsilon - \xi^2} + i\varepsilon \sqrt{\xi^2 - 1}) \sqrt{t^2/\rho'^2 - \xi^2}} \xi d\xi. \quad (8.26)$$

The real and imaginary parts can be separated readily and there is no contribution to the integral for the real part. Then, the integral is simplified as

$$\begin{aligned}
I_1 &= \frac{\partial^2}{\partial t^2} \int_1^{t/\rho'} \frac{2(\varepsilon - \xi^2)\sqrt{\xi^2 - 1}}{(\varepsilon - 1)[(\varepsilon + 1)\xi^2 - \varepsilon]\sqrt{t^2/\rho'^2 - \xi^2}} \xi d\xi \\
&= \frac{2}{\varepsilon - 1} \frac{\partial^2}{\partial t^2} \int_1^{t/\rho'} \frac{-\sqrt{\xi^2 - 1}}{[(\varepsilon + 1)\xi^2 - \varepsilon]\sqrt{t^2/\rho'^2 - \xi^2}} \xi^3 d\xi \\
&\quad + \frac{2\varepsilon}{\varepsilon - 1} \frac{\partial^2}{\partial t^2} \int_1^{t/\rho'} \frac{\sqrt{\xi^2 - 1}}{[(\varepsilon + 1)\xi^2 - \varepsilon]\sqrt{t^2/\rho'^2 - \xi^2}} \xi d\xi. \tag{8.27}
\end{aligned}$$

With the change of the variable $\zeta = \xi^2$, $d\zeta = 2\xi d\xi$, it follows that

$$\begin{aligned}
I_1 &= \frac{1}{\varepsilon - 1} \frac{\partial^2}{\partial t^2} \int_1^{t^2/\rho'^2} \frac{-\sqrt{\zeta - 1}}{[(\varepsilon + 1)\zeta - \varepsilon]\sqrt{t^2/\rho'^2 - \zeta}} \zeta d\zeta \\
&\quad + \frac{\varepsilon}{\varepsilon - 1} \frac{\partial^2}{\partial t^2} \int_1^{t^2/\rho'^2} \frac{\sqrt{\zeta - 1}}{[(\varepsilon + 1)\zeta - \varepsilon]\sqrt{t^2/\rho'^2 - \zeta}} d\zeta. \tag{8.28}
\end{aligned}$$

The following two integrals need to be treated.

$$\vartheta_0^{(1)} = \int_1^{t^2/\rho'^2} \frac{-\sqrt{\zeta - 1}}{[(\varepsilon + 1)\zeta - \varepsilon]\sqrt{t^2/\rho'^2 - \zeta}} \zeta d\zeta, \tag{8.29}$$

$$\vartheta_0^{(2)} = \int_1^{t^2/\rho'^2} \frac{\sqrt{\zeta - 1}}{[(\varepsilon + 1)\zeta - \varepsilon]\sqrt{t^2/\rho'^2 - \zeta}} d\zeta. \tag{8.30}$$

The above two integrals had been solved by Wu and King (1987). The results are

$$\vartheta_0^{(1)} = -\frac{\pi}{2(\varepsilon + 1)} \left[\frac{t^2}{\rho'^2} - 1 + \frac{2\varepsilon}{\varepsilon + 1} - \frac{2\varepsilon}{\varepsilon + 1} \left((\varepsilon + 1) \frac{t^2}{\rho'^2} - \varepsilon \right)^{-1/2} \right], \tag{8.31}$$

$$\vartheta_0^{(2)} = \frac{\pi}{\varepsilon + 1} \left[1 - \left((\varepsilon + 1) \frac{t^2}{\rho'^2} - \varepsilon \right)^{-1/2} \right]. \tag{8.32}$$

Thus,

$$\begin{aligned}
I_1 &= -\frac{\pi}{2(\varepsilon^2 - 1)} \frac{\partial^2}{\partial t^2} \left[\frac{t^2}{\rho'^2} - 1 - \frac{2\varepsilon^2}{\varepsilon + 1} + \frac{2\varepsilon^2}{\varepsilon + 1} \left((\varepsilon + 1) \frac{t^2}{\rho'^2} - \varepsilon \right)^{-1/2} \right]; \\
&\quad 1 < \frac{t}{\rho'} < \sqrt{\varepsilon}. \tag{8.33}
\end{aligned}$$

When $t/\rho' > \sqrt{\varepsilon}$,

$$I_1 = \frac{\partial^2}{\partial t^2} \operatorname{Im} \left\{ \int_1^{\sqrt{\varepsilon}} \frac{2\sqrt{\varepsilon - \xi^2} i \sqrt{\xi^2 - 1}}{(\sqrt{\varepsilon - \xi^2} + i\varepsilon \sqrt{\xi^2 - 1}) \sqrt{t^2/\rho'^2 - \xi^2}} \xi d\xi \right\}$$

$$+ \int_{\sqrt{\varepsilon}}^{t/\rho'} \frac{i2\sqrt{\xi^2 - \varepsilon}\sqrt{\xi^2 - 1}}{(\sqrt{\xi^2 - \varepsilon} + \varepsilon\sqrt{\xi^2 - 1})\sqrt{t^2/\rho'^2 - \xi^2}} \xi d\xi. \quad (8.34)$$

The imaginary part is as follows:

$$\begin{aligned} I_1 &= \frac{2}{\varepsilon - 1} \frac{\partial^2}{\partial t^2} \left\{ \int_1^{\sqrt{\varepsilon}} \frac{(\varepsilon - \xi^2)\sqrt{\xi^2 - 1}}{[(\varepsilon + 1)\xi^2 - \varepsilon]\sqrt{t^2/\rho'^2 - \xi^2}} \xi d\xi \right. \\ &\quad \left. + \int_{\sqrt{\varepsilon}}^{t/\rho'} \frac{\varepsilon(\xi^2 - 1)\sqrt{\xi^2 - \varepsilon} - (\xi^2 - \varepsilon)\sqrt{\xi^2 - 1}}{[(\varepsilon + 1)\xi^2 - \varepsilon]\sqrt{t^2/\rho'^2 - \xi^2}} \xi d\xi \right\} \\ &= \frac{2}{\varepsilon - 1} \frac{\partial^2}{\partial t^2} \left\{ \int_1^{t/\rho'} \frac{(\varepsilon - \xi^2)\sqrt{\xi^2 - 1}}{[(\varepsilon + 1)\xi^2 - \varepsilon]\sqrt{t^2/\rho'^2 - \xi^2}} \xi d\xi \right. \\ &\quad \left. + \int_{\sqrt{\varepsilon}}^{t/\rho'} \frac{\varepsilon(\xi^2 - 1)\sqrt{\xi^2 - \varepsilon}}{[(\varepsilon + 1)\xi^2 - \varepsilon]\sqrt{t^2/\rho'^2 - \xi^2}} \xi d\xi \right\}. \quad (8.35) \end{aligned}$$

With the change in variable $\zeta = \xi^2$, it becomes

$$\begin{aligned} I_1 &= \frac{1}{\varepsilon - 1} \frac{\partial^2}{\partial t^2} \left\{ \int_1^{t^2/\rho'^2} \frac{(\varepsilon - \zeta)\sqrt{\zeta - 1}}{[(\varepsilon + 1)\zeta - \varepsilon]\sqrt{t^2/\rho'^2 - \zeta}} d\zeta \right. \\ &\quad \left. + \int_{\varepsilon}^{t^2/\rho'^2} \frac{\varepsilon(\zeta - 1)\sqrt{\zeta - \varepsilon}}{[(\varepsilon + 1)\zeta - \varepsilon]\sqrt{t^2/\rho'^2 - \zeta}} d\zeta \right\} \\ &= \frac{1}{\varepsilon - 1} \frac{\partial^2}{\partial t^2} \int_1^{t^2/\rho'^2} \frac{-\sqrt{\zeta - 1}}{[(\varepsilon + 1)\zeta - \varepsilon]\sqrt{t^2/\rho'^2 - \zeta}} \zeta d\zeta \\ &\quad + \frac{\varepsilon}{\varepsilon - 1} \frac{\partial^2}{\partial t^2} \int_1^{t^2/\rho'^2} \frac{\sqrt{\zeta - 1}}{[(\varepsilon + 1)\zeta - \varepsilon]\sqrt{t^2/\rho'^2 - \zeta}} d\zeta \\ &\quad + \frac{\varepsilon}{\varepsilon - 1} \frac{\partial^2}{\partial t^2} \int_{\varepsilon}^{t^2/\rho'^2} \frac{\sqrt{\zeta - \varepsilon}}{[(\varepsilon + 1)\zeta - \varepsilon]\sqrt{t^2/\rho'^2 - \zeta}} \zeta d\zeta \\ &\quad + \frac{\varepsilon}{\varepsilon - 1} \frac{\partial^2}{\partial t^2} \int_{\varepsilon}^{t^2/\rho'^2} \frac{-\sqrt{\zeta - \varepsilon}}{[(\varepsilon + 1)\zeta - \varepsilon]\sqrt{t^2/\rho'^2 - \zeta}} d\zeta. \quad (8.36) \end{aligned}$$

The first and second integrals in Eq. (8.36) are shown in Eqs. (8.31) and (8.32). Next, the third and fourth integrals need to be evaluated. They are

$$\vartheta_{\varepsilon}^{(1)} = \int_{\varepsilon}^{t^2/\rho'^2} \frac{\sqrt{\zeta - \varepsilon}}{[(\varepsilon + 1)\zeta - \varepsilon]\sqrt{t^2/\rho'^2 - \zeta}} \zeta d\zeta, \quad (8.37)$$

$$\vartheta_{\varepsilon}^{(2)} = \int_{\varepsilon}^{t^2/\rho'^2} \frac{-\sqrt{\zeta - \varepsilon}}{[(\varepsilon + 1)\zeta - \varepsilon]\sqrt{t^2/\rho'^2 - \zeta}} d\zeta. \quad (8.38)$$

Also the above two integrals were solved by Wu and King (1987). We write

$$v_{\varepsilon}^{(1)} = \frac{\pi}{2(\varepsilon+1)} \left[\frac{t^2}{\rho'^2} - \varepsilon + \frac{2\varepsilon}{\varepsilon+1} - \frac{2\varepsilon^2}{\varepsilon+1} \left((\varepsilon+1) \frac{t^2}{\rho'^2} - \varepsilon \right)^{-1/2} \right], \quad (8.39)$$

$$v_{\varepsilon}^{(2)} = -\frac{\pi}{\varepsilon+1} \left[1 - \varepsilon \left((\varepsilon+1) \frac{t^2}{\rho'^2} - \varepsilon \right)^{-1/2} \right]. \quad (8.40)$$

With substitutions Eqs. (8.31), (8.32), (8.39), and (8.40) into Eq. (8.36), we have

$$I_1 = \frac{\pi}{2(\varepsilon+1)} \frac{\partial^2}{\partial t^2} \left(\frac{t^2}{\rho'^2} - \frac{\varepsilon^2+1}{\varepsilon+1} \right); \quad \frac{t}{\rho'} > \sqrt{\varepsilon}. \quad (8.41)$$

Then, I_1 can be rewritten as follows:

$$I_1 = \frac{\pi}{2} \frac{\partial^2}{\partial t^2} f_1 \left(\frac{t}{\rho'} \right). \quad (8.42)$$

where

$$f_1 \left(\frac{t}{\rho'} \right) = \begin{cases} 0 \\ -\frac{1}{\varepsilon^2-1} \left[\frac{t^2}{\rho'^2} - 1 - \frac{2\varepsilon^2}{\varepsilon+1} + \frac{2\varepsilon^2}{\varepsilon+1} \left((\varepsilon+1) \frac{t^2}{\rho'^2} - \varepsilon \right)^{-1/2} \right] \\ \frac{1}{\varepsilon+1} \left(\frac{t^2}{\rho'^2} - \frac{\varepsilon^2+1}{\varepsilon+1} \right) \end{cases}; \quad \begin{aligned} & \frac{t}{\rho'} < 1 \\ & 1 < \frac{t}{\rho'} < \sqrt{\varepsilon}. \\ & \frac{t}{\rho'} > \sqrt{\varepsilon} \end{aligned} \quad (8.43)$$

It follows that $f_1(1-) = f_1(1+) = 0$ and $f_1(\sqrt{\varepsilon}-) = f_1(\sqrt{\varepsilon}+) = \frac{\varepsilon-1}{(\varepsilon+1)^2}$. Thus, $f_1(t/\rho')$ is everywhere continuous.

$$f_1' \left(\frac{t}{\rho'} \right) = \begin{cases} 0 \\ -\frac{1}{\varepsilon^2-1} \frac{2t}{\rho'^2} \left[1 - \varepsilon^2 \left((\varepsilon+1) \frac{t^2}{\rho'^2} - \varepsilon \right)^{-3/2} \right] \\ \frac{1}{\varepsilon+1} \frac{2t}{\rho'^2} \end{cases}; \quad \begin{aligned} & \frac{t}{\rho'} < 1 \\ & 1 < \frac{t}{\rho'} < \sqrt{\varepsilon}. \\ & \frac{t}{\rho'} > \sqrt{\varepsilon} \end{aligned} \quad (8.44)$$

Since $f_1'(1-) = 0$, $f_1'(1+) = 2/\rho'$, there is a step discontinuity of $2/\rho'$ in $f_1'(t/\rho')$ at $t/\rho' = 1$. Similarly, $f_1'(\sqrt{\varepsilon}-) = -2/[\sqrt{\varepsilon}(\varepsilon+1)\rho']$, $f_1'(\sqrt{\varepsilon}+) = 2\sqrt{\varepsilon}/[(\varepsilon+1)\rho']$, $f_1'(t/\rho')$ has a step discontinuity of $2/(\sqrt{\varepsilon}\rho')$ at $t/\rho' = \sqrt{\varepsilon}$. Thus,

$$f_1'' \left(\frac{t}{\rho'} \right) = \begin{cases} 0 \\ -\left[1 + \frac{\varepsilon^2}{(\varepsilon+1)^{3/2}} \left(\frac{2c^2 t^2}{\rho^2} + \frac{\varepsilon}{\varepsilon+1} \right) \left(\frac{c^2 t^2}{\rho^2} - \frac{\varepsilon}{\varepsilon+1} \right)^{-5/2} \right] \\ \varepsilon - 1 \end{cases};$$

$$1 < \frac{t}{\rho'} < \sqrt{\varepsilon}. \quad (8.45)$$

Finally, the exact formula for I_1 is obtained readily.

$$I_1 = \frac{c\pi}{\rho} \left[\delta\left(t - \frac{\rho}{c}\right) + \frac{1}{\sqrt{\varepsilon}} \delta\left(t - \frac{\sqrt{\varepsilon}\rho}{c}\right) \right] + \frac{c^2\pi}{(\varepsilon^2 - 1)\rho^2} \left\{ - \left[1 + \frac{\varepsilon^2}{(\varepsilon+1)^{3/2}} \left(\frac{2c^2t^2}{\rho^2} + \frac{\varepsilon}{\varepsilon+1} \right) \left(\frac{c^2t^2}{\rho^2} - \frac{\varepsilon}{\varepsilon+1} \right)^{-5/2} \right] \right\};$$

$$1 < \frac{t}{\rho'} < \sqrt{\varepsilon}. \quad (8.46)$$

8.2.2.3 Evaluation of I_2

Following the similar manner used for the evaluation of $B_{2\phi}(\rho, t)$ due the vertical dipole with delta function excitation (Wu and King, 1987), the evaluation of I_2 can be also carried out readily.

$$I_2 = 0; \quad t/\rho' < 1. \quad (8.47)$$

When $1 < t/\rho' < \sqrt{\varepsilon}$,

$$I_2 = -\frac{\partial}{\partial t} \operatorname{Im} \left\{ \int_0^\infty \frac{1}{\xi^2 \rho'} \left[\frac{i\sqrt{\varepsilon - \xi^2} \sqrt{\xi^2 - 1}}{\sqrt{\varepsilon - \xi^2} + i\varepsilon \sqrt{\xi^2 - 1}} - \frac{t}{\rho'} \frac{i\sqrt{\varepsilon - \xi^2} \sqrt{\xi^2 - 1}}{(\sqrt{\varepsilon - \xi^2} + i\varepsilon \sqrt{\xi^2 - 1})(\sqrt{t^2/\rho'^2 - \xi^2})} \right] \xi d\xi \right\}. \quad (8.48)$$

The real and imaginary parts are separated readily and there is no contribution to the integral for the real part. The result reduces to

$$I_2 = -\frac{1}{(\varepsilon - 1)\rho'} \frac{\partial}{\partial t} \left\{ \int_0^\infty \frac{1}{\xi^2} \frac{(\varepsilon - \xi^2)\sqrt{\xi^2 - 1}}{(\varepsilon + 1)\xi^2 - \varepsilon} \xi d\xi - \frac{t}{\rho'} \frac{\partial}{\partial t} \int_0^\infty \frac{1}{\xi^2} \frac{(\varepsilon - \xi^2)\sqrt{\xi^2 - 1}}{[(\varepsilon + 1)\xi^2 - \varepsilon]\sqrt{t^2/\rho'^2 - \xi^2}} \xi d\xi \right\}. \quad (8.49)$$

With the contour in Fig. 8.3, this becomes

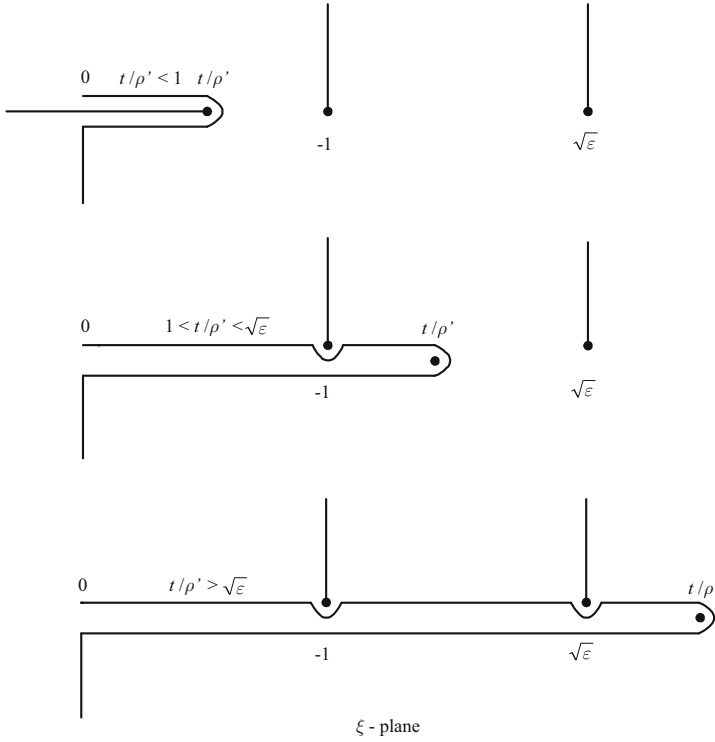


Fig. 8.3. Contours of integration for the integrals in Eqs. (8.21)~(8.23)

$$\begin{aligned}
 I_2 = & -\frac{1}{(\varepsilon-1)\rho'} \frac{\partial}{\partial t} \left\{ \int_1^{t/\rho'} \frac{1}{\xi^2} \frac{(\varepsilon-\xi^2)\sqrt{\xi^2-1}}{(\varepsilon+1)\xi^2-\varepsilon} \xi d\xi \right. \\
 & - \frac{t}{\rho'} \int_1^{t/\rho'} \frac{1}{\xi^2} \frac{(\varepsilon-\xi^2)\sqrt{\xi^2-1}}{[(\varepsilon+1)\xi^2-\varepsilon]\sqrt{t^2/\rho'^2-\xi^2}} \xi d\xi \\
 & - \int_1^{t/\rho'} \frac{1}{\xi^2} \frac{(\varepsilon-\xi^2)\sqrt{\xi^2-1}}{(\varepsilon+1)\xi^2-\varepsilon} \xi d\xi \\
 & \left. + \frac{t}{\rho'} \int_1^{t/\rho'} \frac{1}{\xi^2} \frac{(\varepsilon-\xi^2)\sqrt{\xi^2-1}}{[(\varepsilon+1)\xi^2-\varepsilon](\sqrt{t^2/\rho'^2-\xi^2})} \xi d\xi \right\} \\
 = & \frac{2}{(\varepsilon-1)\rho'} \frac{\partial}{\partial t} \left\{ \frac{t}{\rho'} \int_1^{t/\rho'} \frac{1}{\xi^2} \frac{(\varepsilon-\xi^2)\sqrt{\xi^2-1}}{[(\varepsilon+1)\xi^2-\varepsilon]\sqrt{t^2/\rho'^2-\xi^2}} \xi d\xi \right\}. \quad (8.50)
 \end{aligned}$$

With $\zeta = \xi^2$,

$$I_2 = \frac{1}{(\varepsilon-1)\rho'} \frac{\partial}{\partial t} \left\{ \frac{t}{\rho'} \int_1^{t^2/\rho'^2} \frac{1}{\zeta} \frac{(\varepsilon-\zeta)\sqrt{\zeta-1}}{[(\varepsilon+1)\zeta-\varepsilon]\sqrt{t^2/\rho'^2-\zeta}} d\zeta \right\}$$

$$\begin{aligned}
&= \frac{\varepsilon}{(\varepsilon - 1)\rho'} \frac{\partial}{\partial t} \left\{ \frac{t}{\rho'} \int_1^{t^2/\rho'^2} \frac{1}{\zeta} \frac{\sqrt{\zeta - 1}}{[(\varepsilon + 1)\zeta - \varepsilon]\sqrt{t^2/\rho'^2 - \zeta}} d\zeta \right\} \\
&+ \frac{1}{(\varepsilon - 1)\rho'} \frac{\partial}{\partial t} \left\{ \frac{t}{\rho'} \int_1^{t^2/\rho'^2} \frac{-\sqrt{\zeta - 1}}{[(\varepsilon + 1)\zeta - \varepsilon]\sqrt{t^2/\rho'^2 - \zeta}} d\zeta \right\}. \quad (8.51)
\end{aligned}$$

Then, we write

$$\vartheta_0^{(3)} = \int_1^{t^2/\rho'^2} \frac{1}{\zeta} \frac{\sqrt{\zeta - 1}}{[(\varepsilon + 1)\zeta - \varepsilon]\sqrt{t^2/\rho'^2 - \zeta}} d\zeta, \quad (8.52)$$

$$\vartheta_0^{(4)} = -\vartheta_0^{(2)} = \int_1^{t^2/\rho'^2} \frac{-\sqrt{\zeta - 1}}{[(\varepsilon + 1)\zeta - \varepsilon]\sqrt{t^2/\rho'^2 - \zeta}} d\zeta. \quad (8.53)$$

The first integral needs to be solved and the second one has been solved in Eq. (8.32). Let $x' = \zeta - 1$, $T_0 = t^2/\rho'^2 - 1$, and $E_0 = 1/(\varepsilon + 1)$, then,

$$\begin{aligned}
\vartheta_0^{(3)} &= \int_0^{T_0} \frac{x' dx'}{(x' + 1)[(\varepsilon + 1)x' + 1]\sqrt{(T_0 - x')x'}} \\
&= \frac{1}{\varepsilon + 1} \int_0^{T_0} \frac{x' dx'}{(x' + 1)(x' + E_0)\sqrt{(T_0 - x')x'}} \\
&= \frac{1}{\varepsilon + 1} \frac{1}{1 - E_0} \int_0^{T_0} \left(\frac{1}{x' + E_0} - \frac{1}{x' + 1} \right) \frac{x' dx'}{\sqrt{(T_0 - x')x'}} \\
&= \frac{1}{\varepsilon} \left\{ \int_0^{T_0} \frac{x' dx'}{(x' + E_0)\sqrt{(T_0 - x')x'}} - \int_0^{T_0} \frac{x' dx'}{(x' + 1)\sqrt{(T_0 - x')x'}} \right\}. \quad (8.54)
\end{aligned}$$

Let $x = x' + E_0$ and $X_1 = (T_0 + E_0 - x)(x - E_0)$, then we have

$$\begin{aligned}
\int_0^{T_0} \frac{x' dx'}{(x' + E_0)\sqrt{(T_0 - x')x'}} &= \int_{E_0}^{T_0 + E_0} \frac{(x - E_0) dx}{x \sqrt{(T_0 + E_0 - x)(x - E_0)}} \\
&= \int_{E_0}^{T_0 + E_0} \frac{dx}{X_1^{1/2}} - E_0 \int_{E_0}^{T_0 + E_0} \frac{dx}{x X_1^{1/2}} \\
&= \pi \left[1 - \left((\varepsilon + 1) \frac{t^2}{\rho'^2} - \varepsilon \right)^{-1/2} \right]. \quad (8.55)
\end{aligned}$$

Similarly, let $x = x' + 1$ and $X_2 = (T_0 + 1 - x)(x - 1)$, then we have

$$\begin{aligned}
\int_0^{T_0} \frac{x' dx'}{(x' + 1)\sqrt{(T_0 - x')x'}} &= \int_1^{T_0 + 1} \frac{(x - 1) dx}{x \sqrt{(T_0 + 1 - x)(x - 1)}} \\
&= \int_1^{T_0 + 1} \frac{dx}{X_2^{1/2}} - \int_1^{T_0 + 1} \frac{dx}{x X_2^{1/2}}
\end{aligned}$$

$$= \pi \left[1 - \left(\frac{t^2}{\rho'^2} \right)^{-1/2} \right]. \quad (8.56)$$

With substitutions Eqs. (8.55) and (8.56) into Eq. (8.54), we obtain

$$\vartheta_0^{(3)} = \frac{\pi}{\varepsilon} \left[\left(\frac{t^2}{\rho'^2} \right)^{-1/2} - \left((\varepsilon + 1) \frac{t^2}{\rho'^2} - \varepsilon \right)^{-1/2} \right]. \quad (8.57)$$

Thus,

$$I_2 = \frac{\pi}{(\varepsilon - 1)\rho'} \frac{\partial}{\partial t} \left\{ \frac{t}{\rho'} \left[-\frac{1}{\varepsilon + 1} + \left(\frac{t^2}{\rho'^2} \right)^{-1/2} - \frac{\varepsilon}{\varepsilon + 1} \left((\varepsilon + 1) \frac{t^2}{\rho'^2} - \varepsilon \right)^{-1/2} \right] \right\}; \quad 1 < \frac{t}{\rho'} < \sqrt{\varepsilon}. \quad (8.58)$$

When $t/\rho' > \sqrt{\varepsilon}$,

$$I_2 = -\frac{\partial}{\partial t} \operatorname{Im} \left\{ \int_0^{\sqrt{\varepsilon}} \frac{1}{\xi^2 \rho'} \frac{i\sqrt{\varepsilon - \xi^2} \sqrt{\xi^2 - 1}}{\sqrt{\varepsilon - \xi^2} + i\varepsilon \sqrt{\xi^2 - 1}} \xi d\xi \right. \\ - \frac{t}{\rho'} \int_0^{\sqrt{\varepsilon}} \frac{1}{\xi^2 \rho'} \frac{i\sqrt{\varepsilon - \xi^2} \sqrt{\xi^2 - 1}}{(\sqrt{\varepsilon - \xi^2} + i\varepsilon \sqrt{\xi^2 - 1}) \sqrt{t^2/\rho'^2 - \xi^2}} \xi d\xi \\ + \int_{\sqrt{\varepsilon}}^{\infty} \frac{1}{\xi^2 \rho'} \frac{i\sqrt{\xi^2 - \varepsilon} \sqrt{\xi^2 - 1}}{\sqrt{\xi^2 - \varepsilon} + \varepsilon \sqrt{\xi^2 - 1}} \xi d\xi \\ \left. - \frac{t}{\rho'} \int_{\sqrt{\varepsilon}}^{\infty} \frac{1}{\xi^2 \rho'} \frac{i\sqrt{\xi^2 - \varepsilon} \sqrt{\xi^2 - 1}}{(\sqrt{\xi^2 - \varepsilon} + \varepsilon \sqrt{\xi^2 - 1}) \sqrt{t^2/\rho'^2 - \xi^2}} \xi d\xi \right\}. \quad (8.59)$$

The imaginary part is expressed in the form

$$I_2 = -\frac{1}{(\varepsilon - 1)\rho'} \frac{\partial}{\partial t} \left\{ \int_0^{\sqrt{\varepsilon}} \frac{1}{\xi^2} \frac{(\varepsilon - \xi^2) \sqrt{\xi^2 - 1}}{(\varepsilon + 1)\xi^2 - \varepsilon} \xi d\xi \right. \\ - \frac{t}{\rho'} \int_0^{\sqrt{\varepsilon}} \frac{1}{\xi^2} \frac{(\varepsilon - \xi^2) \sqrt{\xi^2 - 1}}{[(\varepsilon + 1)\xi^2 - \varepsilon] \sqrt{t^2/\rho'^2 - \xi^2}} \xi d\xi \\ + \int_{\sqrt{\varepsilon}}^{\infty} \frac{1}{\xi^2} \frac{\varepsilon(\xi^2 - 1) \sqrt{\xi^2 - \varepsilon} - (\xi^2 - \varepsilon) \sqrt{\xi^2 - 1}}{(\varepsilon + 1)\xi^2 - \varepsilon} \xi d\xi \\ \left. - \frac{t}{\rho'} \int_{\sqrt{\varepsilon}}^{\infty} \frac{1}{\xi^2} \frac{\varepsilon(\xi^2 - 1) \sqrt{\xi^2 - \varepsilon} - (\xi^2 - \varepsilon) \sqrt{\xi^2 - 1}}{[(\varepsilon + 1)\xi^2 - \varepsilon] \sqrt{t^2/\rho'^2 - \xi^2}} \xi d\xi \right\} \\ = -\frac{1}{(\varepsilon - 1)\rho'} \frac{\partial}{\partial t} \left\{ \int_0^{\infty} \frac{1}{\xi^2} \frac{(\varepsilon - \xi^2) \sqrt{\xi^2 - 1}}{(\varepsilon + 1)\xi^2 - \varepsilon} \xi d\xi \right\}$$

$$\begin{aligned}
& -\frac{t}{\rho'} \int_0^\infty \frac{1}{\xi^2} \frac{(\varepsilon - \xi^2)\sqrt{\xi^2 - 1}}{[(\varepsilon + 1)\xi^2 - \varepsilon]\sqrt{t^2/\rho'^2 - \xi^2}} \xi d\xi \\
& + \int_{\sqrt{\varepsilon}}^\infty \frac{1}{\xi^2} \frac{\varepsilon(\xi^2 - 1)\sqrt{\xi^2 - \varepsilon}}{(\varepsilon + 1)\xi^2 - \varepsilon} \xi d\xi \\
& - \frac{t}{\rho'} \int_{\sqrt{\varepsilon}}^\infty \frac{1}{\xi^2} \frac{\varepsilon(\xi^2 - 1)\sqrt{\xi^2 - \varepsilon}}{[(\varepsilon + 1)\xi^2 - \varepsilon]\sqrt{t^2/\rho'^2 - \xi^2}} \xi d\xi \Big\}. \quad (8.60)
\end{aligned}$$

In terms of the variable $\zeta = \xi^2$, $d\zeta = 2\xi d\xi$, this becomes

$$\begin{aligned}
I_2 = & \frac{\varepsilon}{(\varepsilon - 1)\rho'} \frac{\partial}{\partial t} \left\{ \frac{t}{\rho'} \int_1^{t^2/\rho'^2} \frac{1}{\zeta} \frac{\sqrt{\zeta - 1}}{[(\varepsilon + 1)\zeta - \varepsilon]\sqrt{t^2/\rho'^2 - \zeta}} d\zeta \right\} \\
& + \frac{1}{(\varepsilon - 1)\rho'} \frac{\partial}{\partial t} \left\{ \frac{t}{\rho'} \int_1^{t^2/\rho'^2} \frac{-\sqrt{\zeta - 1}}{[(\varepsilon + 1)\zeta - \varepsilon]\sqrt{t^2/\rho'^2 - \zeta}} d\zeta \right\} \\
& + \frac{\varepsilon}{(\varepsilon - 1)\rho'} \frac{\partial}{\partial t} \left\{ \frac{t}{\rho'} \int_\varepsilon^{t^2/\rho'^2} \frac{1}{\zeta} \frac{-\sqrt{\zeta - \varepsilon}}{[(\varepsilon + 1)\zeta - \varepsilon]\sqrt{t^2/\rho'^2 - \zeta}} d\zeta \right\} \\
& + \frac{\varepsilon}{(\varepsilon - 1)\rho'} \frac{\partial}{\partial t} \left\{ \frac{t}{\rho'} \int_\varepsilon^{t^2/\rho'^2} \frac{\sqrt{\zeta - \varepsilon}}{[(\varepsilon + 1)\zeta - \varepsilon]\sqrt{t^2/\rho'^2 - \zeta}} d\zeta \right\}. \quad (8.61)
\end{aligned}$$

The first and second integrals in Eq. (8.61) have been evaluated in Eqs. (8.57) and (8.53). Next, the third and fourth integrals need to be evaluated. They are

$$\vartheta_\varepsilon^{(3)} = \int_\varepsilon^{t^2/\rho'^2} \frac{1}{\zeta} \frac{-\sqrt{\zeta - \varepsilon}}{[(\varepsilon + 1)\zeta - \varepsilon]\sqrt{t^2/\rho'^2 - \zeta}} d\zeta, \quad (8.62)$$

$$\vartheta_\varepsilon^{(4)} = -\vartheta_\varepsilon^{(2)}. \quad (8.63)$$

Let $x' = \zeta - \varepsilon$, $T_\varepsilon = t^2/\rho'^2 - \varepsilon$, $E_\varepsilon = \varepsilon^2/(\varepsilon + 1)$, then, we write

$$\begin{aligned}
\vartheta_\varepsilon^{(3)} = & - \int_0^{T_\varepsilon} \frac{x' dx'}{(x' + \varepsilon)[(\varepsilon + 1)x' + \varepsilon^2]\sqrt{(T_\varepsilon - x')x'}} \\
= & - \frac{1}{\varepsilon + 1} \int_0^{T_\varepsilon} \frac{x' dx'}{(x' + \varepsilon)(x' + E_\varepsilon)\sqrt{(T_\varepsilon - x')x'}} \\
= & - \frac{1}{\varepsilon + 1} \frac{1}{\varepsilon - E_\varepsilon} \int_0^{T_\varepsilon} \left(\frac{1}{x' + E_\varepsilon} - \frac{1}{x' + \varepsilon} \right) \frac{x' dx'}{\sqrt{(T_\varepsilon - x')x'}} \\
= & - \frac{1}{\varepsilon} \left\{ \int_0^{T_\varepsilon} \frac{x' dx'}{(x' + E_\varepsilon)\sqrt{(T_\varepsilon - x')x'}} - \int_0^{T_\varepsilon} \frac{x' dx'}{(x' + \varepsilon)\sqrt{(T_\varepsilon - x')x'}} \right\}. \quad (8.64)
\end{aligned}$$

Let $x = x' + E_\varepsilon$ and $Y_1 = (T_\varepsilon + E_\varepsilon - x)(x - E_\varepsilon)$, we have

$$\begin{aligned}
\int_0^{T_\varepsilon} \frac{x' dx'}{(x' + E_\varepsilon) \sqrt{(T_\varepsilon - x')x'}} &= \int_{E_\varepsilon}^{T_\varepsilon + E_\varepsilon} \frac{(x - E_\varepsilon) dx}{x \sqrt{(T_\varepsilon + E_\varepsilon - x)(x - E_\varepsilon)}} \\
&= \int_{E_\varepsilon}^{T_\varepsilon + E_\varepsilon} \frac{dx}{Y_1^{1/2}} - E_\varepsilon \int_{E_\varepsilon}^{T_\varepsilon + E_\varepsilon} \frac{dx}{x Y_1^{1/2}} \\
&= \pi \left[1 - \varepsilon \left((\varepsilon + 1) \frac{t^2}{\rho'^2} - \varepsilon \right)^{-1/2} \right]. \quad (8.65)
\end{aligned}$$

Similarly, let $x = x' + \varepsilon$ and $Y_2 = (T_\varepsilon + \varepsilon - x)(x - \varepsilon)$, we write

$$\begin{aligned}
\int_0^{T_\varepsilon} \frac{x' dx'}{(x' + \varepsilon) \sqrt{(T_\varepsilon - x')x'}} &= \int_\varepsilon^{T_\varepsilon + \varepsilon} \frac{(x - \varepsilon) dx}{x \sqrt{(T_\varepsilon + \varepsilon - x)(x - \varepsilon)}} \\
&= \int_\varepsilon^{T_\varepsilon + \varepsilon} \frac{dx}{Y_2^{1/2}} - \varepsilon \int_\varepsilon^{T_\varepsilon + \varepsilon} \frac{dx}{x Y_2^{1/2}} \\
&= \pi \left[1 - \varepsilon \left(\frac{\varepsilon t^2}{\rho'^2} \right)^{-1/2} \right]. \quad (8.66)
\end{aligned}$$

With substitutions Eqs. (8.65), (8.66) into Eq. (8.64), we have

$$\vartheta_\varepsilon^{(3)} = \pi \left[- \left(\frac{\varepsilon t^2}{\rho'^2} \right)^{-1/2} + \left((\varepsilon + 1) \frac{t^2}{\rho'^2} - \varepsilon \right)^{-1/2} \right]. \quad (8.67)$$

Thus,

$$I_2 = \frac{\pi}{(\varepsilon - 1)\rho'} \frac{\partial}{\partial t} \left\{ \frac{t}{\rho'} \left[\frac{\varepsilon - 1}{\varepsilon + 1} + (1 - \sqrt{\varepsilon}) \left(\frac{t^2}{\rho'^2} \right)^{-1/2} \right] \right\}; \quad \frac{t}{\rho'} > \sqrt{\varepsilon}. \quad (8.68)$$

Combined with Eqs. (8.47), (8.58), and (8.68), the result is

$$I_2 = \frac{\pi}{(\varepsilon - 1)\rho'} \frac{\partial}{\partial t} f_2 \left(\frac{t}{\rho'} \right) \quad (8.69)$$

where

$$f_2 \left(\frac{t}{\rho'} \right) = \left\{ \begin{array}{c} 0 \\ \frac{t}{\rho'} \left[- \frac{1}{\varepsilon + 1} + \left(\frac{t^2}{\rho'^2} \right)^{-1/2} - \frac{\varepsilon}{\varepsilon + 1} \left((\varepsilon + 1) \frac{t^2}{\rho'^2} - \varepsilon \right)^{-1/2} \right] \\ \frac{t}{\rho'} \left[\frac{\varepsilon - 1}{\varepsilon + 1} + (1 - \sqrt{\varepsilon}) \left(\frac{t^2}{\rho'^2} \right)^{-1/2} \right] \end{array} \right\}; \quad \begin{array}{c} \frac{ct}{\rho} < 1 \\ 1 < \frac{ct}{\rho} < \sqrt{\varepsilon} \\ \frac{ct}{\rho} > \sqrt{\varepsilon} \end{array}. \quad (8.70)$$

Since $f_2(1-) = f_2(1+) = 0$, $f_2(\sqrt{\varepsilon}-) = f_2(\sqrt{\varepsilon}+) = \sqrt{\varepsilon} \left(-\frac{2}{\varepsilon+1} + \frac{1}{\sqrt{\varepsilon}} \right)$, it is continuous at $t/\rho' = 1$ and $t/\rho' = \sqrt{\varepsilon}$.

$$f_2' \left(\frac{t}{\rho'} \right) = \begin{cases} 0 \\ \frac{1}{\rho'} \left[-\frac{1}{\varepsilon+1} + \frac{\varepsilon^2}{\varepsilon+1} \left((\varepsilon+1) \frac{t^2}{\rho'^2} - \varepsilon \right)^{-3/2} \right] \end{cases}; \quad \begin{matrix} \frac{ct}{\rho} < 1 \\ 1 < \frac{ct}{\rho} < \sqrt{\varepsilon} \\ \frac{ct}{\rho} > \sqrt{\varepsilon} \end{matrix}. \quad (8.71)$$

The complete formula for I_2 can be expressed as follows:

$$I_2 = \frac{c^2 \pi}{(\varepsilon^2 - 1) \rho^2} \begin{cases} 0 \\ -1 + \frac{\varepsilon^2}{(\varepsilon+1)^{3/2}} \left(\frac{c^2 t^2}{\rho^2} - \frac{\varepsilon}{\varepsilon+1} \right)^{-3/2} \\ \varepsilon - 1 \end{cases}; \quad \begin{matrix} \frac{ct}{\rho} < 1 \\ 1 < \frac{ct}{\rho} < \sqrt{\varepsilon} \\ \frac{ct}{\rho} > \sqrt{\varepsilon} \end{matrix}. \quad (8.72)$$

8.2.2.4 Evaluation of I_3

Following the same procedures in evaluations of I_2 , I_3 can also be evaluated readily. When $t/\rho' < 1$,

$$I_3 = 0. \quad (8.73)$$

When $1 < t/\rho' < \sqrt{\varepsilon}$,

$$I_3 = \frac{\partial}{\partial t} \operatorname{Im} \left\{ \int_0^\infty \frac{1}{\xi^2 \rho'} \left[\frac{1}{\sqrt{\varepsilon - \xi^2} + i\sqrt{\xi^2 - 1}} - \frac{t}{\rho'} \frac{1}{(\sqrt{\varepsilon - \xi^2} + i\sqrt{\xi^2 - 1})(\sqrt{t^2/\rho'^2 - \xi^2})} \right] \xi d\xi \right\}. \quad (8.74)$$

The real and imaginary parts are readily separated and only the imaginary part is retained. I_3 reduces to

$$I_3 = -\frac{1}{(\varepsilon - 1) \rho'} \frac{\partial}{\partial t} \left\{ \int_0^\infty \frac{1}{\xi^2} \sqrt{\xi^2 - 1} \xi d\xi - \frac{t}{\rho'} \int_0^\infty \frac{1}{\xi^2} \frac{\sqrt{\xi^2 - 1}}{\sqrt{t^2/\rho'^2 - \xi^2}} \xi d\xi \right\}. \quad (8.75)$$

With the contour in Fig. 8.3, this becomes

$$I_3 = \frac{-1}{(\varepsilon - 1) \rho'} \frac{\partial}{\partial t} \left\{ \int_1^{t/\rho'} \frac{1}{\xi^2} \sqrt{\xi^2 - 1} \xi d\xi - \frac{t}{\rho'} \int_1^{t/\rho'} \frac{1}{\xi^2} \frac{\sqrt{\xi^2 - 1}}{\sqrt{t^2/\rho'^2 - \xi^2}} \xi d\xi \right\}$$

$$\begin{aligned}
& - \int_1^{t/\rho'} \frac{1}{\xi^2} \sqrt{\xi^2 - 1} d\xi + \frac{t}{\rho'} \int_1^{t/\rho'} \frac{1}{\xi^2} \frac{\sqrt{\xi^2 - 1}}{\sqrt{t^2/\rho'^2 - \xi^2}} \xi d\xi \Bigg\} \\
= & \frac{2}{(\varepsilon - 1)\rho'} \frac{\partial}{\partial t} \left\{ \frac{t}{\rho'} \int_1^{t/\rho'} \frac{1}{\xi^2} \frac{\sqrt{\xi^2 - 1}}{\sqrt{t^2/\rho'^2 - \xi^2}} \xi d\xi \right\}. \tag{8.76}
\end{aligned}$$

With the change of the variable $\zeta = \xi^2$, $d\zeta = 2\xi d\xi$, it follows that

$$I_3 = \frac{1}{(\varepsilon - 1)\rho'} \frac{\partial}{\partial t} \left\{ \frac{t}{\rho'} \int_1^{t^2/\rho'^2} \frac{1}{\zeta} \frac{\sqrt{\zeta - 1}}{\sqrt{t^2/\rho'^2 - \zeta}} d\zeta \right\}. \tag{8.77}$$

The integral in Eq. (8.77) can be evaluated readily.

$$\begin{aligned}
\vartheta_0^{(5)} &= \int_1^{t^2/\rho'^2} \frac{1}{\zeta} \frac{\sqrt{\zeta - 1}}{\sqrt{t^2/\rho'^2 - \zeta}} d\zeta \\
&= \int_1^{t^2/\rho'^2} \frac{d\zeta}{\sqrt{(t^2/\rho'^2 - \zeta)(\zeta - 1)}} - \int_1^{t^2/\rho'^2} \frac{d\zeta}{\zeta \sqrt{(t^2/\rho'^2 - \zeta)(\zeta - 1)}} \\
&= \pi \left[1 - \left(\frac{t^2}{\rho'^2} \right)^{-1/2} \right]. \tag{8.78}
\end{aligned}$$

When $t/\rho' > \sqrt{\varepsilon}$,

$$\begin{aligned}
I_3 = \frac{\partial}{\partial t} \operatorname{Im} \Bigg\{ & \int_0^{\sqrt{\varepsilon}} \frac{1}{\xi^2 \rho'^2} \frac{1}{\sqrt{\varepsilon - \xi^2} + i\sqrt{\xi^2 - 1}} \xi d\xi \\
& - \frac{t}{\rho'} \int_0^{\sqrt{\varepsilon}} \frac{1}{\xi^2 \rho'^2} \frac{1}{(\sqrt{\varepsilon - \xi^2} + i\sqrt{\xi^2 - 1})\sqrt{t^2/\rho'^2 - \xi^2}} \xi d\xi \\
& + \int_{\sqrt{\varepsilon}}^\infty \frac{1}{\xi^2 \rho'^2} \frac{1}{i\sqrt{\xi^2 - \varepsilon} + i\sqrt{\xi^2 - 1}} \xi d\xi \\
& - \frac{t}{\rho'} \int_{\sqrt{\varepsilon}}^\infty \frac{1}{\xi^2 \rho'^2} \frac{1}{(i\sqrt{\xi^2 - \varepsilon} + i\sqrt{\xi^2 - 1})\sqrt{t^2/\rho'^2 - \xi^2}} \xi d\xi \Bigg\}. \tag{8.79}
\end{aligned}$$

The contributing imaginary part is

$$\begin{aligned}
I_3 = & -\frac{1}{(\varepsilon - 1)\rho'^2} \frac{\partial}{\partial t} \left\{ \int_0^{\sqrt{\varepsilon}} \sqrt{\xi^2 - 1} \frac{\xi d\xi}{\xi^2} - \frac{t}{\rho'} \int_0^{\sqrt{\varepsilon}} \frac{\sqrt{\xi^2 - 1}}{\sqrt{t^2/\rho'^2 - \xi^2}} \frac{\xi d\xi}{\xi^2} \right. \\
& + \int_{\sqrt{\varepsilon}}^\infty \left(\sqrt{\xi^2 - 1} - \sqrt{\xi^2 - \varepsilon} \right) \frac{\xi d\xi}{\xi^2} \\
& \left. - \frac{t}{\rho'} \int_{\sqrt{\varepsilon}}^\infty \frac{\sqrt{\xi^2 - 1} - \sqrt{\xi^2 - \varepsilon}}{\sqrt{t^2/\rho'^2 - \xi^2}} \frac{\xi d\xi}{\xi^2} \right\}
\end{aligned}$$

$$= -\frac{1}{(\varepsilon - 1)\rho'^2} \frac{\partial}{\partial t} \left\{ \int_0^\infty \frac{\sqrt{\xi^2 - 1} \xi d\xi}{\xi^2} - \frac{t}{\rho'} \int_0^\infty \frac{\sqrt{\xi^2 - 1}}{\sqrt{t^2/\rho'^2 - \xi^2}} \frac{\xi d\xi}{\xi^2} \right. \\ \left. - \int_{\sqrt{\varepsilon}}^\infty \frac{\sqrt{\xi^2 - \varepsilon} \xi d\xi}{\xi^2} + \frac{t}{\rho'} \int_{\sqrt{\varepsilon}}^\infty \frac{\sqrt{\xi^2 - \varepsilon}}{\sqrt{t^2/\rho'^2 - \xi^2}} \frac{\xi d\xi}{\xi^2} \right\}. \quad (8.80)$$

In terms of the variable $\zeta = \xi^2$, this becomes

$$I_3 = \frac{1}{(\varepsilon - 1)\rho'^2} \frac{\partial}{\partial t} \left\{ \frac{t}{\rho'} \int_1^{t^2/\rho'^2} \frac{1}{\zeta} \frac{\sqrt{\zeta - 1}}{\sqrt{t^2/\rho'^2 - \zeta}} d\zeta \right\} \\ + \frac{1}{(\varepsilon - 1)\rho'^2} \frac{\partial}{\partial t} \left\{ \frac{t}{\rho'} \int_\varepsilon^{t^2/\rho'^2} \frac{1}{\zeta} \frac{-\sqrt{\zeta - 1}}{\sqrt{t^2/\rho'^2 - \zeta}} d\zeta \right\}. \quad (8.81)$$

The first integral in Eq. (8.81) is shown in Eq. (8.78) and the second one needs to be evaluated.

$$\vartheta_\varepsilon^{(5)} = \int_\varepsilon^{t^2/\rho'^2} \frac{1}{\zeta} \frac{-\sqrt{\zeta - \varepsilon}}{\sqrt{t^2/\rho'^2 - \zeta}} d\zeta \\ = - \int_\varepsilon^{t^2/\rho'^2} \frac{1}{\zeta} \frac{\zeta - \varepsilon}{\sqrt{(t^2/\rho'^2 - \zeta)(\zeta - \varepsilon)}} d\zeta \\ = - \int_\varepsilon^{t^2/\rho'^2} \frac{d\zeta}{\sqrt{(t^2/\rho'^2 - \zeta)(\zeta - \varepsilon)}} + \varepsilon \int_\varepsilon^{t^2/\rho'^2} \frac{d\zeta}{\zeta \sqrt{(t^2/\rho'^2 - \zeta)(\zeta - \varepsilon)}} \\ = -\pi \left[1 - \sqrt{\varepsilon} \left(\frac{t^2}{\rho'^2} \right)^{-1/2} \right]. \quad (8.82)$$

With substitution Eqs. (8.78) and (8.82) into Eq. (8.81), we have

$$I_3 = \frac{\pi}{(\varepsilon - 1)\rho'} \frac{\partial}{\partial t} \left[\frac{t}{\rho'} (\sqrt{\varepsilon} - 1) \left(\frac{t^2}{\rho'^2} \right)^{-1/2} \right]; \quad \frac{ct}{\rho} > \sqrt{\varepsilon}. \quad (8.83)$$

Thus,

$$I_3 = \frac{\pi}{(\varepsilon - 1)\rho'} \frac{\partial}{\partial t} f_3 \left(\frac{t}{\rho'} \right) \quad (8.84)$$

where

$$f_3 \left(\frac{t}{\rho'} \right) = \frac{t}{\rho'} \left\{ \begin{array}{l} 0 \\ \left[1 - \left(\frac{t^2}{\rho'^2} \right)^{-1/2} \right] \\ (\sqrt{\varepsilon} - 1) \left(\frac{t^2}{\rho'^2} \right)^{-1/2} \end{array} \right\}; \quad \begin{array}{l} \frac{ct}{\rho} < 1 \\ 1 < \frac{ct}{\rho} < \sqrt{\varepsilon} \\ \frac{ct}{\rho} > \sqrt{\varepsilon} \end{array}. \quad (8.85)$$

Since $f_3(1-) = f_3(1+) = 0$, $f_3(\sqrt{\varepsilon}-) = f_3(\sqrt{\varepsilon}+) = \sqrt{\varepsilon}-1$. It is continuous at $t/\rho' = 1$ and $t/\rho' = \sqrt{\varepsilon}$.

$$f'_3\left(\frac{t}{\rho'}\right) = \begin{cases} 0 \\ \frac{1}{\rho'} \\ 0 \end{cases}; \quad \begin{matrix} \frac{ct}{\rho} < 1 \\ 1 < \frac{ct}{\rho} < \sqrt{\varepsilon} \\ \frac{ct}{\rho} > \sqrt{\varepsilon} \end{matrix}. \quad (8.86)$$

Finally, the complete formula for I_3 is obtained as follows:

$$I_3 = \frac{c^2\pi}{(\varepsilon-1)\rho^2} \begin{cases} 0 \\ 1 \\ 0 \end{cases}; \quad \begin{matrix} \frac{ct}{\rho} < 1 \\ 1 < \frac{ct}{\rho} < \sqrt{\varepsilon} \\ \frac{ct}{\rho} > \sqrt{\varepsilon} \end{matrix}. \quad (8.87)$$

8.2.2.5 Evaluation of $E_{2\rho}(\rho, 0; t)$

Combined with Eqs. (8.20), (8.46), (8.72), and (8.87), the electric field component $E_{2\rho}(\rho, 0; t)$ can be expressed in the following form:

$$E_{2\rho}(\rho, 0; t) = \frac{1}{2\pi\varepsilon_0 c \rho^2} \left[\delta\left(t - \frac{\rho}{c}\right) + \frac{1}{\sqrt{\varepsilon}} \delta\left(t - \frac{\sqrt{\varepsilon}\rho}{c}\right) \right] + \frac{1}{2\pi\varepsilon_0(\varepsilon+1)\rho^3} \\ \times \begin{cases} 0 \\ 1 - \frac{1}{\varepsilon-1} \frac{\varepsilon^2}{(\varepsilon+1)^{3/2}} \left(\frac{c^2 t^2}{\rho^2} + \frac{2\varepsilon}{\varepsilon+1} \right) \left(\frac{c^2 t^2}{\rho^2} - \frac{\varepsilon}{\varepsilon+1} \right)^{-5/2} \\ 2 \end{cases}; \quad \begin{matrix} \frac{ct}{\rho} < 1 \\ 1 < \frac{ct}{\rho} < \sqrt{\varepsilon} \\ \frac{ct}{\rho} > \sqrt{\varepsilon} \end{matrix}. \quad (8.88)$$

From Eq. (8.88), it is seen that the amplitude of the delta function in Eq. (8.88) includes the factors $1/\rho^2$. It is concluded that when the horizontal dipole is on the boundary, the far pulsed field along the boundary decreases with $1/\rho^2$, which is characteristic of the surface-wave or lateral pulse.

Assuming that the dipole is located on the boundary in Region 1 (the dielectric), at any distance ρ , the electric field $E_{2\rho}(\rho, 0; t)$ is always 0 until the instant $t = \rho/c$. The magnitude of the electric field $E_{2\rho}(\rho, 0; t)$ increases momentarily to infinite and decreases to the value

$$E_{2\rho}(\rho, 0; t) = -\frac{1}{2\pi\varepsilon_0 \rho^3} \frac{3\varepsilon^3 + \varepsilon^2 - \varepsilon + 1}{\varepsilon^2 - 1}. \quad (8.89)$$

The first pulse arrives at $t = \rho/c$ has travelled along the boundary in Region 2 (air) with the velocity c . The magnitude of the field component varies with time according to

$$E_{2\rho}(\rho, 0; t) = \frac{1}{2\pi\varepsilon_0(\varepsilon+1)\rho^3} \left[1 - \frac{1}{\varepsilon-1} \frac{\varepsilon^2}{(\varepsilon+1)^{3/2}} \left(\frac{c^2 t^2}{\rho^2} + \frac{2\varepsilon}{\varepsilon+1} \right) \right]$$

$$\times \left(\frac{c^2 t^2}{\rho^2} - \frac{\varepsilon}{\varepsilon + 1} \right)^{-5/2} \Bigg], \quad (8.90)$$

until $t = \sqrt{\varepsilon}\rho/c$ when it approaches the value

$$E_{2\rho}(\rho, 0; t) = \frac{1}{2\pi\varepsilon_0(\varepsilon + 1)\rho^3} \left[1 - \frac{\varepsilon + 3}{\varepsilon^2(\varepsilon - 1)} \right]. \quad (8.91)$$

At this instant, the magnitude of the field component $E_{2\rho}(\rho, 0; t)$ increases momentarily to infinite and decreases to the value

$$E_{2\rho}(\rho, 0; t) = \frac{2}{2\pi\varepsilon_0(\varepsilon^2 - 1)\rho^3}. \quad (8.92)$$

The second pulse arrives at $t = \sqrt{\varepsilon}\rho/c$ and has travelled along the boundary in Region 1 (dielectric) with the velocity $c/\sqrt{\varepsilon}$.

8.2.3 Time-Dependent Component $E_{2\phi}$

In this section, the time-dependent component $E_{2\phi}$ is evaluated analytically.

8.2.3.1 Finite Integration for Time-Dependent Component $E_{2\phi}$

Similarly, time-dependent component $E_{2\phi}$ due to a horizontal dipole with a delta function excitation can be written in the form

$$E_{2\phi}(\rho', \pi/2; t) = \frac{1}{\pi} \operatorname{Re} \int_0^\infty e^{-i\omega t} \tilde{E}_{2\phi}(\rho', \pi/2; \omega) d\omega. \quad (8.93)$$

With substitution Eq. (8.10) into Eq. (8.93), we have

$$\begin{aligned} E_{2\phi}(\rho', \pi/2; t) &= \frac{\mu_0}{2\pi^2 c} \int_0^\infty e^{-i\omega t} \omega d\omega \\ &\times \operatorname{Re} \int_0^\infty \left\{ \frac{\sqrt{\omega^2 \varepsilon - \lambda'^2} \sqrt{\omega^2 - \lambda'^2}}{\omega^2 \sqrt{\omega^2 \varepsilon - \lambda'^2} + \omega^2 \varepsilon \sqrt{\omega^2 - \lambda'^2}} \frac{J_1(\lambda' \rho')}{\lambda' \rho'} \right. \\ &\quad \left. + \left[J_0(\lambda' \rho') - \frac{1}{\lambda' \rho'} J_1(\lambda' \rho') \right] \right. \\ &\quad \left. \times \frac{1}{\sqrt{\omega^2 \varepsilon - \lambda'^2} + \sqrt{\omega^2 - \lambda'^2}} \right\} \lambda' d\lambda'. \quad (8.94) \end{aligned}$$

With the definition $\lambda' = \omega\xi$, $d\lambda' = \omega d\xi$, Eq. (8.94) reads as

$$E_{2\phi}(\rho', \pi/2; t) = \frac{\mu_0}{2\pi^2 c} \operatorname{Re} \int_0^\infty \left\{ \frac{\sqrt{\varepsilon - \xi^2} \sqrt{1 - \xi^2}}{\sqrt{\varepsilon - \xi^2} + \varepsilon \sqrt{1 - \xi^2}} \frac{i}{\xi \rho'} \right.$$

$$\begin{aligned}
& \times \frac{\partial}{\partial t} \int_0^\infty e^{-i\omega t} J_1(\omega \xi \rho') d\omega - \frac{1}{\sqrt{\varepsilon - \xi^2} + \sqrt{1 - \xi^2}} \\
& \times \left[\frac{\partial^2}{\partial t^2} \int_0^\infty e^{-i\omega t} J_0(\omega \xi \rho') d\omega \right. \\
& \left. + \frac{i}{\xi \rho'} \frac{\partial}{\partial t} \int_0^\infty e^{-i\omega t} J_1(\omega \xi \rho') d\omega \right] \xi d\xi. \quad (8.95)
\end{aligned}$$

Then, Eq. (8.95) can be rewritten as

$$E_{2\phi}(\rho', \pi/2; t) = \frac{\mu_0}{2\pi^2 \rho' c} (I_2 + I_3 + I_4), \quad (8.96)$$

where I_2 and I_3 had been solved and shown in Eqs. (8.72) and (8.87). The next task is to evaluate I_4 .

$$I_4 = -\frac{\partial^2}{\partial t^2} \operatorname{Im} \int_0^\infty \frac{1}{\sqrt{\varepsilon - \xi^2} + \sqrt{1 - \xi^2}} \frac{1}{\sqrt{t^2/\rho'^2 - \xi^2}} \xi d\xi. \quad (8.97)$$

8.2.3.2 Evaluation of I_4

Following the similar procedures in the evaluation of I_2 and I_3 , the evaluation of the integral I_4 can be carried out readily. When $t/\rho' < 1$,

$$I_4 = 0. \quad (8.98)$$

When $1 < t/\rho' < \sqrt{\varepsilon}$,

$$\begin{aligned}
I_4 = -\frac{\partial^2}{\partial t^2} \operatorname{Im} \Bigg\{ & \int_0^1 \left[\frac{1}{(\sqrt{\varepsilon - \xi^2} + \sqrt{1 - \xi^2}) \sqrt{t^2/\rho'^2 - \xi^2}} \right. \\
& \left. - \frac{1}{(\sqrt{\varepsilon - \xi^2} + \sqrt{1 - \xi^2})(-\sqrt{t^2/\rho'^2 - \xi^2})} \right] \xi d\xi \\
& + \int_1^{t/\rho'} \left[\frac{1}{(\sqrt{\varepsilon - \xi^2} + i\sqrt{\xi^2 - 1}) \sqrt{t^2/\rho'^2 - \xi^2}} \right. \\
& \left. - \frac{1}{(\sqrt{\varepsilon - \xi^2} + i\sqrt{\xi^2 - 1})(-\sqrt{t^2/\rho'^2 - \xi^2})} \right] \xi d\xi \Bigg\}. \quad (8.99)
\end{aligned}$$

Because the integrand of the first integral is *real*, the contributing imaginary part is

$$I_4 = -\frac{\partial^2}{\partial t^2} \operatorname{Im} \int_1^{t/\rho'} \frac{2}{(\sqrt{\varepsilon - \xi^2} + i\sqrt{\xi^2 - 1}) \sqrt{t^2/\rho'^2 - \xi^2}} \xi d\xi. \quad (8.100)$$

Then,

$$I_4 = \frac{2}{\varepsilon - 1} \frac{\partial^2}{\partial t^2} \int_1^{t/\rho'} \frac{\sqrt{\xi^2 - 1}}{\sqrt{t^2/\rho'^2 - \xi^2}} \xi d\xi. \quad (8.101)$$

With $\zeta = \xi^2$, it follows that

$$I_4 = \frac{1}{\varepsilon - 1} \frac{\partial^2}{\partial t^2} \int_1^{t^2/\rho'^2} \frac{\sqrt{\zeta - 1}}{\sqrt{t^2/\rho'^2 - \zeta}} d\zeta. \quad (8.102)$$

Let $T_0 = t^2/\rho'^2 - 1$, and $x' = \zeta - 1$, the integral in Eq. (8.102) can be rewritten in the form

$$\vartheta_0^{(6)} = \int_1^{t^2/\rho'^2} \frac{\sqrt{\zeta - 1}}{\sqrt{t^2/\rho'^2 - \zeta}} d\zeta = \int_0^{T_0} \frac{x' dx'}{\sqrt{(T_0 - x')x'}}. \quad (8.103)$$

With $x = x' + E_0$, $E_0 = 1/(\varepsilon + 1)$, and $X_3 = (T_0 + E_0 - x)(x - E_0)$, then,

$$\begin{aligned} \vartheta_0^{(6)} &= \int_{E_0}^{T_0+E_0} \frac{x dx}{X_3^{1/2}} - E_0 \int_{E_0}^{T_0+E_0} \frac{dx}{X_3^{1/2}} \\ &= \frac{\pi}{2} (T_0 + 2E_0) - \pi E_0 = \frac{\pi}{2} \left(\frac{t^2}{\rho'^2} - 1 \right). \end{aligned} \quad (8.104)$$

Thus,

$$I_4 = \frac{\pi}{2(\varepsilon - 1)} \frac{\partial^2}{\partial t^2} \left(\frac{t^2}{\rho'^2} - 1 \right); \quad 1 < \frac{t}{\rho'} < \sqrt{\varepsilon}. \quad (8.105)$$

When $t/\rho' > \sqrt{\varepsilon}$,

$$\begin{aligned} I_4 &= -\frac{\partial^2}{\partial t^2} \operatorname{Im} \left\{ \int_1^{\sqrt{\varepsilon}} \frac{2}{(\sqrt{\varepsilon - \xi^2} + i\sqrt{\xi^2 - 1})\sqrt{t^2/\rho'^2 - \xi^2}} \xi d\xi \right. \\ &\quad \left. + \int_{\sqrt{\varepsilon}}^{t/\rho'} \frac{2}{(i\sqrt{\xi^2 - \varepsilon} + i\sqrt{\xi^2 - 1})\sqrt{t^2/\rho'^2 - \xi^2}} \xi d\xi \right\}. \end{aligned} \quad (8.106)$$

The imaginary part is

$$\begin{aligned} I_4 &= \frac{2}{\varepsilon - 1} \frac{\partial^2}{\partial t^2} \left\{ \int_1^{\sqrt{\varepsilon}} \frac{\sqrt{\xi^2 - 1}}{\sqrt{t^2/\rho'^2 - \xi^2}} \xi d\xi + \int_{\sqrt{\varepsilon}}^{t/\rho'} \frac{\sqrt{\xi^2 - 1} - \sqrt{\varepsilon - \xi^2}}{\sqrt{t^2/\rho'^2 - \xi^2}} \xi d\xi \right\} \\ &= \frac{2}{\varepsilon - 1} \frac{\partial^2}{\partial t^2} \left\{ \int_1^{t/\rho'} \frac{\sqrt{\xi^2 - 1}}{\sqrt{t^2/\rho'^2 - \xi^2}} \xi d\xi - \int_{\sqrt{\varepsilon}}^{t/\rho'} \frac{\sqrt{\varepsilon - \xi^2}}{\sqrt{t^2/\rho'^2 - \xi^2}} \xi d\xi \right\}. \end{aligned} \quad (8.107)$$

In terms of the variable $\zeta = \xi^2$, this becomes

$$I_4 = \frac{1}{\varepsilon - 1} \frac{\partial^2}{\partial t^2} \left\{ \int_1^{t^2/\rho'^2} \frac{\sqrt{\zeta - 1}}{\sqrt{t^2/\rho'^2 - \zeta}} d\zeta - \int_\varepsilon^{t^2/\rho'^2} \frac{\sqrt{\varepsilon - \zeta}}{\sqrt{t^2/\rho'^2 - \zeta}} d\zeta \right\}. \quad (8.108)$$

The first integral has been addressed in Eq. (8.104). In the next step, the second integral needs to be solved. Let $T_\varepsilon = t^2/\rho'^2 - \varepsilon$, and $y' = \zeta - \varepsilon$, the second integral in Eq. (8.108) can be written as

$$\vartheta_\varepsilon^{(6)} = \int_\varepsilon^{t^2/\rho'^2} \frac{\sqrt{\zeta - \varepsilon}}{\sqrt{t^2/\rho'^2 - \zeta}} d\zeta = \int_0^{T_\varepsilon} \frac{y' dy'}{\sqrt{(T_\varepsilon - y')y'}}. \quad (8.109)$$

With $y = y' + E_0$, $E_0 = 1/(\varepsilon + 1)$, and $Y_3 = (T_\varepsilon + E_0 - y)(y - E_0)$, this becomes

$$\begin{aligned} \vartheta_\varepsilon^{(6)} &= \int_{E_0}^{T_\varepsilon + E_0} \frac{y dy}{Y_3^{1/2}} - E_0 \int_{E_0}^{T_0 + E_0} \frac{dy}{Y_3^{1/2}} \\ &= \frac{\pi}{2} (T_\varepsilon + 2E_0) - \pi E_0 = \frac{\pi}{2} \left(\frac{t^2}{\rho'^2} - \varepsilon \right). \end{aligned} \quad (8.110)$$

Thus, we write

$$I_4 = \frac{\pi}{2}; \quad 1 < \frac{t}{\rho'} < \sqrt{\varepsilon}. \quad (8.111)$$

From Eqs. (8.98), (8.105), and (8.111), it is obtained readily.

$$I_4 = \frac{\pi}{2} \frac{\partial^2}{\partial t^2} f_4 \left(\frac{t}{\rho'} \right), \quad (8.112)$$

where

$$f_4 \left(\frac{t}{\rho'} \right) = \begin{cases} 0 \\ \frac{1}{\varepsilon - 1} \left(\frac{t^2}{\rho'^2} - 1 \right) \\ 1 \end{cases}; \quad \begin{aligned} &\frac{ct}{\rho} < 1 \\ &1 < \frac{ct}{\rho} < \sqrt{\varepsilon}. \\ &\frac{ct}{\rho} > \sqrt{\varepsilon} \end{aligned} \quad (8.113)$$

Obviously, $f_4(1-) = f_4(1+) = 0$ and $f_4(\sqrt{\varepsilon}-) = f_4(\sqrt{\varepsilon}+) = 1$, it follows that $f_4(t/\rho')$ is everywhere continuous.

$$f_4' \left(\frac{t}{\rho'} \right) = \begin{cases} 0 \\ \frac{1}{\varepsilon - 1} \frac{2t}{\rho'^2} \\ 0 \end{cases}; \quad \begin{aligned} &\frac{ct}{\rho} < 1 \\ &1 < \frac{ct}{\rho} < \sqrt{\varepsilon}. \\ &\frac{ct}{\rho} > \sqrt{\varepsilon} \end{aligned} \quad (8.114)$$

Since $f_4'(1-) = 0$, $f_4'(1+) = 2/[(\varepsilon - 1)\rho']$, $f_4'(t/\rho')$ has a step discontinuity of $2/\rho'$ at $t/[(\varepsilon - 1)\rho'] = 1$. Similarly, $f_4'(\sqrt{\varepsilon}-) = 2\sqrt{\varepsilon}/[(\varepsilon - 1)\rho']$, $f_4'(\sqrt{\varepsilon}+) = 0$, $f_4'(t/\rho')$ has a step discontinuity of $-2\sqrt{\varepsilon}/[(\varepsilon - 1)\rho']$ at $t/\rho' = \sqrt{\varepsilon}$. Thus, we have

$$f_4''\left(\frac{t}{\rho'}\right) = \begin{Bmatrix} 0 \\ \frac{2}{(\varepsilon-1)\rho'^2} \\ 0 \end{Bmatrix}; \quad \begin{matrix} \frac{ct}{\rho} < 1 \\ 1 < \frac{ct}{\rho} < \sqrt{\varepsilon} \\ \frac{ct}{\rho} > \sqrt{\varepsilon} \end{matrix}. \quad (8.115)$$

The final formula for I_4 can be written in the following form:

$$I_4 = \frac{c\pi}{(\varepsilon-1)\rho} \left[\delta\left(t - \frac{\rho}{c}\right) - \sqrt{\varepsilon}\delta\left(t - \frac{\sqrt{\varepsilon}\rho}{c}\right) \right] \\ + \frac{c^2\pi}{(\varepsilon-1)\rho^2} \begin{Bmatrix} 0 \\ 1 \\ 0 \end{Bmatrix}; \quad \begin{matrix} \frac{ct}{\rho} < 1 \\ 1 < \frac{ct}{\rho} < \sqrt{\varepsilon} \\ \frac{ct}{\rho} > \sqrt{\varepsilon} \end{matrix}. \quad (8.116)$$

8.2.3.3 Evaluation of $E_{2\phi}(\rho, \pi/2; t)$

Combined with Eqs. (8.72), (8.87), (8.96), and (8.116), it is obtained readily.

$$E_{2\phi}(\rho, \pi/2; t) = \frac{1}{2\pi\varepsilon_0 c(\varepsilon-1)\rho^2} \left[\delta\left(t - \frac{\rho}{c}\right) - \sqrt{\varepsilon}\delta\left(t - \frac{\sqrt{\varepsilon}\rho}{c}\right) \right] \\ + \frac{1}{2\pi\varepsilon_0(\varepsilon-1)\rho^3} \begin{Bmatrix} 0 \\ 2 - \frac{1}{\varepsilon+1} + \frac{\varepsilon^2}{(\varepsilon+1)^{5/2}} \left(\frac{c^2 t^2}{\rho^2} - \frac{\varepsilon}{\varepsilon+1} \right)^{-3/2} \\ \frac{\varepsilon-1}{\varepsilon+1} \end{Bmatrix}; \quad \begin{matrix} \frac{ct}{\rho} < 1 \\ 1 < \frac{ct}{\rho} < \sqrt{\varepsilon} \\ \frac{ct}{\rho} > \sqrt{\varepsilon} \end{matrix}. \quad (8.117)$$

Similarly, at the instant $t = \rho/c$, the magnitude of the electric field $E_{2\phi}(\rho, 0; t)$ increases momentarily to infinite and decreases to the value

$$E_{2\phi}(\rho, 0; t) = \frac{1}{2\pi\varepsilon_0\rho^3} \frac{\varepsilon+1}{\varepsilon-1}. \quad (8.118)$$

The magnitude of the electric field varies with time according to

$$E_{2\phi}(\rho, 0; t) = \frac{1}{2\pi\varepsilon_0(\varepsilon-1)\rho^3} \left[2 - \frac{1}{\varepsilon+1} + \frac{\varepsilon^2}{(\varepsilon+1)^{5/2}} \left(\frac{c^2 t^2}{\rho^2} - \frac{\varepsilon}{\varepsilon+1} \right)^{-3/2} \right], \quad (8.119)$$

until $t = \sqrt{\varepsilon}\rho/c$ when it approaches the value

$$E_{2\rho}(\rho, 0; t) = \frac{1}{2\pi\varepsilon_0\rho^3} \frac{2\varepsilon^2 + \varepsilon + 1}{\varepsilon(\varepsilon^2 - 1)}. \quad (8.120)$$

At this instant, the magnitude of the electric field $E_{2\rho}(\rho, 0; t)$ increases momentarily to infinite and decreases to the value

$$E_{2\rho}(\rho, 0; t) = \frac{1}{2\pi\epsilon_0(\epsilon + 1)\rho^3}. \quad (8.121)$$

The second pulse has travelled at $t = \sqrt{\epsilon}\rho/c$ along the boundary in Region 1 (the dielectric) with the velocity $c\sqrt{\epsilon}$.

8.2.4 Time-Dependent Component B_{2z}

When the horizontal electric dipole is excited by a unit moment that is a delta function pulse, the vertical magnetic field, which is *real*, can also be given by the following Fourier transform:

$$B_{2z}(\rho', \pi/2; t) = \frac{1}{\pi} \text{Re} \int_0^\infty e^{-i\omega t} \tilde{B}_{2z}(\rho', \pi/2; \omega) d\omega. \quad (8.122)$$

With Eq. (8.14), it follows that

$$B_{2z}(\rho', \pi/2; t) = \text{Re} \frac{i\mu}{2\pi^2 c^2} \int_0^\infty e^{-i\omega t} d\omega \int_0^\infty \frac{J_1(\lambda' \rho')}{\sqrt{\omega^2 - \lambda'^2} + \sqrt{\omega^2 \epsilon - \lambda'^2}} \lambda'^2 d\lambda'. \quad (8.123)$$

With the definition $\lambda' = \omega\xi$, $d\lambda' = \omega d\xi$, Eq. (8.123) reads as

$$B_{2z}(\rho', \pi/2; t) = \text{Re} \frac{i\mu_0}{2\pi^2 c^2} \frac{\partial^2}{\partial t^2} \int_0^\infty \frac{\xi^2 d\xi}{\sqrt{\epsilon - \xi^2} + \sqrt{1 - \xi^2}} \int_0^\infty e^{-i\omega t} J_1(\omega\xi\rho') d\omega. \quad (8.124)$$

Taking into account the relationship in Eq. (8.19), it is obtained readily.

$$\begin{aligned} B_{2z}(\rho', \pi/2; t) &= \text{Re} \frac{i\mu_0}{2\pi^2 c^2} \\ &\quad \times \frac{\partial^2}{\partial t^2} \int_0^\infty \frac{\xi^2}{\sqrt{\epsilon - \xi^2} + \sqrt{1 - \xi^2}} \frac{1}{\xi\rho'} \left(1 - \frac{t}{\sqrt{t^2 - \xi^2\rho'^2}}\right) d\xi \\ &= \frac{\mu_0}{2\pi^2 c^2 \rho'} \frac{\partial^2}{\partial t^2} \text{Im} \left[\int_0^\infty \frac{\xi d\xi}{\sqrt{\epsilon - \xi^2} + \sqrt{1 - \xi^2}} \right. \\ &\quad \left. - \frac{t}{\rho'} \int_0^\infty \frac{\xi d\xi}{(\sqrt{\epsilon - \xi^2} + \sqrt{1 - \xi^2}) \sqrt{t^2/\rho'^2 - \xi^2}} \right]. \end{aligned} \quad (8.125)$$

Following the same procedures in evaluation of I_2 , the evaluations of the integrals Eq. (8.125) can be carried out readily. When $t/\rho' < 1$,

$$B_{2z}(\rho', \pi/2; t) = 0. \quad (8.126)$$

When $1 < t/\rho' < \sqrt{\epsilon}$,

$$\begin{aligned}
B_{2z}(\rho', \pi/2; t) &= \frac{-\mu_0}{2\pi^2 c^2 \rho'} \frac{\partial^2}{\partial t^2} \operatorname{Im} \left[\frac{t}{\rho'} \int_0^\infty \frac{\xi d\xi}{(\sqrt{\varepsilon - \xi^2} + i\sqrt{\xi^2 - 1})\sqrt{t^2/\rho'^2 - \xi^2}} \right] \\
&= -\frac{\mu_0}{2\pi^2 c^2 \rho'} \frac{1}{\varepsilon - 1} \frac{\partial^2}{\partial t^2} \int_0^\infty \left[\sqrt{\xi^2 - 1} - \frac{t}{\rho'} \frac{\sqrt{\xi^2 - 1}}{\sqrt{t^2/\rho'^2 - \xi^2}} \right] \xi d\xi.
\end{aligned} \tag{8.127}$$

With $\zeta = \xi^2$, we have

$$B_{2z}(\rho', \pi/2; t) = \frac{\mu_0}{2\pi^2 c^2 \rho'} \frac{1}{\varepsilon - 1} \frac{\partial^2}{\partial t^2} \left[\frac{t}{\rho'} \int_1^{t^2/\rho'^2} \frac{\sqrt{\zeta - 1}}{\sqrt{t^2/\rho'^2 - \zeta}} d\zeta \right]. \tag{8.128}$$

The integral in Eq. (8.128) had been evaluated in Eq. (8.104). Then, we write

$$B_{2z}(\rho', \pi/2; t) = \frac{\mu_0}{4\pi c^2 \rho'} \frac{1}{\varepsilon - 1} \frac{\partial^2}{\partial t^2} \left[\frac{t}{\rho'} \left(\frac{t^2}{\rho'^2} - 1 \right) \right]; \quad 1 < \frac{t}{\rho'} < \sqrt{\varepsilon}. \tag{8.129}$$

When $t/\rho' > \sqrt{\varepsilon}$,

$$\begin{aligned}
B_{2z}(\rho', \pi/2; t) &= \frac{\mu_0}{2\pi^2 c^2 \rho'} \frac{\partial^2}{\partial t^2} \operatorname{Im} \left[\int_0^{\sqrt{\varepsilon}} \frac{\xi d\xi}{\sqrt{\varepsilon - \xi^2} + i\sqrt{\xi^2 - 1}} \right. \\
&\quad - \frac{t}{\rho'} \int_0^{\sqrt{\varepsilon}} \frac{\xi d\xi}{(\sqrt{\varepsilon - \xi^2} + i\sqrt{\xi^2 - 1})\sqrt{t^2/\rho'^2 - \xi^2}} \\
&\quad + \int_{\sqrt{\varepsilon}}^\infty \frac{\xi d\xi}{i\sqrt{\xi^2 - \varepsilon} + i\sqrt{\xi^2 - 1}} \\
&\quad \left. - \frac{t}{\rho'} \int_{\sqrt{\varepsilon}}^\infty \frac{\xi d\xi}{(i\sqrt{\xi^2 - \varepsilon} + i\sqrt{\xi^2 - 1})\sqrt{t^2/\rho'^2 - \xi^2}} \right] \\
&= -\frac{\mu_0}{2\pi^2 c^2 \rho'} \frac{1}{\varepsilon - 1} \frac{\partial^2}{\partial t^2} \left[\int_0^{\sqrt{\varepsilon}} \sqrt{\xi^2 - 1} \xi d\xi \right. \\
&\quad - \frac{t}{\rho'} \int_0^{\sqrt{\varepsilon}} \frac{\sqrt{\xi^2 - 1}}{\sqrt{t^2/\rho'^2 - \xi^2}} \xi d\xi \\
&\quad + \int_{\sqrt{\varepsilon}}^\infty i \left(\sqrt{\xi^2 - 1} - \sqrt{\xi^2 - \varepsilon} \right) \xi d\xi \\
&\quad \left. - \frac{t}{\rho'} \int_{\sqrt{\varepsilon}}^\infty \frac{(\sqrt{\xi^2 - 1} - \sqrt{\xi^2 - \varepsilon})}{\sqrt{t^2/\rho'^2 - \xi^2}} \xi d\xi \right]. \tag{8.130}
\end{aligned}$$

Then, we have

$$\begin{aligned}
B_{2z}(\rho', \pi/2; t) = & -\frac{\mu_0}{2\pi^2 c^2 \rho'} \frac{1}{\varepsilon - 1} \frac{\partial^2}{\partial t^2} \left[\int_0^\infty \sqrt{\xi^2 - 1} \xi d\xi \right. \\
& - \frac{t}{\rho'} \int_0^\infty \frac{\sqrt{\xi^2 - 1}}{\sqrt{t^2/\rho'^2 - \xi^2}} \xi d\xi - \int_{\sqrt{\varepsilon}}^\infty \sqrt{\xi^2 - \varepsilon} \xi d\xi \\
& \left. + \frac{t}{\rho'} \int_{\sqrt{\varepsilon}}^\infty \frac{\sqrt{\xi^2 - \varepsilon}}{\sqrt{t^2/\rho'^2 - \xi^2}} \xi d\xi \right]. \quad (8.131)
\end{aligned}$$

In terms of the variable $\zeta = \xi^2$, $d\zeta = 2\xi d\xi$, it follows that

$$\begin{aligned}
B_{2z}(\rho', \pi/2; t) = & \frac{\mu_0}{2\pi^2 c^2 \rho'} \frac{1}{\varepsilon - 1} \frac{\partial^2}{\partial t^2} \left[\frac{t}{\rho'} \left(\int_1^{t^2/\rho'^2} \frac{\sqrt{\zeta - 1}}{\sqrt{t^2/\rho'^2 - \zeta}} d\zeta \right. \right. \\
& \left. \left. - \int_\varepsilon^{t^2/\rho'^2} \frac{\sqrt{\zeta - \varepsilon}}{\sqrt{t^2/\rho'^2 - \zeta}} d\zeta \right) \right]. \quad (8.132)
\end{aligned}$$

The above two integrals have been evaluated in Eqs. (8.104) and (8.110). Then, we write

$$B_{2z}(\rho', \pi/2; t) = \frac{\mu_0}{4\pi c^2 \rho'} \frac{1}{\varepsilon - 1} \frac{\partial^2}{\partial t^2} \left[\frac{t}{\rho'} (\varepsilon - 1) \right]; \quad \frac{t}{\rho'} > \sqrt{\varepsilon}. \quad (8.133)$$

With substitutions (8.126), (8.129), and (8.133) into Eq. (8.125), we have

$$B_{2z}(\rho', \pi/2; t) = \frac{\mu_0}{4\pi c^2 \rho'} \frac{\partial^2}{\partial t^2} f_7 \left(\frac{t}{\rho'} \right), \quad (8.134)$$

where

$$f_7 \left(\frac{t}{\rho'} \right) = \frac{1}{\varepsilon - 1} \frac{t}{\rho'} \left\{ \frac{0}{\frac{t^2}{\rho'^2} - 1} \right\}; \quad 1 < \frac{\frac{ct}{\rho}}{\frac{ct}{\rho}} < \sqrt{\varepsilon}. \quad (8.135)$$

Since $f(1-) = f(1+) = 0$ and $f(\sqrt{\varepsilon}-) = f(\sqrt{\varepsilon}+) = \sqrt{\varepsilon}$, $f_7(t/\rho')$ is everywhere continuous.

$$f_7' \left(\frac{t}{\rho'} \right) = \frac{1}{(\varepsilon - 1)\rho'} \left\{ \frac{0}{\frac{3t^2}{\rho'^2} - 1} \right\}; \quad 1 < \frac{\frac{ct}{\rho}}{\frac{ct}{\rho}} < \sqrt{\varepsilon}. \quad (8.136)$$

Since $f_7'(1-) = 0$ and $f_7'(1+) = 2/[(\varepsilon - 1)\rho']$, $f_7'(t/\rho')$ has a step discontinuity of $2/[(\varepsilon - 1)\rho']$ at $\frac{t}{\rho'} = 1$. Similarly, $f_7'(\sqrt{\varepsilon}-) = (3\varepsilon - 1)/[(\varepsilon - 1)\rho']$, $f_7'(\sqrt{\varepsilon}+) = 1/\rho'$, $f_7'(t/\rho')$ has a step discontinuity of $-2\varepsilon/[(\varepsilon - 1)\rho']$ at $t/\rho' = \sqrt{\varepsilon}$. Thus, we have

$$f_7'' \left(\frac{t}{\rho'} \right) = \frac{1}{(\varepsilon - 1)\rho'^3} \left\{ \begin{matrix} 0 \\ 6t \\ 0 \end{matrix} \right\}; \quad 1 < \frac{\frac{ct}{\rho}}{\frac{ct}{\rho}} < \sqrt{\varepsilon}. \quad (8.137)$$

With substitution Eq. (8.137) into Eq. (8.134) and $\rho' = \rho/c$, the final formula for the vertical magnetic field is expressed as follows:

$$B_{2z}(\rho, \pi/2; t) = \frac{\mu_0}{2\pi\rho^2} \frac{1}{\varepsilon - 1} \left[\delta\left(t - \frac{\rho}{c}\right) - \varepsilon \delta\left(t - \frac{\sqrt{\varepsilon}\rho}{c}\right) \right] - \frac{\mu_0 c}{2\pi\rho^3} \frac{1}{\varepsilon - 1} \begin{Bmatrix} 0 \\ \frac{3ct}{\rho} \\ 0 \end{Bmatrix}; \quad \begin{matrix} \frac{ct}{\rho} < 1 \\ 1 < \frac{ct}{\rho} < \sqrt{\varepsilon} \\ \frac{ct}{\rho} > \sqrt{\varepsilon} \end{matrix}. \quad (8.138)$$

8.2.5 Discussions and Conclusions

We start with the Fourier-Bessel integral representations for the electromagnetic field radiated by a delta function current in a horizontal electric dipole located on the planar boundary between air and a homogeneous dielectric. Similar to the case of the vertical dipole, the tangential electric field components due to a horizontal dipole consist of a delta function pulse travelling in the air with the velocity c , the oppositely directed delta function pulse travelling in the dielectric with the velocity $c/\varepsilon^{1/2}$ for the component E_ρ and the velocity $c\varepsilon^{1/2}$ for the component E_ϕ , and the final static electric field due to the charge left on the dipole. The structures of the three field components $E_{2\rho}(\rho, 0; t)$, $E_{2\phi}(\rho, \pi/2; t)$, and $E_{2z}(\rho, \pi/2; t)$ between the two delta function pulses are different from each other. Also, the structures of the field components are, of course, different from those of the field components in the case of the vertical dipole.

The time-dependent component $E_{2\rho}(\rho, t)$ due to a vertical dipole cannot be expressed in terms of elementary functions. Similarly, the three time-dependent components $E_{2z}(\rho, 0; t)$, $B_{2\rho}(\rho, \pi/2; t)$, and $B_{2\phi}(\rho, \pi/2; t)$ due to a horizontal electric dipole with a delta function excitation are also not expressible in terms of elementary functions.

8.3 Exact Transient Field with Gaussian Excitation

In what follows, we will treat the exact transient field of a horizontal electric dipole with Gaussian excitation on the plane boundary between two dielectrics.

8.3.1 Exact Formulas for the Transient Field of Horizontal Dipole Excited by a Gaussian Pulse on the Boundary Between Two Dielectrics

If the unit horizontal electric dipole, as shown in Fig. 8.1, is excited by a Gaussian pulse, the exact formulas for the transient field with Gaussian excitation

can be obtained from the exact formulas with delta function excitation by using Fourier's transform technique (King, Owens, and Wu, 1992). It is necessary to rewrite the exact formulas for the transient field with delta function excitation in the following forms:

$$\begin{aligned}
 [E_{2\rho}(\rho, 0; t)]_\delta &= \frac{1}{2\pi\varepsilon_0 c\rho^2} \left[\delta\left(t - \frac{\rho}{c}\right) + \frac{1}{\sqrt{\varepsilon}} \delta\left(t - \frac{\sqrt{\varepsilon}\rho}{c}\right) \right] + \frac{1}{2\pi\varepsilon_0(\varepsilon+1)\rho^3} \\
 &\quad \times \left\{ \begin{array}{c} 0 \\ 1 - \frac{1}{\varepsilon-1} \frac{\varepsilon^2}{(\varepsilon+1)^{3/2}} \left(\frac{c^2 t^2}{\rho^2} + \frac{2\varepsilon}{\varepsilon+1} \right) \left(\frac{c^2 t^2}{\rho^2} - \frac{\varepsilon}{\varepsilon+1} \right)^{-5/2} \\ 2 \end{array} \right\}; \\
 &\quad \begin{array}{c} \frac{ct}{\rho} < 1 \\ 1 < \frac{ct}{\rho} < \sqrt{\varepsilon}, \\ \frac{ct}{\rho} > \sqrt{\varepsilon} \end{array}, \quad (8.139)
 \end{aligned}$$

$$\begin{aligned}
 [E_{2\phi}(\rho, \pi/2; t)]_\delta &= \frac{1}{2\pi\varepsilon_0 c(\varepsilon-1)\rho^2} \left[\delta\left(t - \frac{\rho}{c}\right) - \sqrt{\varepsilon} \delta\left(t - \frac{\sqrt{\varepsilon}\rho}{c}\right) \right] \\
 &\quad + \frac{1}{2\pi\varepsilon_0(\varepsilon-1)\rho^3} \left\{ \begin{array}{c} 0 \\ 2 - \frac{1}{\varepsilon+1} + \frac{\varepsilon^2}{(\varepsilon+1)^{5/2}} \left(\frac{c^2 t^2}{\rho^2} - \frac{\varepsilon}{\varepsilon+1} \right)^{-3/2} \\ \frac{\varepsilon-1}{\varepsilon+1} \end{array} \right\}; \\
 &\quad \begin{array}{c} \frac{ct}{\rho} < 1 \\ 1 < \frac{ct}{\rho} < \sqrt{\varepsilon}, \\ \frac{ct}{\rho} > \sqrt{\varepsilon} \end{array}, \quad (8.140)
 \end{aligned}$$

$$\begin{aligned}
 [B_{2z}(\rho, \pi/2; t)]_\delta &= \frac{\mu_0}{2\pi\rho^2} \frac{1}{\varepsilon-1} \left[\delta\left(t - \frac{\rho}{c}\right) - \varepsilon \delta\left(t - \frac{\sqrt{\varepsilon}\rho}{c}\right) \right] \\
 &\quad - \frac{\mu_0 c}{2\pi\rho^3} \frac{1}{\varepsilon-1} \left\{ \begin{array}{c} 0 \\ \frac{3ct}{\rho} \\ 0 \end{array} \right\}; \quad \begin{array}{c} \frac{ct}{\rho} < 1 \\ 1 < \frac{ct}{\rho} < \sqrt{\varepsilon}, \\ \frac{ct}{\rho} > \sqrt{\varepsilon} \end{array}. \quad (8.141)
 \end{aligned}$$

The exact transient field with Gaussian excitation can be expressed as follows:

$$E_{2\rho}(\rho, 0; t) = \frac{1}{t_1 \sqrt{\pi}} \int_{-\infty}^{\infty} [E_{2\rho}(\rho, 0; t - \zeta)]_\delta e^{-\zeta^2/t_1^2} d\zeta, \quad (8.142)$$

$$E_{2\phi}(\rho, \pi/2; t) = \frac{1}{t_1 \sqrt{\pi}} \int_{-\infty}^{\infty} [E_{2\phi}(\rho, \pi/2; t - \zeta)]_\delta e^{-\zeta^2/t_1^2} d\zeta, \quad (8.143)$$

$$B_{2z}(\rho, \pi/2; t) = \frac{1}{t_1 \sqrt{\pi}} \int_{-\infty}^{\infty} [B_{2z}(\rho, \pi/2; t - \zeta)]_\delta e^{-\zeta^2/t_1^2} d\zeta, \quad (8.144)$$

where t_1 is the half-width of the Gaussian pulse defined by

$$f(t) = \frac{e^{-t^2/t_1^2}}{t_1\sqrt{\pi}}. \quad (8.145)$$

Thus, the exact formulas of the field components can be written in terms of several integrals.

$$\begin{aligned} t_1\sqrt{\pi}E_{2\rho}(\rho, 0; t) &= \frac{1}{2\pi\epsilon_0 c\rho^2} \left(I_1 + \varepsilon^{-1/2} I_2 \right) + \frac{1}{2\pi\epsilon_0(\varepsilon + 1)\rho^3} \\ &\times \left[I_3 - \frac{1}{\varepsilon - 1} \frac{\varepsilon^2}{(\varepsilon + 1)^{3/2}} I_4 + 2I_5 \right], \end{aligned} \quad (8.146)$$

$$\begin{aligned} t_1\sqrt{\pi}E_{2\phi}(\rho, \pi/2; t) &= \frac{1}{2\pi\epsilon_0 c(\varepsilon - 1)\rho^2} \left(I_1 - \varepsilon^{1/2} I_2 \right) + \frac{1}{2\pi\epsilon_0(\varepsilon - 1)\rho^3} \\ &\times \left[\left(2 - \frac{1}{\varepsilon + 1} \right) I_3 + \frac{\varepsilon^2}{(\varepsilon + 1)^{5/2}} I_6 + \frac{\varepsilon - 1}{\varepsilon + 1} I_5 \right], \end{aligned} \quad (8.147)$$

$$t_1\sqrt{\pi}B_{2z}(\rho, \pi/2; t) = \frac{\mu_0}{2\pi\rho^2} \frac{1}{\varepsilon - 1} (I_1 - \varepsilon I_2) - \frac{\mu_0 c}{2\pi\rho^3} \frac{3I_7}{\varepsilon - 1}. \quad (8.148)$$

The several integrals are as follows:

$$I_1 = \int_{-\infty}^{\infty} \delta\left(t - \frac{\rho}{c} - \zeta\right) e^{-\zeta^2/t_1^2} d\zeta, \quad (8.149)$$

$$I_2 = \int_{-\infty}^{\infty} \delta\left(t - \frac{\sqrt{\varepsilon}\rho}{c} - \zeta\right) e^{-\zeta^2/t_1^2} d\zeta, \quad (8.150)$$

$$I_3 = \int_{t-\sqrt{\varepsilon}\rho/c}^{t-\rho/c} e^{-\zeta^2/t_1^2} d\zeta, \quad (8.151)$$

$$I_4 = \int_{t-\sqrt{\varepsilon}\rho/c}^{t-\rho/c} \left[\frac{c^2(t-\zeta)^2}{\rho^2} + \frac{2\varepsilon}{\varepsilon + 1} \right] \left[\frac{c^2(t-\zeta)^2}{\rho^2} - \frac{\varepsilon}{\varepsilon + 1} \right]^{-5/2} e^{-\zeta^2/t_1^2} d\zeta, \quad (8.152)$$

$$I_5 = \int_{-\infty}^{t-\sqrt{\varepsilon}\rho/c} e^{-\zeta^2/t_1^2} d\zeta, \quad (8.153)$$

$$I_6 = \int_{t-\sqrt{\varepsilon}\rho/c}^{t-\rho/c} \left[\frac{c^2(t-\zeta)^2}{\rho^2} - \frac{\varepsilon}{\varepsilon + 1} \right]^{-3/2} e^{-\zeta^2/t_1^2} d\zeta, \quad (8.154)$$

$$I_7 = \int_{t-\sqrt{\varepsilon}\rho/c}^{t-\rho/c} \frac{c(t-\zeta)}{\rho} e^{-\zeta^2/t_1^2} d\zeta. \quad (8.155)$$

It is found that the integrals I_1 , I_2 , I_3 , and I_5 have been evaluated (King, Owens, and Wu, 1992). The results are

$$I_1 = e^{-(t' - \rho_1)^2}, \quad (8.156)$$

$$I_2 = e^{-(t' - \sqrt{\varepsilon}\rho_1)^2}, \quad (8.157)$$

$$I_3 = \frac{t_1\sqrt{\pi}}{2} [\operatorname{erf}(t' - \rho_1) - \operatorname{erf}(t' - \sqrt{\varepsilon}\rho_1)], \quad (8.158)$$

$$I_5 = \frac{t_1\sqrt{\pi}}{2} [1 + \operatorname{erf}(t' - \sqrt{\varepsilon}\rho_1)], \quad (8.159)$$

where

$$t' = \frac{t}{t_1}; \quad \rho_1 = \frac{\rho}{ct_1}, \quad (8.160)$$

and the error function is defined by

$$\operatorname{erf}(z) = \frac{2}{\sqrt{\pi}} \int_0^z e^{-t^2} dt. \quad (8.161)$$

Next, the main tasks are to evaluate the integrals I_4 , I_6 , and I_7 . For the purpose of evaluating those integrals, it is convenient to introduce the additional notations:

$$\zeta' = \frac{\zeta}{t_1}; \quad a^2 = \frac{\varepsilon}{\varepsilon + 1}. \quad (8.162)$$

Substituting Eq. (8.162) into Eqs. (8.152)~(8.154), we write

$$I_4 = t_1 \int_{t' - \sqrt{\varepsilon}\rho_1}^{t' - \rho_1} \left[\frac{(t' - \zeta')^2}{\rho_1^2} + 2a^2 \right] \left[\frac{(t' - \zeta')^2}{\rho_1^2} - a^2 \right]^{-5/2} e^{-\zeta'^2} d\zeta', \quad (8.163)$$

$$I_6 = t_1 \int_{t' - \sqrt{\varepsilon}\rho_1}^{t' - \rho_1} \left[\frac{(t' - \zeta')^2}{\rho_1^2} - a^2 \right]^{-3/2} e^{-\zeta'^2} d\zeta', \quad (8.164)$$

$$I_7 = t_1 \int_{t' - \sqrt{\varepsilon}\rho_1}^{t' - \rho_1} \frac{t' - \zeta'}{\rho_1} e^{-\zeta'^2} d\zeta'. \quad (8.165)$$

With the change of the variable $x = (t' - \zeta')/\rho_1$, $dx = -d\zeta'/\rho_1$, and $\zeta' = t' - \rho_1 x$, it follows that

$$I_4 = \rho_1 t_1 \int_1^{\sqrt{\varepsilon}} \frac{x^2 + 2a^2}{(x^2 - a^2)^{5/2}} e^{-(t' - \rho_1 x)^2} dx, \quad (8.166)$$

$$I_6 = \rho_1 t_1 \int_1^{\sqrt{\varepsilon}} \frac{e^{-(t' - \rho_1 x)^2}}{(x^2 - a^2)^{3/2}} dx, \quad (8.167)$$

$$I_7 = \rho_1 t_1 \int_1^{\sqrt{\varepsilon}} e^{-(t' - \rho_1 x)^2} x dx. \quad (8.168)$$

The above three integrals can be readily evaluated numerically.

8.3.2 Computations and Conclusions

We started this chapter with the exact formulas for the transient field due to a delta function current in a horizontal electric dipole on the planar boundary between two dielectrics. The final exact formulas for the transient field generated by a horizontal dipole with Gaussian excitation are expressed in terms of several fundamental functions and finite integrals.

The integrals I_4 , I_6 , and I_7 have been evaluated numerically and combined with the other integrals to give the field components $t_1 \sqrt{\pi} E_{2\rho}$, $t_1 \sqrt{\pi} E_{2\phi}$, and $t_1 \sqrt{\pi} B_{2z}$. From the above derivations and the numerical results shown in Figs. 8.4~8.6, it is concluded that the transient field component $t_1 \sqrt{\pi} E_{2\rho}$ consists of the two lateral pulses which decrease with the amplitude factor ρ^{-2} and travel in Region 2 with the velocity c and in Region 1 with the velocity $c/\varepsilon^{1/2}$. Similarly, the component $t_1 \sqrt{\pi} E_{2\phi}$ consists of the two pulses decreasing with the amplitude factor ρ^{-2} and travelling in Region 2 with the velocity c and in Region 1 with the velocity $c\varepsilon^{1/2}$.

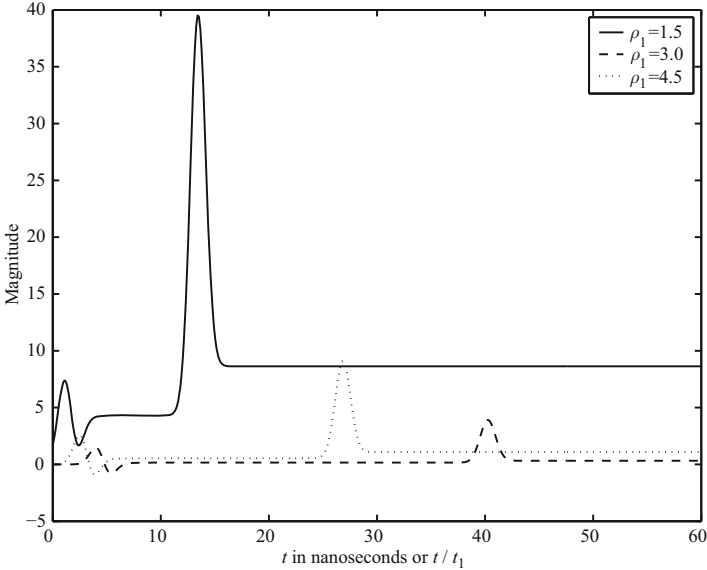


Fig. 8.4. Exact electric field $t_1 \sqrt{\pi} E_{2\rho}(\rho, 0; t)$ on the boundary in air due to a horizontal dipole on the boundary in a dielectric with relative permittivity $\varepsilon = 80$. The horizontal dipole is excited by a Gaussian pulse with $t_1 = 1$ nsec; $\rho_1 = \rho/ct_1$

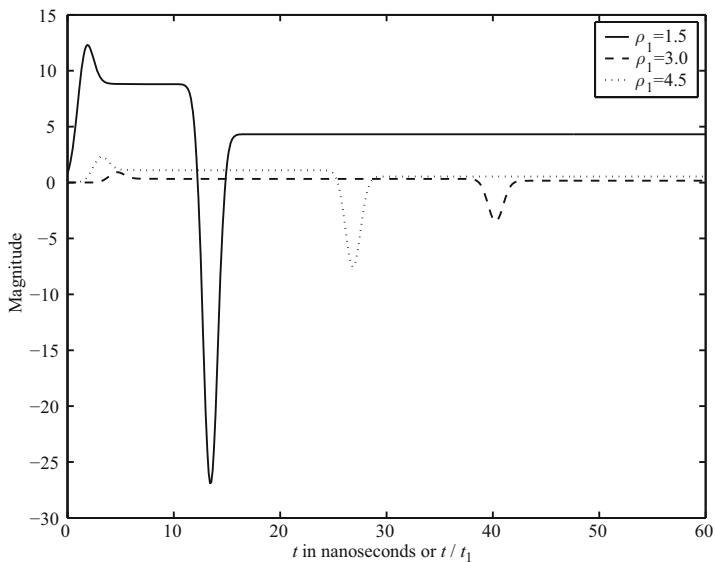


Fig. 8.5. Exact electric field $t_1\sqrt{\pi}E_{2\phi}(\rho, \pi/2; t)$ on the boundary in air due to a horizontal dipole on the boundary in a dielectric with relative permittivity $\varepsilon = 80$. The horizontal dipole is excited by a Gaussian pulse with $t_1 = 1$ nsec; $\rho_1 = \rho/ct_1$

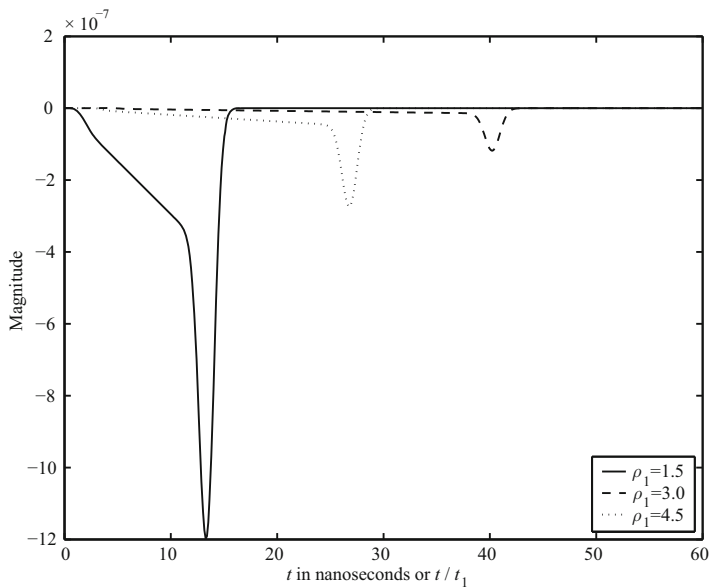


Fig. 8.6. Exact vertical magnetic field $t_1\sqrt{\pi}B_{2z}(\rho, \pi/2; t)$ on the boundary in air due to a horizontal dipole on the boundary in a dielectric with relative permittivity $\varepsilon = 80$. The horizontal dipole is excited by a Gaussian pulse with $t_1 = 1$ nsec; $\rho_1 = \rho/ct_1$

In actual fact, the second pulse for $t_1\sqrt{\pi}E_{2\rho}$ has a Gaussian shape with an amplitude that is very smaller than the first pulse. However, the term including the integral I_4 in Eq. (8.150) has a large negative value near the the first pulse, and this means that the second pulse has Gaussian shape with amplitude that is larger than the first one. The other two field components $t_1\sqrt{\pi}E_{2\phi}$ and $t_1\sqrt{\pi}B_{2z}$ have similar characteristics to those of the component $t_1\sqrt{\pi}E_{2\rho}$.

Similar to the the case of delta function excitation as addressed in the preceding section, the components $t_1\sqrt{\pi}E_{2z}$, $t_1\sqrt{\pi}B_{2\rho}$, and $t_1\sqrt{\pi}B_{2\phi}$ of a horizontal electric dipole with Gaussian excitation cannot be expressed in terms of elementary functions and finite integrals.

References

- Abamowitz M and Stegun IA (1972) *Handbook of Mathematical Functions*. New York, NY, USA: Dover Publications.
- Baños A Jr (1966) *Dipole Radiation in the Presence of a Conducting Half-Space*. Oxford, UK: Pergamon Press.
- Cicchetti R (1991) Transient analysis of radiated field from electric dipoles and microstrip lines. *IEEE Transactions on Antennas and Propagation*, 39(7): 910–918.
- Dai R and Young CT (1997) Transient fields of a horizontal electric dipole on multilayered dielectric medium. *IEEE Transactions on Antennas and Propagation*, 45(6): 1023–1031.
- De Hoop AT and Frankena HJ (1960) Radiation of pulses generated by a vertical electric dipole above a plane, non-conducting earth. *Applied Scientific Research*, Section B, 8: 369–377.
- Ezzeddine A, Kong JA, and Tsang L (1981a) Time response of a vertical electric dipole over a two-layer medium by the double deformation technique. *Journal of Applied Physics*, 53(2): 813–822.
- Ezzeddine A, Kong JA, and Tsang L (1981b) Transient fields of a vertical electric dipole over a two-layer nondispersive dielectric. *Journal of Applied Physics*, 53(3): 1202–1208.
- Frankena HJ (1960) Transient phenomena associated with Sommerfeld's horizontal dipole problem. *Applied Scientific Research*, Section B, 8: 357–368.
- Gradshteyn IS and Ryzhik IM (1980) *Table of Integrals, Series, and Products*. New York, NY, USA: Academic Press.
- King RWP (1982). New formulas for the electromagnetic field of a vertical electric dipole in a dielectric or conducting half-space near its horizontal interface. *Journal of Applied Physics*, 53: 8476–8482; (1984). Erratum, 56: 3366.
- King RWP and Wu TT (1983). Lateral waves: Formulas for the magnetic field. *Journal of Applied Physics*, 54: 507–514; (1984). Erratum, 56: 3365.
- King RWP (1984). Lateral electromagnetic waves along plane boundaries: A summarizing approach. *Proceedings of the IEEE*, 72: 595–611.

- King RWP (1986) Properties of the lateral electromagnetic field of a vertical dipole and their application. *IEEE Transactions on Geosciences and Remote Sensing*, GE-24: 813–825.
- King RWP, Owens M, and Wu TT (1986) Properties of lateral electromagnetic fields and their application. *Radio Science*, 21: 12–23.
- King RWP (1988) Lateral electromagnetic pulses generated by a vertical dipole on a plane boundary dielectrics. *Journal of Electromagnetic Waves and Applications*, 2: 225–243.
- King RWP (1989) Lateral electromagnetic pulses generated on a plane boundary between dielectrics by vertical and horizontal dipole source with Gaussian pulse excitation. *Journal of Electromagnetic Waves and Applications*, 2: 589–597.
- King RWP, Owens M, and Wu TT (1992) *Lateral Electromagnetic Waves: Theory and Applications to Communications, Geophysical Exploration, and Remote Sensing*. New York, NY, USA: Springer-Verlag.
- Li K, Lu Y, and Li M (2005) Approximate formulas for lateral electromagnetic pulses from a horizontal electric dipole on the surface of one-dimensionally anisotropic medium. *IEEE Transactions on Antennas and Propagation*, 53(3): 933–937.
- Li K, Lu Y, and Pan WY (2005a) Exact formulas for the lateral electromagnetic pulses generated by a horizontal electric dipole on the boundary of two dielectrics. *Progress In Electromagnetics Research*, PIER 55: 249–283. Cambridge, MA, USA: EMW Publishing.
- Li K, Lu Y, and Pan WY (2005b) Exact transient field of a horizontal electric dipole excited by a Gaussian pulse on the boundary between two dielectrics. *IEEE Antennas and Wireless Propagation Letters*, 4: 337–340.
- Margetis D (2001) Exactly calculable field components of electric dipoles in planar boundary. *Journal of Mathematical Physics*, 42: 713–745.
- Nikoskinen KI and Lindell IV (1990) Time-domain analysis of Sommerfeld VMD problem based on the exact image theory, *IEEE Transactions on Antennas and Propagation*, 38(2): 241–250.
- Nikoskinen KI (1990) Time-domain analysis of horizontal dipoles in front of planar dielectric interface. *IEEE Transactions on Antennas and Propagation*, 38(12): 1951–1957.
- Sommerfeld AN (1909). Propagation of waves in wireless telegraphy. *Annalen der Physik* (Leipzig), 28: 665–737.
- Sommerfeld AN (1926). Propagation of waves in wireless telegraphy. *Annalen der Physik*(Leipzig), 81: 1135–1153.
- Van der Pol B (1956) On discontinuous electromagnetic waves and occurrence of a surface wave. *IRE Transactions on Antennas and Propagation*, 4: 288–293.
- Wait JR (1957) The transient behavior of the electromagnetic ground wave on a spherical earth. *IRE Transactions on Antennas and Propagation*, AP5: 198–202.
- Wait JR (1970) *Electromagnetic Waves in Stratified Media* (2nd, Ed.). New York, NY, USA: Pergamon Press.
- Wait JR (1981) *Wave propagation Theory*. New York, NY, USA: Pergamon Press.
- Wu TT and King RWP (1987) Lateral electromagnetic pulses generated by a vertical dipole on the boundary between two dielectrics. *Journal of Applied Physics*, 62: 4345–4355.

- Xia MY, Chan CH, Xu Y, and Chew WC (2004) Time-domain Green's functions for microstrip structures using the Cagniard-de Hoop method. *IEEE Transactions on Antennas and Propagation*, 52(6): 1578–1585.
- Zenneck J (1907) Propagation of plane electromagnetic waves along a plane conducting surface and its bearing on the theory of transmission in wireless telegraphy. *Annalen der Physik* (Leipzig), 23: 846–866.

Approximate Transient Field of Horizontal Electric Dipole on the Boundary Between a Homogeneous Isotropic Medium and One-Dimensionally Anisotropic Medium

Approximate solutions are carried out for the transient field of a horizontal electric dipole with a delta function excitation and Gaussian excitation located on the planar boundary between a homogeneous isotropic medium and one-dimensionally anisotropic medium. The derivations and analysis show that the components of the electric field consist of two delta function lateral pulses which decrease with the amplitude factor $1/\rho^2$ and travel along the boundary with different velocities and different amplitudes. With the Gaussian excitation, the final formulas of the transient field are expressed in terms of several fundamental functions. In particular, the Fresnel-integral terms in those formulas do not completely cancel for the electric field components.

9.1 Statements of Problem

The approximate transient field and its applications due to a dipole with delta function excitation and Gaussian excitation have been examined analytically (King, 1988; 1989; 1990). In this chapter, further investigation will be extended to the anisotropic uniaxially case.

Consider a \hat{x} -directed horizontal electric dipole as shown in Fig. 9.1 at $(0, 0, d)$ in the upper half-space (Region 1, $z \geq 0$) with a homogeneous isotropic medium. Region 2 ($z \leq 0$) is the remaining half-space with a one-dimensionally anisotropic medium characterized by a permittivity tensor of the form

$$\hat{\epsilon}_2 = \epsilon_0 \begin{bmatrix} \epsilon_T & 0 & 0 \\ 0 & \epsilon_T & 0 \\ 0 & 0 & \epsilon_L \end{bmatrix}. \quad (9.1)$$

It is assumed that both regions are nonmagnetic so that $\mu_1 = \mu_2 = \mu_0$. The wave numbers of the two regions are

$$k_1 = \omega \sqrt{\mu_0 \epsilon_0 \epsilon_1} = \frac{\omega \sqrt{\epsilon_1}}{c}, \quad (9.2)$$

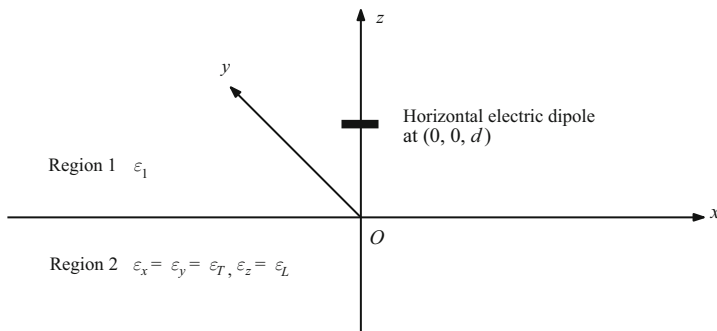


Fig. 9.1. Geometry of a \hat{x} -directed horizontal electric dipole on the boundary between a homogeneous, isotropic medium and one-dimensionally anisotropic medium

$$k_T = \omega \sqrt{\mu_0 \epsilon_0 \epsilon_T} = \frac{\omega \sqrt{\epsilon_T}}{c}, \quad (9.3)$$

$$k_L = \omega \sqrt{\mu_0 \epsilon_0 \epsilon_L} = \frac{\omega \sqrt{\epsilon_L}}{c}. \quad (9.4)$$

When the conditions

$$|k_1| \geq 3|k_L|; \quad |k_1| \geq 3|k_T|, \quad (9.5)$$

are satisfied, the approximate formulas are obtained for the frequency-domain electromagnetic field generated by a horizontal electric dipole on or near the planar boundary between a homogeneous isotropic medium and one-dimensionally anisotropic medium in the 1985 Pan's paper (Pan, 1985). By using Fourier's transform techniques, the corresponding formulas for the transient electromagnetic pulse with delta function excitation and Gaussian excitation are derived readily (Li and Lu, 2005; Xu, Li, and Ren, 2007).

9.2 The Approximate Transient Field with Delta Function Excitation

In the mid 1980's, the formulas were evaluated analytically for the frequency-domain field components generated by a horizontal electric dipole near the boundary between a homogeneous isotropic medium and one-dimensionally anisotropic medium (Pan, 1985). These approximate formulas for the three electric field components are rewritten in the following forms:

$$\begin{aligned}
E_{1\rho}(\rho, \phi, z) = & -\frac{\omega\mu_0}{2\pi k_1^2} \cos \phi \\
& \times \left(e^{ik_1(z+d)} \left\{ e^{ik_L\rho} \left[\frac{ik_L k_T}{\rho} - \frac{k_T}{\rho^2} \right. \right. \right. \\
& \quad \left. \left. - \frac{k_L^2 k_T^2}{k_1} \left(\frac{\pi}{k_L \rho} \right)^{1/2} e^{-ip_e \mathbf{F}(p_e)} \right] - \frac{ie^{ik_T \rho}}{\rho^3} \right\} \\
& \left. - e^{ik_1 r_1} \left(\frac{k_1}{\rho^2} + \frac{i}{\rho^3} \right) + e^{ik_1 r_2} \left(\frac{z+d}{\rho} \right) \left(\frac{ik_1}{\rho^2} - \frac{3}{2\rho^3} \right) \right), \tag{9.6}
\end{aligned}$$

$$\begin{aligned}
E_{1\phi}(\rho, \phi, z) = & \frac{\omega\mu_0}{2\pi k_1^2} \sin \phi \\
& \times \left(k_T e^{ik_1(z+d)} \left\{ e^{ik_L\rho} \left[\frac{1}{\rho^2} + \frac{ik_L k_T}{k_1 \rho} \left(\frac{\pi}{k_L \rho} \right)^{1/2} e^{-ip_e \mathbf{F}(p_e)} \right] \right. \right. \\
& \quad \left. \left. + e^{ik_T \rho} \left(\frac{1}{\rho^2} + \frac{2i}{k_T \rho^3} \right) \right\} \right. \\
& + \frac{k_1}{2} \left[e^{ik_1 r_2} \left(\frac{ik_1}{\rho} - \frac{3}{\rho^2} - \frac{3i}{k_1 \rho^3} \right) \right. \\
& \quad \left. - e^{ik_1 r_1} \left(\frac{ik_1}{\rho} - \frac{1}{\rho^2} - \frac{i}{k_1 \rho^3} \right) \right] \\
& \left. + ik_1 e^{ik_1 r_2} \left(\frac{z+d}{\rho} \right) \left(\frac{ik_1}{\rho} - \frac{3}{2\rho^2} - \frac{5i}{8k_1 \rho^3} \right) \right), \tag{9.7}
\end{aligned}$$

$$\begin{aligned}
E_{1z}(\rho, \phi, z) = & \frac{\omega\mu_0}{2\pi k_1^2} \cos \phi \\
& \times \left(\frac{k_L k_T}{k_1} \left\{ e^{ik_1(z+d)} e^{ik_L\rho} \left[\frac{ik_L}{\rho} - \frac{1}{\rho^2} - \frac{k_L^2 k_T}{k_1} \right. \right. \right. \\
& \quad \left. \left. \times \left(\frac{\pi}{k_L \rho} \right)^{1/2} e^{-ip_e \mathbf{F}(p_e)} \right] - e^{ik_1 r_2} \left(\frac{i}{\rho^2} - \frac{3}{2k_1 \rho^3} \right) \right\} \right. \\
& \left. - \frac{1}{2} \left[e^{ik_1 r_1} \left(\frac{z-d}{\rho} \right) + e^{ik_1 r_2} \left(\frac{z+d}{\rho} \right) \right] \right. \\
& \left. \times \left(\frac{ik_1^2}{\rho} - \frac{3k_1}{\rho^2} - \frac{3i}{\rho^3} \right) \right). \tag{9.8}
\end{aligned}$$

In these formulas, $r_1 = \sqrt{\rho^2 + (z-d)^2}$, $r_2 = \sqrt{\rho^2 + (z+d)^2}$, p_e and the Fresnel integral $\mathbf{F}(p_e)$ are defined by

$$p_e = k_L \rho \left(\frac{k_T^2}{2k_1^2} \right), \quad (9.9)$$

and

$$\mathbf{F}(p_e) = \frac{1}{2}(1 + i) - C_2(p_e) - iS_2(p_e), \quad (9.10)$$

where

$$C_2(p_e) + iS_2(p_e) = \int_0^{p_e} \frac{e^{it}}{(2\pi t)^{1/2}} dt. \quad (9.11)$$

With $z = d = 0$, $k_1 = \omega \varepsilon_1^{1/2}/c$, $k_T = \omega \varepsilon_T^{1/2}/c$, $k_L = \omega \varepsilon_L^{1/2}/c$, and $\rho' = \rho/c$, we have

$$\begin{aligned} \tilde{E}_{1\rho}(\rho', 0; \omega) = & -\frac{\mu_0}{2\pi\varepsilon_1 c} \left\{ e^{i\omega\sqrt{\varepsilon_L}\rho'} \left[\frac{i\omega\sqrt{\varepsilon_L\varepsilon_T}}{\rho'} - \frac{\sqrt{\varepsilon_T}}{\rho'^2} \right. \right. \\ & \left. \left. - \omega^{\frac{3}{2}}\varepsilon_L\varepsilon_T \left(\frac{\pi}{\varepsilon_1\sqrt{\varepsilon_L}\rho'} \right)^{1/2} e^{-ip\mathbf{F}(p)} \right] \right. \\ & \left. - \frac{i e^{i\omega\sqrt{\varepsilon_T}\rho'}}{\omega\rho'^3} - e^{i\omega\sqrt{\varepsilon_1}\rho'} \left(\frac{\sqrt{\varepsilon_1}}{\rho'^2} + \frac{i}{\omega\rho'^3} \right) \right\}, \quad (9.12) \end{aligned}$$

$$\begin{aligned} \tilde{E}_{1\phi}(\rho', \pi/2; \omega) = & \frac{\mu_0}{2\pi\varepsilon_1 c} \left(\sqrt{\varepsilon_T} \left\{ e^{i\omega\sqrt{\varepsilon_L}\rho'} \right. \right. \\ & \times \left[\frac{1}{\rho'^2} + \frac{i\sqrt{\omega}\sqrt{\varepsilon_L\varepsilon_T}}{\rho'} \left(\frac{\pi}{\varepsilon_1\sqrt{\varepsilon_L}\rho'} \right)^{1/2} e^{-ip\mathbf{F}(p)} \right] \\ & \left. + e^{i\omega\sqrt{\varepsilon_T}\rho'} \left(\frac{1}{\rho'^2} + \frac{2i}{\omega\sqrt{\varepsilon_T}\rho'^3} \right) \right\} \\ & \left. - e^{i\omega\sqrt{\varepsilon_1}\rho'} \left(\frac{\sqrt{\varepsilon_1}}{\rho'^2} + \frac{i}{\omega\rho'^3} \right) \right), \quad (9.13) \end{aligned}$$

$$\begin{aligned} \tilde{E}_{1z}(\rho', 0; \omega) = & \frac{\mu_0}{2\pi\varepsilon_1 c} \frac{\sqrt{\varepsilon_L\varepsilon_T}}{\sqrt{\varepsilon_1}} \left\{ e^{i\omega\sqrt{\varepsilon_L}\rho'} \left[\frac{i\omega\sqrt{\varepsilon_L}}{\rho'} - \frac{1}{\rho'^2} \right. \right. \\ & \left. \left. - \omega^{\frac{3}{2}}\varepsilon_L\sqrt{\varepsilon_T} \left(\frac{\pi}{\varepsilon_1\sqrt{\varepsilon_L}\rho'} \right)^{1/2} e^{-ip\mathbf{F}(p)} \right] \right. \\ & \left. - e^{i\omega\sqrt{\varepsilon_1}\rho'} \left(\frac{i}{\rho'^2} - \frac{3}{2\omega\sqrt{\varepsilon_1}\rho'^3} \right) \right\}, \quad (9.14) \end{aligned}$$

where

$$p = \frac{\omega \rho' \varepsilon_T \sqrt{\varepsilon_L}}{2\varepsilon_1}; \quad \mathbf{F}(p) = \frac{1}{2}(1 + i) - \int_0^p \frac{e^{i\tau}}{(2\pi\tau)^{1/2}} d\tau. \quad (9.15)$$

With a delta function excitation, the time-dependent electric field components are the transforms of the corresponding frequency-domain field components. The time-dependent electric field components are expressed in the forms

$$\begin{aligned} E_{1\rho}(\rho', 0; t) &= \operatorname{Re} \frac{1}{\pi} \int_0^\infty e^{-i\omega t} \tilde{E}_{1\rho}(\rho', 0; \omega) d\omega \\ &= -\frac{\mu_0}{2\pi\varepsilon_1 c} \left(\frac{\sqrt{\varepsilon_L \varepsilon_T} I_1}{\rho'} - \frac{\sqrt{\varepsilon_T} I_2}{\rho'^2} - \frac{I_3}{\rho'^3} \right. \\ &\quad \left. + \frac{\varepsilon_L \varepsilon_T I_5}{\sqrt{\pi\varepsilon_1 \sqrt{\varepsilon_L} \rho'}} - \frac{\sqrt{\varepsilon_1} I_7}{\rho'^2} - \frac{I_8}{\rho'^3} \right), \end{aligned} \quad (9.16)$$

$$\begin{aligned} E_{1\phi}(\rho', \pi/2; t) &= \operatorname{Re} \frac{1}{\pi} \int_0^\infty e^{-i\omega t} \tilde{E}_{1\phi}(\rho', \pi/2; \omega) d\omega \\ &= \frac{\mu_0}{2\pi\varepsilon_1 c} \left(\frac{\sqrt{\varepsilon_T} I_2}{\rho'^2} - \frac{\varepsilon_T \sqrt{\varepsilon_L} I_6}{\sqrt{\pi\varepsilon_1 \sqrt{\varepsilon_L} \rho'^{3/2}}} + \frac{\sqrt{\varepsilon_T} I_4}{\rho'^2} \right. \\ &\quad \left. + \frac{2I_3}{\rho'^3} - \frac{\sqrt{\varepsilon_1} I_7}{\rho'^2} - \frac{I_8}{\rho'^3} \right), \end{aligned} \quad (9.17)$$

$$\begin{aligned} E_{1z}(\rho', 0; t) &= \operatorname{Re} \frac{1}{\pi} \int_0^\infty e^{-i\omega t} \tilde{E}_{1z}(\rho', 0; \omega) d\omega \\ &= \frac{\mu_0}{2\pi\varepsilon_1 c} \frac{\sqrt{\varepsilon_L \varepsilon_T}}{\sqrt{\varepsilon_1}} \left(\frac{\sqrt{\varepsilon_L} I_1}{\rho'} - \frac{I_2}{\rho'^2} + \frac{\varepsilon_L \sqrt{\varepsilon_T} I_5}{\sqrt{\pi\varepsilon_1 \sqrt{\varepsilon_L} \rho'}} \right. \\ &\quad \left. - \frac{iI_7}{\rho'^2} - \frac{i3I_8}{2\sqrt{\varepsilon_1} \rho'^3} \right), \end{aligned} \quad (9.18)$$

where

$$I_1 = \operatorname{Re} \frac{1}{\pi} \int_0^\infty i\omega e^{-i\omega(t - \sqrt{\varepsilon_L} \rho')} d\omega, \quad (9.19)$$

$$I_2 = \operatorname{Re} \frac{1}{\pi} \int_0^\infty e^{-i\omega(t - \sqrt{\varepsilon_L} \rho')} d\omega, \quad (9.20)$$

$$I_3 = \operatorname{Re} \frac{1}{\pi} \int_0^\infty \frac{i}{\omega} e^{-i\omega(t - \sqrt{\varepsilon_T} \rho')} d\omega, \quad (9.21)$$

$$I_4 = \operatorname{Re} \frac{1}{\pi} \int_0^\infty e^{-i\omega(t - \sqrt{\varepsilon_T} \rho')} d\omega, \quad (9.22)$$

$$I_5 = -\text{Re} \int_0^\infty \omega^{\frac{3}{2}} e^{-i\omega(t - \sqrt{\varepsilon_L}\rho' + \frac{\varepsilon_T\sqrt{\varepsilon_L}}{2\varepsilon_1}\rho')} \times \left[\frac{1}{2}(1+i) - \int_0^{\frac{\omega\rho'\varepsilon_T\sqrt{\varepsilon_L}}{2\varepsilon_1}} \frac{e^{i\tau}}{(2\pi\tau)^{1/2}} d\tau \right] d\omega, \quad (9.23)$$

$$I_6 = -\text{Re} \int_0^\infty i\omega^{\frac{1}{2}} e^{-i\omega(t - \sqrt{\varepsilon_L}\rho' + \frac{\varepsilon_T\sqrt{\varepsilon_L}}{2\varepsilon_1}\rho')} \times \left[\frac{1}{2}(1+i) - \int_0^{\frac{\omega\rho'\varepsilon_T\sqrt{\varepsilon_L}}{2\varepsilon_1}} \frac{e^{i\tau}}{(2\pi\tau)^{1/2}} d\tau \right] d\omega, \quad (9.24)$$

$$I_7 = \text{Re} \frac{1}{\pi} \int_0^\infty e^{-i\omega(t - \sqrt{\varepsilon_1}\rho')} d\omega, \quad (9.25)$$

$$I_8 = \text{Re} \frac{1}{\pi} \int_0^\infty \frac{i}{\omega} e^{-i\omega(t - \sqrt{\varepsilon_1}\rho')} d\omega. \quad (9.26)$$

Similar to the manner addressed in the book by King, Owens, and Wu (1992), the integrals of Eqs. (9.19)~(9.26) are evaluated exactly as follows:

$$I_1 = -\delta'(t - \sqrt{\varepsilon_L}\rho'), \quad (9.27)$$

$$I_2 = \delta(t - \sqrt{\varepsilon_L}\rho'), \quad (9.28)$$

$$I_3 = \begin{cases} 1, & t > \sqrt{\varepsilon_T}\rho' \\ 0, & t < \sqrt{\varepsilon_T}\rho' \end{cases}, \quad (9.29)$$

$$I_4 = \delta(t - \sqrt{\varepsilon_T}\rho'), \quad (9.30)$$

$$I_5 = \left(\frac{\pi}{2}\right)^{1/2} \left[\left(\frac{2\varepsilon_1}{\varepsilon_T\sqrt{\varepsilon_L}\rho'}\right)^{1/2} \delta'(t - \sqrt{\varepsilon_L}\rho') - \frac{1}{2} \left(\frac{2\varepsilon_1}{\varepsilon_T\sqrt{\varepsilon_L}\rho'}\right)^{3/2} \delta(t - \sqrt{\varepsilon_L}\rho') + \frac{3}{4} \left(t - \sqrt{\varepsilon_L}\rho' + \frac{\varepsilon_T\sqrt{\varepsilon_L}\rho'}{2\varepsilon_1}\right)^{-5/2} U(t - \sqrt{\varepsilon_L}\rho') \right], \quad (9.31)$$

$$I_6 = \left(\frac{\pi}{2}\right)^{1/2} \left[\left(\frac{2\varepsilon_1}{\varepsilon_T\sqrt{\varepsilon_L}\rho'}\right)^{1/2} \delta(t - \sqrt{\varepsilon_L}\rho') - \frac{1}{2} \left(t - \sqrt{\varepsilon_L}\rho' + \frac{\varepsilon_T\sqrt{\varepsilon_L}\rho'}{2\varepsilon_1}\right)^{-3/2} U(t - \sqrt{\varepsilon_L}\rho') \right], \quad (9.32)$$

$$I_7 = \delta(t - \sqrt{\varepsilon_1}\rho'), \quad (9.33)$$

$$I_8 = \begin{cases} 1, & t > \sqrt{\varepsilon_1}\rho' \\ 0, & t < \sqrt{\varepsilon_1}\rho' \end{cases}. \quad (9.34)$$

With substitutions Eqs. (9.27)~(9.34) into Eqs. (9.16)~(9.18) and ρ' replaced by ρ/c , the approximate formulas of the time-dependent electric field components are written readily.

$$E_{1\rho}(\rho, 0; t) = \frac{1}{2\pi\varepsilon_0 c\rho^2} \left[\frac{1}{\sqrt{\varepsilon_T}} \left(1 + \frac{\varepsilon_T}{\varepsilon_1} \right) \delta \left(t - \frac{\sqrt{\varepsilon_L}\rho}{c} \right) + \frac{1}{\sqrt{\varepsilon_1}} \delta \left(t - \frac{\sqrt{\varepsilon_1}\rho}{c} \right) \right] \\ + \frac{1}{2\pi\varepsilon_0\varepsilon_1\rho^3} \left\{ \begin{array}{c} 0 \\ -3\varepsilon_1^2\varepsilon_T\varepsilon_L^{3/4} \left[2\varepsilon_1 \left(\frac{ct}{\rho} - \sqrt{\varepsilon_L} \right) + \varepsilon_T\sqrt{\varepsilon_L} \right]^{-\frac{5}{2}} \\ 1 - 3\varepsilon_1^2\varepsilon_T\varepsilon_L^{3/4} \left[2\varepsilon_1 \left(\frac{ct}{\rho} - \sqrt{\varepsilon_L} \right) + \varepsilon_T\sqrt{\varepsilon_L} \right]^{-\frac{5}{2}} \\ 2 - 3\varepsilon_1^2\varepsilon_T\varepsilon_L^{3/4} \left[2\varepsilon_1 \left(\frac{ct}{\rho} - \sqrt{\varepsilon_L} \right) + \varepsilon_T\sqrt{\varepsilon_L} \right]^{-\frac{5}{2}} \end{array} \right\}; \quad (9.35)$$

$$\begin{array}{c} ct/\rho < \sqrt{\varepsilon_L} \\ \sqrt{\varepsilon_L} < ct/\rho < \sqrt{\varepsilon_T} \\ \sqrt{\varepsilon_T} < ct/\rho < \sqrt{\varepsilon_1} \\ ct/\rho > \sqrt{\varepsilon_1} \end{array},$$

$$E_{1\phi}(\rho, \pi/2; t) = \frac{1}{2\pi\varepsilon_0\varepsilon_1 c\rho^2} \left[\sqrt{\varepsilon_T}\delta \left(t - \frac{\sqrt{\varepsilon_T}\rho}{c} \right) - \sqrt{\varepsilon_1}\delta \left(t - \frac{\sqrt{\varepsilon_1}\rho}{c} \right) \right] \\ + \frac{1}{2\pi\varepsilon_0\varepsilon_1\rho^3} \left\{ \begin{array}{c} 0 \\ \varepsilon_1\varepsilon_T\varepsilon_L^{1/4} \left[2\varepsilon_1 \left(\frac{ct}{\rho} - \sqrt{\varepsilon_L} \right) + \varepsilon_T\sqrt{\varepsilon_L} \right]^{-\frac{3}{2}} \\ 2 + \varepsilon_1\varepsilon_T\varepsilon_L^{1/4} \left[2\varepsilon_1 \left(\frac{ct}{\rho} - \sqrt{\varepsilon_L} \right) + \varepsilon_T\sqrt{\varepsilon_L} \right]^{-\frac{3}{2}} \\ 1 + \varepsilon_1\varepsilon_T\varepsilon_L^{1/4} \left[2\varepsilon_1 \left(\frac{ct}{\rho} - \sqrt{\varepsilon_L} \right) + \varepsilon_T\sqrt{\varepsilon_L} \right]^{-\frac{3}{2}} \end{array} \right\}; \quad (9.36)$$

$$\begin{array}{c} ct/\rho < \sqrt{\varepsilon_L} \\ \sqrt{\varepsilon_L} < ct/\rho < \sqrt{\varepsilon_T} \\ \sqrt{\varepsilon_T} < ct/\rho < \sqrt{\varepsilon_1} \\ ct/\rho > \sqrt{\varepsilon_1} \end{array},$$

$$E_{1z}(\rho, 0; t) = -\frac{1}{2\pi\varepsilon_0\sqrt{\varepsilon_1}c\rho^2} \sqrt{\frac{\varepsilon_L}{\varepsilon_T}} \left(1 + \frac{\varepsilon_T}{\varepsilon_1} \right) \delta \left(t - \frac{\sqrt{\varepsilon_L}\rho}{c} \right) \\ + \frac{1}{2\pi\varepsilon_0\varepsilon_1\rho^3} \left\{ \begin{array}{c} 0 \\ 3\varepsilon_1^{3/2}\varepsilon_T\varepsilon_L^{5/4} \left[2\varepsilon_1 \left(\frac{ct}{\rho} - \sqrt{\varepsilon_L} \right) + \varepsilon_T\sqrt{\varepsilon_L} \right]^{-\frac{5}{2}} \end{array} \right\};$$

$$\begin{aligned} ct/\rho &< \sqrt{\varepsilon_L} \\ ct/\rho &> \sqrt{\varepsilon_L}. \end{aligned} \quad (9.37)$$

For the transient field due to a horizontal electric dipole on the boundary between a homogeneous isotropic medium and one-dimensionally anisotropic medium, the significant features of Eqs. (9.35)~(9.37) are addressed as follows:

- At any radical distance ρ , both $E_{1\rho}$ and E_{1z} consist of two delta function pulses that travel along the boundary with the velocities $c/\sqrt{\varepsilon_L}$ and $c/\sqrt{\varepsilon_1}$ and arrive at $t = \rho\sqrt{\varepsilon_L}/c$ and $t = \rho\sqrt{\varepsilon_1}/c$. Similarly, $E_{1\phi}$ consists of two delta function pulses with the velocities $c/\sqrt{\varepsilon_T}$ and $c/\sqrt{\varepsilon_1}$ and arrive at $t = \rho\sqrt{\varepsilon_T}/c$ and $t = \rho\sqrt{\varepsilon_1}/c$.
- When both the dipole and observation point are located on the boundary, the lateral pulses decrease with the amplitude factor $1/\rho^2$.
- For $E_{1\rho}$, it is seen that both the amplitudes of the first and second pulses are $\sqrt{\varepsilon_T}/(1 + \varepsilon_T/\varepsilon_1)$ and $1/\sqrt{\varepsilon_1}$, respectively. When the conditions in Eq. (9.5) are satisfied, the amplitude factor of the second pulse is very small compared to that of the first one. Similarly, for E_{1z} , the amplitude of the second pulse with the factor $\sqrt{\varepsilon_L\varepsilon_T}/\varepsilon_1$ also very small compared to that of the first one with $\sqrt{\varepsilon_L/\varepsilon_T}/(1 + \varepsilon_T/\varepsilon_1)$. In contrast, for $E_{1\phi}$, the amplitude of the second pulse with the factor $\sqrt{\varepsilon_1}$ is large compared to that of the first one with $\sqrt{\varepsilon_T}$.

From Eqs. (9.35)~(9.37), the complete transient electric field components of a horizontal electric dipole with delta function excitation at all points on the surface are given by

$$E_{1\rho}(\rho, \phi; t) = E_{1\rho}(\rho, 0; t) \cos \phi, \quad (9.38)$$

$$E_{1\phi}(\rho, \phi; t) = E_{1z}(\rho, \pi/2; t) \sin \phi, \quad (9.39)$$

$$E_{1z}(\rho, \phi; t) = E_{1z}(\rho, 0; t) \cos \phi. \quad (9.40)$$

With $\varepsilon_1 = 80$, $\varepsilon_T = 4$, and $\varepsilon_L = 2$, a graph of $E_{1\rho}(\rho, 0; t)$ due to a horizontal electric dipole on the boundary between a homogeneous isotropic medium and one-dimensionally anisotropic medium is shown in Fig. 9.2. In contrast to that of an anisotropic case, a graph for the corresponding isotropic case with $\varepsilon_1 = 80$ and $\varepsilon_2 = 1$ is also computed and plotted in Fig. 9.2. It is seen that when $ct/\rho > \sqrt{\varepsilon_T}$, the graph for the anisotropic case is closer to that for the isotropic case, namely the effect by the anisotropic properties is small under the condition of $ct/\rho > \sqrt{\varepsilon_T}$. The properties of $E_{1\phi}(\rho, \pi/2; t)$ and $E_{1z}(\rho, 0; t)$ are similar to that of $E_{1\rho}(\rho, 0; t)$.

From the above derivations and computations, it is seen that the three time-dependent electric field components consist of two delta function lateral pulses which decrease with an amplitude factor ρ^{-2} and travel along the boundary with different velocities and different amplitudes.

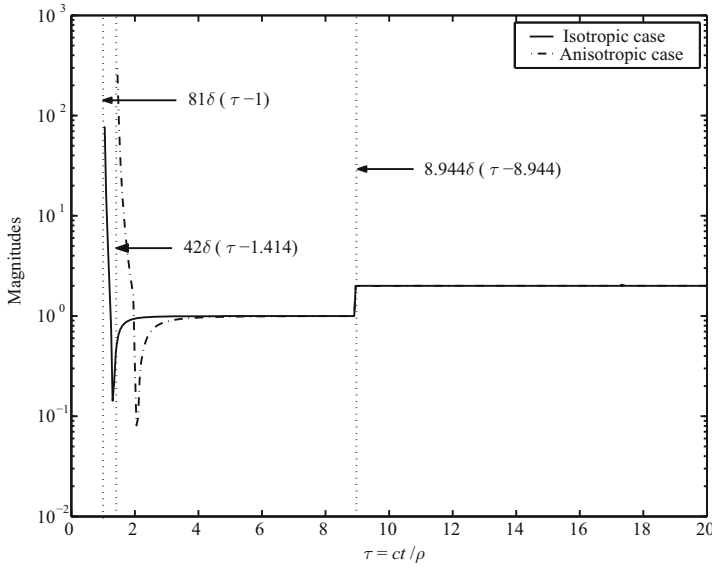


Fig. 9.2. Comparison between the electric field $E_{1\rho}(\rho, 0; t)$ in the anisotropic case with $\varepsilon_1 = 80$, $\varepsilon_T = 4$, and $\varepsilon_L = 2$ and that in the isotropic case with $\varepsilon_1 = 80$ and $\varepsilon_2 = 1$

When the dipole source is placed at the height d , the formulas can be derived for the components of the electric field at the height z . Subject to $\rho \geq 5|z|$ and $\rho \geq 5d$, the formula for $E_{1\rho}(\rho, 0; t)$ is written in the form

$$\begin{aligned}
 E_{1\rho}(\rho, 0, z; t) = & \frac{1}{2\pi\varepsilon_0 c\rho^2} \left[\frac{1}{\sqrt{\varepsilon_T}} \left(1 + \frac{\varepsilon_T}{\varepsilon_1} \right) \delta \left(t - \frac{\sqrt{\varepsilon_L} s_L}{c} \right) \right. \\
 & \left. + \frac{1}{\sqrt{\varepsilon_1}} \delta \left(t - \frac{\sqrt{\varepsilon_1} r_1}{c} \right) \right] + \frac{1}{2\pi\varepsilon_0 \varepsilon_1 \rho^3} \\
 & \times \left\{ \begin{array}{l} 0 \\ -3\varepsilon_1^2 \varepsilon_T \varepsilon_L^{3/4} \left[2\varepsilon_1 \left(\frac{ct - \sqrt{\varepsilon_L} s_L}{\rho} \right) + \varepsilon_T \sqrt{\varepsilon_L} \right]^{-5/2} \\ 1 - 3\varepsilon_1^2 \varepsilon_T \varepsilon_L^{3/4} \left[2\varepsilon_1 \left(\frac{ct - \sqrt{\varepsilon_L} s_L}{\rho} \right) + \varepsilon_T \sqrt{\varepsilon_L} \right]^{-5/2} \\ 2 - 3\varepsilon_1^2 \varepsilon_T \varepsilon_L^{3/4} \left[2\varepsilon_1 \left(\frac{ct - \sqrt{\varepsilon_L} s_L}{\rho} \right) + \varepsilon_T \sqrt{\varepsilon_L} \right]^{-5/2} \end{array} \right\}; \\
 & \begin{array}{l} ct < \sqrt{\varepsilon_L} s_L \\ \sqrt{\varepsilon_L} s_L < ct < \sqrt{\varepsilon_T} s_T \\ \sqrt{\varepsilon_T} s_T < ct < \sqrt{\varepsilon_1} r_1 \\ ct > \sqrt{\varepsilon_1} r_1 \end{array}, \quad (9.41)
 \end{aligned}$$

where

$$s_L = \rho + \sqrt{\varepsilon_1/\varepsilon_L}(z + d), \quad (9.42)$$

$$s_T = \rho + \sqrt{\varepsilon_1/\varepsilon_T}(z + d), \quad (9.43)$$

$$r_1 = [\rho^2 + (z - d)^2]^{1/2}. \quad (9.44)$$

In a similar manner, the final formulas for the other two transient electric field components can also be obtained readily.

9.3 Approximate Formulas for the Transient Field with Gaussian Excitation

In what follows, we will attempt to treat the approximate transient field of a horizontal electric dipole excited by a Gaussian pulse on the plane boundary between a homogeneous isotropic medium and one-dimensionally anisotropic medium. The normalized Gaussian pulse is defined by

$$f(t) = \frac{e^{-t^2/t_1^2}}{\sqrt{\pi}t_1}, \quad (9.45)$$

where t_1 is the half-width of the Gaussian pulse. Correspondingly, the Fourier transform of the Gaussian pulse is written in the form

$$\tilde{f}(\omega) = \int_{-\infty}^{\infty} \frac{e^{-t^2/t_1^2}}{\sqrt{\pi}t_1} e^{i\omega t} dt = e^{-\omega^2 t_1^2/4}. \quad (9.46)$$

To examine the transient electric field with Gaussian excitation, use is made of the available approximate formulas in Eqs. (9.12)~(9.14) for the frequency-domain field. The corresponding formulas in the time domain can be expressed in the following forms:

$$\begin{aligned} E_{1\rho}(\rho', 0; t) &= \text{Re} \frac{1}{2\pi} \int_{-\infty}^{\infty} e^{-i\omega t} \tilde{f}(\omega) \tilde{E}_{1\rho}(\rho', 0; \omega) d\omega \\ &= -\frac{\mu_0}{2\pi\varepsilon_1 c} \left(\frac{\sqrt{\varepsilon_L \varepsilon_T} I_1}{\rho'} - \frac{\sqrt{\varepsilon_T} I_2}{\rho'^2} - \frac{I_3}{\rho'^3} \right. \\ &\quad \left. + \frac{\varepsilon_L \varepsilon_T I_5}{\sqrt{\pi \varepsilon_1 \sqrt{\varepsilon_L \rho'}}} - \frac{\sqrt{\varepsilon_1} I_7}{\rho'^2} - \frac{I_8}{\rho'^3} \right), \end{aligned} \quad (9.47)$$

$$\begin{aligned} E_{1\phi}(\rho', \pi/2; t) &= \text{Re} \frac{1}{2\pi} \int_{-\infty}^{\infty} e^{-i\omega t} \tilde{f}(\omega) \tilde{E}_{1\phi}(\rho', \pi/2; \omega) d\omega \\ &= \frac{\mu_0}{2\pi\varepsilon_1 c} \left(\frac{\sqrt{\varepsilon_T} I_2}{\rho'^2} - \frac{\varepsilon_T \sqrt{\varepsilon_L} I_6}{\sqrt{\pi \varepsilon_1 \sqrt{\varepsilon_L \rho'^3/2}}} \right) \end{aligned}$$

$$+ \frac{\sqrt{\varepsilon_T} I_4}{\rho'^2} + \frac{2I_3}{\rho'^3} - \frac{\sqrt{\varepsilon_1} I_7}{\rho'^2} - \frac{I_8}{\rho'^3} \Bigg), \quad (9.48)$$

$$\begin{aligned} E_{1z}(\rho', 0; t) &= \operatorname{Re} \frac{1}{2\pi} \int_{-\infty}^{\infty} e^{-i\omega t} \tilde{f}(\omega) \tilde{E}_{1z}(\rho', 0; \omega) d\omega \\ &= \frac{\mu_0}{2\pi\varepsilon_1 c} \frac{\sqrt{\varepsilon_L \varepsilon_T}}{\sqrt{\varepsilon_1}} \left(\frac{\sqrt{\varepsilon_L} I_1}{\rho'} - \frac{I_2}{\rho'^2} + \frac{\varepsilon_L \sqrt{\varepsilon_T} I_5}{\sqrt{\pi\varepsilon_1 \sqrt{\varepsilon_L} \rho'}} \right), \end{aligned} \quad (9.49)$$

where

$$I_1 = \operatorname{Re} \frac{1}{2\pi} \int_{-\infty}^{\infty} i\omega e^{-\omega^2 t_1^2/4} e^{-i\omega(t-\sqrt{\varepsilon_L}\rho')} d\omega, \quad (9.50)$$

$$I_2 = \operatorname{Re} \frac{1}{2\pi} \int_{-\infty}^{\infty} e^{-\omega^2 t_1^2/4} e^{-i\omega(t-\sqrt{\varepsilon_L}\rho')} d\omega, \quad (9.51)$$

$$I_3 = \operatorname{Re} \frac{1}{2\pi} \int_{-\infty}^{\infty} \frac{i}{\omega} e^{-\omega^2 t_1^2/4} e^{-i\omega(t-\sqrt{\varepsilon_T}\rho')} d\omega, \quad (9.52)$$

$$I_4 = \operatorname{Re} \frac{1}{2\pi} \int_{-\infty}^{\infty} e^{-\omega^2 t_1^2/4} e^{-i\omega(t-\sqrt{\varepsilon_T}\rho')} d\omega, \quad (9.53)$$

$$\begin{aligned} I_5 &= -\operatorname{Re} \frac{1}{2} \int_{-\infty}^{\infty} \omega^{\frac{3}{2}} e^{-\omega^2 t_1^2/4} e^{-i\omega\left(t-\sqrt{\varepsilon_L}\rho' + \frac{\varepsilon_T \sqrt{\varepsilon_L}}{2\varepsilon_1} \rho'\right)} \\ &\quad \times \left[\frac{1}{2}(1+i) - \int_0^p \frac{e^{i\tau}}{(2\pi\tau)^{1/2}} d\tau \right] d\omega, \end{aligned} \quad (9.54)$$

$$\begin{aligned} I_6 &= -\operatorname{Re} \frac{1}{2} \int_{-\infty}^{\infty} i\omega^{\frac{1}{2}} e^{-\omega^2 t_1^2/4} e^{-i\omega\left(t-\sqrt{\varepsilon_L}\rho' + \frac{\varepsilon_T \sqrt{\varepsilon_L}}{2\varepsilon_1} \rho'\right)} \\ &\quad \times \left[\frac{1}{2}(1+i) - \int_0^p \frac{e^{i\tau}}{(2\pi\tau)^{1/2}} d\tau \right] d\omega, \end{aligned} \quad (9.55)$$

$$I_7 = \operatorname{Re} \frac{1}{2\pi} \int_{-\infty}^{\infty} e^{-\omega^2 t_1^2/4} e^{-i\omega(t-\sqrt{\varepsilon_1}\rho')} d\omega, \quad (9.56)$$

$$I_8 = \operatorname{Re} \frac{1}{2\pi} \int_{-\infty}^{\infty} \frac{i}{\omega} e^{-\omega^2 t_1^2/4} e^{-i\omega(t-\sqrt{\varepsilon_1}\rho')} d\omega. \quad (9.57)$$

Examination of these integrals reveals that

$$I_1 = -\frac{\partial I_2}{\partial t}; \quad \frac{\partial I_3}{\partial t} = I_4; \quad \frac{\partial I_8}{\partial t} = I_7. \quad (9.58)$$

With the notations

$$\tau_L \equiv t - \sqrt{\varepsilon_L} \rho' = t - \frac{\sqrt{\varepsilon_L} \rho}{c}, \quad (9.59)$$

$$\tau_T \equiv t - \sqrt{\varepsilon_T} \rho' = t - \frac{\sqrt{\varepsilon_T} \rho}{c}, \quad (9.60)$$

$$\tau_1 \equiv t - \sqrt{\varepsilon_1} \rho' = t - \frac{\sqrt{\varepsilon_1} \rho}{c}. \quad (9.61)$$

By using the similar manner addressed in Sec. 14.8 of the book by King, Owens, and Wu (1992), the integrals I_2 , I_4 , and I_7 are evaluated exactly. They are

$$I_2 = \frac{1}{\sqrt{\pi} t_1} e^{-\tau_L^2/t_1^2}; \quad I_4 = \frac{1}{\sqrt{\pi} t_1} e^{-\tau_T^2/t_1^2}; \quad I_7 = \frac{1}{\sqrt{\pi} t_1} e^{-\tau_1^2/t_1^2}. \quad (9.62)$$

Thus, with Eq. (9.58), the three integrals I_1 , I_3 , and I_8 can be evaluated readily.

$$I_1 = \frac{2\tau_L}{\sqrt{\pi} t_1^3} e^{-\tau_L^2/t_1^2}; \quad I_3 = \frac{1}{2} [1 + \operatorname{erf}(\tau_T/t_1)]; \quad I_8 = \frac{1}{2} [1 + \operatorname{erf}(\tau_1/t_1)], \quad (9.63)$$

where the definition of the error function is

$$\operatorname{erf} z = \frac{2}{\sqrt{\pi}} \int_0^z e^{-u^2} du; \quad \frac{2}{\sqrt{\pi}} \int_0^\infty e^{-u^2} du = 1. \quad (9.64)$$

Next, the main tasks are to evaluate the integrals I_5 and I_6 . With the similar procedure for the evaluation of the integral I_4 addressed in Sec. 14.8 of the book by King, Owens, and Wu (1992), I_5 is evaluated readily.

$$I_5 = -\frac{\pi}{2} \frac{2^{1/4}}{t_1^{5/2}} e^{-T^2/2t_1^2} \left\{ \pi^{-1/2} \left[V\left(0, \frac{\sqrt{2}T}{t_1}\right) - \frac{\sqrt{2}T}{t_1} V\left(-1, \frac{\sqrt{2}T}{t_1}\right) \right. \right. \\ \left. \left. U\left(0, -\frac{\sqrt{2}T}{t_1}\right) + \frac{2\sqrt{2}T}{t_1} U\left(-1, -\frac{\sqrt{2}T}{t_1}\right) \right] \right\}; \quad (9.65)$$

$$\begin{aligned} T/t_1 &\geq 0 \\ T/t_1 &\leq 0, \end{aligned}$$

where $V(a, z)$ and $U(a, z)$ are parabolic cylinder functions defined on page 687 of the mathematical handbook by Abamowitz and Stegun (1972), and

$$T \equiv t - \sqrt{\varepsilon_L} \rho' + \frac{\varepsilon_T \sqrt{\varepsilon_L}}{2\varepsilon_1} \rho'. \quad (9.66)$$

It is noted that the notation $U(a, z)$ is not related to the step function $U(x)$. From Eq. (9.55), we have

$$I_6 = \frac{\partial}{\partial t} \operatorname{Re} \left[\frac{1}{4} (1 + i) \int_{-\infty}^{\infty} e^{-\omega^2 t_1^2/4} e^{-i\omega T} d\omega \right]$$

$$- \int_{-\infty}^{\infty} e^{-\omega^2 t_1^2/4} e^{-i\omega T} d\omega \int_0^P \frac{e^{i\tau}}{(2\pi\tau)^{1/2}} d\tau \Bigg]. \quad (9.67)$$

The integral in Eq. (9.55) is like Eq. (14.6.22) in the book by King, Owens, and Wu (1992) except for the factor $\omega^{3/2}$ being replaced by $i\omega$. Similarly, the second integral in Eq. (9.67) yields a pure imaginary that contributes nothing to I_6 in Eq. (9.67). Then, we write

$$I_6 = \frac{\partial}{\partial t} \operatorname{Re} \frac{1}{4} (1 + i) \int_{-\infty}^{\infty} e^{-\omega^2 t_1^2/4} e^{-i\omega T} d\omega. \quad (9.68)$$

With $\omega = \sqrt{2}\tau/t_1$ and $z = \sqrt{2}T/t_1$, I_6 becomes

$$I_6 = \operatorname{Re} \frac{e^{i\pi/4} 2^{1/4}}{2\sqrt{2}t_1^{1/2}} \frac{\partial}{\partial t} \vartheta_0, \quad (9.69)$$

where

$$\vartheta_0 = \int_{-\infty}^{\infty} \tau^{-1/2} e^{-\tau^2/2 - iz\tau} d\tau. \quad (9.70)$$

Then, we have

$$\vartheta_0 = \left(\frac{z}{2}\right)^{1/2} e^{-z^2/4} e^{-i\pi/4} f\left(\frac{1}{4}z^2\right), \quad (9.71)$$

$$f\left(\frac{1}{4}z^2\right) = \sqrt{2}K_{1/4}\left(\frac{1}{4}z^2\right) + 2\pi I_{1/4}\left(\frac{1}{4}z^2\right). \quad (9.72)$$

Taking into account the following relations:

$$y = \left(\frac{1}{2}z\right) f\left(\frac{1}{4}z^2\right) = \frac{2\pi}{\sqrt{2}} V(0, z), \quad (9.73)$$

$$\frac{dy}{dz} = \frac{2\pi}{\sqrt{2}} V'(0, z) = \frac{2\pi}{\sqrt{2}} \left[\frac{z}{2} V(0, z) - \frac{1}{2} V(-1, z) \right], \quad (9.74)$$

we have

$$\begin{aligned} \frac{\partial \vartheta_0}{\partial t} &= \frac{\partial \vartheta_0}{\partial T} = \frac{\sqrt{2}}{t_1} \frac{\partial \vartheta_0}{\partial z} \\ &= -\frac{\pi e^{-i\pi/4} e^{-z^2/4}}{t_1} V(-1, z); \quad z \geq 0. \end{aligned} \quad (9.75)$$

For negative values of z , using the Eq. (19.4.2) in the handbook by Gradshteyn and Ryzhik (1980) with $a = -1$, we write

$$V(-1, z) = -\frac{\Gamma(-\frac{1}{2})}{\pi} U(-1, -z). \quad (9.76)$$

With $\Gamma(-1/2) = -2\pi^{1/2}$, this yields to

$$\frac{\partial \vartheta_0}{\partial t} = -\frac{\pi e^{-i\pi/4} e^{-z^2/4}}{t_1} 2\pi^{-1/2} U(-1, -z); \quad z \leq 0. \quad (9.77)$$

Substituting Eqs. (9.75) and (9.77) into Eq. (9.69), I_6 becomes

$$I_6 = -\frac{2^{1/4} \pi e^{-z^2/4}}{2\sqrt{2} t_1^{3/2}} \left\{ \begin{array}{l} V\left(-1, \frac{\sqrt{2}T}{t_1}\right) \\ 2\pi^{-1/2} U\left(-1, -\frac{\sqrt{2}T}{t_1}\right) \end{array} \right\}; \quad \begin{array}{l} T/t_1 \geq 0 \\ T/t_1 \leq 0 \end{array}. \quad (9.78)$$

With the following new notation introducing dimensionless variables:

$$t' \equiv \frac{t}{t_1}; \quad \tau'_L \equiv \frac{\tau_L}{t_1} = t' - \sqrt{\varepsilon_L} \rho_1, \quad (9.79)$$

$$\tau'_T \equiv \frac{\tau_T}{t_1} = t' - \sqrt{\varepsilon_T} \rho_1; \quad \tau'_1 \equiv \frac{\tau_1}{t_1} = t' - \sqrt{\varepsilon_1} \rho_1, \quad (9.80)$$

$$\rho_1 \equiv \frac{\rho'}{t_1} = \frac{\rho}{ct_1}; \quad T' \equiv \frac{T}{t_1} = t' - \sqrt{\varepsilon_L} \rho_1 + \frac{\varepsilon_T \sqrt{\varepsilon_L}}{2\varepsilon_1} \rho_1, \quad (9.81)$$

the formulas of the transient electric field components with Gaussian excitation are derived readily.

$$\begin{aligned} E_{1\rho}(\rho, 0; t) = & \frac{1}{2\pi\varepsilon_0\varepsilon_1} \frac{\pi^{-1/2}}{c^3 t_1^3} \\ & \times \left[\left(-\frac{2\sqrt{\varepsilon_L\varepsilon_T}\tau'_L}{\rho_1} + \frac{\sqrt{\varepsilon_L}}{\rho_1} \right) e^{-\tau'^2_L} + \frac{\pi^{1/2}}{2\rho_1^3} (1 + \operatorname{erf}\tau'_T) \right. \\ & + \left(\frac{\sqrt{\varepsilon_1}}{\rho_1} e^{-\tau'^2_1} + \frac{\pi^{1/2}}{2\rho_1^3} (1 + \operatorname{erf}\tau'_1) \right) + \frac{\pi}{2} \frac{2^{1/4}\varepsilon_L\varepsilon_T}{\sqrt{\varepsilon_1}\sqrt{\varepsilon_L}\rho_1} e^{-T'^2/2} \\ & \left. \times \left\{ \begin{array}{l} V(0, \sqrt{2}T') - \sqrt{2}T'V(-1, \sqrt{2}T') \\ \pi^{-1/2} [U(0, -\sqrt{2}T') + 2\sqrt{2}T'U(-1, \sqrt{2}T')] \end{array} \right\} \right]; \\ & \begin{array}{l} T' \geq 0 \\ T' \leq 0 \end{array}, \end{aligned} \quad (9.82)$$

$$\begin{aligned} E_{1\phi}(\rho, \pi/2; t) = & \frac{1}{2\pi\varepsilon_0\varepsilon_1} \frac{\pi^{-1/2}}{c^3 t_1^3} \\ & \times \left[\left(e^{-\tau'^2_L} + e^{-\tau'^2_T} \right) \frac{\sqrt{\varepsilon_T}}{\rho_1^2} + \frac{\pi^{1/2}}{\rho_1^3} (1 + \operatorname{erf}\tau'_T) \right] \end{aligned}$$

$$\begin{aligned}
& - \left(\frac{\sqrt{\varepsilon_1}}{\rho_1^2} e^{-\tau_1'^2} + \frac{\pi^{1/2}}{2\rho_1^3} (1 + \operatorname{erf} \tau_1') \right) \\
& + \frac{2^{1/4} \pi \varepsilon_T \sqrt{\varepsilon_L} e^{-T'^2/2}}{2\sqrt{2} \sqrt{\varepsilon_1} \sqrt{\varepsilon_L} \rho_1^{3/2}} \left\{ \frac{V(-1, \sqrt{2}T')}{2\pi^{-1/2} U(-1, -\sqrt{2}T')} \right\}; \\
& \qquad \qquad \qquad \begin{matrix} T' \geq 0 \\ T' \leq 0 \end{matrix}, \tag{9.83}
\end{aligned}$$

$$\begin{aligned}
E_{1z}(\rho, 0; t) &= - \frac{\sqrt{\varepsilon_L \varepsilon_T} \pi^{-1/2}}{2\pi \varepsilon_0 \varepsilon_1^{3/2} c^3 t_1^3} \\
& \times \left[\left(- \frac{2\sqrt{\varepsilon_L} \tau_L'}{\rho_1} + \frac{1}{\rho_1^2} \right) e^{-\tau_L'^2} + \frac{\pi^{1/4} \varepsilon_L \sqrt{\varepsilon_T}}{2 \sqrt{\varepsilon_1 \sqrt{\varepsilon_L} \rho_1}} e^{-T'^2/2} \right. \\
& \times \left. \left\{ \frac{V(0, \sqrt{2}T') - \sqrt{2}T' V(-1, \sqrt{2}T')}{\pi^{-1/2} [U(0, -\sqrt{2}T') + 2\sqrt{2}T' U(-1, \sqrt{2}T')]} \right\} \right]; \\
& \qquad \qquad \qquad \begin{matrix} T' \geq 0 \\ T' \leq 0 \end{matrix}. \tag{9.84}
\end{aligned}$$

From above derivations, it is seen that the final approximate formulas for the transient field excited by a Gaussian pulse in a horizontal electric dipole can be expressed in terms of fundamental functions. It is noted that the transient electric field components with Gaussian excitation at all points on the surface are obtained by using the following formulas:

$$E_{1\rho}(\rho, \phi; t) = E_{1\rho}(\rho, 0; t) \cos \phi, \tag{9.85}$$

$$E_{1\phi}(\rho, \phi; t) = E_{1\phi}(\rho, \pi/2; t) \sin \phi, \tag{9.86}$$

$$E_{1z}(\rho, \phi; t) = E_{1z}(\rho, 0; t) \cos \phi. \tag{9.87}$$

With $\varepsilon_1 = 80$, $\varepsilon_T = 4$, and $\varepsilon_L = 2$, graph of $E_{1\phi}(\rho, \pi/2; t)$ of a horizontal electric dipole on the boundary between a homogeneous isotropic medium and one-dimensionally anisotropic medium is shown in Fig. 9.3. Similarly, the properties of $E_{1\rho}(\rho, 0; t)$ and $E_{1z}(\rho, 0; t)$ are shown in Figs. 9.4 and 9.5, respectively. From the above derivations and the results in Figs. 9.3~9.5, it is seen that the three time-dependent electric field components consist of two lateral pulses which decrease with the amplitude factor ρ^{-2} . One pulse travels in the isotropic medium (Region 1) with the velocity $c/\sqrt{\varepsilon_1}$, and the second one travels in the one-dimensionally anisotropic medium (Region 2) with the velocity $c/\sqrt{\varepsilon_L}$ for the components $E_{1\rho}(\rho, 0; t)$ and $E_{1z}(\rho, 0; t)$ and the velocity $c/\sqrt{\varepsilon_T}$ for the component $E_{1\phi}(\rho, \pi/2; t)$. The ρ^{-3} terms constitute the static field generated by the charges left on the ends of the dipole. This field remains after both pulses have travelled an infinite distance.

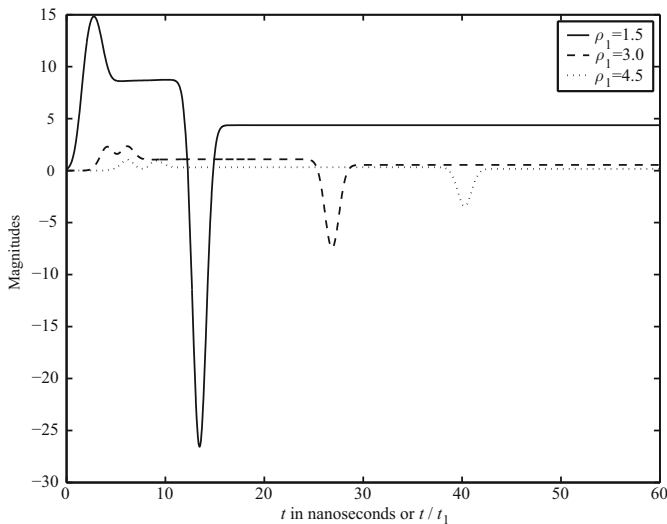


Fig. 9.3. The approximate electric field $t_1\sqrt{\pi}E_{1\phi}(\rho, \pi/2; t)$ on the boundary due to a horizontal electric dipole on the boundary between a homogeneous isotropic medium with relative permittivity $\varepsilon_1 = 80$ and an anisotropic media. The horizontal dipole is excited by a Gaussian pulse with $t_1 = 1$ nsec; $\rho_1 = \rho/ct_1$

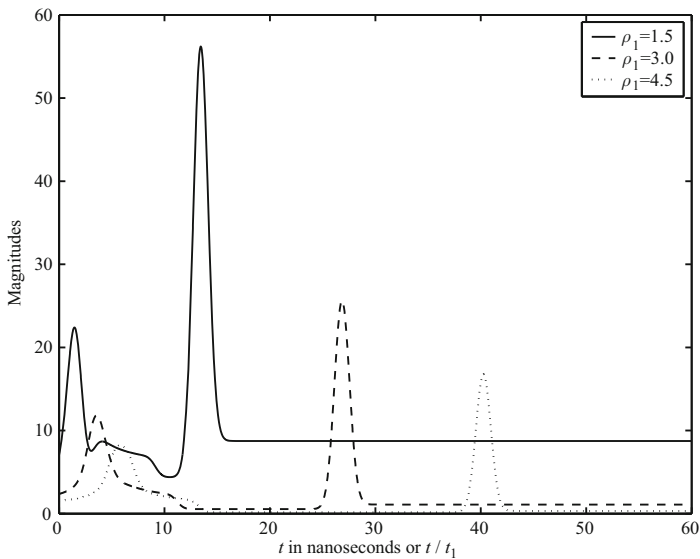


Fig. 9.4. The approximate electric field $t_1\sqrt{\pi}E_{1\rho}(\rho, 0; t)$ on the boundary due to a horizontal electric dipole on the boundary between a homogeneous isotropic medium with relative permittivity $\varepsilon_1 = 80$ and an anisotropic media. The horizontal dipole is excited by a Gaussian pulse with $t_1 = 1$ nsec; $\rho_1 = \rho/ct_1$

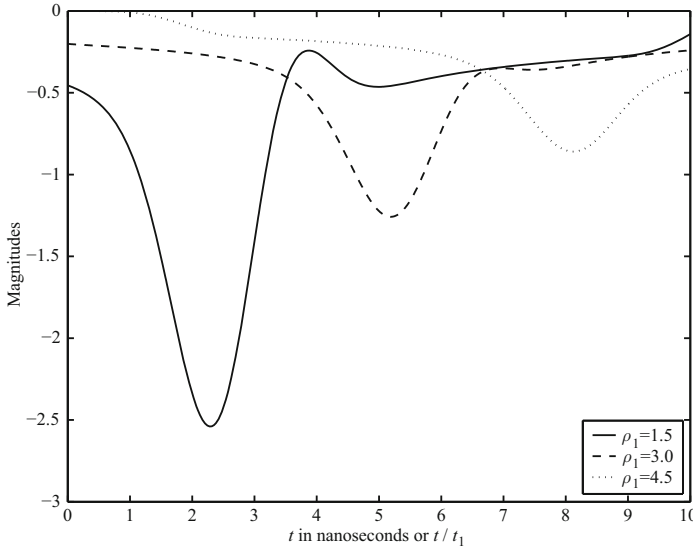


Fig. 9.5. The approximate electric field $t_1 \sqrt{\pi} E_{1z}(\rho, 0; t)$ on the boundary in to a horizontal electric dipole on the boundary between a homogeneous isotropic medium with relative permittivity $\varepsilon_1 = 80$ and an anisotropic media. The horizontal dipole is excited by a Gaussian pulse with $t_1 = 1$ nsec; $\rho_1 = \rho/ct_1$

Furthermore, it should be pointed out that, unlike the field with delta function excitation in this chapter, the terms due to the Fresnel integral do not completely cancel the $\rho^{-1/2}$ term for the components $E_{1\rho}(\rho, 0; t)$ and $E_{1z}(\rho, 0; t)$ and the $\rho^{-3/2}$ term for the component $E_{1\phi}$. Obviously, the Fresnel-integral term for the component $E_{1\phi}(\rho, \pi/2; t)$ decreases rapidly so that the Fresnel-integral term for the isotropic case was omitted in Eq. (14.8.16) in the book by King, Owens, and Wu (1992).

References

- Abamowitz M and Stegun IA (1972) *Handbook of Mathematical Functions*. New York, NY, USA: Dover Publications.
- Gradshteyn IS and Ryzhik IM (1980) *Table of Integrals, Series, and Products*. New York, NY, USA: Academic Press.
- King RWP (1982) New formulas for the electromagnetic field of a vertical electric dipole in a dielectric or conducting half-space near its horizontal interface. *Journal of Applied Physics*, 53: 8476–8482; (1984) Erratum, 56: 3366.
- King RWP and Brown MF (1984) Lateral electromagnetic waves along plane boundaries: A summarizing approach. *Proceedings of the IEEE*, 72: 595–611.
- King RWP (1985) Electromagnetic surface waves: New formulas and applications. *IEEE Transactions on Antennas and Propagation*, AP-33: 1204–1212.

- King RWP (1988) Lateral Electromagnetic pulses generated by a vertical electric dipole on a plane boundary between dielectrics. *Journal of Electromagnetic Waves and Applications*, 2: 225–243.
- King RWP (1989) Lateral Electromagnetic pulses generated on a plane boundary between dielectrics by vertical and horizontal dipole source with Gaussian pulse excitation. *Journal of Electromagnetic Waves and Applications*, 2: 589–597.
- King RWP (1990) Lateral Electromagnetic waves and pulses on open microstrip. *IEEE Transactions on Microwave Theory and Techniques*, 38: 38–47.
- King RWP, Owens M, and Wu TT (1992) *Lateral Electromagnetic Waves: Theory and Applications to Communications, Geophysical Exploration, and Remote Sensing*. New York, NY, USA: Springer-Verlag.
- Li K, Lu Y, and Li M (2005) Approximate formulas for lateral electromagnetic pulses from a horizontal electric dipole on the surface of one-dimensionally anisotropic medium. *IEEE Transactions on Antennas and Propagation*, 53(3): 933–937.
- Pan WY (1985) Surface-wave propagation along the boundary between sea water and one-dimensionally anisotropic rock. *Journal of Applied Physics*, 58: 3963–3974.
- Sommerfeld A (1909) Propagation of waves in wireless telegraphy. *Annalen der Physik* (Leipzig), 28: 665–736.
- Sommerfeld A (1926) Propagation of waves in wireless telegraphy. *Annalen der Physik* (Leipzig), 81: 1135–1153.
- Wu TT and King RWP (1982a) Lateral waves: New formulas for $E_{1\phi}$ and E_{1z} . *Radio Science*, 17: 532–538; (1984) Correction, 19: 1422.
- Wu TT and King RWP (1982b) Lateral waves: A new formula and interference pattern. *Radio Science*, 17: 521–531.
- Wu TT and King RWP (1987) Lateral Electromagnetic pulses generated by a vertical electric dipole on the boundary between two dielectrics. *Journal of Applied Physics*, 62: 4543–4555.
- Xu YH, Li K, and Ren W (2007) The approximate transient field of a horizontal electric dipole excited by a Gaussian pulse on the boundary between a homogeneous isotropic medium and one-dimensionally anisotropic medium. *IEEE Antennas and Wireless Propagation Letters*, 6: 427–431.

Index

- additional notations, 196
- admittance boundary condition, 154
- air-dielectric boundary, 7, 28
- air-earth boundary, 2
- Airy function of the second kind, 127, 138, 155
- amplitude factor, 197, 210
- amplitude of delta function, 184
- analytical solution, 147
- angular distance, 9
- anisotropic properties, 210
- anisotropic uniaxially case, 203
- approximate formulas, 148, 212, 217
- approximate transient field, 203, 212
- asphalt- and cement-coated planar and spherical Earth, 157
- asphalt- and cement-coated spherical Earth, 136
- asymptotic methods, 87
- attenuation factor, 39, 61
- azimuthal field variations, 149

- based-insulated dipole, 45, 73
- Bessel function, 21, 59, 90
- boundary condition, 154
- branch cut, 21, 62, 91
- branch line, 24, 63, 91
- branch-cut structure, 171

- Cartesian coordinate system, 16, 56
- Cartesian coordinates, 17
- characteristic impedance, 78
- complex parameter, 131
- complex plane, 35

- complex plane technique, 8
- conducting base, 77, 84
- conducting or electrically spherical Earth, 147
- contour integrations, 87
- convergence of series, 142
- corrugated metal plane and cylinder, 3
- current density, 8, 149
- current-density distribution, 77
- cylindrical coordinates, 19, 73, 167
- cylindrical surface wave, 1

- delta function current, 165, 197
- delta function excitation, 175, 194, 203
- delta function lateral pulse, 210
- delta function pulse, 190, 193, 210
- dielectric base, 84
- dielectric image line, 3
- dielectric layer, 3, 6, 16, 124, 132
- dielectric rod or optical fiber, 3
- dielectric-coated Earth, 123, 157
- dielectric-coated plane and cylinder, 3
- differential equation, 128, 138, 152
- diffraction of ground wave, 9
- dimensionless variable, 216
- direct wave, 20, 90
- discontinuity, 174, 192
- driving-point current, 78
- dyadic Green's function, 87

- electric field component, 46, 184, 204
- electric type, 142
- electric-type field, 115, 150
- electric-type lateral wave, 62

- electric-type term, 108, 157
- electric-type trapped surface wave, 65
- electric-type wave, 66
- electrically Earth, 148
- electrically medium, 136
- electrically narrow microstrip line, 73
- electrically short and long horizontal antennas, 157
- electromagnetic theory, 123
- elementary functions, 193, 199
- error function, 26, 94, 196
- even function, 21, 90, 108
- exact formulas, 166, 193
- exact solution, 166
- excitation condition, 128
- excitation efficiency, 140, 157
- excitation source, 137, 153
- exciting current, 169

- far-field condition, 24, 36, 93
- far-field region, 7, 15, 78
- field factor, 78
- finite integral, 197, 199
- four-layered forest environment, 87
- four-layered region, 88, 96, 103
- Fourier transform, 17, 212
- Fourier's transform technique, 194, 204
- Fourier-Bessel integral representations, 193
- fourth quadrant, 34
- frequency-domain electromagnetic field, 204
- frequency-domain field component, 204, 207
- frequency-domain properties, 165
- Fresnel integral, 26, 94, 205
- Fresnel-integral term, 219
- fundamental function, 197, 217

- Gaussian excitation, 194, 203, 212
- Gaussian pulse, 193, 212, 217
- Gaussian shape, 199
- general formulas, 157
- ground-wave attenuation factor, 9
- guiding-wave mechanism, 2

- half-width, 195, 212
- Hankel function, 2, 21, 90
- harmonic series, 8

- Helmholtz equation, 125, 149
- Hertz potential, 165, 166
- homogeneous isotropic medium, 204, 212
- horizontal antenna, 55
- horizontal electric dipole, 56, 140, 203

- ice-coated spherical seawater, 136
- ideal image wave, 6
- ideal reflected wave, 6, 27, 90
- impedance boundary condition, 127, 150
- impedance load, 79
- impedance of patch, 78
- imperfect conductor, 32, 35
- infinite integral, 170
- infinitesimal vertical Hertzian dipole, 2
- initial value, 132
- integral contour, 34
- integrand function, 23
- interference, 136, 157
- intermediate region, 79
- isotropic medium, 217

- lateral pulse, 184, 210
- lateral wave, 27, 88
- lateral-wave characteristics, 6
- Legendre function, 126, 131, 149
- logarithmic graphs, 49
- low frequencies, 124, 136

- magnetic field component, 95
- magnetic type, 142
- magnetic-type field, 62, 153, 157
- magnetic-type lateral wave, 65
- magnetic-type term, 108, 113, 157
- magnetic-type trapped surface wave, 65
- magnetic-type wave, 66
- matched line, 79
- mathematical challenges, 123
- Maxwell's equations, 16, 56, 88
- microstrip antenna, 55
- microstrip transmission line, 78
- microstrip transmission lines, 78
- monopole base-driven against a buried ground system, 45, 74
- multi-layered Earth, 147
- multi-layered region, 88

- N-layered dielectric, 124, 148

- Newton's iteration method, 28, 91, 97
- non-zero components, 149, 153
- nonzero field components, 124
- normalized height-gain function, 128, 138, 153, 155
- normalized surface impedance, 9, 150
- numerical integration, 34, 59
- numerical method, 132
- one-dimensionally anisotropic medium, 203, 212
- operating frequency, 28, 78
- parabolic cylinder function, 214
- patch antenna, 77
- perfect conducting Earth, 136
- perfect conducting sphere, 8, 123, 128
- perfect conductor, 16, 88, 136
- permeability, 88, 124, 147
- permittivity tensor, 203
- physical significance, 123
- Planar-Earth formulas, 143
- pole equation, 59, 91
- poles of electric-type wave, 109
- potential function, 128, 149, 153
- propagating distance, 136
- propagation factor, 62, 65
- propagation modes, 153
- prospecting and diagnostics, 72
- pulsed field, 184
- radiation condition, 127
- radio practice, 123
- receiving dipole, 6
- reciprocity theorem, 140, 155
- rectangular patch antenna, 77
- reflection coefficient, 20, 32
- relative effective permittivity, 78
- relative permittivity, 16, 124, 132
- removable pole, 62, 91, 113
- resonant lines, 79
- scalar Helmholtz equation, 153
- significant feature, 210
- Sommerfeld radiation condition, 18
- spherical and electrically homogeneous Earth, 123
- spherical boundary, 126
- spherical coordinate system, 147
- spherical coordinates, 44, 73, 125
- spherical dielectric Earth, 147
- spherical Earth, 132, 149
- spherical electrically Earth, 152, 157
- spherical interface, 153
- spherical layering, 147
- spherical layers, 147
- spherical perfectly conducting Earth, 138
- spherical surface, 123, 148, 149
- spherical-Earth formulas, 143
- spherical-Earth surface, 9
- spherically bounded layer, 147, 149, 152
- static electric field, 193
- static field, 217
- step function, 214
- Stokes equation, 9, 126
- stratified media, 3
- strip transmission lines, 77
- subsurface and close-to-the-surface communication, 72
- sum of residues of poles, 24, 61, 96
- surface admittance, 147, 154
- surface communication, 124
- surface impedance, 127, 150
- surface-wave pulse, 184
- tangential electric field component, 57, 193
- three- and four-layered region, 123
- three-dimensional diagrams, 79
- three-layered region, 16, 32, 55
- three-layered spherical Earth, 124
- three-layered spherical region, 140
- time domain, 166, 212
- time-dependent electric field component, 207, 217
- total field, 97
- transient electric field, 212
- transient electromagnetic pulse, 204
- transient field, 165, 193, 217
- transmission lines, 77
- transmitting dipole, 6
- transverse electric (TE) field, 58
- transverse electric (TE) wave, 5
- transverse magnetic (TM) field, 58
- transverse magnetic (TM) wave, 4
- trapped surface wave, 7, 96, 117
- travelling-wave currents, 79

- two dielectric layers, 88
- two different media, 6, 55, 165
- two half-spaces, 165
- two- and three-layered region, 87

- uniaxial substrate, 73
- uniaxially anisotropic medium, 84
- uniform permittivity, 1, 124, 147

- velocity of light, 168
- vertical components, 140, 155

- vertical electric dipole, 16, 124, 149
- vertical electric field, 8
- vertical magnetic dipole, 137, 153
- vertical magnetic field, 190, 193
- volume current density, 17, 57

- Watson's theory, 8, 123
- wave of a ideal image dipole, 57

- Zenneck surface wave, 1